

**GLULAM CONNECTIONS
USING EPOXY GLUED-IN REBARS**

by

Robert Wiktor

Mgr inż. (M.Eng.), Warsaw Technical University, Warsaw, Poland, 1990

**A THESIS SUBMITTED IN PARTIAL FULFILLMENT OF
THE REQUIREMENTS FOR THE DEGREE OF
MASTER OF APPLIED SCIENCE**

in

**THE FACULTY OF GRADUATE STUDIES
Department of Civil Engineering**

We accept this thesis as conforming
to the required standard

THE UNIVERSITY OF BRITISH COLUMBIA

October 1994

© **Robert Wiktor, 1994**

In presenting this thesis in partial fulfilment of the requirements for an advanced degree at the University of British Columbia, I agree that the Library shall make it freely available for reference and study. I further agree that permission for extensive copying of this thesis for scholarly purposes may be granted by the head of my department or by his or her representatives. It is understood that copying or publication of this thesis for financial gain shall not be allowed without my written permission.

(Signature)

Department of CIVIL ENGINEERING

The University of British Columbia
Vancouver, Canada

Date OCTOBER 13th, 1994

ABSTRACT

This thesis is a part of the research aimed at developing a reliable moment resisting connection method for timber structures based on gluing the reinforcing bars to the wood.

The aims of this thesis are:

- **to investigate the influence of atmospheric factors (such as moisture and temperature) on the performance of the glued-in rebar joints,**
- **to examine the possibility of increasing the bearing resistance of the glulam (compression perpendicular to the grain) by gluing the rebars perpendicularly to the grain,**
- **to implement the glued-in rebar technique in creating a moment resisting joint of a statically indeterminate glulam frame for a multi-storey building,**
- **to provide the designers of timber buildings with information on how to design the glued-in rebar joints,**
- **to verify the possible savings derived from the use of the moment resisting joints in glulam frames.**

The findings of this research are:

- **the glued-in rebar connection may be considered reliable in the temperature and moisture conditions which can occur in the building; the connection was found to be influenced by those conditions to a lesser degree than the glulam structure itself,**
- **the gluing of the rebars under the bearing plates can increase the compressive resistance of the glulam in the direction perpendicular to the grain by 100%,**
- **the rebars glued perpendicularly to the grain have an additional effect of increasing the shear capacity of the glulam members,**
- **full size beam-to-column joints using the glued-in rebar idea were tested; the connection proved**

to have bending and shear resistance equal or greater than the resistance of the glulam members which were joined,

- a ductile behaviour of the beam-to-column connections was observed prior to the failures,
- a set of guidelines was developed to facilitate the design of glued-in rebar joints in the multi-storey timber frames,
- by using moment resisting glued-in rebar connections it is possible to save 15% of the glulam volume versus the traditional hinged frame design.

TABLE OF CONTENTS

Abstract	ii
Table of Contents	iv
List of Tables	vii
List of Figures	ix
Acknowledgements	xiii
Chapter 1 INTRODUCTION AND LITERATURE OVERVIEW	1
1.1 Introduction.	1
1.2 Literature Overview.	3
Chapter 2 MOISTURE CONTENT AND TEMPERATURE TESTS	15
2.1 Test Objectives.	15
2.2 Development of a Test Specimen.	17
2.3 Moisture Content Tests.	28
2.4 Temperature Tests.	42
2.5 Conclusions.	52
Chapter 3 COMPRESSION PERPENDICULAR TO THE GRAIN	54
3.1 Test Objective.	54
3.2 Materials, Test Setups, and Test Procedures.	55
3.3 Flush Rebar Tests.	59
3.4 Protruding Rebar Tests.	72
3.5 Guidelines for Bearing Reinforcement with #15 Rebars.	79
3.6 Conclusions.	80

Chapter 4	BEAM-TO-COLUMN JOINTS	81
4.1	Test Objectives.	81
4.2	Preliminary Analysis of the Frame for a Multi-storey Building.	82
4.3	Test Setup.	87
4.4	Materials.	92
4.5	Joint Design.	94
4.6	Test T-1.	99
4.7	Test T-2.	110
4.8	Test T-3.	124
4.9	Conclusions.	135
Chapter 5	DESIGN GUIDELINES FOR GLUED-IN REBAR JOINTS	136
5.1	Objective.	136
5.2	Design Philosophy.	137
5.3	Design Assumptions.	138
5.4	Moment Resistance of the Joint.	140
5.5	Bearing Reinforcement of the Column Plates.	141
5.6	Axial Resistance of the Joint.	143
5.7	Combined Axial and Bending Resistance of the Joint.	143
5.8	Shear Resistance of the Joint.	144
5.9	Resistance of the Bolts, Plates, and Welds.	145
5.10	Serviceability Check.	146
Chapter 6	COMPARISON WITH STATICALLY DETERMINATE FRAME	147
6.1	Objective.	147
6.2	Design of the Pinned Frame.	147
6.3	Design of the Members.	148
6.4	Cost Comparison.	154

Chapter 7	CONCLUSIONS	156
Bibliography		158
Appendix A	THEORETICAL DEFORMATIONS AND STRESSES IN A GLUED-IN REBAR SPECIMEN DURING FREEZING/HEATING CYCLE	161
	1. Assumptions.	161
	2. Freezing Cycle: from +20°C to -30°C.	163
	3. Heating Cycle: from +20°C to +50°C.	168
	4. Summary.	172
Appendix B	THE ANALYSIS OF THE RIGID FRAME FOR A MULTI-STOREY OFFICE BUILDING	173
	1. General Design Assumptions.	173
	2. Loads.	175
	3. Load Combinations.	181
	4. Frame Analysis.	182
	5. Results of the Analysis.	183
	6. Design of the Members.	201

LIST OF TABLES

Table 2.1	Selected thermal properties of steel and wood.	15
Table 2.2	Results of tension tests performed on #15 rebars.	19
Table 2.3	Results of the control sample testing.	24
Table 2.4	Results of the M.C. sample testing.	40
Table 2.5	Results of the temperature sample testing.	50
Table 3.1	Results of the preliminary tests with bearing plates.	60
Table 3.2	Results of the "beam specimen" tests with bearing plates.	63
Table 3.3	Results of the tests with two bearing plates.	68
Table 3.4	Results of the multi-rebar tests.	70
Table 3.5	Results of the preliminary tests with protruding rebars.	73
Table 3.6	Results of the "beam specimen" tests with protruding rebars.	76
Table 4.1	Internal forces governing the design of the elements.	85
Table 4.2	Calculated resistance and size of the elements.	85
Table 4.3	Results of tension tests performed on #20 rebars.	92
Table 4.4	Capability of glued-in rebars to transfer tension loads.	96
Table 4.5	Components of the total deflection in test T-1.	107
Table 4.6	Components of the total deflection in test T-2.	120
Table 4.7	Comparison of the LVDT 3 readings in tests T-1 and T-2.	121
Table 4.8	Comparison of the LVDT 4 readings in tests T-1 and T-2.	121
Table 4.9	Components of the total deflection in test T-3.	131
Table 4.10	Comparison of the LVDT 3 readings in tests T-1, T-2, and T-3.	132
Table 4.11	Comparison of the LVDT 4 readings in tests T-1, T-2, and T-3.	133
Table 5.1	Minimum embedment length for various size of the rebars.	139

Table 6.1	Maximum internal forces in the hinged frame.	148
Table 6.2	Volume of the glulam used for different types of frame.	154
Table 6.3	Cost of a glued-in rebar joint.	154
Table 6.4	Cost comparison between frames.	155
Table B.1	Load cases used in the numerical analysis of the frame.	182
Table B.2	Internal forces due to the load combination "a".	183
Table B.3	Internal forces due to the load combination "b".	186
Table B.4	Internal forces due to the load combination "c".	188
Table B.5	Internal forces due to the load combination "d".	191
Table B.6	Internal forces due to the load combination "e".	193
Table B.7	Internal forces due to the load combination "f".	196
Table B.8	Internal forces due to the load combination "g".	198
Table B.9	Internal forces governing the design of the elements.	201

LIST OF FIGURES

Fig. 1.1	Typical column base connection as developed by H.Riberholt.	4
Fig. 1.2	Purlin joint (Riberholt, 1986).	4
Fig. 1.3	Moment resisting knee joint (Riberholt, 1986).	4
Fig. 1.4	Beam-column connection used in timber classrooms (McIntosh, 1989).	5
Fig. 1.5	Beam-column connection used in the Te Awamutu College Gymnasium (McIntosh, 1989).	5
Fig. 1.6	Portal frames at Jellie Park (Buchanan and Fletcher, 1989).	6
Fig. 1.7	Portal apex connection (Buchanan and Fletcher, 1989).	6
Fig. 1.8	Beam splice (Townsend, 1990).	7
Fig. 1.9	Portal knee connection using structural bracket.	7
Fig. 1.10	Beam-column connections (Fairweather, 1992).	8
Fig. 1.11	Bearing connection using glued-in rods.	9
Fig. 1.12	Shear reinforcement of the glulam beam.	9
Fig. 1.13	Moment resisting splice connection of the glulam beam.	10
Fig. 1.14	Knee joint and column to foundation joint (Turkovskij, 1991).	10
Fig. 1.15	Pull-out test (Malczyk, 1993).	12
Fig. 1.16	Beam splice test (Malczyk, 1993).	12
Fig. 1.17	Racking test of the glulam column (Malczyk, 1993).	13
Fig. 1.18	Knee joint test (Malczyk, 1993).	14
Fig. 2.1	Specimen used for M.C. and temperature tests.	18
Fig. 2.2	Typical L-D curve obtained from the rebar tension test.	20
Fig. 2.3	Specimen during the test in the tension apparatus.	21
Fig. 2.4	Typical L-D relationship for the control specimens.	23
Fig. 2.5	Failure Mode I - rebar yielding.	25
Fig. 2.6	Stress distribution along the rebar.	27

Fig. 2.7	Stress distribution at different load levels.	27
Fig. 2.8	An example of the M.C. changes.	29
Fig. 2.9	Drying of the specimens.	30
Fig. 2.10	Load-deformation curves for the M.C. specimens.	32
Fig. 2.11	Failure Mode II - pull-out.	34
Fig. 2.12	Failure Mode III - glulam split.	35
Fig. 2.13	Specimens K1 and K2 after failure.	36
Fig. 2.14	Deformation range observed after pull-out failure.	37
Fig. 2.15	Stresses, deformations, and M.C. in function of time.	39
Fig. 2.16	Comparison of the control sample and the M.C. sample.	41
Fig. 2.17	Temperature variations during the treatment.	42
Fig. 2.18	Load-deformation curves for the temperature specimens.	44
Fig. 2.19	Dimensional changes of the specimen as a function of time.	47
Fig. 2.20	Internal stresses as a function of the temperature.	48
Fig. 2.21	Internal stresses as a function of time.	49
Fig. 2.22	Comparison of the control sample and the temperature sample.	51
Fig. 3.1	Preliminary test setup.	55
Fig. 3.2	Specimen in the testing machine during preliminary test.	56
Fig. 3.3	Simple supported beam setup.	57
Fig. 3.4	Specimen with top and bottom bearing plates.	58
Fig. 3.5	Load-deformation curves for the specimens with 76x102mm plate.	65
Fig. 3.6	Load-deformation curves for the specimens with 102x152mm plate.	65
Fig. 3.7	Comparison of L-D curves for the specimens with 76x102mm plate.	66
Fig. 3.8	Comparison of L-D curves for the specimens with 102x152mm plate.	67
Fig. 3.9	Load-deformation curves for the specimens with two bearing plates.	69
Fig. 3.10	Comparison of L-D curves for the multi-rebar specimens.	71
Fig. 3.11	Specimens after the preliminary tests.	75
Fig. 3.12	Specimens after the preliminary tests.	75

Fig. 3.13	Typical L-D curves for the "beam" specimens with protruding rebars.	77
Fig. 3.14	Failure loads versus the embedment length for the specimens with protruding rebars.	78
Fig. 4.1	Overall dimensions of the building.	83
Fig. 4.2	Locations of the splice joints in the beams.	86
Fig. 4.3	Overall dimensions of the reaction frame and the specimen.	87
Fig. 4.4	Specimen in the reaction frame.	89
Fig. 4.5	Load, reactions, and resulting moment and shear diagrams.	90
Fig. 4.6	Locations of the gauges in the frame.	91
Fig. 4.7	Locations of the gauges within the connection region.	91
Fig. 4.8	Moment transfer from the column to the beam.	94
Fig. 4.9	Forces created at the end of the column.	95
Fig. 4.10	Column part of the specimen T-1.	99
Fig. 4.11	Beam part of the specimen T-1.	100
Fig. 4.12	Specimen T-1 before the test.	102
Fig. 4.13	Locations of the gauges in the specimen T-1.	103
Fig. 4.14	Joint in the specimen T-1 after failure.	104
Fig. 4.15	Fracture of the rebar in the specimen T-1.	105
Fig. 4.16	Deflections of the column during the test T-1.	106
Fig. 4.17	Behaviour of the tension side of the connection.	108
Fig. 4.18	Bending of the beam plate.	109
Fig. 4.19	Column part of the specimen T-2.	111
Fig. 4.20	Beam part of the specimen T-2.	112
Fig. 4.21	Routing grooves.	113
Fig. 4.22	Drilling perpendicular holes.	113
Fig. 4.23	Gluing perpendicular rebars.	114
Fig. 4.24	Drilling inclined holes.	114
Fig. 4.25	Fitting inclined rebars and plates.	115
Fig. 4.26	Loading procedures for the specimen T-2.	116

Fig. 4.27	Joint in the specimen T-2 during final loading.	117
Fig. 4.28	Failure of the specimen T-2.	118
Fig. 4.29	Deflections of the column during the test T-2.	119
Fig. 4.30	Partial pull-out of the beam rebar in the specimen T-2.	122
Fig. 4.31	Column part of the specimen T-3.	124
Fig. 4.32	Beam part of the specimen T-3.	125
Fig. 4.33	Loading procedures for the specimen T-3.	127
Fig. 4.34	Specimen T-3 during final loading.	128
Fig. 4.35	Joint in the specimen T-3 after failure.	129
Fig. 4.36	Deflections of the column during the test T-3.	130
Fig. 5.1	Forces in the connection.	138
Fig. 5.2	Geometry of the beam to column joint.	140
Fig. 5.3	Forces perpendicular to the grain in the column.	142
Fig. 5.4	Bending of the beam plates.	146
Fig. 6.1	Braced frame of the building.	147
Fig. A.1	Internal stresses in the specimen due to temperature changes.	162
Fig. A.2	Deformation of the specimen in phase 1.	164
Fig. A.3	Deformation of the specimen in phase 2.	166
Fig. A.4	Deformation of the specimen in phase 5.	168
Fig. A.5	Deformation of the specimen in phase 6.	170
Fig. B.1	Overall dimensions of the building.	174
Fig. B.2	Model of the frame used in the numerical analysis.	182

ACKNOWLEDGEMENTS

I am very grateful to my supervisor Professor Borg Madsen for his guidance, valuable suggestions, and encouragement throughout this research.

I would like to express my gratitude to Professor R.O. Foschi and Professor R.G. Sexsmith for reviewing the manuscript and constructive criticism.

I would like to thank Mr. Paul Symons for his helpful participation in preparing and maintaining instrumentation used in the experimental part of this research.

My appreciation is extended to Mr. Dick Postgate and all technicians for their assistance during various phases of the experiments.

Research grant from the Science Council of British Columbia is gratefully acknowledged.

The support from the following companies is much appreciated: Industrial Formulators of Canada, Surrey Laminated Products Ltd., Structurlam, Dickie Dee Ice Cream.

Finally, I wish to thank my family and my friends for their support throughout my graduate career.

This thesis is joyfully dedicated to my loving wife Justyna.

CHAPTER 1

INTRODUCTION AND LITERATURE OVERVIEW.

1.1 INTRODUCTION.

Connections are essential parts of structures. In many cases, they are the most difficult parts to design and to accomplish. This is especially true for timber structures. It is relatively simple to design a timber member but, usually, the challenge starts when it has to be connected to the other members.

Over the years, engineers invented many connection techniques but still the most commonly used are the traditional connectors: bolts, nails and pins. Unfortunately, these connectors can't be successfully used in statically indeterminate timber structures due to their lack of stiffness. In those structures, the joints should be able to resist reversed bending moments due to dynamic loads on the structure such as wind loads or earthquake loads. The traditional connectors do not provide enough stiffness for the joint, often due to oversized holes. Therefore, the need of a reliable, moment resisting connection method for glulam structures still exists.

One of the most promising new techniques is the use of steel rods bonded to the timber by glues. This idea originated in Scandinavia and was used in the industry for over 30 years. Various modifications have been developed, some of them with very narrow applications. Recently, an increasing interest in this technique was observed. Several research programs in this field are presently performed in Finland, Russia, Australia, New Zealand, and Canada.

This thesis is part of a Canadian research program which started in 1992 at the University of British Columbia under supervision of Professor Borg Madsen.

1.1.1 Scope of Thesis.

This thesis is the second one dealing with glued-in rebar connections being part of the research program at UBC. The first one was presented by Robert Malczyk in 1993

(R.Malczyk, "Glued-in Re-bar Connection", 1993). The work presented here is a natural continuation of previous research.

The main aims of this thesis are:

- to implement the glued-in rebar technique developed earlier, in moment resisting joints for multi-storey frame structures,
- to provide the designers of timber buildings with design information on the behaviour of glued-in rebar connections,
- to investigate the influence of atmospheric factors (such as moisture and temperature) on the performance of the glued-in rebar joints,
- to develop a reinforcement technique for glulam members subjected to bearing (compression perpendicular to the grain).

1.1.2 Outline of Thesis.

The thesis consists of three parts: one theoretical part and two practical parts.

An overview of recent experimental work in the use of steel rods glued into timber members is presented in Chapter 1.

Chapter 2 deals with the general behaviour of the glued-in rebars when subjected to severe changes of temperature or moisture content in the glulam. An impact of those changes on the capacity of the connection is presented. The stresses created in the connection by the atmospheric factors are discussed.

Chapter 3 and 4 presents practical implementation of the glued-in rebar technique. Chapter 3 describes the reinforcing of glulam in compression perpendicular to the grain creating a very efficient bearing connection method. Chapter 4 describes the beam-to-column moment resisting connection and the tests conducted at UBC on full scale specimens.

Finally, chapter 5 contains design guidelines for the glued-in rebar joints and chapter 6 provides a comparison to the traditional design.

1.2 LITERATURE OVERVIEW.

Two different approaches of the glued-in rebar idea have been adopted by the researchers. In New Zealand and in Australia the steel rods are glued parallel to the grain of the glulam. This is continuation of an original idea developed in Scandinavia and improved by Danish researchers in 1960's. A different approach was developed in Russia and Finland. The researchers there are creating rigid connections by gluing rebars at an angle to the grain. This later idea is also followed (with some modifications) in the research program conducted at the University of British Columbia.

A comprehensive overview of the research related to the topic of this thesis is presented below.

1.2.1 Scandinavian Research.

The first research on glued-in steel rods in laminated timber was performed in Sweden around 1965.

Special glued-in bolts were used in Denmark to provide connection for a glulam rotor in wind turbines (Riberholt, 1982).

The major work on steel bars glued into the glulam was performed by Riberholt (1986, 1988) in Denmark. The idea of the rods glued parallel to the grain was followed in that research. Riberholt completed tension and shear tests on steel rods glued into the end grain of glulam beams (Riberholt, 1986) and recommended design procedures for the connection. The collected information was then applied to the splice joint in a beam. The beams were tested under both wet and dry, service conditions. The same report also describes a moment resisting column to foundation joint (see Fig.1.1). This type of joint became a standard connection method for the glulam industry in Scandinavia.

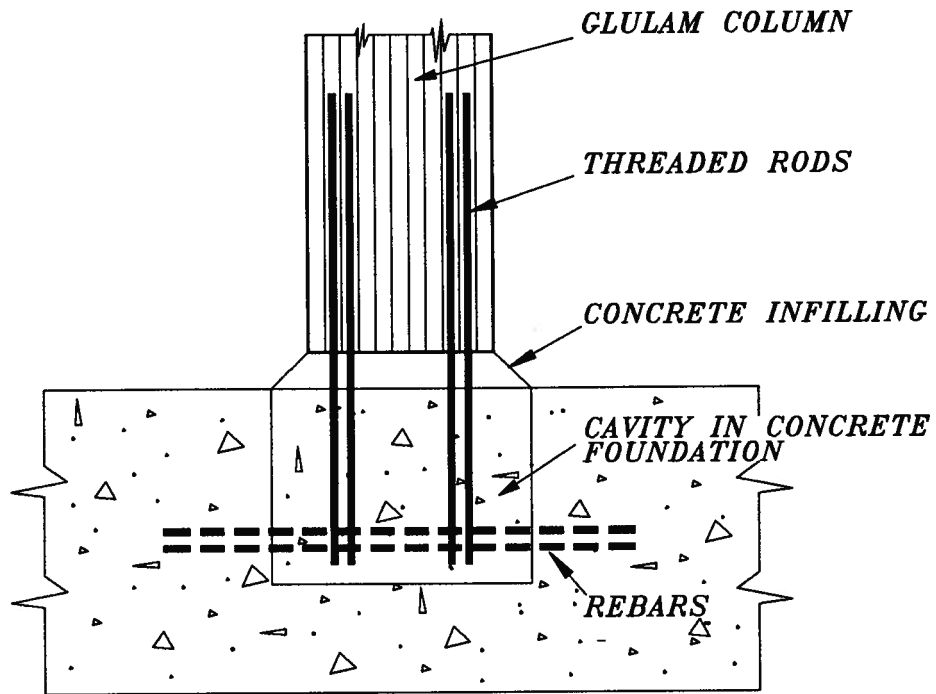


Fig.1.1 Typical column base connection as developed by H.Riberholt.

His report (Riberholt, 1986) also describes tests on purlin joints (Fig.1.2) and moment resisting knee joints for portal frames (Fig.1.3). Further reports provide more test results and some empirical formulae for failure loads in this type of connection (Riberhold, 1988).

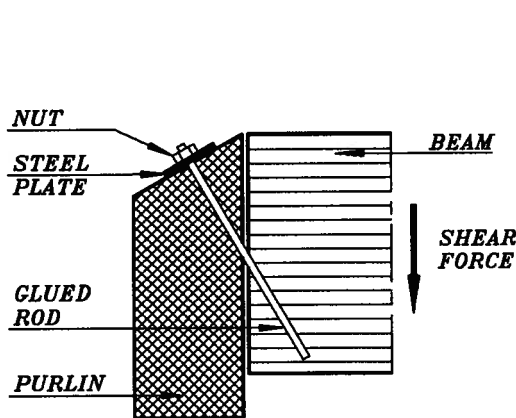


Fig.1.2 Purlin joint
(Riberholt, 1986).

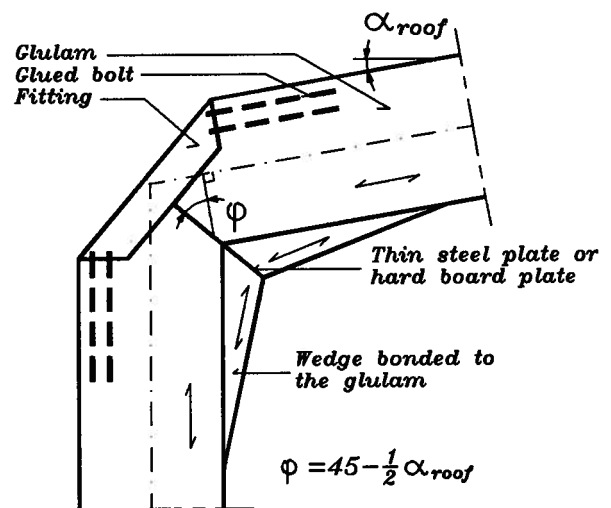


Fig.1.3 Moment resisting knee joint
(Riberholt, 1986).

1.2.2 New Zealand Research.

An extensive program of glued-in dowels has been carried out in New Zealand since late 1980's. The epoxied steel rods were used in beam-column connection for timber classrooms (Fig.1.4) and in the Te Awamutu College Gymnasium (Fig.1.5).

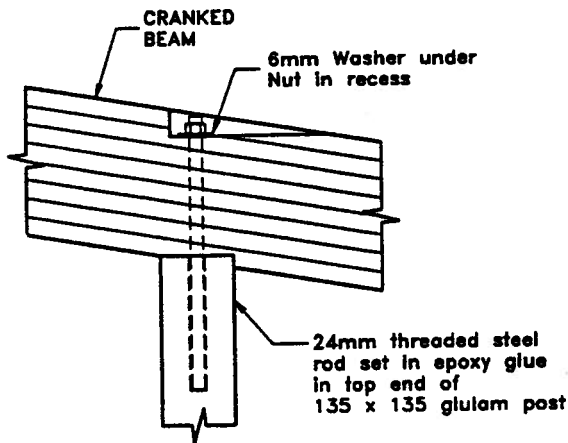


Fig.1.4 *Beam-column connection used in timber classrooms (McIntosh, 1989).*

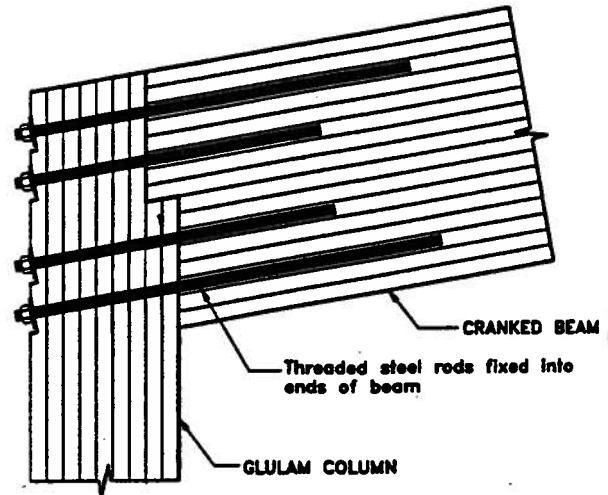


Fig.1.5 *Beam-column connection used in the Te Awamutu College Gymnasium (McIntosh, 1989).*

Buchanan and Fletcher (1989) report on the design and construction of two indoor swimming pools which use epoxied steel dowels for attaching curved glulam portal frames (Fig.1.6).

The base connection was similar to that developed by Riberhold. The beam-column connections also used threaded rods glued into the end grains of the beams and pass through the column.

The same researchers also reported on the use of epoxy glued steel rods in portal apex connection (Fig.1.7).

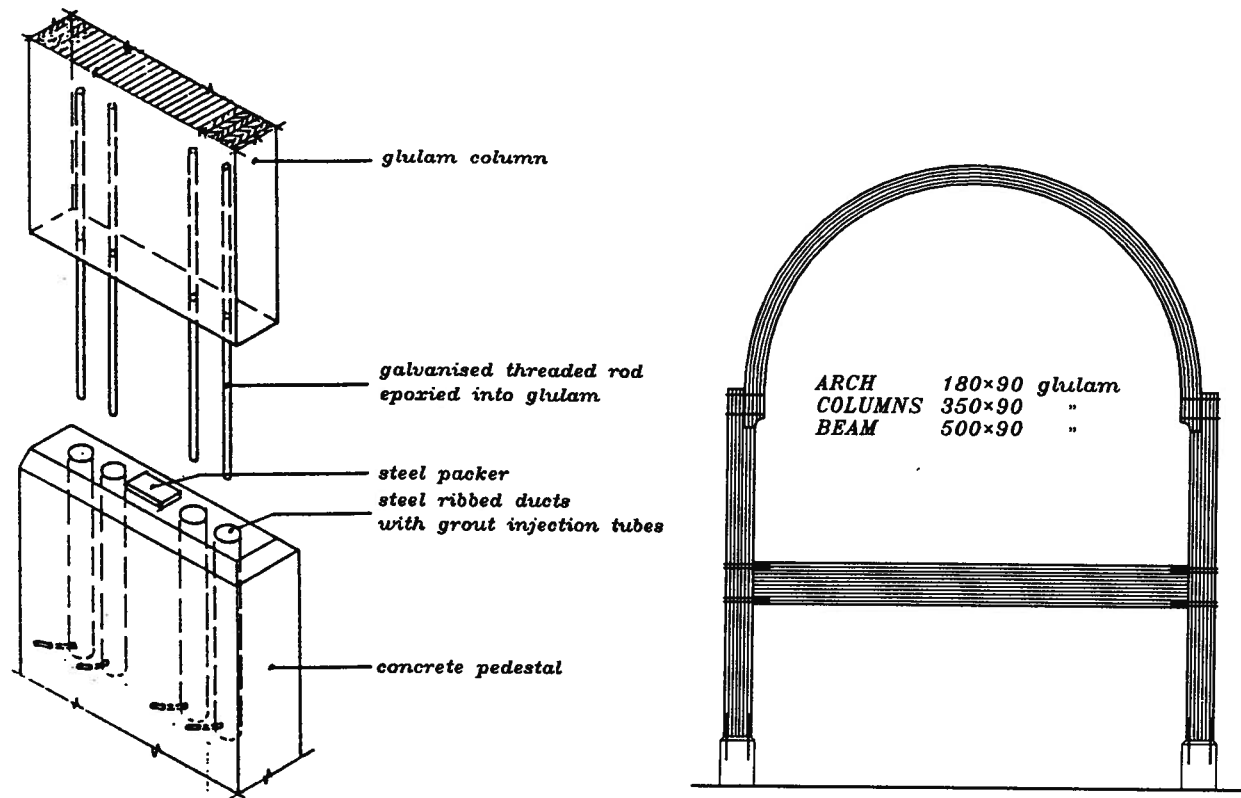


Fig.1.6 Portal frames at Jellie Park (Buchanan and Fletcher, 1989).

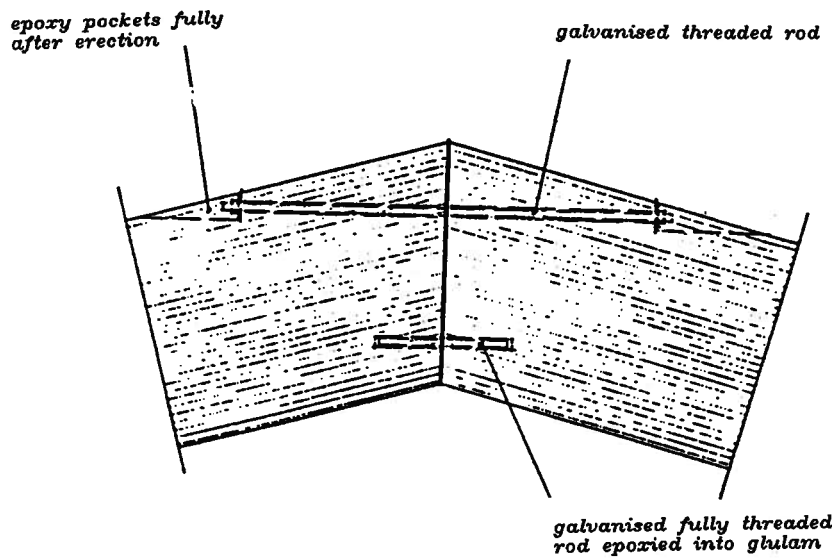


Fig.1.7 Portal apex connection (Buchanan and Fletcher, 1989).

Townsend (1990) carried out an extensive testing program on epoxy glued steel dowels using New Zealand materials. The tests considered loading in both tension and shear, different types of epoxy and various rod geometries. Townsend (1990) also reports on some full size beam splices that were tested in bending. High strength deformed bars glued parallel to the grain were used in that joint (see Fig.1.8). The splice connection performed very well and results showed they were generally stronger than the beams themselves.

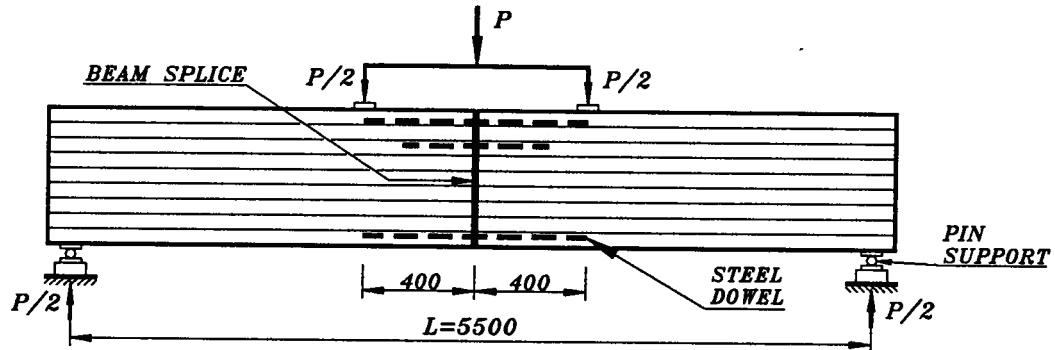


Fig.1.8 *Beam splice (Townsend, 1990).*

Several types of knee joints were tested by Buchanan and Townsend (1990). The most successful one, using a structural steel bracket is shown on Fig.1.9.

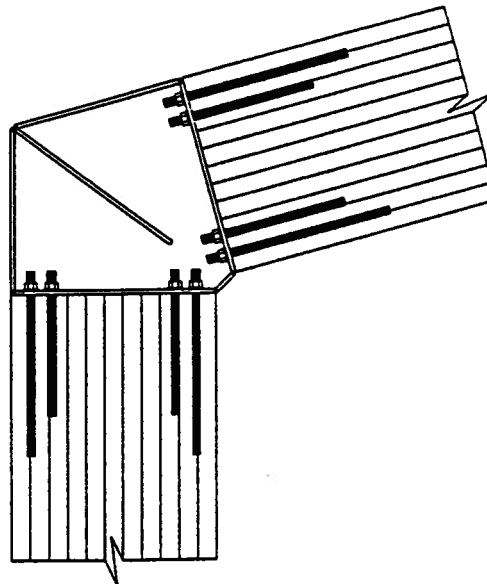


Fig.1.9 *Portal knee connection using structural bracket.*

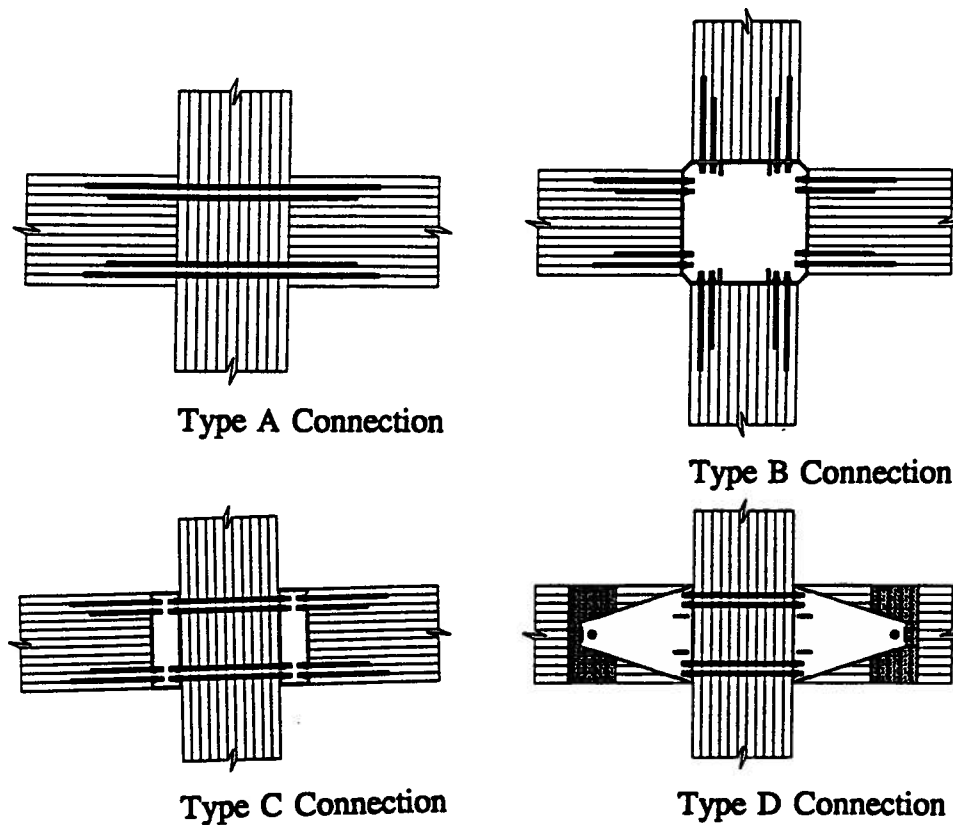


Fig.1.10 *Beam-column connections (Fairweather, 1992).*

Fairweather (1992) reports the tests of beam-column connection under quasi-static cyclic loading with a horizontal load applied at the top of the column. Four types of joints were tested (see Fig.1.10):

A- direct beam-column connection,

B- connection using inside steel bracket,

C- connection using steel brackets on each side of the continuous column,

D- connection between continuous column and twin continuous beams using steel side brackets nailed to the beams and bolted to the rods epoxied into the column.

Fairweather reports strong and stiff behaviour of those connections and excellent ductility.

Some problems with brittle fracture of the wood have been encountered.

1.2.3 Russian Research.

Connections using reinforcing bars glued into the glulam were introduced in Russia in mid 1970's (Turkovskij, 1991). The idea originated with a problem where the bearing stresses in the beam were too high. Instead of providing a larger bearing plate, a steel rod was glued perpendicularly to the grain close to the end of the beam so the concentrated load was distributed throughout the length of the rod (Fig.1.11). This detail was found to work very well.

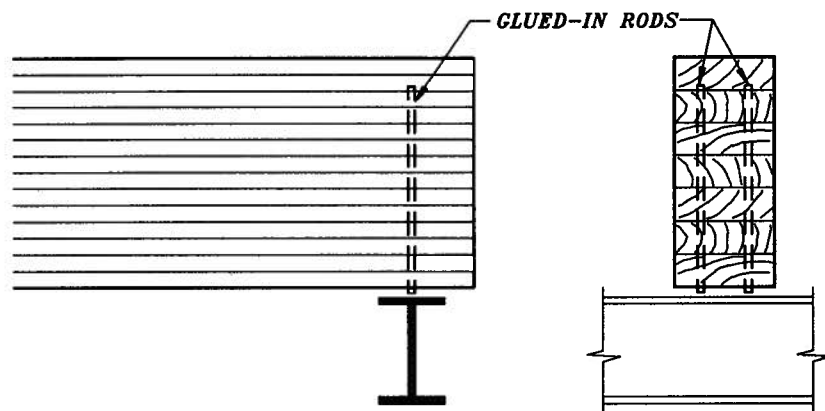


Fig.1.11 *Bearing connection using glued-in rods.*

The concept was then applied to increase shear capacity of the beams (Fig.1.12) and was later used as a repair method. The innovation here was to use the rods glued into the glulam at an angle of 45°.

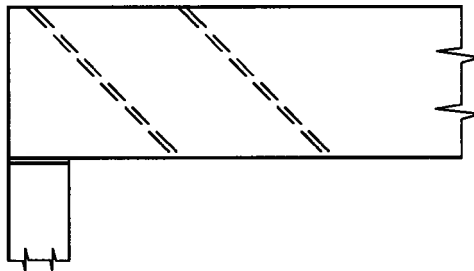


Fig.1.12 *Shear reinforcement of the glulam beam.*

Turkovskij (1991) also reports the use of similar technique to create moment resisting joints for glulam. The main difference with respect to the connections described in previous two sections is the use of inclined steel rods (the Russians use reinforcing bars). Commonly the angle of inclination is 30° . The other innovation is that the bars are glued separately into both members and then joined on site by an extra steel plate welded to the rebars. Fig.1.13 shows how this concept is applied to the moment resisting splice connection of the beam.

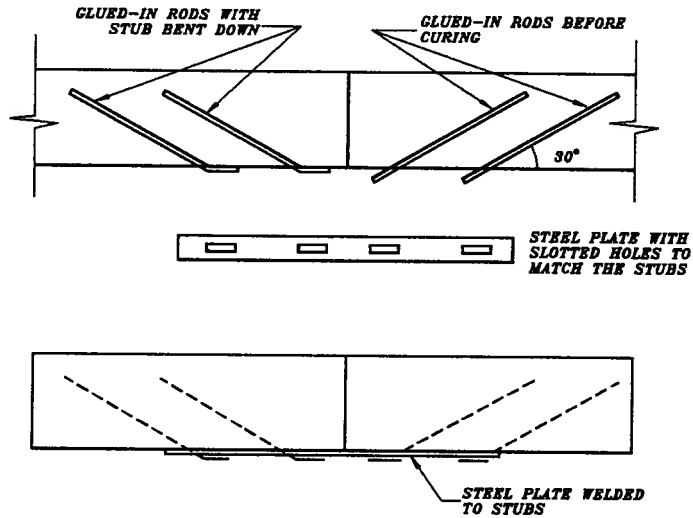


Fig.1.13 *Moment resisting splice connection of the glulam beam.*

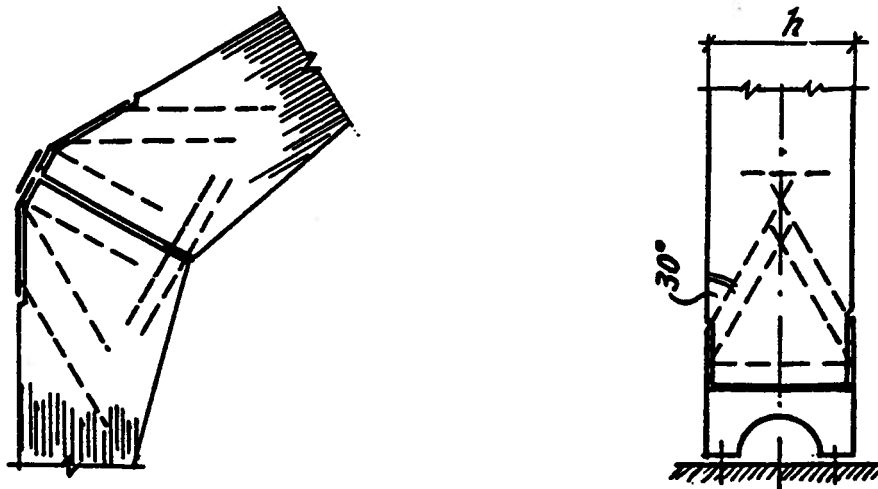


Fig.1.14 *Knee joint and column to foundation joint (Turkovskij, 1991).*

The rebars are glued with the stubs about 100mm sticking out of the beam. After the glue has cured these stubs are bent down to lay flat on the beam's edge. On the site a steel plate with slotted holes matching the position of the stubs is welded to the stubs. Some other examples of moment resisting joints which were tested and later implemented in practice are shown on Fig.1.14

A very interesting aspect of the glued-in rod methods is the forcing of the failure into the steel elements of the joint. After establishing the embedment length of the rebar required to yield it and exceeding this length in practice, the joints can be designed as the steel joints! In that way, the advantage of the small variability of the steel properties can be utilized in the glulam structures. It is especially important in an earthquake design where a highly predictable behaviour of the structure is desirable together with a high ductility level.

1.2.4 Canadian Research.

The idea of forcing the failure into the steel is followed in the research conducted at the University of British Columbia.

Malczyk (1993) reports series of pull-out tests conducted on the rebars glued at an angle to the grain (Fig.1.15). Three parameters were investigated: an angle of inclination of the rebar, the embedment length, and the rebar's diameter. Although the tests were similar to those conducted by the researchers described in previous section, some improvements in the connection method was made:

- welding close to the glulam surface was eliminated (so called "pre-welded" connection was developed),
- overall appearance of the connection was improved by welding the rebars to the bottom face of the steel plates,
- bolted connection was preferred instead of welding on the building site.

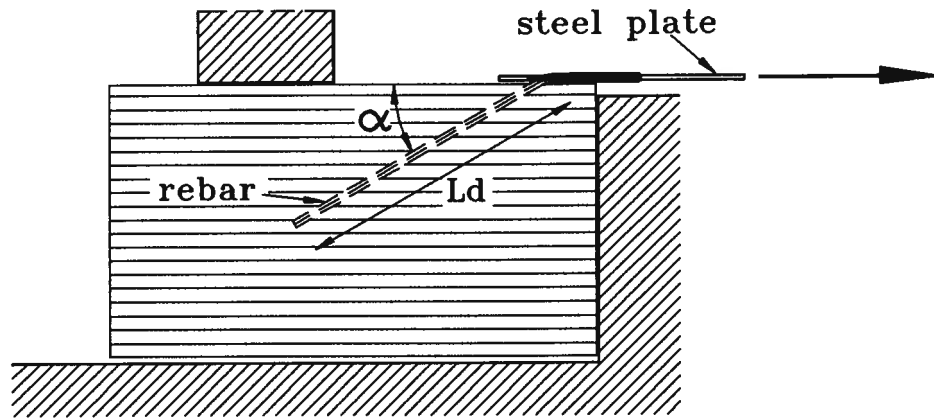


Fig.1.15 *Pull-out test (Malczyk, 1993).*

Some full scale tests were conducted (Malczyk, 1993) to verify the behaviour of the glued-in rebar connection in different joint configurations. The pre-welded technique and the rebars glued at 30° angle were consistently used in the following research.

First, a beam splice joint was tested (Fig.1.16). Then, a column to foundation joint was tested under lateral loading (Fig.1.17), and finally, some tests of the knee joint in the portal frame were conducted (Fig.1.18).

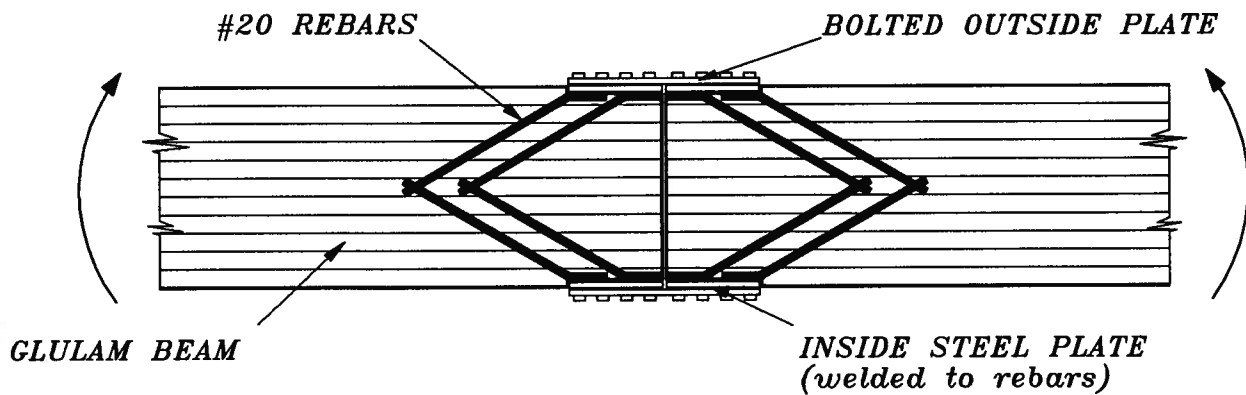


Fig.1.16 *Beam splice test (Malczyk, 1993).*

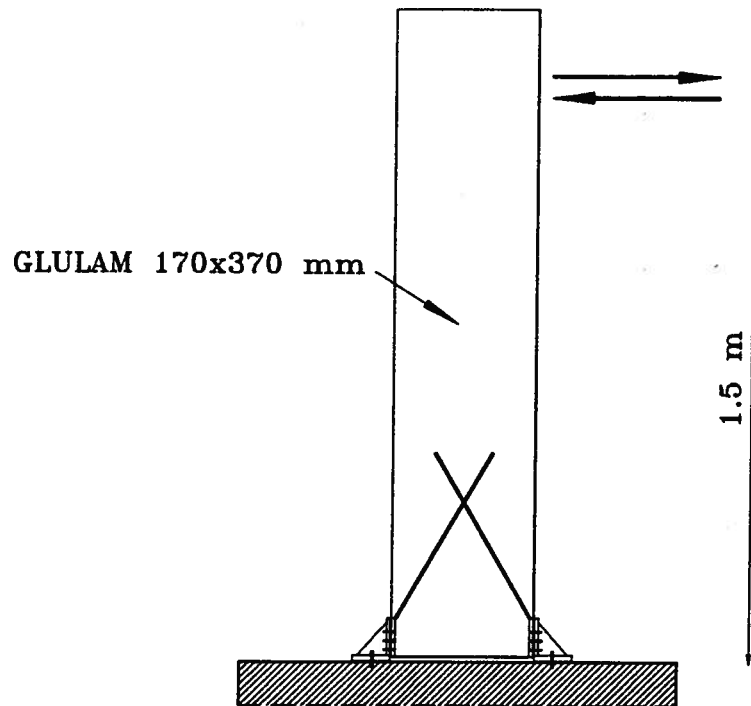


Fig.1.17 *Racking test of the glulam column (Malczyk, 1993).*

The foundation and knee joint tests were conducted under reversed loading conditions, i.e. positive and negative moments were created in the joint.

Steel failures were observed consistently. A steel-like ductile behaviour of the connections was reported. Some bearing problems under the plates were encountered, however, they were later solved by increasing the bearing area of the plates.

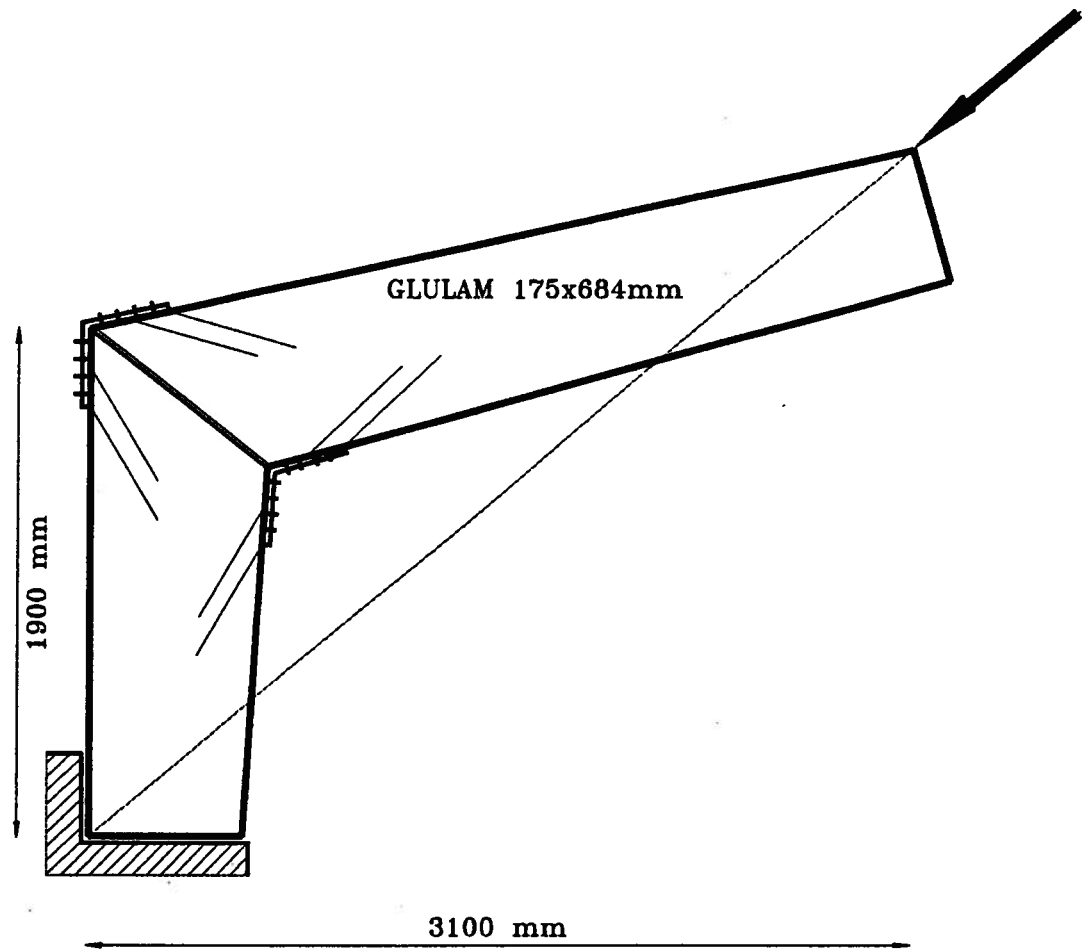


Fig.1.18 *Knee joint test (Malczyk, 1993).*

1.2.5 Summary.

1. The idea of gluing steel rods into the glulam has been used in several countries for a long time.
2. The bars glued at an angle to the grain engage significant portion of the glulam cross-section, whereas, the bars glued parallel to the grain behave more like skin connectors.
3. Inclined bars increase the shear capacity of the glulam cross-section.
4. If the embedment length of the bar is larger than the length required to yield the bar, the joints may be designed as the steel joints.

CHAPTER 2

MOISTURE CONTENT AND TEMPERATURE TESTS.

2.1 TEST OBJECTIVES.

The primary objectives of moisture content (M.C.) and temperature tests were to establish whether changes of the connection's environment would have a deteriorating influence on the strength and durability of the connection.

The glulam is highly sensitive to changes in the moisture content and the steel is sensitive to changes in the temperature. These two materials are combined in the joint and bonded by the epoxy glue, however, their thermal expansion coefficients as well as their thermal conductivity differ significantly. It is commonly known that the steel expands more than the glulam when both materials are exposed to the same increase of temperature. That, however, is true, but only in the direction parallel to the grain. The coefficient of thermal expansion for wood perpendicularly to the grain is roughly 4 times larger than the same coefficient for steel (see Table 2.1; note: the values for wood depend on M.C. and density; they are quoted below for oven-dry wood of density $\rho=500 \text{ kg/m}^3$).

Thermal property	steel	wood parallel	wood perpendicular
expansion coefficient [$\times 10^{-6}$ per K]	11	4	40
conductivity [W/mK]	58	0.30	0.16

Table 2.1 *Selected thermal properties of steel and wood.*

The thermal conductivity of each material plays an important role as well. It can be seen from the Table 2.1 that the conductivity of the steel is approximately 200 times larger than the conductivity of the glulam parallel to the grain, and almost 400 times larger than the conductivity of the glulam perpendicular to the grain. That means, the same amount of heat energy will flow through a material of one unit area and one unit thickness 400 times faster in the case of the steel rebar than in the case of the glulam block in the direction perpendicular to the grain.

The differences in thermal properties of the materials used in the glued-in rebar connection create internal stresses within both materials when the outside temperature changes. The magnitude of those stresses depends on the change in temperature, time, and the joint's configuration. A particular example of this phenomenon (for tested specimens) is discussed in section 2.4.2. Here, a more general illustration will be presented.

Let us consider the case of a joint (a rebar glued parallel to the grain) located under the roof of an industrial hall. Further let us assume that the temperature at that location can reach +40°C during the sunny winter day and rapidly drop below 0°C at night. The rebar will shrink faster and will shrink more than the glulam part of the joint. The steel will develop tension stresses while the glulam will be in compression. Eventually, after several hours, an equilibrium will be reached. The process will be reversed by the increasing temperature during the day. The situation may repeat over several days. At the end a heavy snowfall may occur creating additional stresses. *Will the connection, under these extreme conditions, behave as well as the one which was not subjected to the temperature changes at all? Will the bond, provided by epoxy, be reliable despite the relatively high temperature?*

In another situation the glulam may expand due to the high humidity of the surrounding air while the rebar is not affected by this factor. The result is similar: internal stresses are created in both materials and the process is time dependant. Thus, the question may be restated - *can the connection still be relied upon after many changes in the glulam's moisture content?*

Tests conducted at UBC from May to December 1993 were designed to clarify the above questions. Unfortunately, to answer them fully, much more time would be necessary - specially for M.C. tests. In a real structure, it takes months for moisture to penetrate the glulam element and even more time to dry it out. Additionally, this process repeats many times during the life

span of the structure. To get the answers quicker, a reasonable reduction of size of the tested specimens was desirable. The number of cycles had to be limited, due to time constraints, as well. Yet, the tests should give the results which could be extrapolated on the real structures. To compensate for the reduction of size and number of cycles the severity of the changes was made greater than what is normally found in a structure. The process of developing a suitable test specimen is discussed in the next section.

2.2 DEVELOPMENT OF A TEST SPECIMEN.

It was necessary to develop a test specimen because it wasn't practical to test a full size connection. A control sample, consisting of 6 test specimens, was chosen to give a better picture of the variability of the test results. This sample was tested before the other samples (i.e. M.C. sample and temperature sample). The control specimens were tested in a constant temperature of +20°C and their moisture contents were measured to be 11%.

The test specimens had to meet some functional requirements to allow for the future extrapolation of the results to the real structures. The requirements were as follows:

- the control specimens should be loaded identically to the M.C. and temperature specimens, but the loading conditions didn't need to reflect the real structure (although they need to be realistic);
- a tension test should be performed to comply with the idea of forcing the failure into the steel (described in chapter 1);
- the most disadvantageous orientation of the rebar with respect to the glulam fibres should be chosen, but excessive stress concentrations should be avoided;
- the specimens should have realistic dimensions - as close to the real structures as practical;
- the specimens should be small enough to allow reasonably quick moisture penetration and heat transfer;
- the manufacturing of the specimens should be as simple as possible;
- the specimens should be easy to handle during the treatment (wetting, drying, heating, etc.) as well as during the strength testing;

Unfortunately, some of above requirements were in conflict. A judgement of the priorities was made and it was decided that the length (dimension parallel to the grain) of the specimens should be reduced, but the other dimensions, as well as the size of a rebar, should be kept realistic. The moisture penetrates the glulam faster in the direction of the fibres than across the fibres. Thus, the time necessary for this process can be reduced by making the specimens shorter than in the real structure. The length of the specimen was chosen to be 250mm (see a sketch on Fig. 2.1). The rebar was glued perpendicularly to the grain, so the weakest direction of glulam was tested.

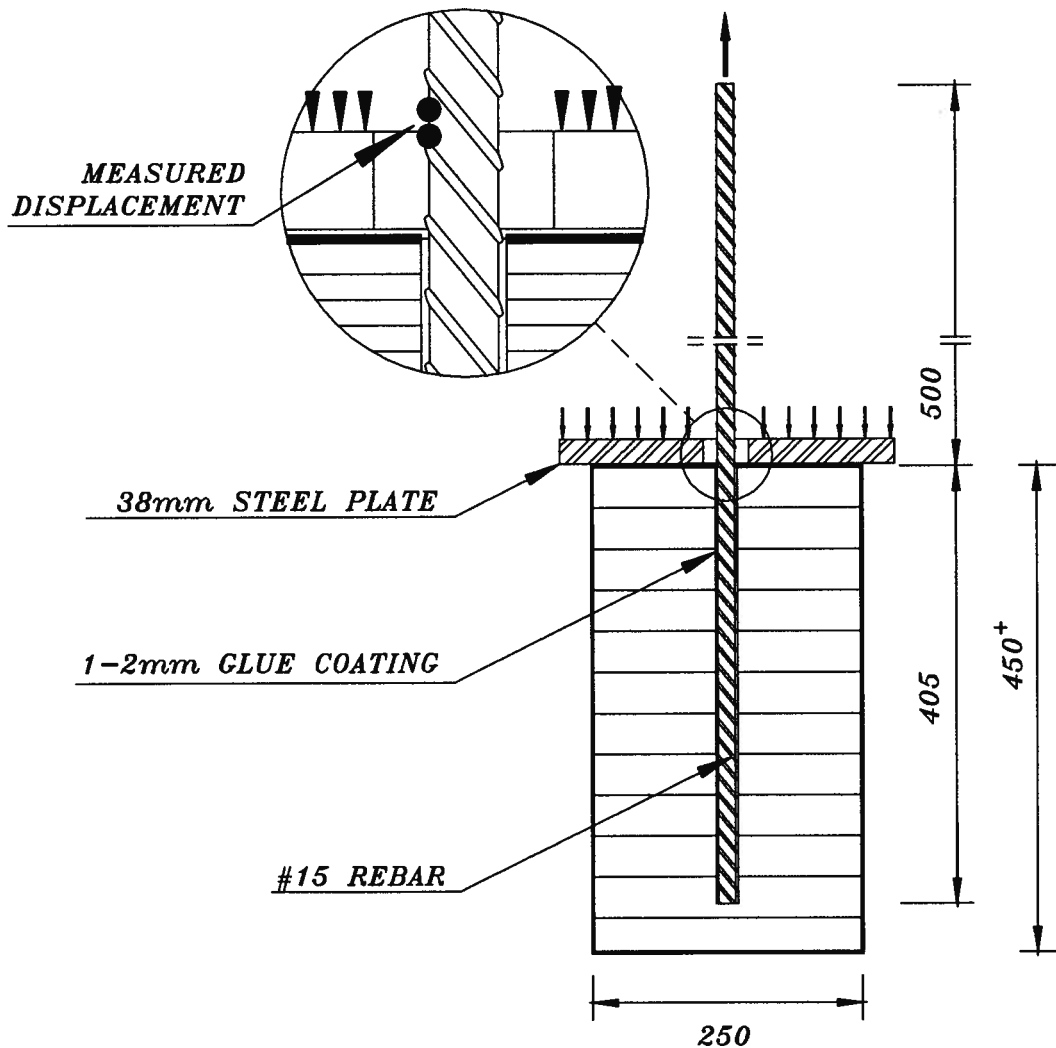


Fig.2.1 Specimen used for M.C. and temperature tests.

2.2.1 Materials.

GLULAM.

Material used for all the tests described in this chapter was Douglas Fir glulam 24f manufactured by Structurlam Ltd. in Penticton, B.C. The dimensions of the glulam block were as follows:

thickness - 175mm;

length - 250mm;

height - varied because the blocks were prepared from glulam beams of different sizes
- minimum was 450mm.

A 19mm ($\frac{3}{4}$ ") hole was drilled in the center of the block which is 3mm larger than the rod diameter. The depth of the hole was 405mm.

REBAR.

Deformed weldable reinforcing bars (rebars) of grade 400 (yield stress = 400MPa) were used. All tests were conducted with #15 rebars. Their nominal diameter was 16mm and nominal area 200mm². The nominal dimensions are equivalent to those of a plain round bar having the same mass per meter as the deformed bar. Table 2.2 summarizes the results of tension tests of these rebars and Fig. 2.2 shows typical load deformation curve obtained during the tests.

#	yield			E elastic [MPa]	ultimate		
	load [kN]	stress [MPa]	strain		load [kN]	stress [MPa]	strain
1	88.6	443	0.0024	184600	129.3	647	0.117
2	89.5	448	0.0023	194800	133.2	666	0.148
3	89.0	445	0.0024	185400	129.9	650	0.188
4	89.4	447	0.0023	194300	130.2	651	0.129
Average	89.1	446	0.0024	189800	130.7	654	n/a

Table 2.2 Results of tension tests performed on #15 rebars.

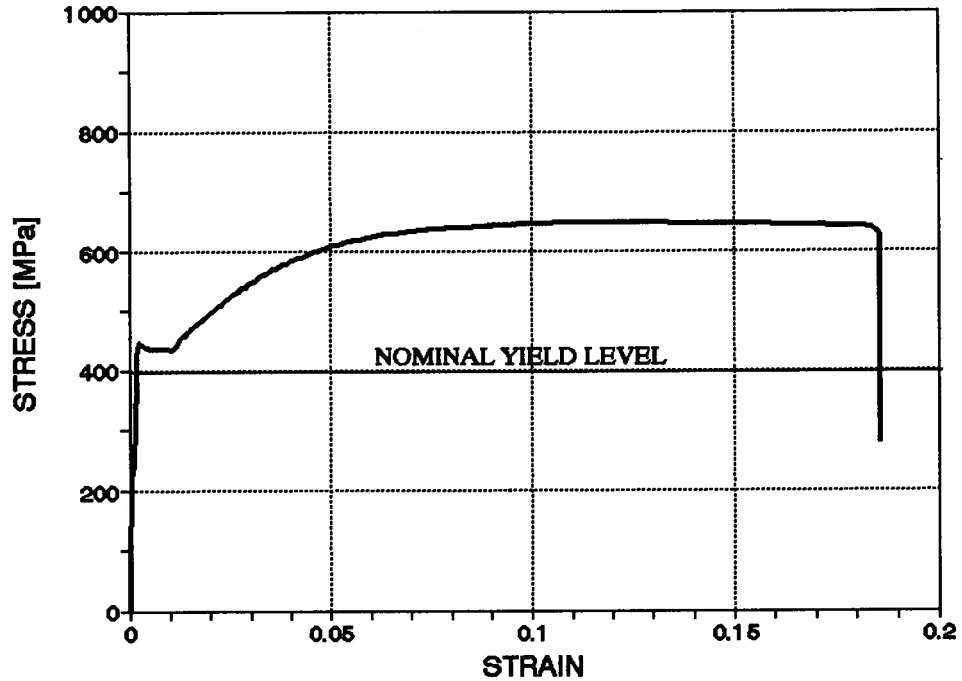


Fig.2.2 *Typical load-deformation curve obtained from the rebar tension test.*

The total length of the rebar was 905mm. It was embedded in the glulam block for a distance of 405mm while protruding 500mm (see Fig. 2.1).

GLUE.

The epoxy glue "IFC-SP" was used for the connections. It is manufactured by Industrial Formulators of Canada Ltd., Burnaby, B.C. It consists of two parts: resin and hardener. The mixing ratio is 100 to 42 (by weight) respectively.

The glue was poured into the hole just before the rebar was inserted. By inserting the rebar slowly, the glue was pushed up, and in this way, the creation of air pockets was avoided. The air pockets, as described in chapter 1, did cause a lot of problems for previous researchers because the hole was drilled horizontally.

An average of 65cm³ of glue per hole was used (+/- 5%). The pot life of the glue

varied from 1 to 3 hours depending on the outside temperature and the volume of the glue used. The glued specimens were cured at least 7 days before testing in order to reach the full strength of the glue.

2.2.2 Test Setup and Test Procedures.

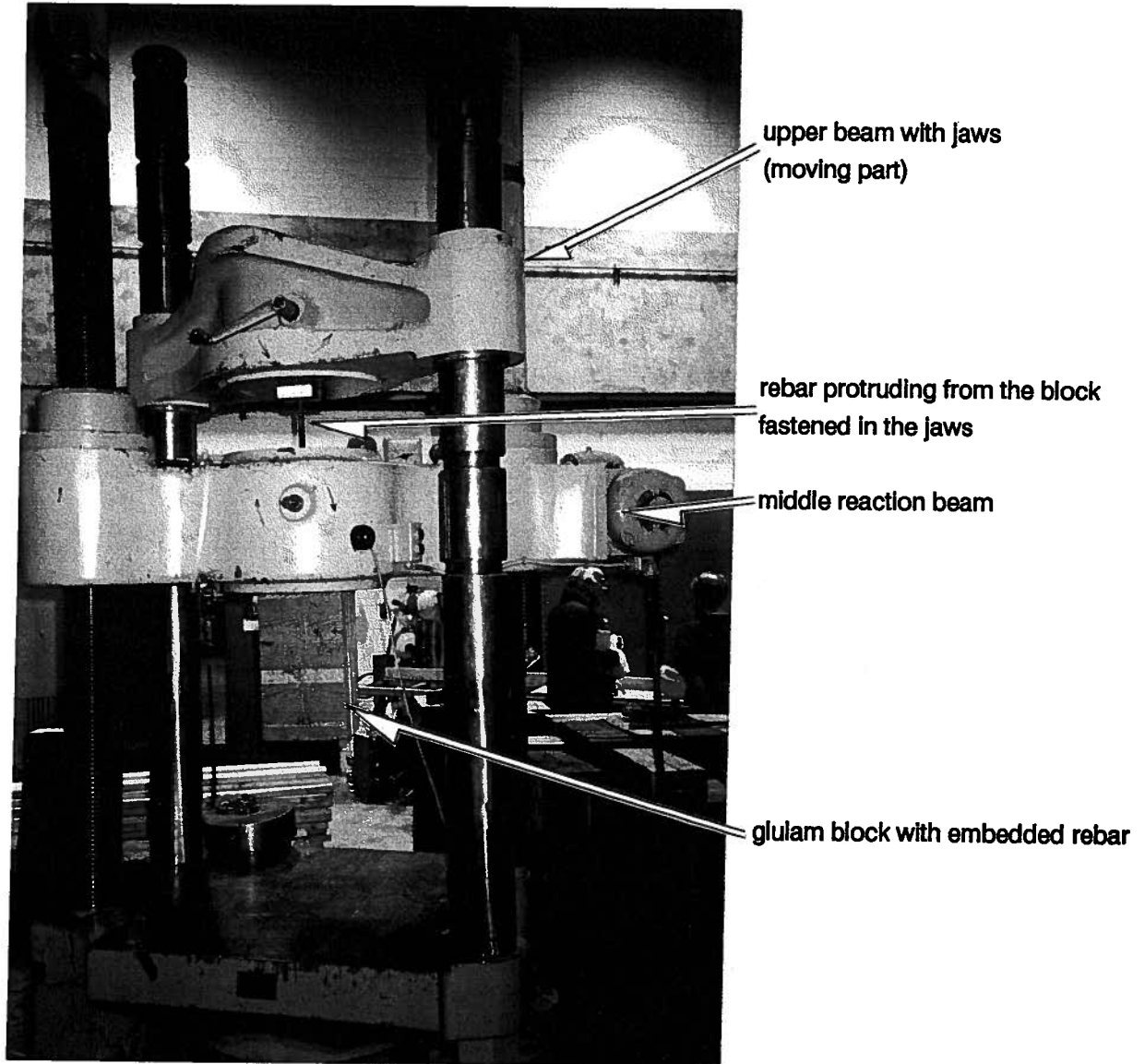


Fig.2.3 Specimen during the test in the tension apparatus.

A Baldwin tension apparatus was available in the Structures Laboratory of UBC Civil Engineering Department. This machine has 3 different ranges of loading:

low	0 - 71kN	(16000lb),
medium	0 - 356kN	(80000lb),
high	0 - 1779kN	(400000lb).

The apparatus was set for medium range and used to perform all tests.

The protruding end of the rebar was fastened in upper jaws of the apparatus while the top surface of glulam was supported (via 38mm thick steel plate with a hole for the rebar) by the middle reaction beam of the apparatus. The applied load created tension in the rebar and compression in the glulam block. The specimen set for testing in the apparatus is shown on Fig. 2.3. This setup was chosen for its simplicity and it was not intended to reflect any particular situation in the real life structures.

It was decided to measure the displacement of a point located on the rebar's surface, as close to the glue line as possible (see Fig.2.1), relative to the top surface of the glulam (or plate). This displacement consisted of the elongation of the embedded part of the rebar plus the deformation of the wood fibres at the perimeter of the glue coating.

The body of the displacement gauge (LVDT) was fixed to the steel plate while its moving tip was resting on a stud glued to the rebar at the measuring point. The load applied to the rebar was measured by the load cell of the apparatus. Both measurements, i.e. load and displacement were recorded by the data acquisition system every second.

The test was considered to be finished when:

- the rebar broke, or
- a significant drop of the load was observed (accompanied by increase of the displacement).

The testing procedure took approximately 10 minutes.

elongation of the rebar (over 20mm), at almost constant load (final yield plateau), leads to the failure of the rebar. The failure is preceded by necking.

This kind of the load-deformation relationship was observed in all the control specimen tests. The results are summarized in Table 2.3.

Specimen	Ultimate force [kN]	Ultimate stress		Ductility ratio	Failure mode
		glulam [MPa]	rebar [MPa]		
H1	126.9	2.90	635	13	rebar yielding
H2	129.3	2.97	647	15	rebar yielding
H3	130.2	2.98	651	13	rebar yielding
H4	127.1	2.92	636	14	rebar yielding
H5	128.9	2.93	645	17	rebar yielding
I1	130.2	2.98	651	17	rebar yielding
Average	128.8	2.95	645	15	n/a

Table 2.3 Results of the control sample testing.

The results of all 6 tests are highly consistent. The ultimate force varied among the specimens slightly (+/_ 2.6%) and yielding failure occurred in the rebar during each test. The total elongation of the rebar varied more than the force (from 14mm to 24mm). The plastic deformations were fairly large and resulted in the average ductility ratio (total elongation/elastic elongation) of 13. This level of ductility for the connection can be considered as very desirable (for example, the bolted connections in timber have ductility ratio of 2 to 6).

2.2.4 Discussion of Failure Mode I - Rebar Yielding.

The dimensions of the control specimen (glulam block, glue area, rebar's size, and embedment length) were intentionally chosen to force failure in the steel as this will also be the case in the real connection. However, after the treatment of the M.C. and temperature samples, other failure modes could be expected (pull-out, for example). It was important to recognize the mechanism of failure in the control sample. The performance of the bond between the glue, steel, and the glulam was essential to understand the process. After the temperature treatment the bond between glue and steel could have been affected.

After the M.C. treatment the glue-wood bond could have lost its strength. Therefore all the imperfections of the bond in the control sample had to be detected to form the basis for later comparisons with the specimens in other samples.

After the test the blocks were split open so the interfaces between the materials could be examined. The idealized picture of the connection after the failure is shown on Fig.2.5.

Yielding failure in the rebar was named Failure Mode I.

Fig.2.5 *Failure Mode I - rebar yielding.*

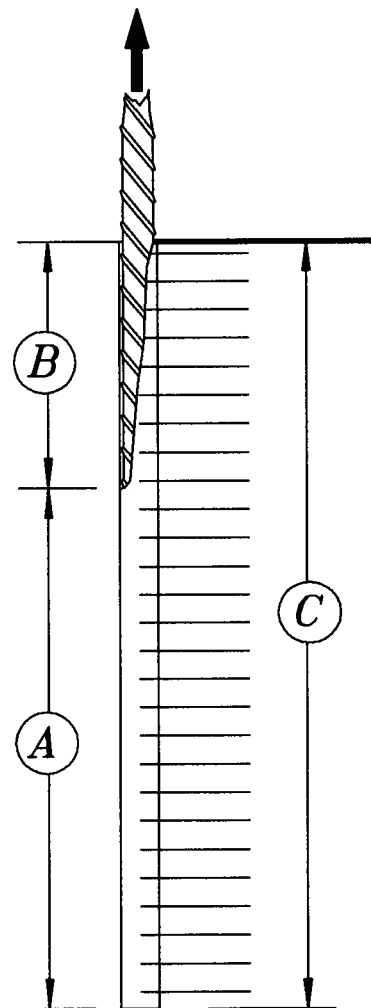
STEEL-GLUE BOND:

(A) sound,

(B) damaged;

WOOD-GLUE BOND:

(C) uninterrupted, straight wood fibres.



The top part of steel-glue bond (*B*) was damaged - probably due to large deformations in the rebar at the very end of the test when high loads were experienced. The length of this part varied from 1/10 to 1/3 of the total embedment length. The rest of the bond was not affected (*A*). Also the bond between the glue and the wood fibres was not affected during the test (*C*). This picture indicates that part *A* provided the effective embedment length for the connection. This was a very important observation.

2.2.5 Instrumented Rebar Tests.

To establish the stress distribution along the rebar two instrumented rebar tests were conducted. Five strain gauges were placed on one side of the rebar. Because of the axial tension loading of the specimen, the strain was predicted to be uniform across the cross-section of the rebar. The readings from the strain gauges were recorded during the test by the data acquisition system. The usual measurements of the loads and the displacements were recorded as well. The location of the gauges and the stress distribution along the rebar at an external force of 80 kN (400 MPa) is shown on Fig.2.6.

Unfortunately, the stress distribution close to the edge of the glue line (top part) remains uncertain. However, the damage of the glue-steel bond described in the previous section indicates a stress concentration (marked as a dashed line) in that region. When the load was increased beyond 80 kN, the overstressed region propagated deeper into the specimen which resulted in the breaking of the gauge closest to the top. That happened because of a large deformation in the rebar exceeding the range of the gauge. Before the load reached its ultimate value, 3 out of 5 gauges were broken. The readings of the gauges at 6 different levels of the external force (5 kN, 40 kN, 80 kN, 86 kN, 130 kN) are shown on Fig.2.7.

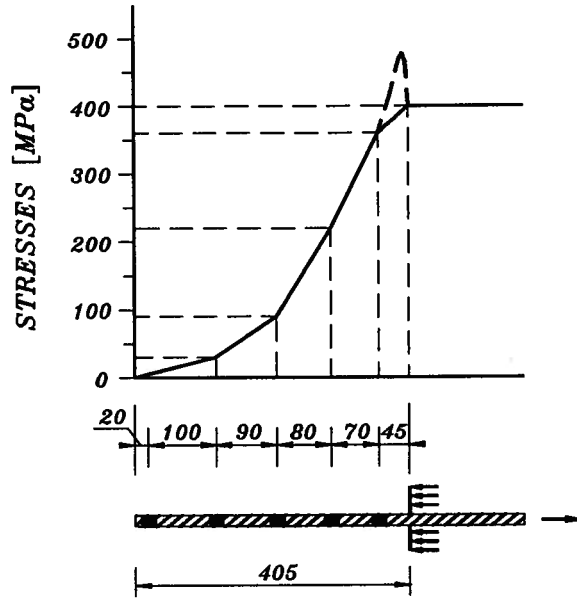


Fig.2.6 Stress distribution along the rebar.

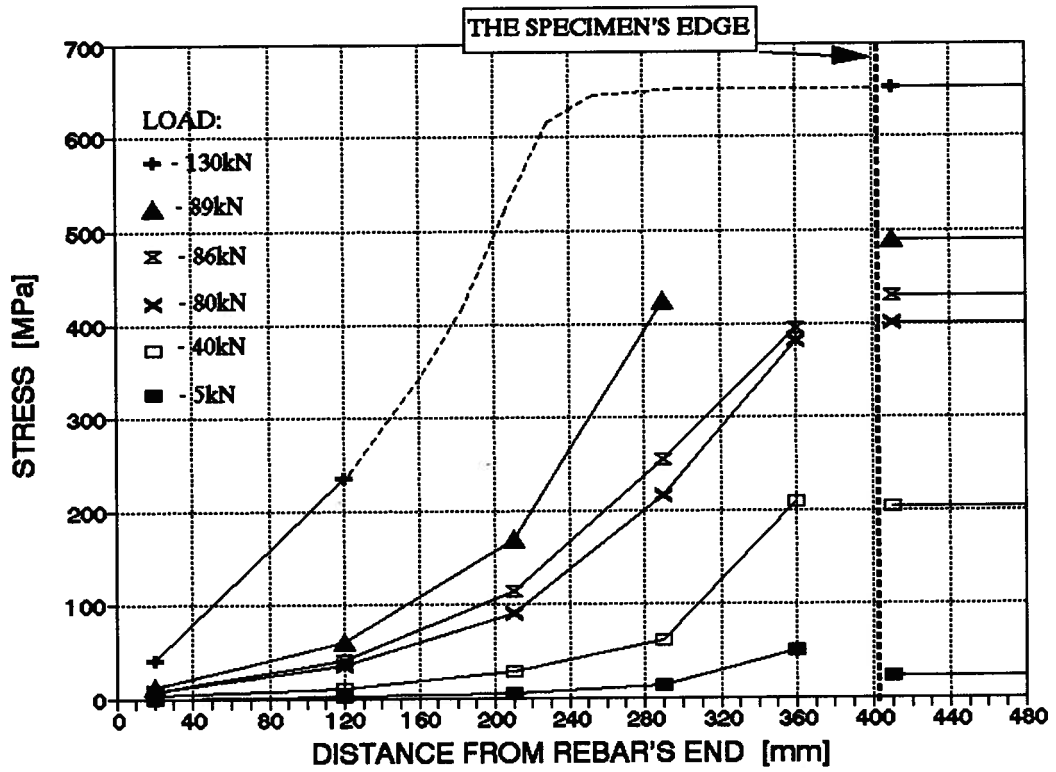


Fig.2.7 Stress distribution at different load levels.

On the graph above the heavy dotted vertical line represents the edge of the specimen. The lines shown on the right side of the dotted line represent the stress in the protruding part of the rebar at different load levels. These stresses are calculated as load/rebar's area. The curves on the left side of the dotted line represent the stress in the glued part of the rebar. These stresses are calculated according to Hooke's law (strain x modulus of elasticity). The actual yielding plateau for this specimen started at 430 MPa so there are 4 curves in the elastic region (at 5 kN, 40 kN, 80 kN, and 86 kN load levels). The 89 kN level represents the beginning of the strain hardening phase. The ultimate level is 130 kN.

About 85-90% of the total load is transferred from the rebar to the glue (and later to the glulam) within half the embedment length (i.e. within first 200mm counting from the top face of the glulam). The point located 120mm from the bottom of the rebar (second from left) experienced only 50 MPa at the 89 kN load, which is only 12% of the stress in the protruding part of the rebar. The increase of the stress at that point was observed after the large elongations occurred, i.e. far beyond the design load for the connection. The stress at the very bottom of the rebar remained small even at the ultimate load showing that extra safety is available.

2.3 MOISTURE CONTENT TESTS.

In this section, the influence of the changes in moisture content in the glulam member on the behaviour of the connection is described.

2.3.1 Parameters Investigated.

2.3.1.1 Moisture content range.

The moisture content of the glulam block was varied between 10% and 30%. The M.C. was measured in two ways:

- a) by weight (all specimens),

b) with M.C. meter (additionally in the selected specimens).

The two measurements in the selected specimens were found to be highly correlated during the whole treatment because moisture could easily enter the wood through the end grain. Usually, the average M.C. (measured by weight) was higher than local (measured with the meter) when the specimen was dry. The reverse happened when the specimen was wet. The changes in M.C. of one specimen during the treatment are shown on Fig.2.8.

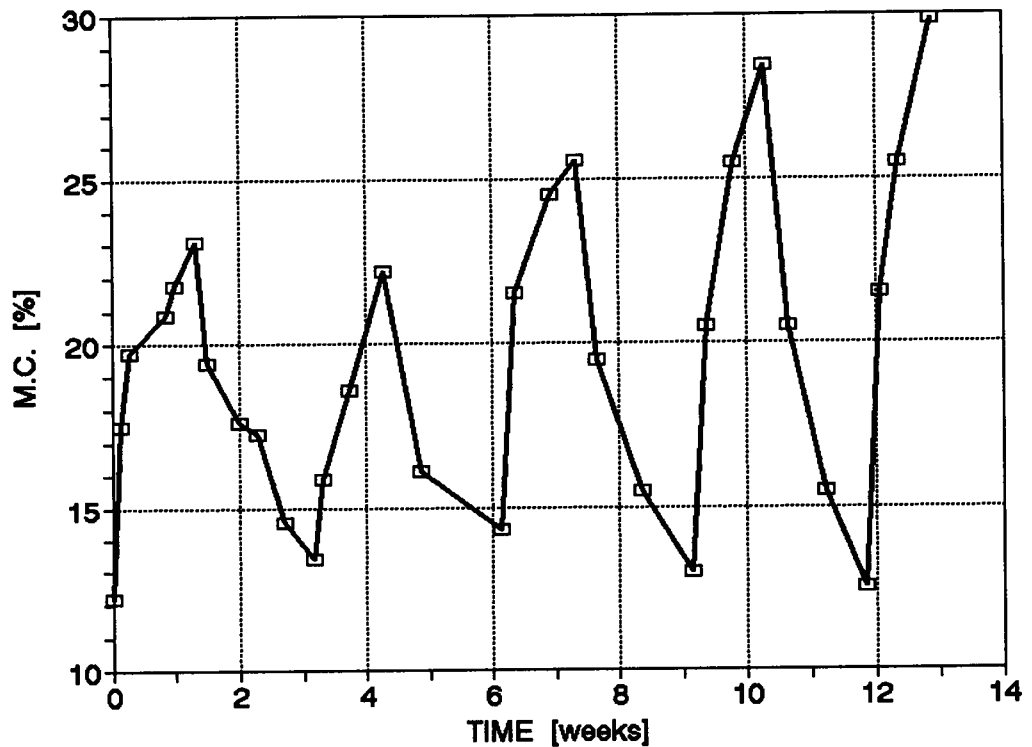


Fig.2.8 Example of the moisture content changes.

The wetting part of the cycle took place in the moist room of Material Laboratory. The specimens were sprinkled with water twice a day and covered with a plastic tarpaulin to maintain high humidity in the vicinity of the specimen. The relative humidity of the room was about 90% which was not sufficient for these tests. Immersion of the specimens in water, although more effective, were not considered to be realistic and didn't take place. The fastest increase of M.C. was observed in first two days of wetting. Usually,

the final M.C. of the specimen in the wetting part increased slightly with the number of cycles.

Under the conditions described above the wetting phase of the treatment lasted from 7 to 9 days.

The drying of the specimens was performed in a plywood tunnel (shown on Fig. 2.9) built in the basement of the Structures Laboratory. The specimens were placed in

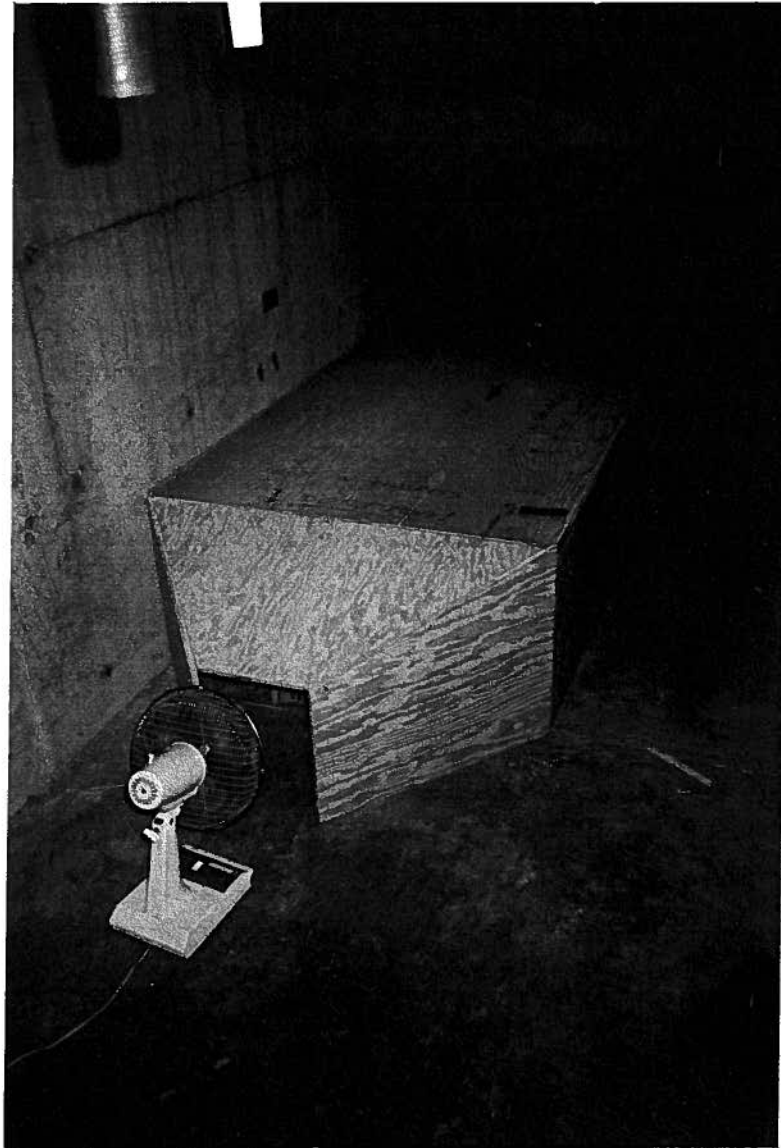


Fig.2.9 Drying of the specimens.

the tunnel in two layers. Each layer and each specimen were separated to allow proper ventilation. To accelerate the drying a fan was installed at the inlet. Heating of the air (and the specimens) was avoided. The weighting of the specimens (to calculate M.C.) took place every 4-5 days. After the measurements the location of the specimens in the tunnel was changed - the top layer became the bottom one and the specimens placed on the left side were moved to the right side of the tunnel. In that manner more uniform drying conditions were achieved. The drying phase of the cycle lasted from 22 to 12 days. The rate of the drying increased slightly with the number of cycles.

Because of the accelerated drying process the cracks formed on the surface of the specimens. Most of them appeared during the first drying cycle and continued to expand throughout the additional cycles. The increase in the drying (or wetting) rate can be explained by increased access area for the moisture.

2.3.1.2 Number of cycles.

Each cycle consisted of one wetting phase and one drying phase. A full cycle lasted around 3 weeks. Five cycles were conducted. However, some specimens were tested before completion of the full treatment so the number of cycles a particular specimen experienced varied from 1 to 5. In this way the correlation between the number of cycles and the change in the ultimate strength could be detected.

2.3.1.3 Testing condition.

The tests were performed on wet specimens as well as on dry specimens. Five specimens were tested after one of their wetting phases was completed. The M.C. of those specimens during the test varied from 28% to 30% (specimens tested wet). Twelve other specimens were tested after the drying phase was completed. Their M.C. varied from 11% to 13% (specimens tested dry).

2.3.1.4 Angle to the grain.

Out of the total number of 17 specimens, 5 specimens were prepared with rebars glued in an angle of 30° to the grain (30° sample). In the remaining specimens the rebars were glued perpendicularly to the grain. Both arrangements of the rebars can be used in the real structures. Generally gluing perpendicularly to the grain is considered to be more critical. The 30° sample was tested to detect possible differences.

2.3.2 Discussion of Typical Load-Deformation Curves.

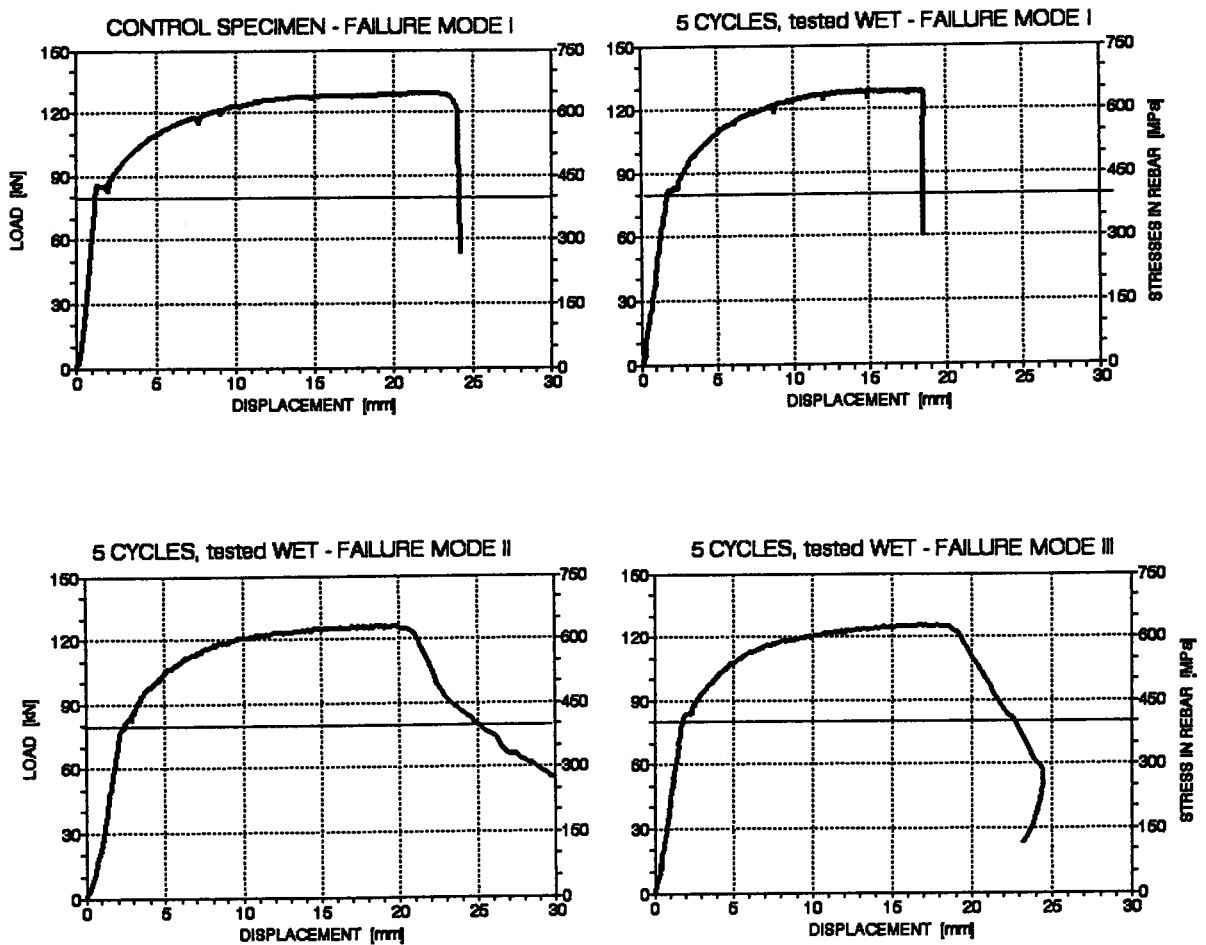


Fig.2.10 Load-deformation curves for the specimens after M.C. treatment and a control specimen.

Generally speaking, the load-deformation curves obtained from the tests after M.C. treatment were similar to those from the control sample. The only differences were observed in the specimens tested wet during the final stage of the tests (i.e. when large plastic deformations in the rebar occurred). Two more failure modes were observed: Failure Mode II - pull-out, and Failure Mode III - wood split. These will be explained in the following sections. The comparison of load-deformation curves obtained after M.C. treatment versus the control curve is presented on Fig.2.10.

All the curves have the same characteristics as that discussed in section 2.2.3 except the final stage (failure). The ranges of the elastic and plastic parts of the curves are identical to the control curves. However, a drop of stiffness within the elastic range (15%-20%) can be observed. This last observation is valid for all M.C. treated specimens regardless of test condition or angle to the grain. The ultimate loads oscillate around 130 kN. The ductility levels are also similar to those observed in the control sample (11-18).

The differences in the curves begin after the ultimate load has been reached. For Mode II as well as for Mode III the drop in the load is not as sudden as for Mode I. This is because some resistance still exists in those specimens - friction in Mode II and shear in Mode III.

The similar shapes, location of characteristic points (first yielding plateau, ultimate load), and magnitudes of load and deformation can lead to the conclusion that the behaviour of the described specimens is almost identical to the control specimens and would not affect the design range.

2.3.3 Discussion of Failure Mode II - Pull-out.

The pull-out failures were observed in 3 tests out of 17. They took place at the same level of stresses and deformations as Mode I which indicates similar mechanism of failure.

Because of the large deformations in the rebar the damage of steel-glue bond propagated deeper into the specimen (zone *B* on Fig.2.11). In effect, the remaining length (*A*)

dropped below the necessary embedment length and the rebar started to come out of the glulam pulling the bonded wood fibres up (E). The fibres located above moved as well (D). Top fibres remained bonded to the glue coating (C) because the rebar was free to move in that zone due to the failure of steel-g glue bond.

STEEL-GLUE BOND:

- (A) sound,
- (B) damaged;

WOOD-GLUE BOND:

- (C) uninterrupted, straight wood fibres,
- (D) uninterrupted, curved wood fibres,
- (E) interrupted, curved wood fibres (shear failure).

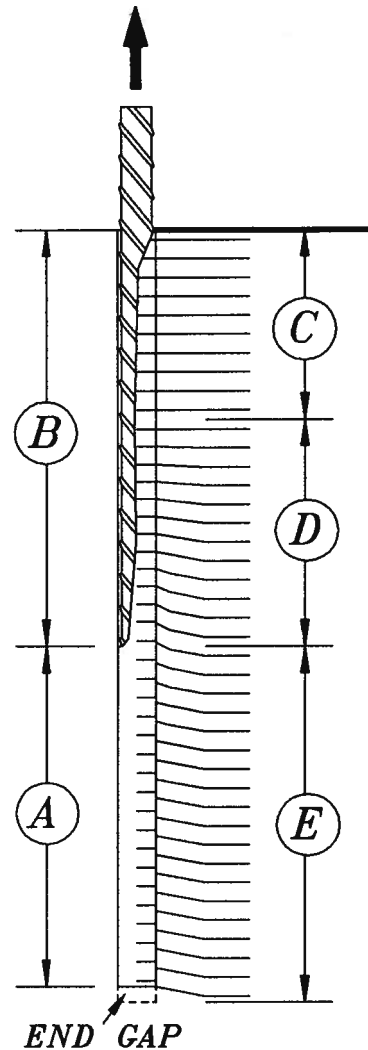


Fig.2.11 Failure Mode II - pull-out.

Some friction resistance was still present after the failure. In the lower part (A) the friction occurred on the wood-g glue line. In the upper part (B) the friction between glue and the rebar took place.

2.3.4 Discussion of Failure Mode III - Wood Split.

Glulam failure occurred during 2 (out of 17) tests. This Failure Mode was observed exclusively in the specimens tested wet.

STEEL-GLUE BOND:
 (A) sound,
 (B) damaged;

WOOD-GLUE BOND:
 (C) uninterrupted, straight wood fibres,
 (D) uninterrupted, curved wood fibres.

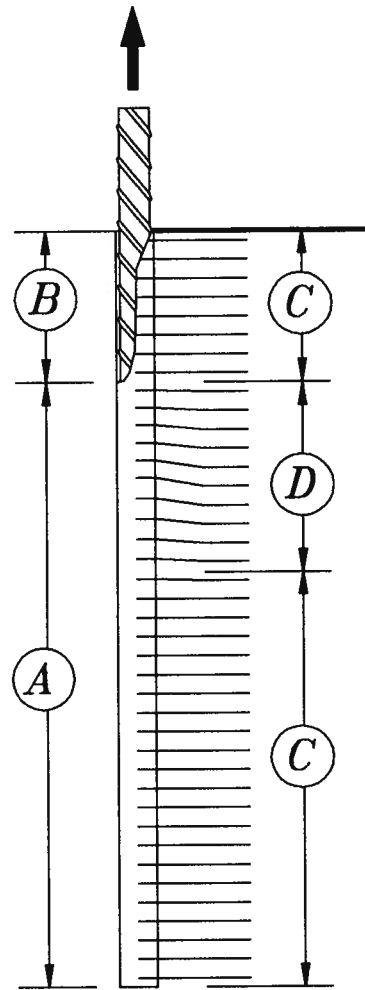


Fig.2.12 Failure Mode III - glulam split.

The damaged part of steel-glue bond (B) was very short and only a small movement of neighboring fibres was observed (see Fig.2.12). Probably the local variation of the glulam properties combined with high moisture content (30%) are responsible for this kind of failure.

The splitting of the glulam block originated in the middle of the specimen (close to the rebar's end) and propagated up along the glue line. However, the crack did not reach the top surface of the block but deflected sideways. This indicates that the top part of rebar (B) was free to move at that moment.



Fig.2.13 Photo of the specimens K2 (Failure Mode II) and K1 (Failure Mode III). Note that the top surface of the specimen K1 is not split.

2.3.5 Deformation Range.

After the failure some specimens were bisected along the grain to expose the interior of the glulam and the glue coating. In the case of pull-out failure the deformations of the wood fibres due to the movement of the rebar were observed. The distance where those deformations could be seen (with an unaided eye) varied significantly depending on the direction to the grain (see Fig.2.14).

In the parallel direction the fibres were curved within 50-60mm from the glue coating (60-70mm from the center of the rebar). In the perpendicular direction, a couple millimeters

away from the coating any deformation of the wood fibres could not be detected. This can be a good indication for future spacing rules in multi-bar connections. The spacing along the grain has to be much larger than across.

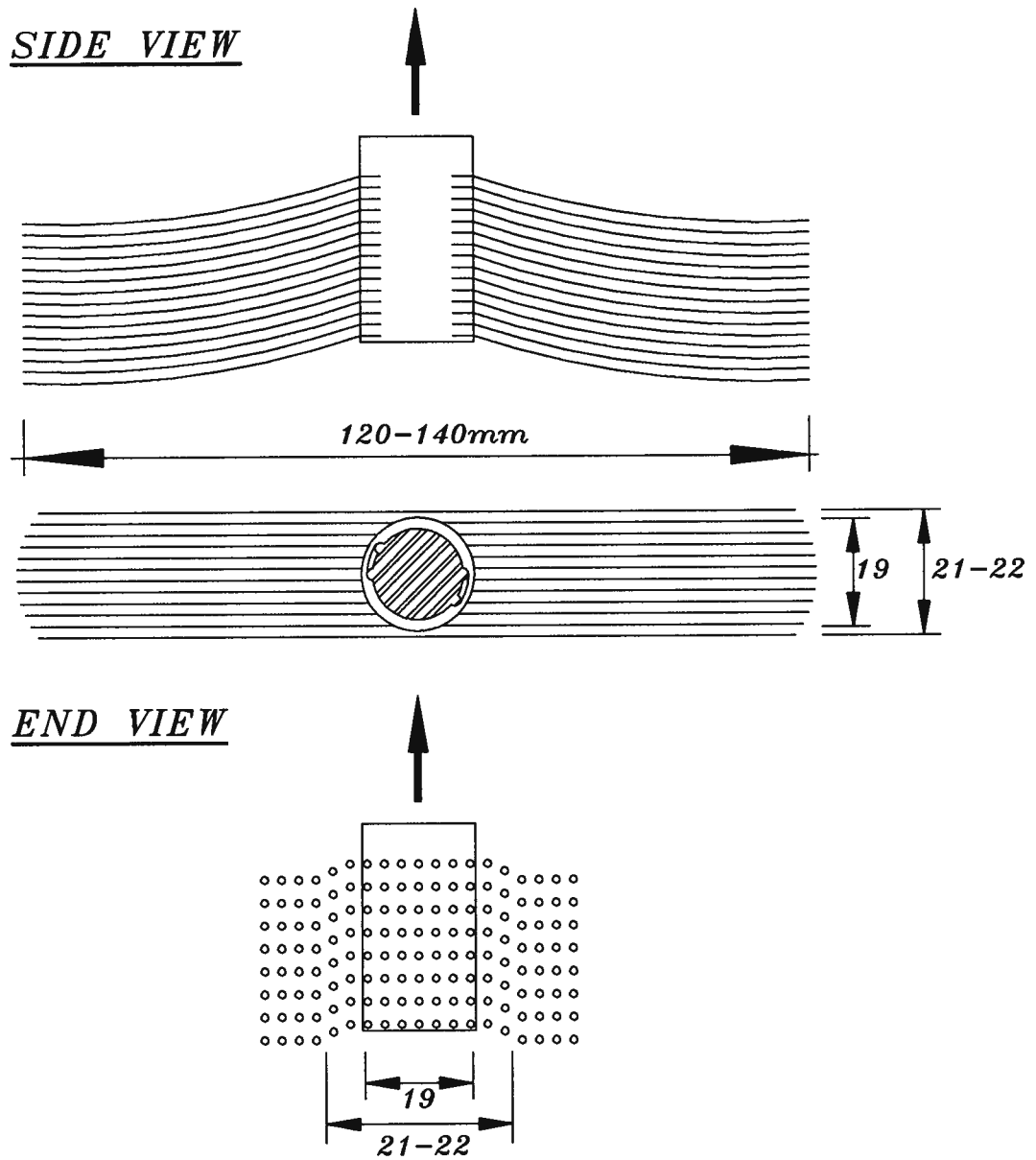


Fig.2.14 Deformation range observed after pull-out failure.

2.3.6 Stresses Due to M.C. Changes.

The change in M.C. of the glulam causes changes in the dimensions of the block. With rising M.C. the glulam swells and with falling M.C. the glulam shrinks. In the transverse direction (i.e. perpendicular to the grain) these dimensional changes can be very large. Within the discussed range of M.C. (10%-30%) the height of the glulam block can vary by 3-4% (12-16mm). When the dimensional changes are restricted, stresses develop in the glulam. The relationship between stress and strain is viscoelastic in nature and cannot be explained so easily as in case of temperature related stresses (see section 2.4.3).

In the case of the investigated connection, the rebar restricts the deformation of the glulam block in the direction perpendicular to the grain. In effect, opposing stresses develop both in the glulam block and in the rebar. Their magnitude and direction depends on actual M.C., time, and M.C. during manufacturing of the specimens.

The gluing of the rebar took place in the laboratory. The glulam blocks had been stored there, before cutting and drilling, for about 2 months. That allowed them to reach equilibrium moisture content (EMC) of 11-12%. The M.C. treatment described in previous sections started with wetting of the specimen. Because swelling of the glulam was restrained by the rebar compression stresses developed in the glulam and tension stresses were created in the rebar. Some increase of the height of the specimen also occurred due to elastic elongation of the rebar (due to the inducted stresses). When the limit of the swelling was approached a relaxation of the swelling stresses occurred. After reaching the fibre saturation point (M.C.=24%) the swelling stopped and the relaxation lowered the stresses to a level slightly above zero. At the end of the wetting the glulam was subjected to compression and the rebar to tension stresses. When the drying part of the treatment started the situation reversed. The glulam shrank and released the tension in the rebar. But shrinkage continued and, most probably (due to lack of relaxation), the stresses were reversed. The compression stresses were created in the rebar and tension stresses in the glulam. The hypothetical relationship between stresses, deformation, and moisture content during the first cycle of treatment is presented on Fig.2.15.

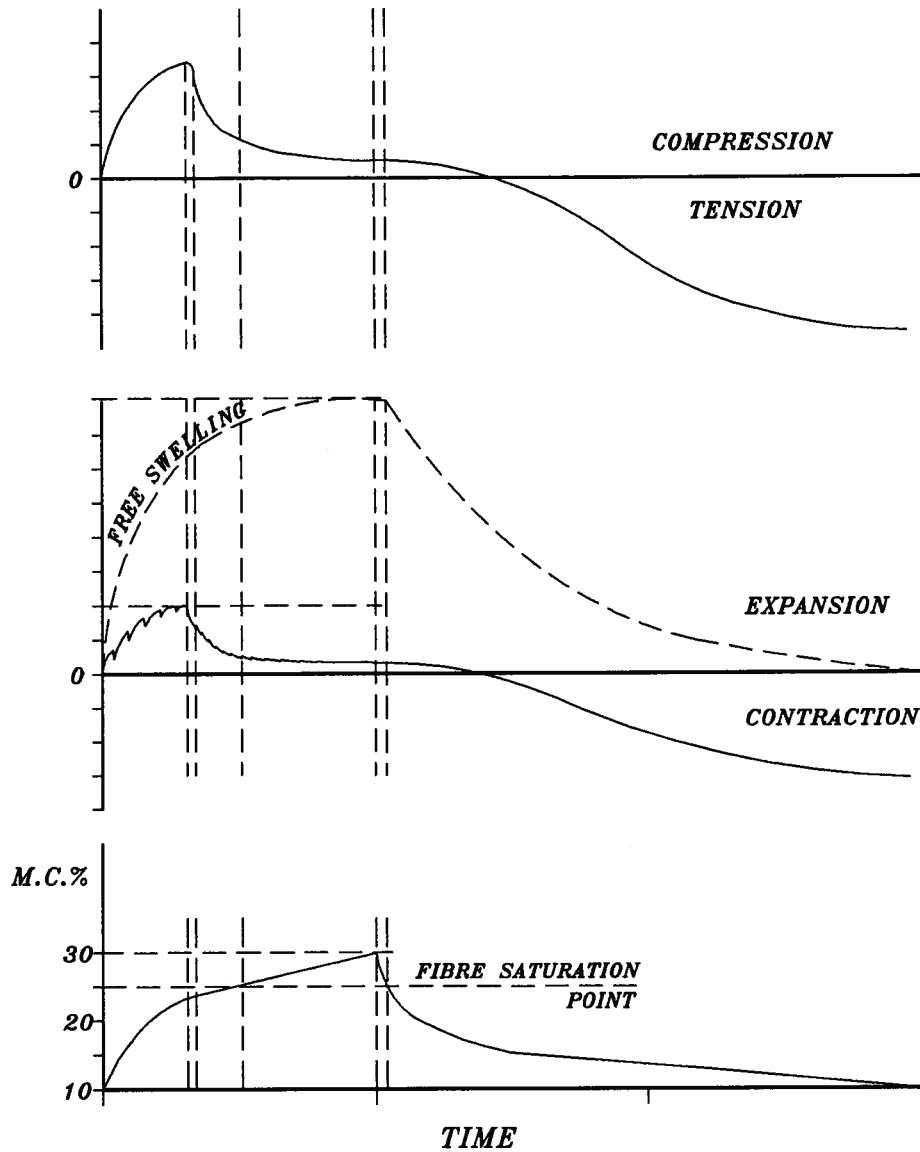


Fig.2.15 Relationship between stresses, partially restrained deformation, and moisture content in function of time (based on Sasaki & Yamada 1972, and Perkitny & Kingston 1972).

It is very difficult to evaluate the magnitude of those stresses. At the end of drying they couldn't be very high because tension perpendicular to the grain is the weakest property of glulam (0.89MPa according to the code). There was no evidence that the limit strength of the glulam was reached. Similarly, there was no evidence that the glulam reached its compression capacity during swelling. However, the glulam split failures could be related to the level of the stress developed during the treatment.

2.3.7 Results and Comments.

The results of moisture content tests are given in Table 2.4 and illustrated on Fig.2.16.

Spec.	Angle to the grain	Testing conditions	No. of cycles	Ultimate force [kN]	Ultimate stress in rebar [MPa]	Ductility ratio	Failure Mode
J1	90°	wet	5	132.0	660	18	I
K1	90°	wet	5	126.3	632	16	II
K2	90°	wet	5	125.5	628	10	III
K3	90°	wet	4	124.7	624	13	II
K4	90°	wet	3	117.4	589	6	III
L1	90°	dry	3	127.8	639	12	I
L2	90°	dry	3	129.7	649	13	I
L3	90°	dry	5	128.9	645	12	I
L4	90°	dry	5	130.5	653	17	I
L5	90°	dry	1	123.9	620	11	II
L6	90°	dry	2	129.3	647	18	I
Q1	90°	dry	5	127.0	635	14	I
M1	30°	dry	5	127.8	639	15	I
M2	30°	dry	1	131.0	655	19	I
M3	30°	dry	3	126.6	633	14	I
M4	30°	dry	3	128.2	641	16	I
M5	30°	dry	5	128.9	645	18	I

Table 2.4 Results of the tests conducted after M.C. treatment of the specimens.

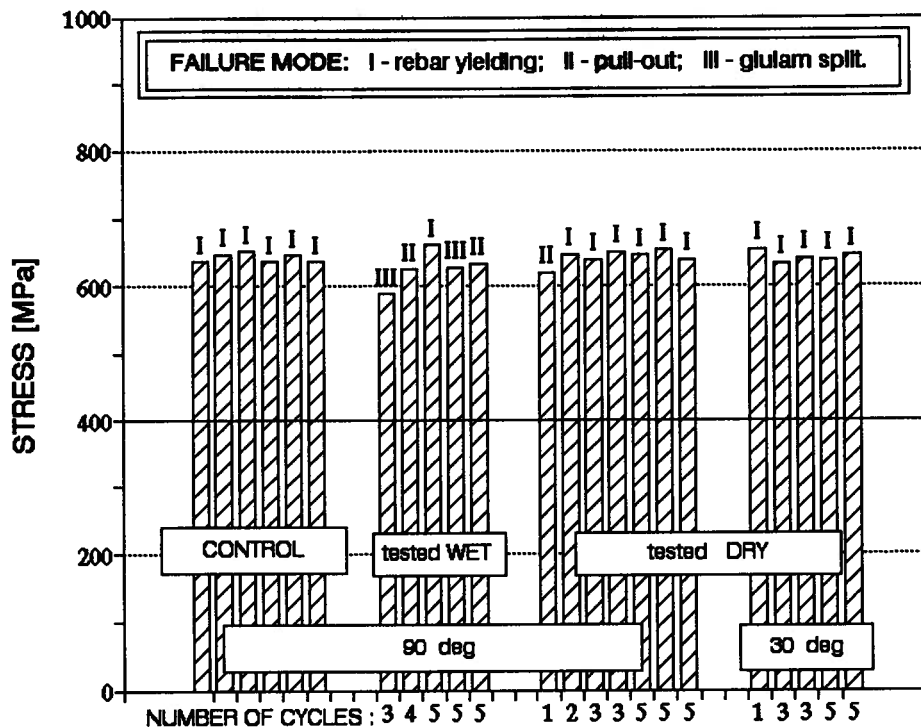


Fig.2.16 Graphical comparison of the ultimate load between the control sample and the M.C. samples. A horizontal line at 400MPa represents the design level for the connection (elastic deformations).

The main conclusion from all M.C. tests is that

there are no significant differences within the elastic range,

when compared to control sample. The elastic range is the design range for future connections. The only variation which should be taken into consideration is the decrease in stiffness of the connection.

Other findings are:

- the ultimate strength of the specimens apparently did not depend on number of cycles (within the range tested);
- no differences in ultimate strength between 90° sample and 30° sample were observed;
- the ultimate strength didn't vary significantly;

- the deformations developed during the treatment did not deteriorate the glue bonding;
- all specimens had similar level of ductility.

Although three failure modes were established, all the specimens experienced steel yielding and, in effect, large deformations of the rebars. Therefore, yielding of the rebar may be considered the primary cause of failure in tested glued-in connections.

2.4 TEMPERATURE TESTS.

In this section, the influence of temperature changes on behaviour of the connection is presented.

2.4.1 Parameters Investigated.

2.4.1.1 Temperature range.

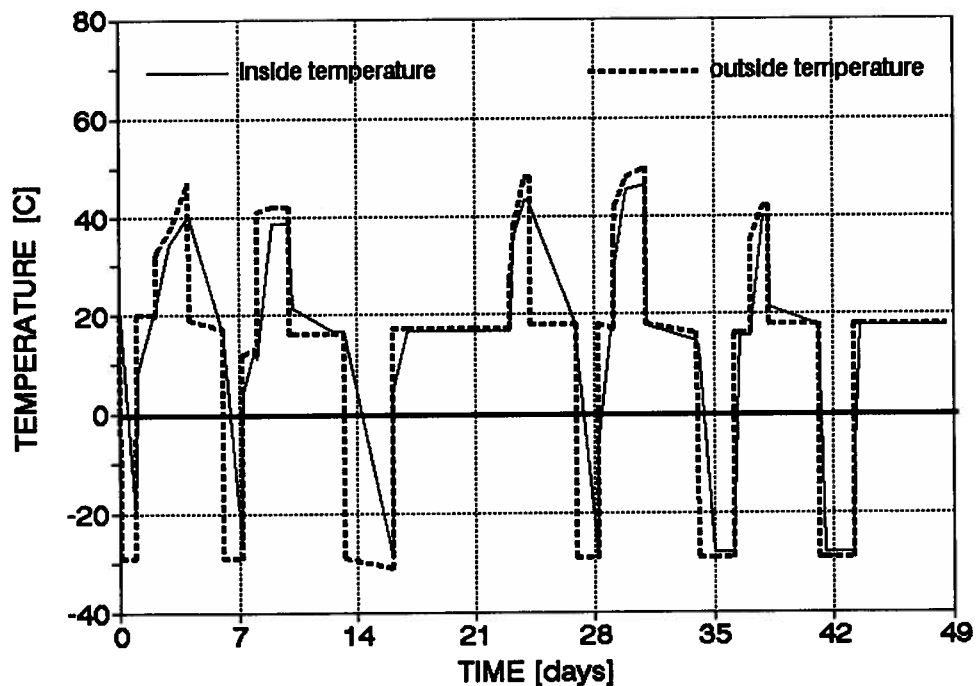


Fig.2.17 *Temperature variation outside and inside the specimens.*

The temperature of the specimens during treatment varied from -30°C to $+50^{\circ}\text{C}$ - well beyond the range expected in normal building practice. The temperature was measured outside the specimens and inside the specimens (small holes were drilled in 2 specimens). Usually, both readings matched after 24 hours stay in constant ambient temperature. The temperature variations are shown on Fig.2.17.

The freezing part of the cycle took place in a walk-in freezer of Dickie Dee Ice Cream, Coquitlam, B.C. The specimens were placed there for 2-3 days. After that, they were transported to the Structure Lab and left in the temperature about $+20^{\circ}\text{C}$ for the period of at least 24 hours.

To heat the specimens the plywood tunnel with sealed outlet (same as described in section 2.3.1.1) was used. At the inlet a heater with a fan was located. To reduce drying of the specimens, shallow open tanks with water were placed close to the heater. Usually, this phase lasted 2-3 days. After the heating the specimens were left in the lab's temperature for another 24 hours before freezing.

2.4.1.2 Number of cycles.

Each cycle consisted of the freezing part and the heating part. A full cycle lasted 6-10 days. Five cycles were conducted. However, some specimens were tested before completion of the treatment, so the number of cycles a particular specimen experienced varied from 1 to 5. In this way the correlation between the number of cycles and the change in the ultimate strength could be detected.

2.4.1.3 Test condition.

The specimens stayed in the lab's temperature for at least 24 hours prior to the testing. Usually this temperature was around $+20^{\circ}\text{C}$. The changes of the test temperature within few degrees were considered to be insignificant when compared to the temperature range during the treatment.

2.4.2 Discussion of Typical Load-Deformation Curve.

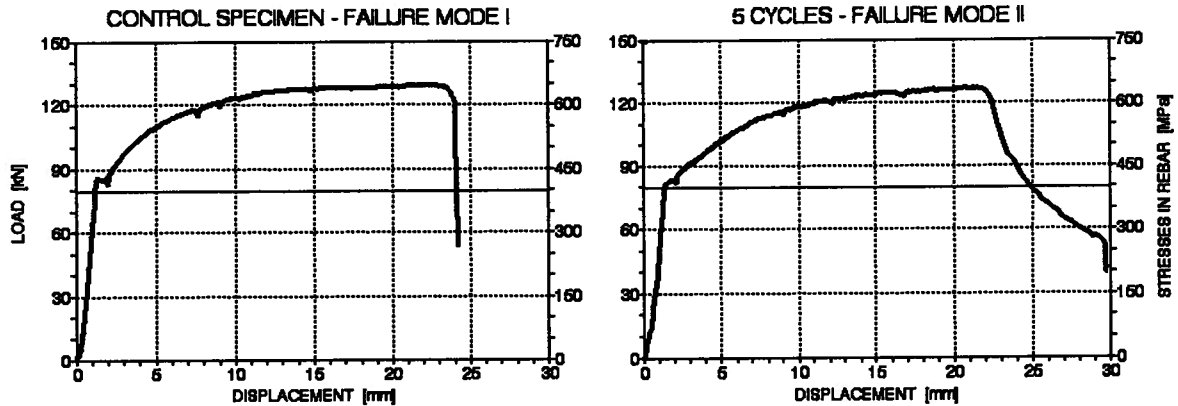


Fig.2.18 Typical load-deformation curve from the temperature treated specimen compared to the control one.

The comparison between the load-deformation curves of the temperature treated specimen versus a control specimen is shown on Fig.2.18.

The pull-out failure (Mode II) dominated in the temperature treated sample. But two other failure modes were observed as well. Again, all the curves were similar to those from the control sample except close to failure. The differences were identical to those described for the M.C. sample in section 2.3.2. Similar drop of stiffness within elastic range (20%) was observed.

2.4.3 Stresses Due to the Temperature Changes.

Unlike in the case of M.C. changes, the internal stresses due to the temperature changes are easy to establish because of their elastic nature. However, the process of developing these stresses is quite complicated. It depends on the magnitude of the tem-

perature change and the location of the rebar with respect to the grain. It is also time dependent. Two thermal properties of the materials are important here:

linear expansion coefficient - responsible for the magnitude of the deformations, and conductivity - responsible for the time after which the deformations develop.

The values for both coefficients are given in Table 2.1 at the beginning of this chapter.

In case of the investigated specimens the following phases of stress development can be observed (see Fig.2.19, Fig.2.20, and Fig.2.21):

phase 0 the specimen is manufactured at about +20°C; internal forces in the specimen are in equilibrium with zero stresses in rebar and glulam;

phase 1 the specimen is moved into the freezer; the surrounding temperature drops to -30°C; however, due to the poor conductivity of glulam, only the rebar is affected by the changed temperature and starts to contract (the protruding part of the rebar creates a large surface through which the heat can be transmitted); the glulam resists contraction of the rebar; tension stress develops in the rebar and compression stress develops in the glulam; eventually, an extreme of the stresses is reached (theoretically at 40MPa for the rebar and 0.18MPa for the glulam - see Appendix A for the calculations); this phase lasts about 1 hour;

phase 2 the glulam cools and shrinks; the tension in the rebar is released; because the wood contracts more than steel the specimen passes the neutral (zero stresses) point and continues to shrink; compression is introduced into the rebar and tension into the glulam; after about 24 hours the equilibrium is reached and the specimen doesn't contract any more; the stresses are: 101MPa in the rebar and 0.46MPa in the glulam; total contraction of the specimen is 0.44mm (based on 405mm total length); these conditions last until the end of the freezing (2-3 days);

- phase 3* the specimen is moved out of the freezer; the temperature jumps to about +20°C; again, only the rebar is affected by the change at the very beginning; the rebar expands creating even more compression in it and more tension in the glulam; the stresses can reach 142MPa for the rebar and 0.65MPa for the glulam; however, the glulam starts to expand as well and the stresses at the end of this phase are, probably, slightly lower; this phase is also very short and lasts about an hour;
- phase 4* the glulam expands more and more, and during the next 24 hours, the original state of equilibrium is restored; zero stresses both in the rebar and in the glulam;
- phase 5* the specimen is moved into the heating box; the surrounding temperature reaches +50°C; the rebar elongates immediately; the compression is created in the rebar and tension in the glulam; the stresses reach 25MPa in the rebar and 0.11MPa in the glulam;
- phase 6* the glulam starts to expand and reduces the stresses; the specimen passes the neutral point and continues to expand; the tension is created in the rebar and compression in the glulam; after about 24 hours the specimen reaches its maximum elongation of about 0.26mm; the stresses are: 61MPa for the rebar and 0.28MPa for the glulam; this equilibrium lasts until the end of the heating;
- phase 7* the specimen is moved out of the box; the temperature changes to about +20°C; the rebar reacts first and tends to contract creating more compression in the glulam and more tension in the steel; the stresses can reach about 86MPa for the rebar and 0.39MPa for the glulam (practically they are slightly lower due to some contraction of the glulam); this phase is quite short and lasts about an hour;

phase 8 the glulam shrinks and releases the stresses; after about 20 hours the original state of equilibrium is restored; there are no stresses in the glulam as well as in the rebar.

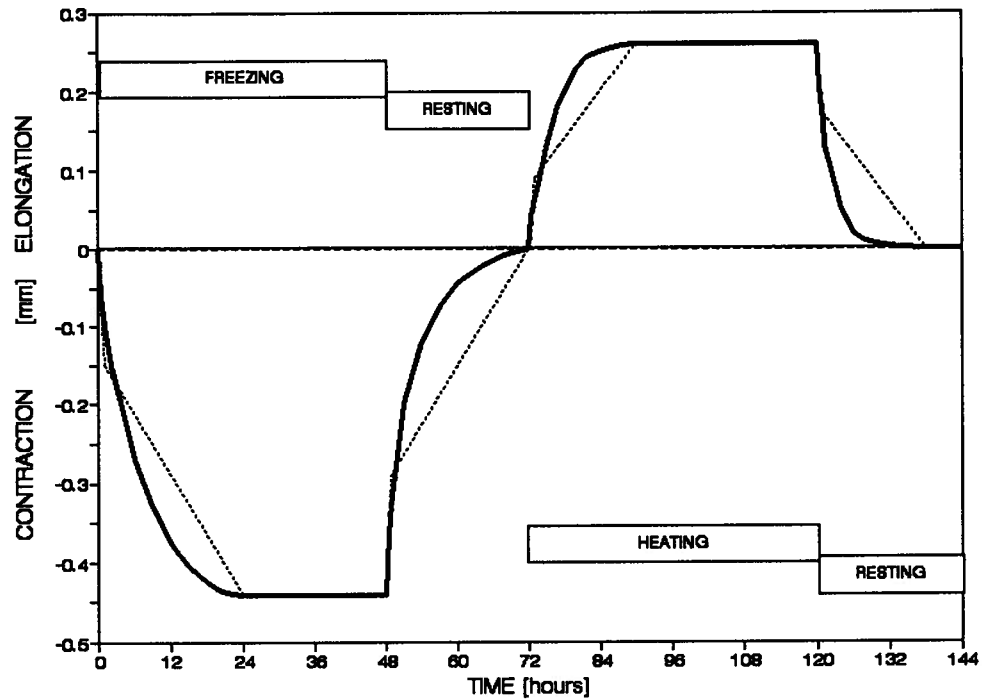
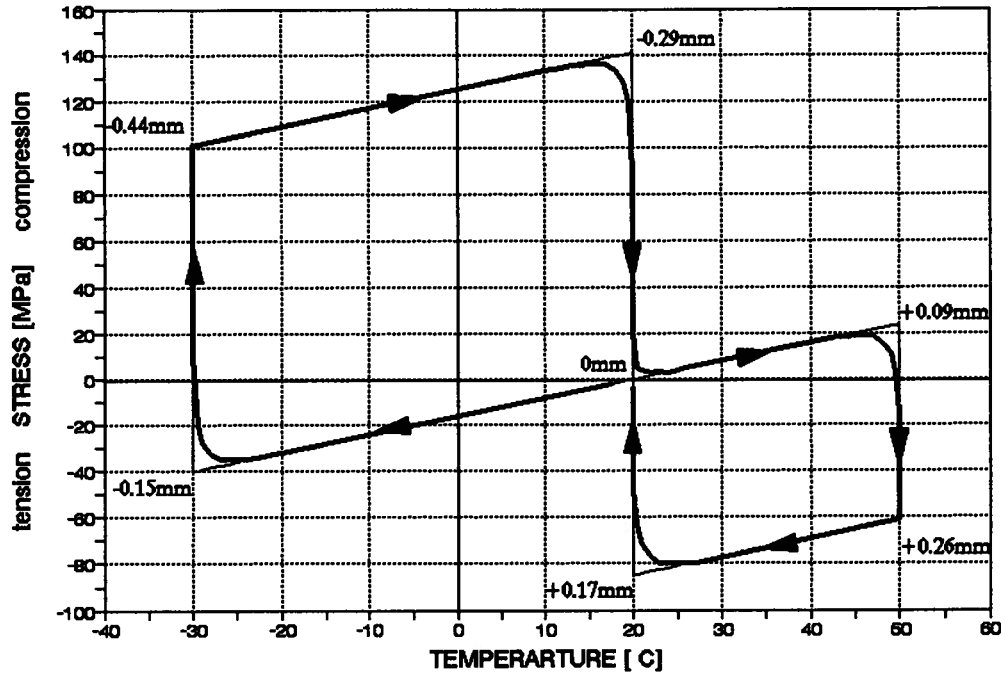


Fig.2.19 *Dimensional changes of the specimen (perpendicular to the grain) as a function of time. The dotted line shows theoretical calculations, the solid one represents more realistic behaviour.*

The changes of internal stresses due to the varying temperature are presented graphically on Fig.2.20 as a function of temperature and on Fig.2.21 as a function of time. The deformations of the specimen (based on 405mm length) during one cycle of the treatment are shown on Fig.2.19.

STRESS IN REBAR



STRESS IN GLULAM

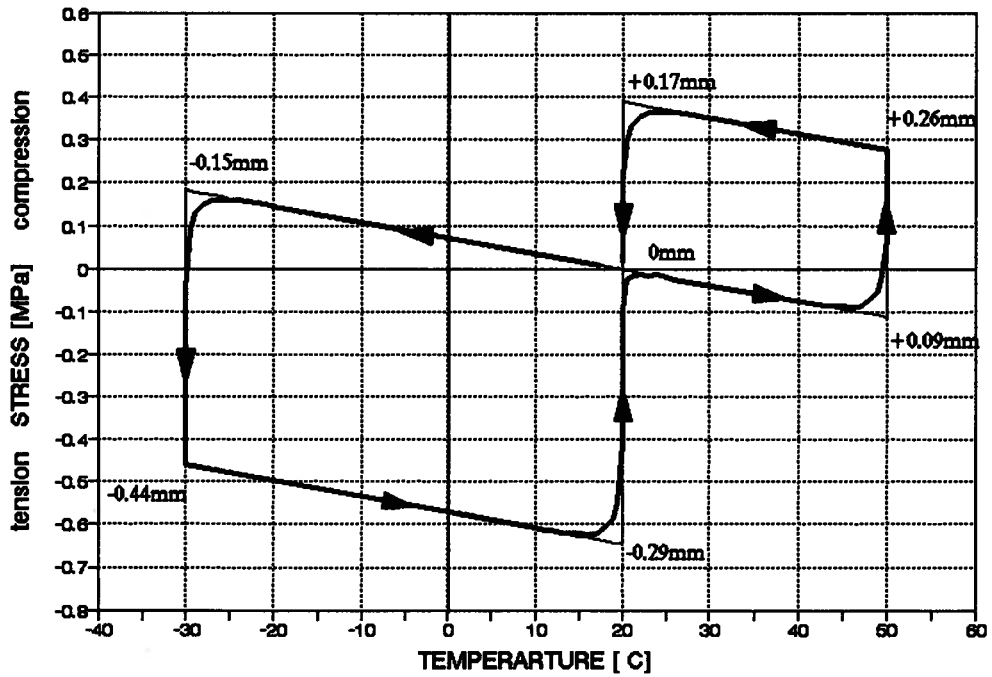
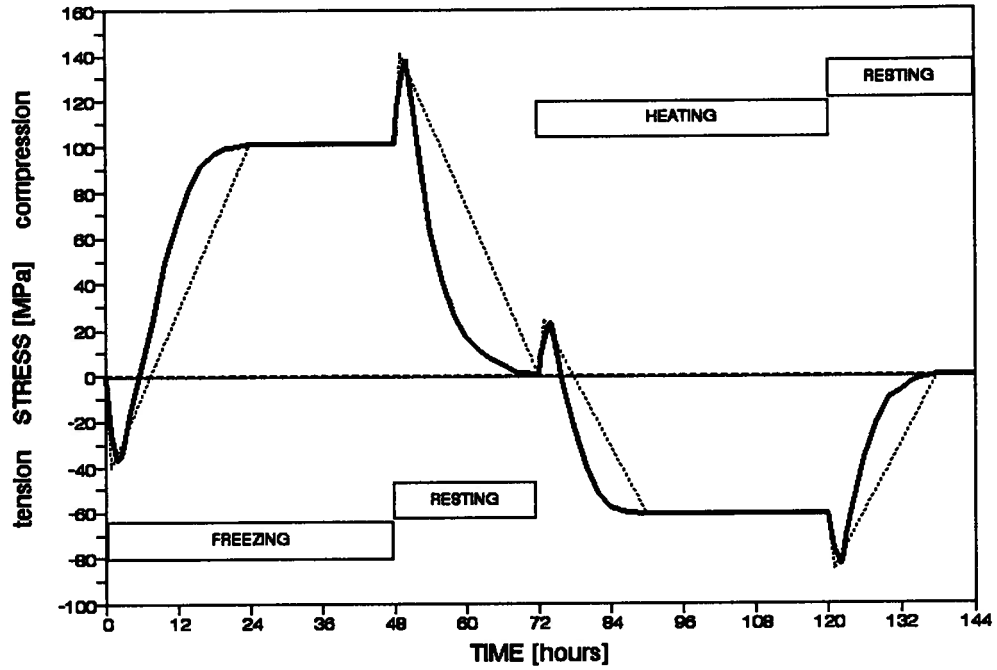


Fig.2.20 Internal stresses as a function of the temperature.

STRESS IN REBAR



STRESS IN GLULAM

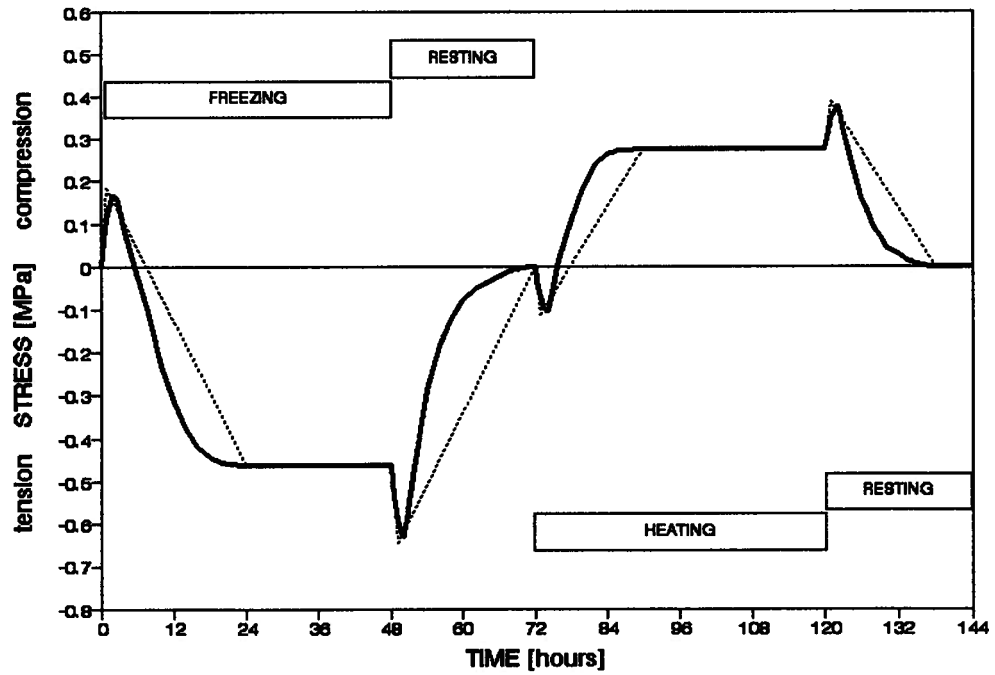


Fig.2.21 Internal stresses as a function of time.

Above graphs present the calculated stresses and deformations. The relaxation of stresses was not taken into consideration. However, due to the short time, the relaxation couldn't be significant. The thin solid line on Fig.2.20 presents theoretical situation when the dimensional change of the glulam starts right after the expansion (or contraction) of the rebar was completed. The heavy solid line presents more likely behaviour.

2.4.4 Results and Comments.

The results of the temperature tests are given in Table 2.5 and illustrated on Fig.2.22.

Spec.	Angle to the grain	No. Of cycles	Ultimate force [kN]	Ultimate stress in rebar [MPa]	Ductility ratio	Failure Mode
N1	90°	5	112.0	560	6	III
N2	90°	3	128.2	641	10	II
N3	90°	5	127.4	637	14	II
N4	90°	1	131.3	656	12	I
N5	90°	5	127.0	635	22	II
N6	90°	3	117.2	586	14	II
Q2	90°	5	128.0	640	11	I

Table 2.5 *Results of the tests conducted after the temperature treatment of the specimens.*

The main conclusion from the temperature tests is, again, that

there are no significant differences within the elastic range,

when compared to the control sample. The decrease in stiffness, however, was even more significant than in the M.C. samples.

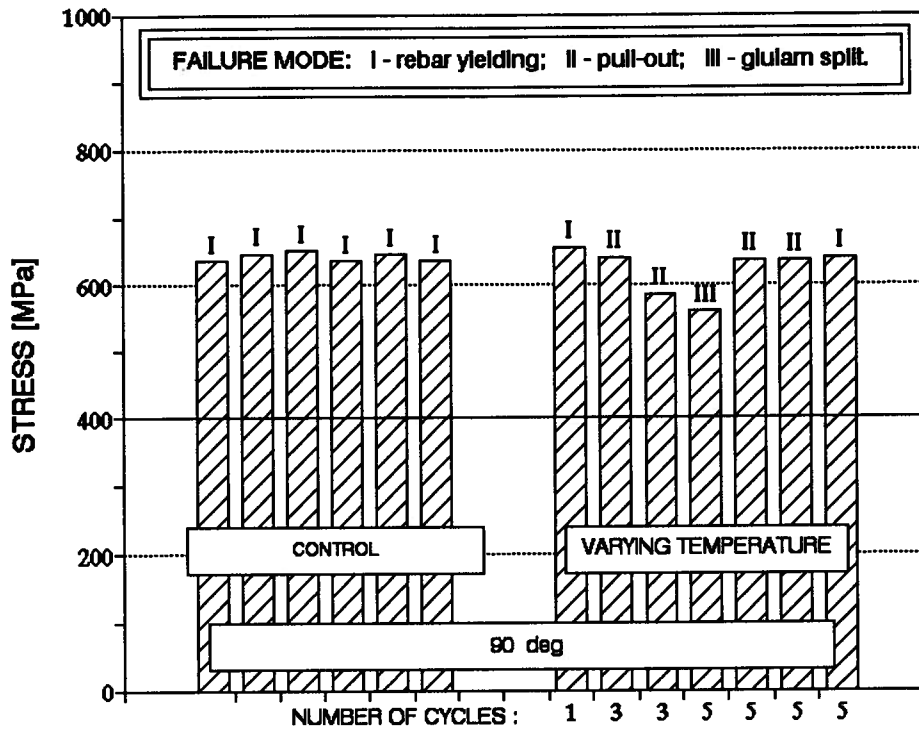


Fig.2.22 Graphical comparison of the ultimate load between the control sample and the temperature sample. A horizontal line at 400MPa represents the design level for the connection (elastic deformations).

The other findings are similar to those from M.C. tests:

- the ultimate strength of the specimens apparently did not depend on number of cycles;
- the ultimate strength didn't vary significantly;
- the deformations developed during the treatment did not deteriorate the glue bonding;
- the ductility of the specimens varied significantly within the temperature sample but the average ductility ratio (13) was only slightly lower than the one obtained from the control sample (15).

Although reduced by the procedure described in section 2.4.1.1, an intensive drying of the surface of the glulam blocks occurred during the heating part of the cycle. In effect, a lot of

cracks formed in the specimens. Certainly the cracking did influence the stiffness of the specimen. In the real structure, however, the dimensions of glulam pieces are much larger and the temperature changes not so severe (it's hard to imagine a situation where the temperature jumps by 50°C within few minutes). Therefore, cracking in the real life wouldn't be so serious.

It can be seen that the effect of the temperature treatment on the specimens was almost exactly the same as the effect of the M.C. treatment (described in section 2.3.7). In both cases the stresses were introduced into the specimen due to the relative movement of the glulam versus the rebar. Both tension and compression stresses were experienced by each part of the connection (i.e. the glulam and the rebar) during each cycle of the treatment. Although the magnitude of the stresses during the M.C. treatment was not established it can be assumed (based on the behaviour of the specimens during the treatment and testing) that these stresses had a similar range to those during the temperature treatment. Thus, the temperature test could also represent the M.C. changes in the specimen.

2.5 CONCLUSIONS.

It can be concluded, from the tests described in this chapter, that

the changes in surrounding environment, i.e. humidity and temperature, influence the glued-in rebar connection not any more than the glulam member itself.

The treated specimens proved to have the same or similar ultimate strength, yield stress, ductility, and general behaviour when compared to the non-treated specimens. Therefore, it can be assumed that the connections used in the real structures in different environment conditions will have similar properties and behaviour as those tested in the laboratory. Of course, all usual effects of long term loading of glulam will influence the structure and have to be considered.

It should be emphasized that within the elastic range, which is the design range of the

connection, only the stiffness decreased (about 20%). Similar drop of glulam properties could be expected due to higher moisture content. All other properties, such as strength and ductility, remained unchanged.

It is necessary, however, to further investigate this subject. Specially, the internal stresses developed during the treatment (both M.C. and temperature) should be studied more precisely. The time seems to be a very important factor here. Also an accumulation of stresses during larger number of cycles should be established.

The tests described in this chapter were conducted on the specimens which returned to their original condition (except the sample tested wet). It is important, however, to establish the extent to which the internal stresses can be superimposed with the stresses caused by the external loads. Therefore, the future research should include the treatment of loaded specimens.

Because, in this research program, time of the treatment as well as the size of the specimens were limited, the need of full scale, long term tests still exists. Some assumptions have been made (for example, occurrence of the Failure Mode III), which can be verified only by testing full size members.

The future research could be based on the temperature tests only since they would also represent the M.C. changes. The temperature test is much easier to conduct and saves a lot of time.

CHAPTER 3

COMPRESSION PERPENDICULAR TO THE GRAIN.

3.1 TEST OBJECTIVE.

Compression perpendicular to the grain is the second weakest property of timber (tension perpendicular to the grain being the weakest). It is quite often that this property limits the design of an element. Usually, this happens when large concentrated forces have to be transferred from horizontal to vertical members in the structure through bearing type connection. The most common case is a beam supported by a column or a wall, where bearing stresses are developed in the beam.

The objective of the tests described in this chapter was to investigate the possibility of increasing the bearing capacity of the glulam members, by gluing a rebar into the glulam, perpendicularly to the grain. The problem became apparent when knee joints were tested by Robert Malczyk in summer 1993 (described in chapter 1). Very high compression stresses under the steel plates were observed during those tests - far beyond the resistance of the glulam - causing excessive overall deformations of the structure. Although other solution was applied to improve the performance of the knee joint, reinforcing of the glulam was seriously considered. It was also anticipated that similar problems may occur in the future with other joint configurations. It was decided that a separate research program should be developed to obtain more information about bearing reinforcing of the glulam. A part of it was incorporated into this thesis.

The tests started in June 1993 and were conducted with varying intensity until December 1993.

3.2 MATERIALS, TEST SETUPS, AND TEST PROCEDURES.

3.2.1 Materials.

The glulam used for the tests described in this chapter were some 30 years old beams recovered from the UBC bookstore when it was demolished. The width of the beams was 178mm and so was the width of all test specimens. Both length and height of the specimens varied according to the needs of the test setup and parameters investigated.

Deformed weldable reinforcing bars (rebars) of grade 400 (yield stress = 400MPa) were used. Two sizes of rebars were tested: #10 and #15. Their nominal diameters were 11.3mm and 16.0mm, and their nominal areas 100mm^2 and 200mm^2 respectively (refer to section 2.2.1 for more information).

The epoxy glue IFC-SP manufactured by Industrial Formulators of Canada Ltd., Burnaby, B.C., was used for the connections. It consists of two parts: resin and hardener. The mixing ratio is 100 to 42 (by weight) respectively. The glued specimens were cured at least 7 days before testing in order to reach full strength of the glue.

The steel plates used for the testing were 12.7mm ($\frac{1}{2}$ ") thick, cut from flat bars of A-36 type steel. The specified minimum tensile strength of the steel was $F_u=450\text{MPa}$.

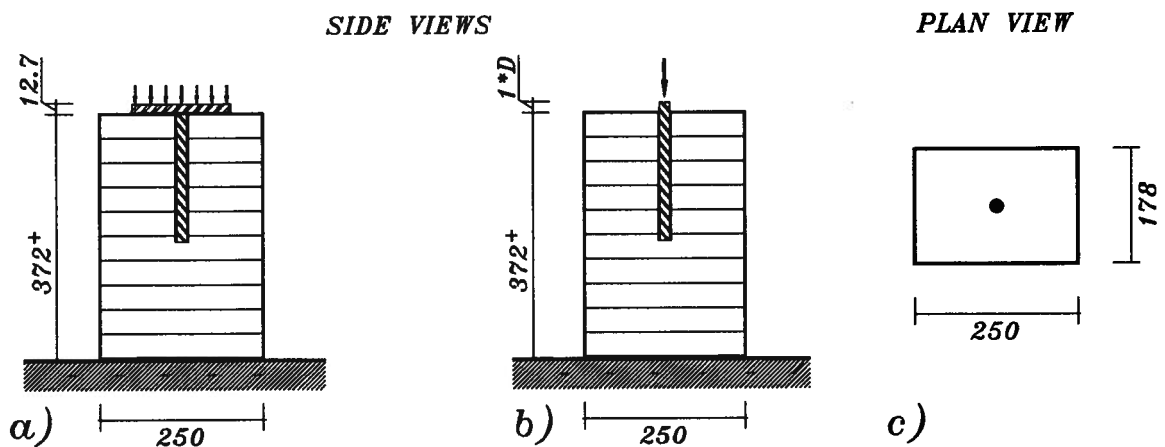
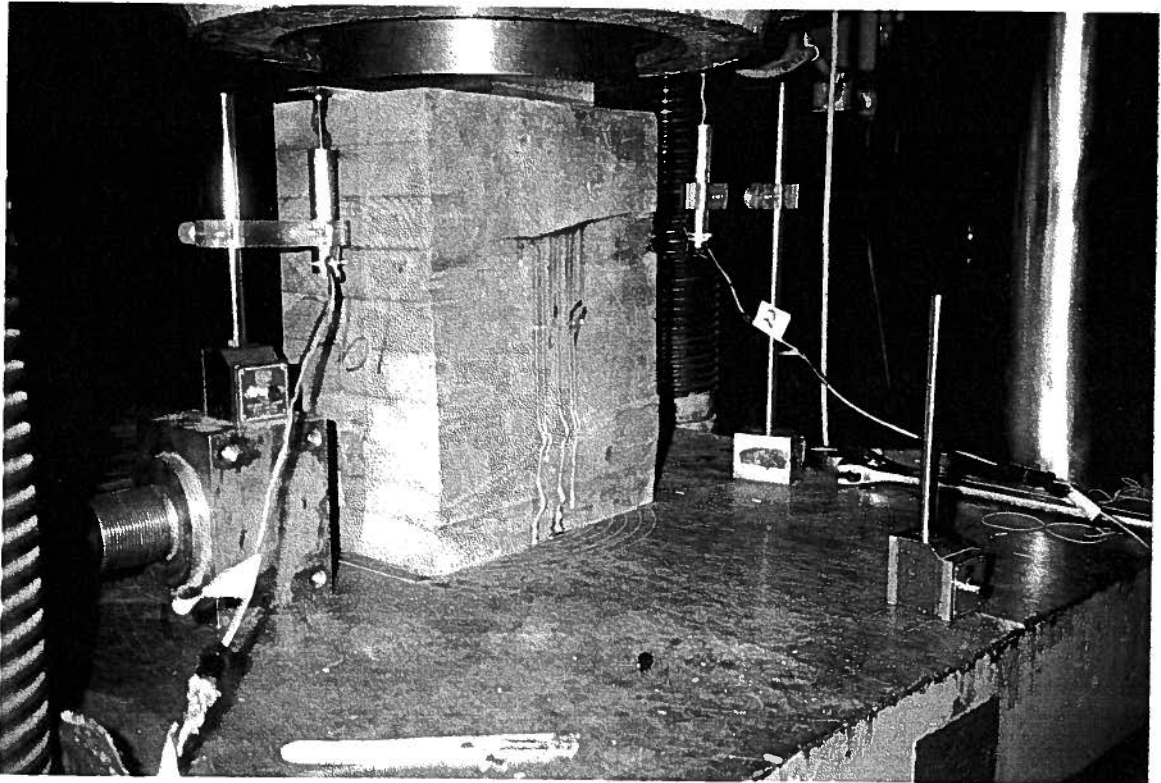


Fig.3.1 Preliminary test setup: a) a specimen with bearing plate, b) a specimen with protruding rebar, c) cross section.

3.2.2 Test Setup.

The Baldwin testing machine described in section 2.2.2 was used to perform all tests. This time a compression configuration of the Baldwin machine was used. In most cases the machine was set for medium range (0 to 356 kN). The high range (0 to 1780 kN) was used only for multi-rebar tests.



*Fig.3.2 Specimen in the testing machine during preliminary test
(note the deformations of the lower part of the glulam block).*

Three different test arrangements were used. The preliminary tests were conducted on the glulam blocks supported uniformly on the entire area of the specimen (see Fig.3.1

and Fig.3.2). Because some unwanted failure (described in section 3.3.3) occurred during these tests, the setup was later changed to the simple supported beam arrangement (see Fig.3.3). The compression force was applied to the specimen in two different ways:

- a) to the steel plate located on the top surface of the specimen (the rebar was flush with the surface of the glulam),
- b) directly to the rebar (the rebar was protruding by the length equal to its diameter).

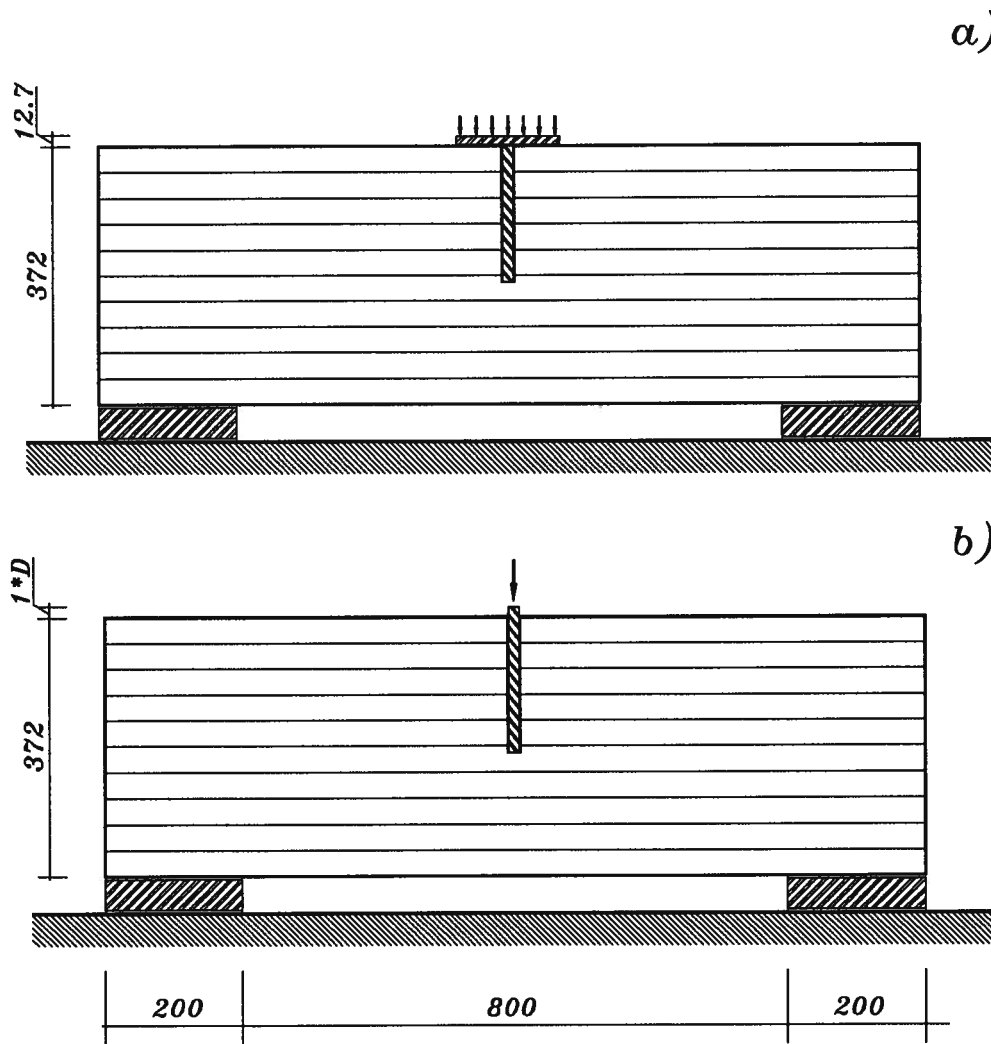


Fig.3.3 *Simple supported beam setup:*

a) a specimen with bearing plate,

b) a specimen with protruding rebar.

The third arrangement involved a block with two bearing plates (placed on the opposite faces of the glulam). The rebar was going through the entire depth of the specimen and was flush on both sides (see Fig.3.4). This setup was designed to check the likelihood of buckling of the rebar within the specimen.

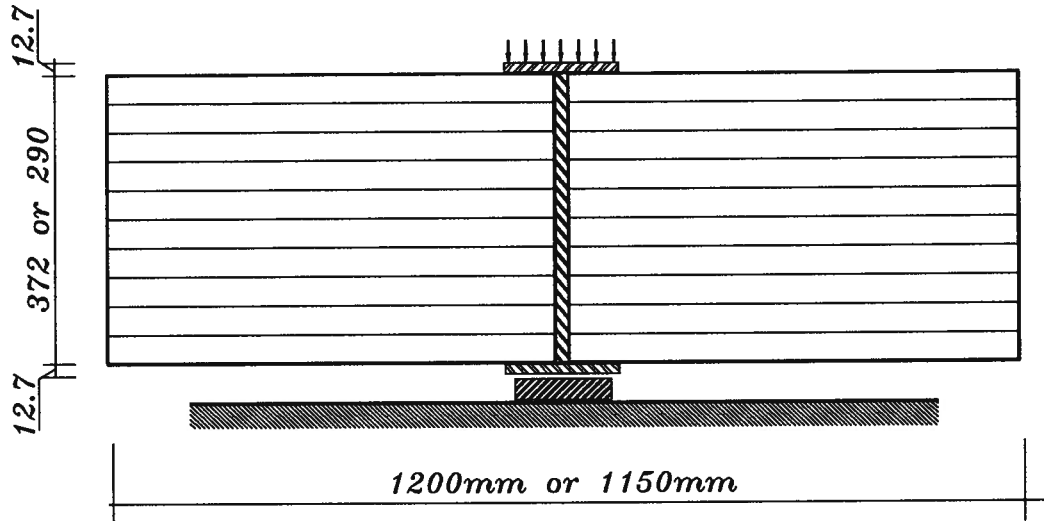


Fig.3.4 Specimen with top and bottom bearing plates.

3.2.3 Test Procedures.

Three measurements were recorded by the data acquisition system: a load measured by the load cell of the Baldwin, a relative displacement between the base and middle reaction beam of the machine, and a relative displacement between the base and the top (or bottom) surface of glulam (see Fig.3.2). The displacements were measured by LVDT gauges. A set of data was recorded every second.

The test was considered to be completed when:

- a) the protruding part of the rebar (or the plate in case of flush rebar) was completely

- pressed into the glulam (after 12mm indentation),
- b) the protruding part of the rebar buckled,
- c) glulam failure occurred (shear failure or bearing failure at the support).

3.3 FLUSH REBAR TESTS.

In the tests described in this section a combined action of the glued-in rebar and the glulam in bearing was induced.

3.3.1 Manufacturing of the Specimens.

The manufacturing of the specimens proceeded as follows. First, the hole (or holes) was drilled in the centre of the glulam block. Then the glue was poured into the hole and the rebar inserted. After the glue had set, the rebar was ground flush with the surface of the glulam. The specimens were cured 7 days before testing. Before the test the steel plate (12.7mm thick) was placed on top of the specimen in such way that the centre of the plate matched the centre of the glulam block and the centre of the rebar or rebar group (to obtain equal forces in all rebars).

In cases where the rebar was welded to the plate, the gluing took place after the welding.

3.3.2 Parameters Investigated.

The following parameters were investigated during these tests:

- rebar's size #10 and #15
- rebar's length from 50mm to 372mm
- number of rebars from 1 to 4
- size of the plate 76x102, 102x152, 127x152, 152x124 mm

- effect of welding rebar welded to the plate or not
- support conditions uniform (Fig.3.1.a), simple supported beam (Fig.3.4.a),
uniform with two plates (Fig.3.4.)

3.3.3 Preliminary Tests.

The results of the tests conducted on the plain specimens and the reinforced specimens are presented in Table 3.1.

Spec.	Rbl mm	Pls mm	Pde kN	Pdu kN	Ste MPa	Stu MPa	Remarks
Plain glulam specimens, block size: 178x372x250mm (width x depth x length)							
Glm6x5a	-	127x152	118	149	6.1	7.7	comp./bearing failure
Glm6x5b	-	"	136	170	7.0	8.8	"
Glm6x6a	-	152x152	134	157	5.8	6.8	"
Glm6x6b	-	"	121	153	5.2	6.6	"
Glm6x7b *)	-	152x178	164	265	6.1	9.8	bearing failure
Glm370a	-	152x250	142	180	3.7	4.7	comp./bearing failure
Glm200a	-	127x152	117	-	6.1	-	no failure
Glm100a	-	"	112	-	5.8	-	"
Specimens reinforced with one #10 rebar, block size: 178x372x250mm							
R10-050b	50	127x152	115	136	6.0	7.0	compression failure
R10-100b	100	"	109	135	5.6	7.0	"
R10-200b	200	"	110	137	5.7	7.1	"

Table 3.1 continues on the next page...

Spec.	Rbl mm	Pls mm	Pde kN	Pdu kN	Ste MPa	Stu MPa	Remarks
Specimens reinforced with one #15 rebar, block size: 178x372x250mm							
R15-100b	100	127x152	118	136	6.1	7.0	compression failure
R15-100a	"	152x250	130	173	3.4	4.6	"
R15-200a	200	"	135	187	3.6	4.9	"
R15-200b	"	127x152	117	135	6.1	7.0	"
R15-300a	300	152x250	130	189	3.4	5.0	"
R15-300b	"	127x152	120	164	6.2	8.5	"
<i>Note:</i> Rbl - embedment length of the rebar [mm] Pls - plate size width x length [mm] (thickness 12.7mm) Pde - maximum load within elastic region (approximate) [kN] Pdu - ultimate load [kN] Ste - equivalent stress under the plate (within elastic region) [MPa] Stu - ultimate equivalent stress under the plate [MPa] *) length of the block increased to 600mm							

Table 3.1 Results of the preliminary tests with bearing plate and flush rebar.

The main goal of these tests was to quantify the difference in bearing capacity between plain glulam specimens and the specimens reinforced with glued-in rebars. Unfortunately, the size of the specimens combined with uniform support created compression failure of the glulam in most cases, not bearing failure under the plate. However, it was noticed that the compression failure occurred beneath the reinforced part of the specimen (see Fig.3.2). This fact indicated that the glued-in rebar spread the bearing stresses from under the plate deeper into the glulam. It was suggested that larger glulam blocks would be needed to obtain evident bearing failures. It was confirmed during a test Glm6x7b (with the length of the glulam block increased to 660mm).

3.3.4 "Beam" Setup Tests.

During the tests described in previous section the bearing plates were located directly above the support surface of the specimens. In cases where the rebar was glued-in, the bearing stresses were "moved" into the unreinforced part of the glulam. That created relatively short (especially where the rebar was 300mm long), highly stressed zone, where the support stresses interfered with the stresses transferred by the rebar. To avoid that situation, it was decided to move the support location away from the reinforced section of the specimen. To achieve this a short simple supported beam setup was chosen.

An initial clearance between the base and the bottom face of the beam was set to 51mm (2"). That clearance allowed the beam to deflect freely at midspan, i.e. at the location of the bearing reinforcement. The clear span was kept approximately twice the depth of the specimen so the influence of compression stresses at the supports on the midspan cross section could be diminished. The usual support length was 200mm. The total length of the specimen was calculated according to the empirical formula:

$$\text{total length} > 2 \times (\text{rebar's embedment length} + \text{support length})$$

The maximum length of the specimen that could be tested in the Baldwin machine was 1300mm. The majority of the specimens had dimensions 178x372x1200mm. Three specimens (Bm15, Bm17, Bm20) were 178x290x1150mm and one (#1) was 178x372x960mm.

The results of the tests conducted on "beam specimens" without reinforcement and with one #15 rebar glued-in are presented in Table 3.2.

Spec.	Rbl mm	Pde kN	Pdf kN	Pdu kN	Ste MPa	Stf MPa	Stu MPa	Remarks
Plain glulam specimens with bearing plates								
Bm5	-	60	-	137	7.7	-	17.5	pa
Bm6	-	110	-	215	7.1	-	13.9	pb
#1	-	175	-	295	4.9	-	8.2	* pc
Specimens reinforced with one #15 rebar, bearing plate size: 76x102mm								
Bm9	100	110	116.5	133	14.2	15.0	17.2	
Bm7	200	143	177.5	140	18.4	22.9	18.1	
Bm17	"	148	178.5	160	19.1	23.0	20.6	
Bm18	"	155	181.2	170	20.0	23.4	21.9	
Bm19	"	150	178.6	155	19.3	23.0	20.0	
Bm2	300	150	220.0	162	19.3	28.4	20.9	
Bm3	"	130	181.0	145	16.8	24.7	18.7	
Bm12	"	140	244.0	240	18.1	31.5	31.0	wld
Bm13	372	150	264.6	220	19.3	34.1	28.4	gt
Bm15	290	140	203.1	155	18.1	26.2	20.0	gt

Table 3.2 continues on the next page...

Spec.	Rbl mm	Pde kN	Pdf kN	Pdu kN	Ste MPa	Stf MPa	Stu MPa	Remarks
Specimens reinforced with one #15 rebar, bearing plate size: 102x152mm								
Bm20	100	180	206.0	225	11.6	13.3	14.5	
Bm8	200	200	227.1	238	12.9	14.6	15.4	
Bm1	300	190	233.5	215	12.3	15.1	13.9	
Bm11	"	180	331.5	300	11.6	21.4	19.3	wld
<p><i>Note:</i> Rbl - embedment length of the rebar [mm] Pde - maximum load within elastic region (approximate) [kN] Pdf - load at failure of reinforced bearing area [kN] Pdu - load at the end of the test [kN] Ste - equivalent stress under the plate (within elastic region) [MPa] Stf - equivalent stress under the plate at failure [MPa] Stu - equivalent stress under the plate at the end of the test [MPa] p - plate size: a) 76x102mm, b) 102x152mm, c) 178x202mm * - support length 240mm wld - rebar welded to the plate gt - rebar going through the entire depth of the specimen</p>								

Table 3.2 Results of the tests conducted on beam specimens with bearing plate and flush rebar.

The comparison of load-deformation curves obtained during these tests is presented on Fig.3.5 for 76x102mm plate and on Fig.3.6 for 102x152mm plate.

The indentation of the plate with respect to the top surface of the glulam is presented on the abscissa. The applied load and the corresponding bearing stress under the plate is shown on the ordinate. The stress was calculated as the applied force divided by the area of the plate (uniform stress distribution under the plate was assumed). It represents a real stress in the glulam only in case of non-reinforced specimen. When the rebar is present this value represents the combined action of the glulam and the rebar. Thus, the values of stress from Fig.3.5 and Fig.3.6 cannot be compared directly.

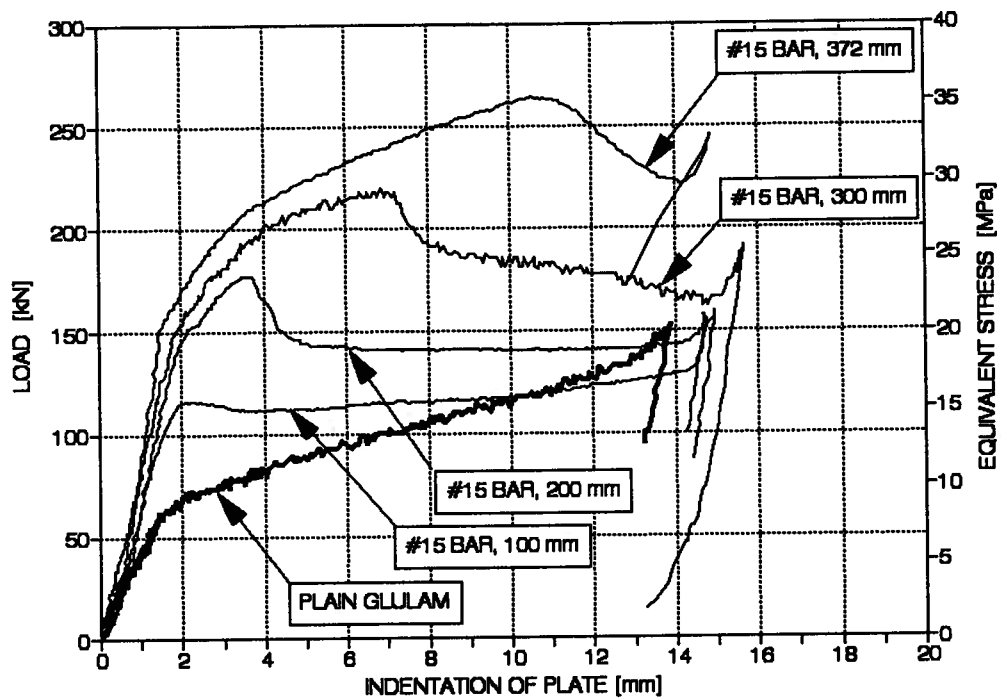


Fig.3.5 Load-deformation curves for the specimens with 76x102mm plate.

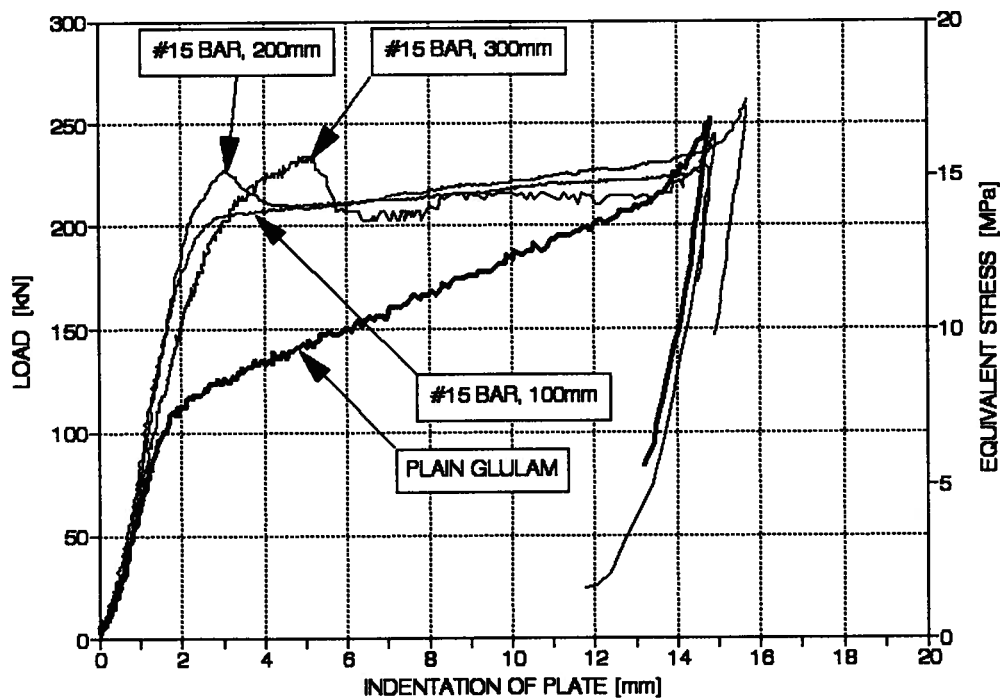


Fig.3.6 Load-deformation curves for the specimens with 102x152mm plate.

From the presented curves it is obvious that even the shortest rebar (100mm) improves the bearing capacity of the glulam significantly. By gluing the rebar the ultimate capacity can be increased (almost 2 times) and, what is even more important, the elastic region of the curve is 2.5 times larger when compared to the plain glulam specimen. This can be achieved by using just 200mm long rebar. The improvement in stiffness is also very significant - from 1.5 times for 100mm rebar up to 2.5 times for 372mm rebar.

Of course, the relative increase of the elastic or ultimate load depends on the size of the plate used. The larger the plate the smaller is an influence of a single rebar.

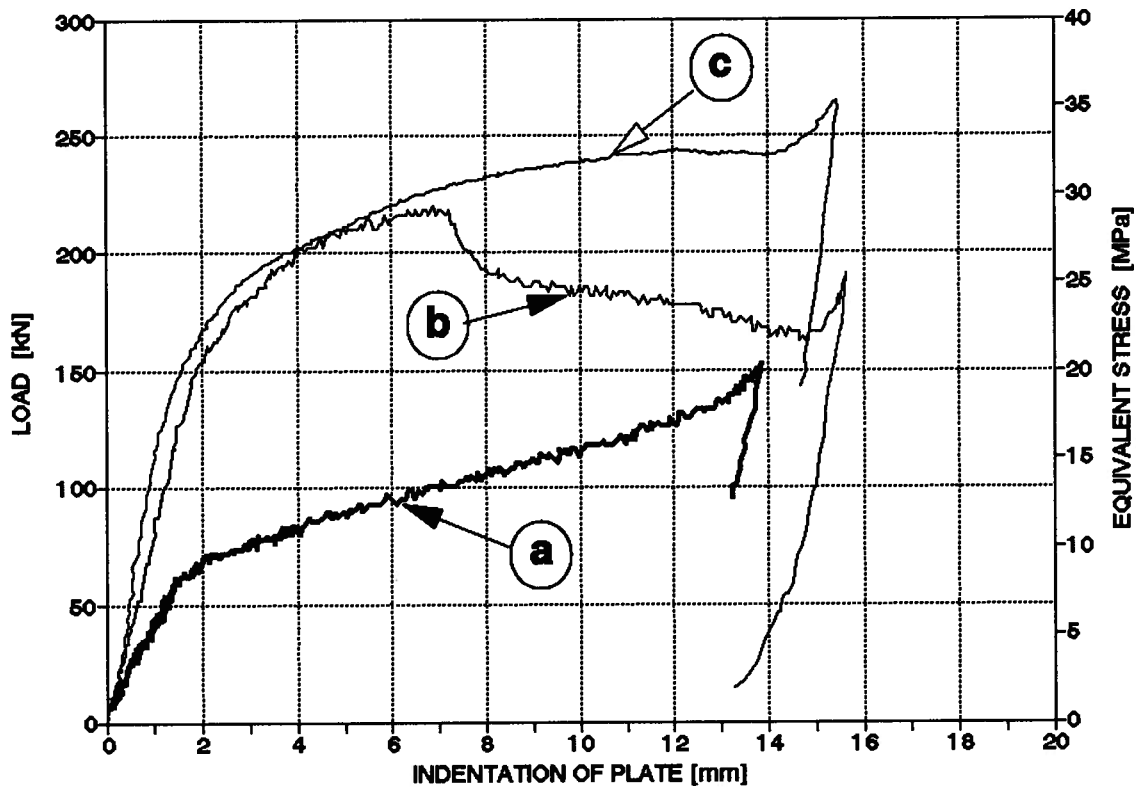


Fig.3.7 Comparison of L-D curves for the specimens with 76x102mm plates:

- a) plain glulam, b) 300mm rebar not welded to the plate,
- c) 300mm rebar welded to the plate.

Another interesting observation was made when load-deformation curves of the specimens with the rebars welded to the plate were compared with the non-welded specimens of the same rebar's length (see Fig.3.7 and Fig.3.8). Although the elastic load is the same, an additional increase in initial stiffness is observed. Also the ultimate load was over 20% larger for welded specimen than for non-welded. The effect of welding wasn't of much interest at that stage and it wasn't investigated further because it would require an extra operation for the manufacturers. However, it appears that providing better contact between the rebar and the plate can additionally increase the bearing capacity of reinforced glulam.

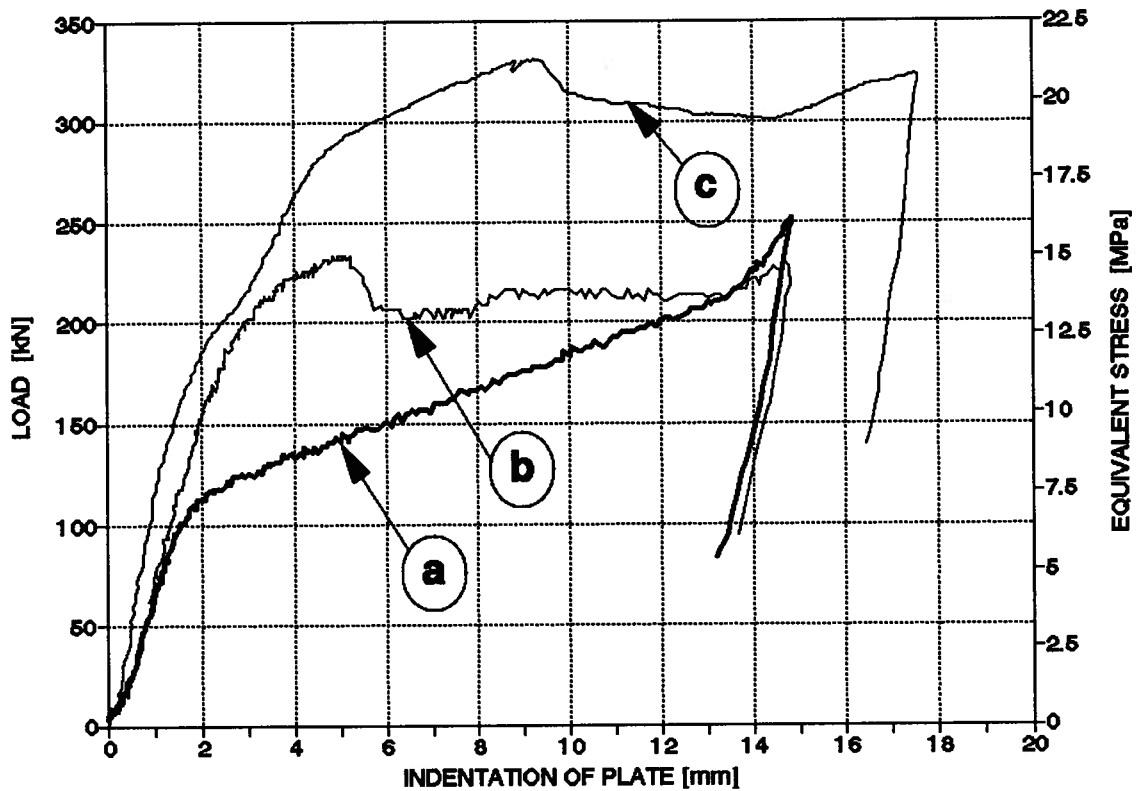


Fig.3.8 Comparison of L-D curves for the specimens with 102x152mm plates:

- a) plain glulam, b) 300mm rebar not welded to the plate,
- c) 300mm rebar welded to the plate.

3.3.5 "Two Plates" Tests.

It is possible that the bearing plates are required on opposite sides of the glulam member at the same time. That is the case of a column to beam connection, where the beam is continuous over the joint and the structure has more than one story. The test setup described in this section (see Fig.3.4) was intended to verify if only one rebar can be used to reinforce the compression resistance of the glulam member on both sides.

These tests were designed to check if the glulam provides sufficient resistance against buckling of the rebar.

The glulam block was of the size as the "beam" specimen. A #15 rebar was going through the entire depth of the glulam and was flush on both sides. Two steel plates of identical size were placed at the rebar's location. A compression load was applied until one of the plates was completely pressed into the glulam. The results of the tests are presented in Table 3.3 and on Fig.3.9.

Spec.	Gls mm	Rbl mm	Pls mm	Pde kN	Pdf kN	Ste MPa	Stf MPa	Remarks
Bm14	372x1200	372	76x102	142	259.3	18.3	33.9	gt
Bm16	290x1150	290	102x152	130	366.5	8.4	22.9	gt
<p><i>Note:</i> Gls - glulam size: 178 x depth x length [mm] Rbl - embedment length of #15 rebar [mm] Pls - plate size: width x length [mm] (thickness 12.7mm) Pde - maximum load within elastic region (approximate) [kN] Pdf - load at failure of reinforced bearing area [kN] Ste - equivalent stress under the plate (within elastic region) [MPa] Stf - equivalent stress under the plate at failure [MPa] gt - rebar going through the entire depth of the specimen</p>								

Table 3.3 Results of the tests with two bearing plates and flush rebar.

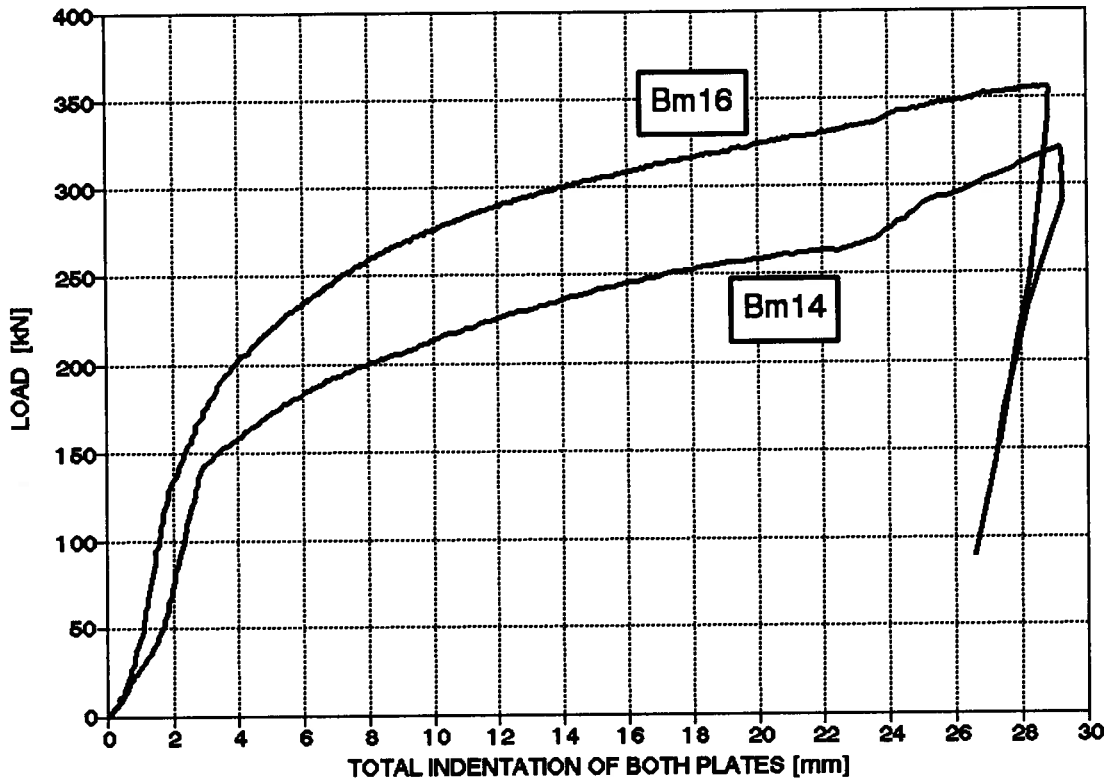


Fig.3.9 *L-D curves for the specimens with two bearing plates.*

The results are very much similar to those obtained from the "beam" tests for the same length of the rebar, i.e. similar increase in bearing capacity of the glulam was observed.

The buckling of the rebar did not take place.

3.3.6 Multi-rebar Tests.

Some specimens with multi-rebar reinforcement were tested as well. Three or four #15 rebars were glued-in under the plate. The "beam" setup was used for testing. The results of multi-rebar tests are presented in Table 3.4 and on Fig.3.10.

Spec.	Gls mm	Nr	Rbl mm	Pls mm	Pde kN	Pdf kN	Pdu kN	Ste MPa	Stf MPa	Stu MPa	Remar.
#1	372x960	-	-	178x202	175	-	295	4.9	-	8.2	*
Bm21	410x1300	3	200	152x204	410	nf	455	13.2	-	14.7	sf bf
Bm23	372x1200	3	200	"	388	419.9	330	12.5	13.5	10.6	sf
Bm22	"	3	200	"	400	433.3	340	12.9	14.0	11.0	sbr
#2	372x960	4	300	178x202	480	nf	586	13.3	-	16.3	* wld bf

Note:

- Gls* - glulam size: 178 x depth x length [mm]
- Nr* - number of rebars
- Rbl* - embedment length of the rebars [mm]
- Pls* - plate size width x length [mm] (thickness 12.7mm)
- Pde* - maximum load within elastic region (approximate) [kN]
- Pdf* - load at failure of reinforced bearing area [kN]
- Pdu* - load at the end of the test [kN]
- Ste* - equivalent stress under the plate (within elastic region) [MPa]
- Stf* - equivalent stress under the plate at failure [MPa]
- Stu* - equivalent stress under the plate at the end of the test [MPa]
- nf* - failure under plate not observed
- sf* - shear failure of the beam
- bf* - bearing failure of the supports
- sbr* - shear reinforcement and supports bearing reinforcement added
- ** - supports length 240mm
- wld* - rebars welded to the plate

Table 3.4 Results of the multi-rebar tests.

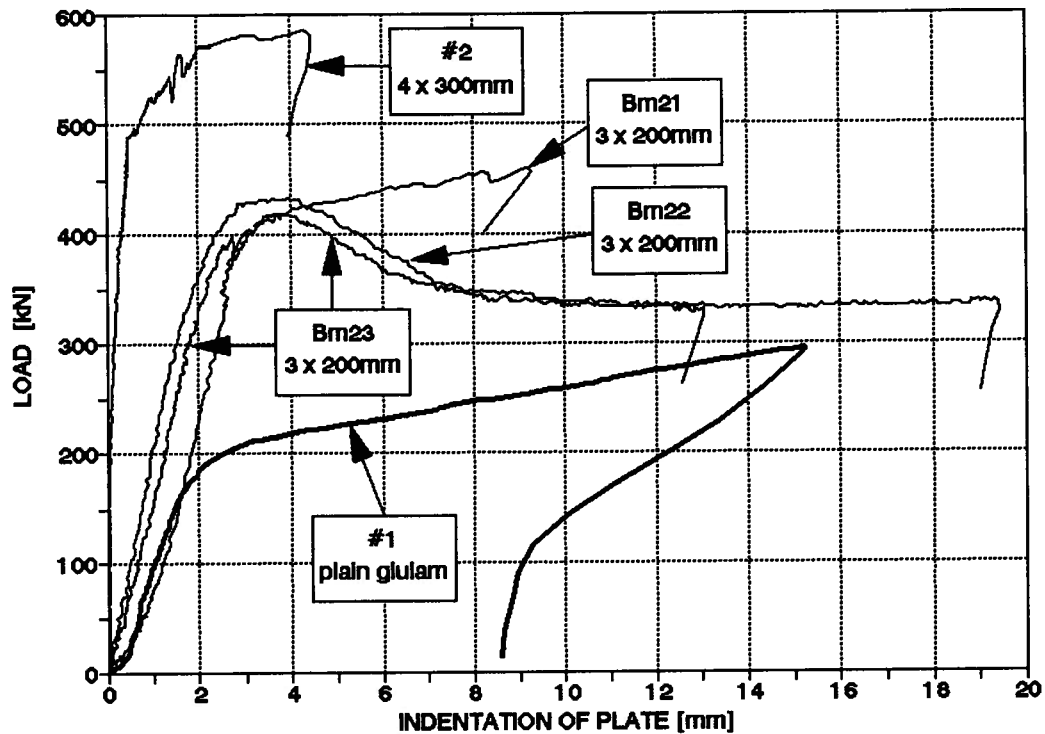


Fig.3.10 Comparison of L-D curves for the plain glulam specimen and the multi-rebar specimens.

A large increase in load carrying capacity was observed. It was proportional to the increase in the plate's surface and total rebars' length. The equivalent stress was comparable to that obtained with single rebar test. Unfortunately, the limitations of the Baldwin machine didn't allow larger specimens to be tested and shear failures occurred in two specimens as well as bearing failures at the supports. To prevent that, the specimen Bm22 was reinforced by gluing one #15 rebar 350mm long at each support (perpendicularly to the grain). Those rebars acted as bearing and shear reinforcement simultaneously. This reinforcement allowed for a clear picture of failure at the location of the compression force since the shear capacity of the glulam was increased.

One of the specimens (#2) had its rebars welded to the plate. In that case the increase of the stiffness was much more significant than in the specimens described in section 3.3.4 (about 8 times larger than the plain glulam specimen and 5 times larger than non-welded specimens).

Sp	Rbl mm	Pde kN	Pdf kN	Sre MPa	Srf MPa	Sgf MPa	Sbf MPa	Remarks
Specimens reinforced with one #10 rebar, protruding length 11mm								
R10-050c	50	32	33	320	330	0.7	16.5	embedment failure
R10-050d	"	32	32	320	320	0.7	16.0	"
R10-100c	100	55	64	550	640	1.4	16.0	"
R10-100d	"	54	56	540	560	1.3	14.0	"
R10-150a	150	54	79	540	790	1.8	13.2	rebar buckling
R10-150b	"	49	81	490	810	1.8	13.5	"
R10-150c	"	54	86	540	860	1.9	14.4	"
R10-150d	"	49	74	490	740	1.7	12.4	"
R10-200c	200	44	79	440	790	1.8	9.9	"
R10-200d	"	46	83	460	830	1.9	10.4	"
R10-250a	250	45	86	450	860	1.9	8.6	"
R10-250b	"	47	78	470	780	1.8	7.8	"
Specimens reinforced with one #15 rebar, protruding length 16mm								
R15-100c	100	56	58	280	290	1.3	9.7	embedment failure
R15-100d	"	59	62	295	310	1.4	10.4	"
R15-150c	150	85	96	425	480	2.2	10.7	"
R15-150d	"	82	88	410	440	2.0	9.8	"
R15-200c	200	86	109	430	545	2.4	9.1	"
R15-200d	"	89	113	445	565	2.5	9.4	"
R15-250c	250	91	126	455	630	2.8	8.4	"
R15-250d	"	91	130	455	650	2.9	8.7	rebar buckling
R15-320a	300	92	140	460	700	3.1	7.8	"

Table 3.5 continues on the next page...

Spec.	Rbl mm	Pde kN	Pdf kN	Sre MPa	Srf MPa	Sgf MPa	Sbf MPa	Remarks
R15-300c	300	78	115	390	575	2.6	6.4	rebar buckling
R15-300d	"	91	143	455	715	3.2	8.0	"
R15-350a	350	88	147	440	735	3.3	7.0	"
R15-350b	"	89	134	445	670	3.0	6.4	"
R15-400a *	400	91	151	455	755	3.4	6.3	"
R15-400b *	"	93	152	465	760	3.4	6.3	"

Note: Rbl - embedment length of the rebar [mm]
Pde - maximum load within elastic region (approximate) [kN]
Pdf - rebar's failure load [kN]
Sre - stress in the rebar at maximum load within elastic region [MPa]
Srf - stress in the rebar at failure load [MPa]
Sgf - stress in the glulam at failure load [MPa]
Sbf - bond stress between wood and glue at failure [MPa]
* - depth increased to 420mm

Table 3.5 Results of the preliminary tests with protruding rebars.

The embedment length established on the basis of these tests was 150mm for #10 rebar and 250mm for #15 rebar. In the specimens where the length of the rebar increased the embedment length the failure occurred due to buckling of the rebar (see Fig.3.11 and Fig.3.12). Where the length was smaller the shear around the glue coating (in the glulam) occurred without any signs of buckling of the rebar (see Fig.3.12).

The failure load of the specimens with full embedment length was larger (up to 18%) than the ultimate load for the same rebar tested in tension (compare with the values presented in section 2.2.1). Although the boundary between the elastic region and the plastic region in the compression test wasn't so distinct as in the tension test it can be assumed that it was located at the same load level.



Fig.3.11 *Specimens after the preliminary test. Note buckled rebars.*



Fig.3.12 *Specimens after the preliminary test. Note buckled rebar in the specimen with 300mm long rebar and glulam deformations around the rebar in the specimens with 250mm rebars.*

3.4.3 "Beam" Setup Tests.

Although the preliminary tests gave rather consistent results it was decided to verify them using the "beam" setup. Again, the reason for this was to eliminate possible influence of the support condition - specially in the specimens with long rebars.

The tests were conducted on the glulam beams of uniform size (178x372x1200mm), supported on 200mm long supports at each end. Only #15 rebars were tested. The protruding length of the rebar was equal to its diameter (i.e. 16mm).

The results of these tests are presented in Table 3.6. The typical load-deformation curves obtained during the tests are shown on Fig.3.13.

Spec.	Rbl mm	Pde kN	Pdf kN	Sre MPa	Srf MPa	Sbf MPa	Remarks
Bm24	100	60	65.5	300	328	10.9	embedment failure
Bm25	"	55	62.8	275	314	10.5	"
Bm26	"	57	62.8	285	314	10.5	"
Bm27	200	73	111.4	365	557	9.3	"
Bm28	"	88	112.0	440	560	9.4	"
Bm29	"	90	117.0	450	585	9.8	"
Bm30	300	93	148.0	465	730	8.2	rebar buckling
Bm31	"	92	154.3	460	772	8.6	"
Bm32	"	87	149.1	435	746	8.3	"

Note: Rbl - embedment length of the rebar [mm]
Pde - maximum load within elastic region (approximate) [kN]
Pdf - failure load [kN]
Sre - stress in the rebar at maximum load within elastic region [MPa]
Srf - stress in the rebar at failure load [MPa]
Sbf - bond stress between wood and glue at failure [MPa]

Table 3.6 Results of the beam tests with the protruding rebars.

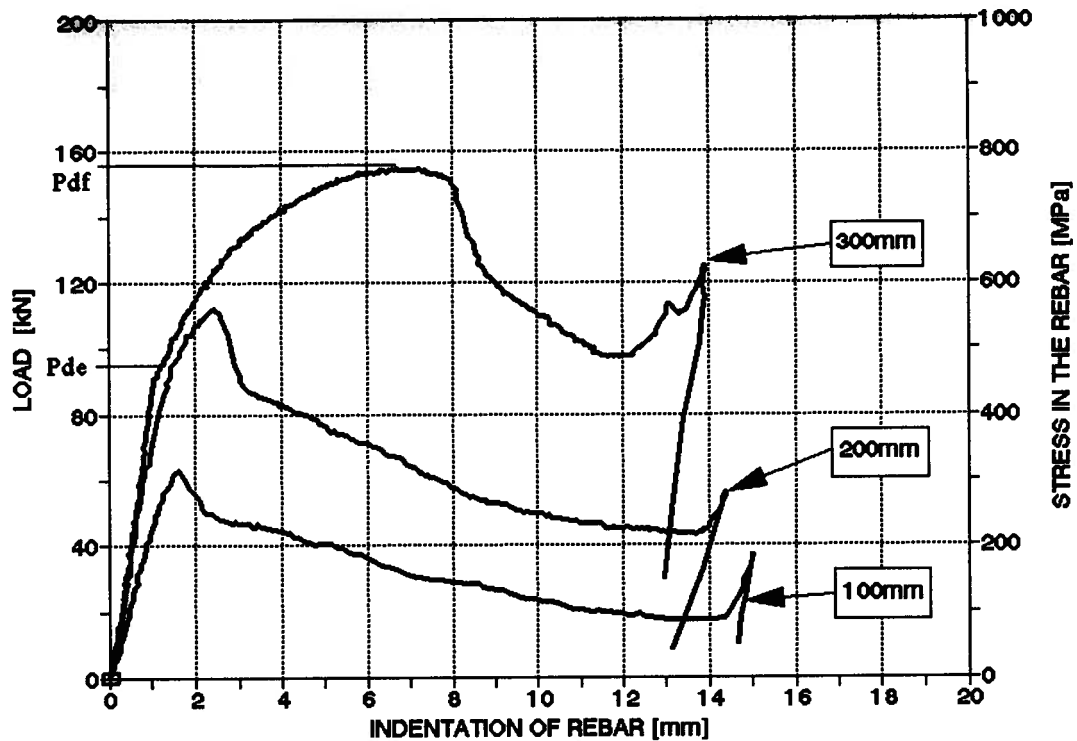


Fig.3.13 Typical load-deformation curves for the "beam" specimens with protruding rebars.

It can be seen from Table 3.6 that the results conducted on "beam" specimens confirmed results from the preliminary tests: the minimum embedment length for # 15 rebar loaded in compression was greater than 200mm and smaller than 300mm (embedment length established previously was 250mm). All specimens with the rebars longer than 200mm failed by buckling of top part of the rebar.

It was also noticed that after the embedment failure (100mm and 200mm rebars) the specimens were able to carry some load due to the friction around sheared surface and some bearing under the rebar. Although this carrying capacity decreased as the indentation increased but finally it stabilized at 40% of the failure load.

The plot of the failure loads for all specimens - regardless of the support condition - is presented on Fig.3.14.

- allows reliable and convenient connection method with supporting structure (specially in case of concrete walls or columns);
- can provide some resistance against uplift forces (tension perpendicular to the grain).

There are also some disadvantages:

- the rebars sticking out of the beam may cause some transportation (or storing) problems;
- the faces of the beam (top and bottom) cannot be switched;
- the connection is very sensitive to high temperatures and fire when not protected.

3.5 GUIDELINES FOR BEARING REINFORCEMENT WITH #15 REBARS.

The tests described in this chapter proved that gluing the rebars perpendicularly to the grain at the location of high concentrated compression force is a very effective way to increase the bearing capacity of the glulam member.

The following could be used as guidelines for bearing reinforcement where #15 rebars are used:

- the rebars should be glued-in perpendicularly to the grain;
- the hole diameter should be 19mm ($\frac{3}{4}$ ");
- for multi-rebar connection the spacing parallel to the grain should be 100mm (4"), and 75mm (3") perpendicularly to the grain;
- the steel plate should provide uniform distribution of the compression force to all glued-in rebars;
- the protruding part of the rebar should be shorter than the diameter of the rebar;
- the resistance of the glulam under the plate should be taken not more than the specified value in compression perpendicular to the grain;
- the elastic resistance of a single rebar 300mm or longer may be taken as its nominal resistance

i.e. 80kN (400MPa);

- the elastic resistance of a single rebar shorter than 300mm but longer than 100mm may be calculated according to the empirical formula:

$$\text{resistance [kN]} = 35 + 0.15 \times \text{embedment length [mm]}$$

- the combined resistance of the plate and the rebar may be taken as a summarized resistance of the plate and the rebar acting separately;
- the elastic resistance of up to 4 rebars may be assumed to be directly proportional to the number of rebars used.

3.6 CONCLUSIONS.

As can be seen from the tests presented in this chapter, the gluing of the rebar perpendicularly to the grain is a very effective way of increasing the bearing capacity of the glulam. According to obtained results the failure load and the elastic range of the bearing connection can be doubled with respect to the plain glulam bearing. The increase of the stiffness is even more significant and can exceed 2.5 times.

Although the tests conducted at UBC gave a relatively clear picture of the possible benefits coming from reinforcing of the glulam they didn't answer all questions related to that topic. Here are some of the unknowns that should be established during future research:

- spacing of the rebars,
- the group effect,
- evaluation of shear stresses around the rebar,
- evaluation of bearing stresses under the rebar,
- contribution of bearing reinforcement to the shear capacity of the glulam.

CHAPTER 4

BEAM-TO-COLUMN JOINTS.

4.1 TEST OBJECTIVES.

A moment resisting frame is widely used as a primary structural system for low-rise office or apartment buildings. It provides significant savings of materials when compared to statically determinate structures. It has also ability to resist lateral loads without additional bracing elements.

Unfortunately, glulam has not generally been successfully used for this type of structure in Canada. The main reason for this was a lack of a reliable connection methods which would be able to transfer bending moments under reversed loading conditions, i.e. in case of wind loads or seismic loads. The glued-in rebar connection is one possible means to solve that problem.

The primary objective of the tests described in this chapter was to confirm that expectation. The other objectives were:

- develop manufacturing and design techniques for the beam-to-column joints in a moment resisting frame,
- investigate the behaviour of glued-in rebar connection under cyclic loading,
- verify the effectiveness of the reinforcement perpendicular to the grain as described in chapter 3,
- investigate the behaviour of perpendicularly glued rebars under reversed loads (tension/compression).

The tests were prepared and conducted at the University of British Columbia between January and May 1994.

4.2 PRELIMINARY ANALYSIS OF THE FRAME FOR A MULTI-STOREY BUILDING.

It was decided that the tested connections should imitate the real structure's joints as closely as possible. To achieve this, a specific structure was chosen to provide background for later comparison. It was a 3-storey office building with a steel moment resisting frame as a main structural system. The complete design of that building can be found in "Metric Design Notes for Limit States Design in Steel" (Canadian Institute of Steel Construction, 1979).

The goal was to design a similar building using glulam members assuming that a moment resisting joint can be created. Then, a specific beam-to-column connection was chosen for further investigation. It was designed using the glued-in rebar idea (i.e. the rebars glued into the glulam providing a rigid connection between the beam and the column in the structure). It was then manufactured and tested in the laboratory. The last step was to compare the strength data collected during the tests with the design loads and deformations obtained from the analysis.

A full analysis of the building's frame can be found in Appendix B. Essential information and assumptions, as well as the results of the analysis are presented below for convenience.

4.2.1 Basic Dimensions.

The building was rectangular in shape, 63.0m long and 36.0m wide. The main frame was placed in the longitudinal direction. The span was 9.0m and the spacing 4.5m. The requirements for the clear heights were: 3.0m for the ground floor, and 2.7m for 2nd and 3rd floors. It was found that a storey height equal to 4.0m would satisfy those requirements.

It was assumed that the lateral forces in the direction perpendicular to the plane of the frame were resisted by bracing between frames.

A plan and a cross section of the building are shown on Fig.4.1.

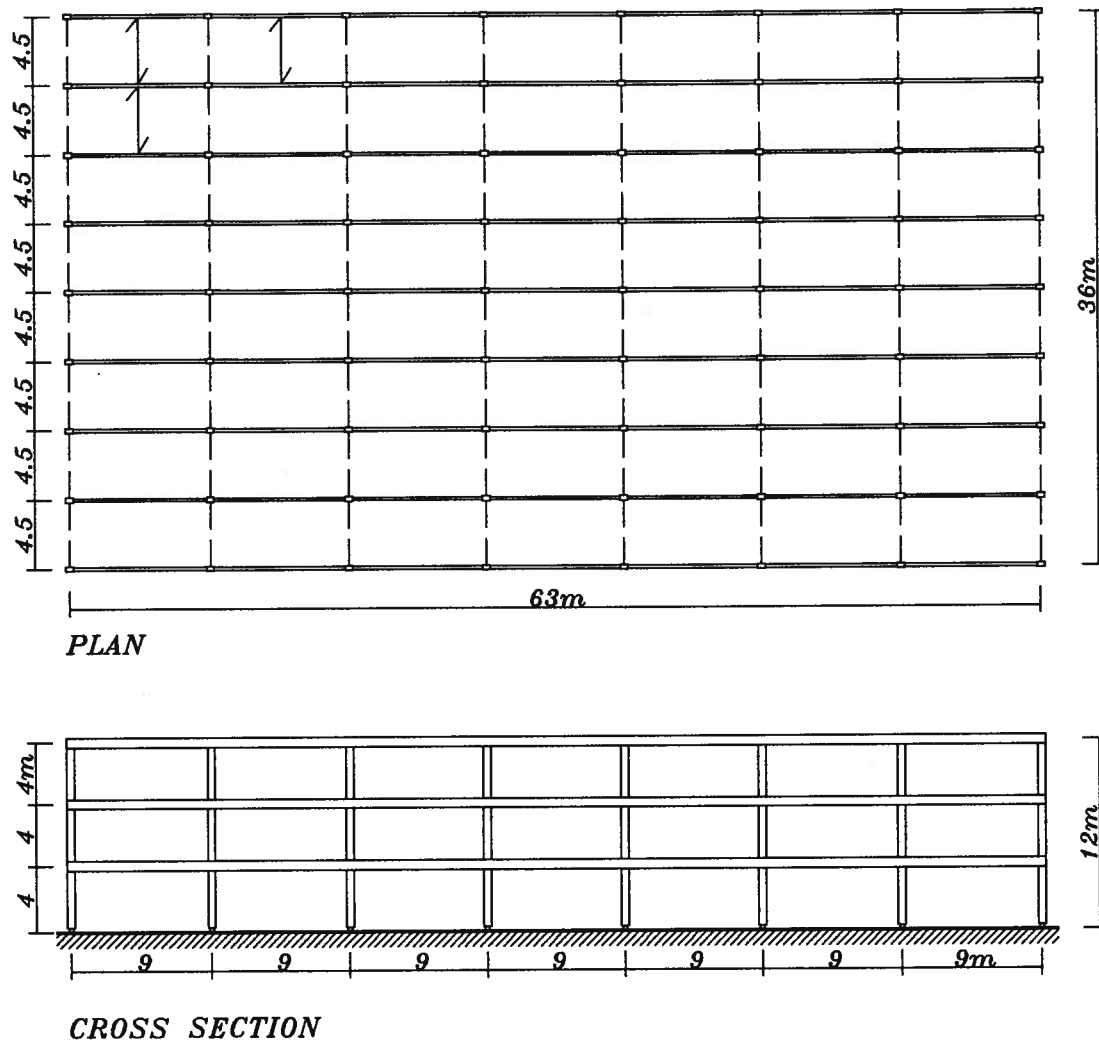


Fig.4.1 Overall dimensions of the building.

4.2.2 Loads and Load Combinations.

The following specified loads were calculated to act on the frame:

- | | |
|--------------------|------------------------|
| 1. floor dead load | 2.00 kN/m ² |
| 2. roof dead load | 1.15 kN/m ² |

3. floor live load	1.90 kN/m ²
4. snow load	2.30 kN/m ²
5. wind load on the windward wall (pressure)	0.43 kN/m ²
6. wind on the leeward wall (suction)	0.32 kN/m ²
7. wind load on the roof (suction)	0.75 kN/m ²
8. first storey seismic force	50 kN
9. second storey seismic force	101 kN
10. roof seismic force	131 kN

The following factored load combinations were included in the analysis:

- A. $1.25x(\text{Dead Loads}) + 1.5x(\text{Live Loads})$
- B. $1.25x(\text{Dead Loads}) + 1.5x(\text{Wind Loads})$
- C. $0.85x(\text{Dead Loads}) + 1.5x(\text{Wind Loads})$
- D. $1.25x(\text{Dead Loads}) + 1.0x(\text{Seismic Forces})$
- E. $0.85x(\text{Dead Loads}) + 1.0x(\text{Seismic Forces})$
- F. $1.25x(\text{Dead Loads}) + 0.7x\{1.5x(\text{Live Loads}) + 1.5x(\text{Wind Loads})\}$
- G. $1.25x(\text{Dead Loads}) + 0.7x\{1.5x(\text{Live Loads}) + 1.0x(\text{Seismic Forces})\}$

A load combination giving the largest internal forces in the element was chosen to design that element.

4.2.3 Design Forces.

The internal maximum forces governing the design of the elements of the frame are summarized in Table 4.1.

element	internal force governing design	load combination
first storey beam	bending moment 235 kNm	G
second storey beam	bending moment 191 kNm	G
roof beam	bending moment 172 kNm	A
first storey column	bending moment 159 kNm axial force 283 kN	D
second storey column	bending moment 78 kNm axial force 168 kN	G
third storey column	bending moment 80 kNm axial force 73 kN	G

Table 4.1 *Internal forces governing the design of the elements.*

4.2.4 Element Sizes.

The sizes of the elements and their resistance are presented in Table 4.2.

element	moment resistance [kNm]	axial resistance [kN]	size [mm]
first storey beam	250		130x684
second storey beam	202	-	130x608
roof beam	180		130x570
first storey column	221	1093	175x532
second storey column	99	439	130x418
third storey column	99	449	130x418

Table 4.2 *Calculated resistance and size of the elements.*

4.2.5 Configuration of the Elements.

There are two possible arrangements of the beams and the columns in the discussed frame. The first one in which the columns are continuous through the joints and the second one is where the beams are continuous. The second option was chosen for investigation in this research.

In this situation the beams required some moment resisting splice connections to make them continuous over the entire length of the building. This kind of the joint, using glued-in rebars idea, was described in chapter 1. The proposed locations of those joints are shown on Fig.4.2 and represent places with small moments.

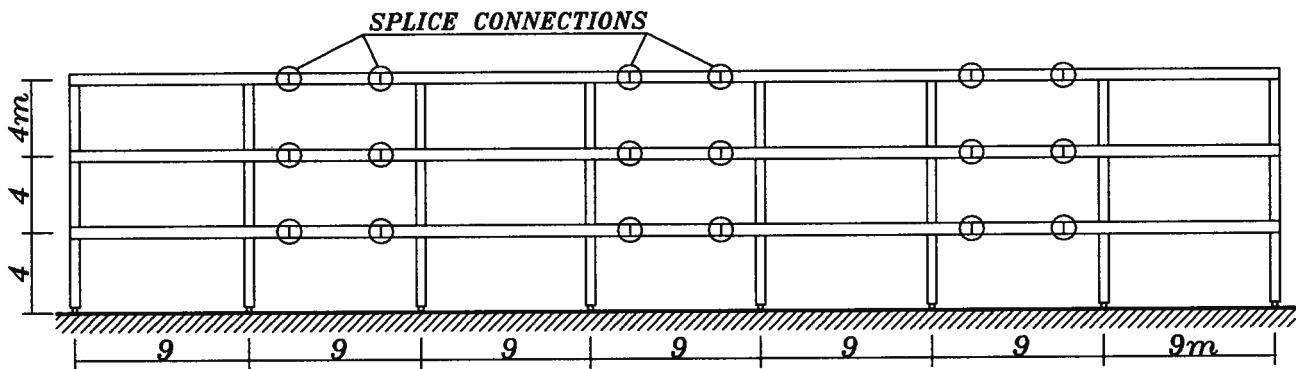


Fig.4.2 Locations of the splice joints in the beams.

The splice connections have one more very important function. It is fairly easy to shape the joint in that way so the steel elements will yield at certain load to create a plastic hinge at that location (for example by varying the thickness of the steel plates used in the connection). From the earthquake design point of view it is much safer that the plastic hinges are created in the beams than in the columns (so called "weak beams" approach). When an earthquake occurs plastic hinges in the beams do not create collapse of the structure but allow accommodation of large movements in a relatively safe way.

4.3 TEST SETUP.

It was decided that a connection of a second storey column to a second storey beam would be tested. That was an arbitrary choice and any other would be as good as this one. An axial force, a bending moment, and a shear force acted in that connection in a real structure. However, reflecting all those forces in a test would be not only difficult, but could also produce unclear picture of the failure. Because the main goal of the test was to prove the ability of the glued-in rebar connection to transfer bending moments it was decided to design the test setup in such way that it would create moments similar to those in a real joint. Furthermore, the moment in the beam was not of much interest because the beam was designed to be continuous over the joint. In effect, the moment in the column was the only one related to the real joint's forces.

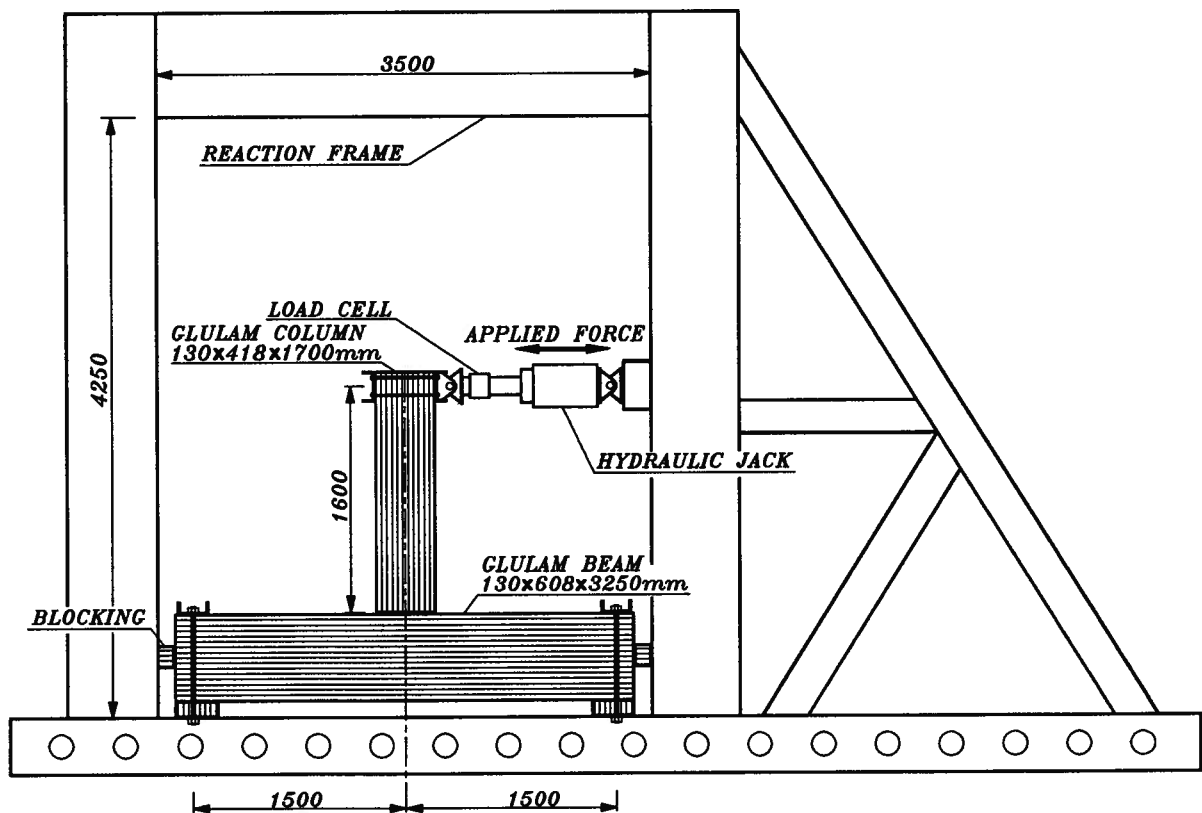


Fig.4.3 Overall dimensions of the reaction frame and the specimen.

Other moments (in the beam) resulted from the moment in the column and their magnitude was about 30% of those in the real joint. The magnitude of the shear forces created in the beam was about 40% of the real shear. The shear force in the real column was close to zero but it wasn't possible to avoid shear in the column during the test. In effect, the shear force in the test column was several times larger than the shear force in the real joint. An axial force in the column was not simulated at that stage of testing.

A total of 3 tests were performed. The testing took place in a steel reaction frame erected in the Structures Laboratory at UBC. The dimensions of the specimens were designed to fit the available space inside the frame and reflect the column moments as closely as possible. The overall dimensions of the frame and the specimen are shown on Fig.4.3.

The load was applied by a hydraulic jack equipped with a load cell. The working range of the jack was 0-445kN (0-100,000lb) and its stroke was 152mm (6"). The load from the jack was transferred to the column by two channels bolted together on opposite sides of the column and pin connected to the jack. The bearing length between the channels and the column was 200mm.

The beam was clamped down on both ends to the reaction frame. The bottom supports were provided by glulam blocks which created a 300mm bearing length. The top supports were provided by 200mm wide channels bolted down to the frame by 1½" threaded bars. The lateral movement of the specimen was prevented by blocking between the frame and both ends of the beam.

The out-of-plane movement of the specimen was restricted at 3 locations. The angles were bolted to the frame in front of and behind the beam at both ends. They were placed at the mid-height of the beam. Additionally, out-of-plane bracing was installed in the frame 1300mm above the top face of the beam (300mm below the applied force). The bracing allowed free in-plane movement of the column (within the jack's stroke). The bracing is shown on Fig.4.4.

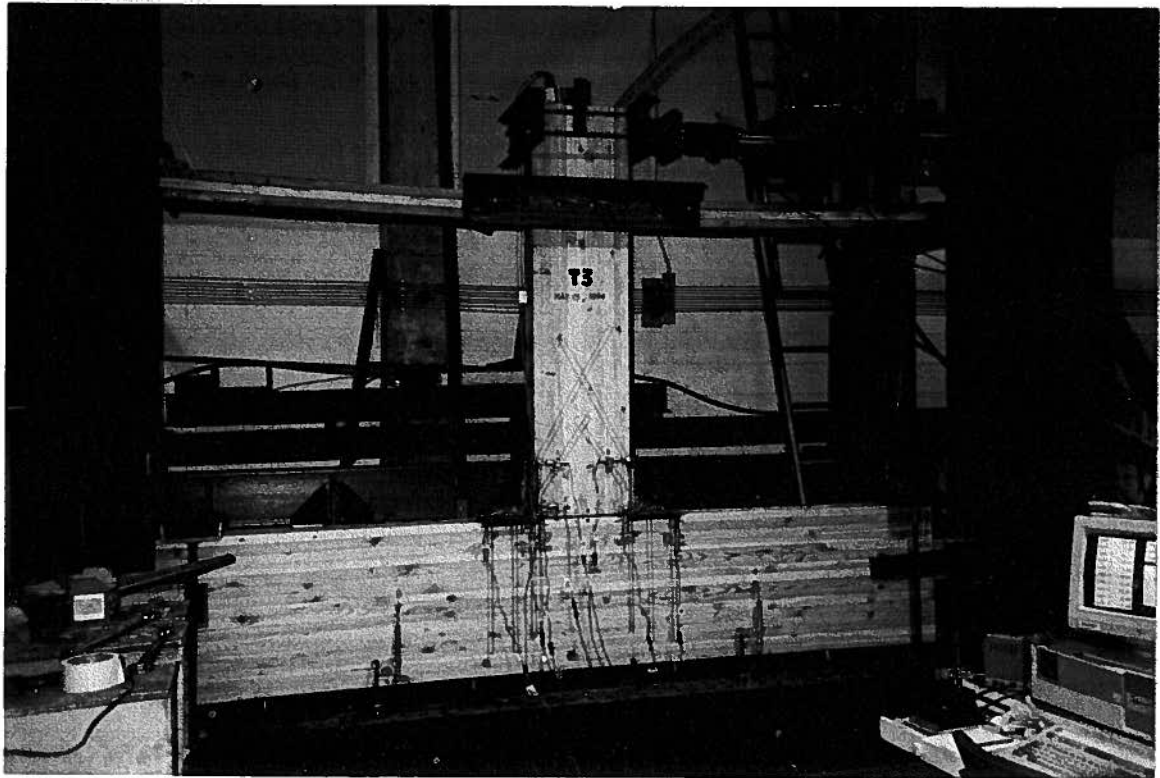


Fig.4.4 Photograph of the specimen T-3 in the reaction frame. Note a bracing just below the hydraulic jack.

The load was sequentially applied in both directions (i.e. pushing and pulling) to obtain reversing of the moments in the joint. The loading procedures varied slightly among the tests and they will be described in the sections related to the specific test (4.6 through 4.8). The forces acting on the specimen during the test, as well as the resulted moment and shear diagrams, are shown on Fig.4.5.

The following data were collected during the test:

- applied force measured by the load cell in the hydraulic jack,
- displacement of the jack's cylinder,
- three measurements of an overall movement of the specimen (LVDT 7 through 9),
- six displacements of various parts of the connection (LVDT 1 through 6),
- two displacements of the column versus the beam (LVDT 10 and LVDT 11) - these readings were recorded only during the last test (T-3).

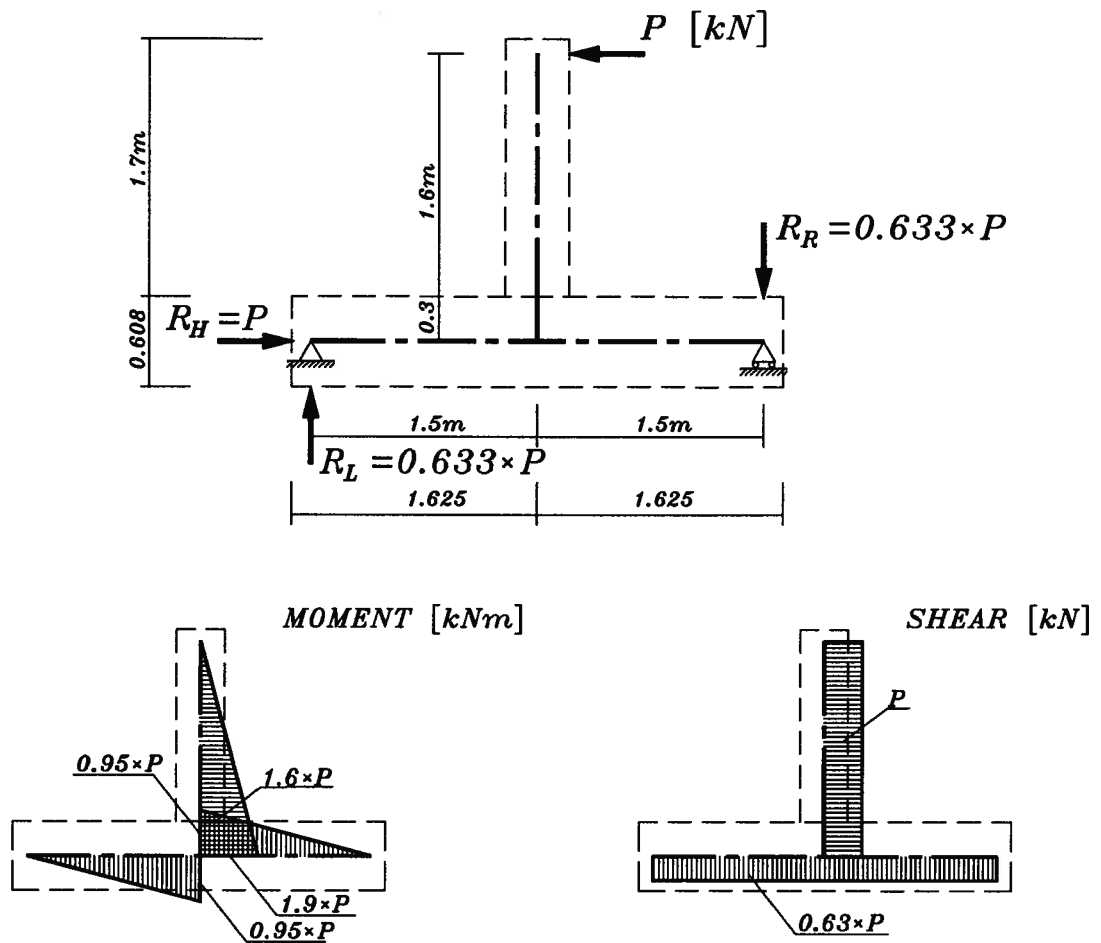


Fig.4.5 Load, reactions, and resulting moment and shear diagrams for the specimen. Note, only one direction of the load is shown.

All gauges, except LVDT 7, were placed on the front side of the glulam members. LVDT 7 was placed on top of the column at the center of its cross section. The general location of the displacement gauges is shown on Fig.4.6 and Fig.4.7.

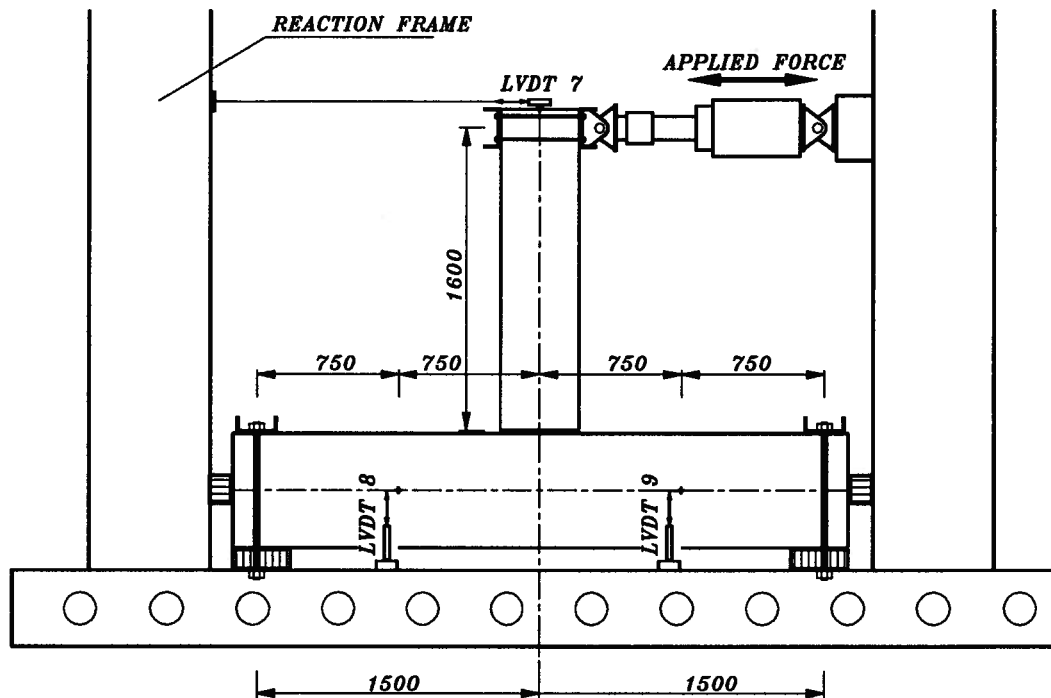


Fig.4.6 Locations of the gauges monitoring the overall movement of the specimen.

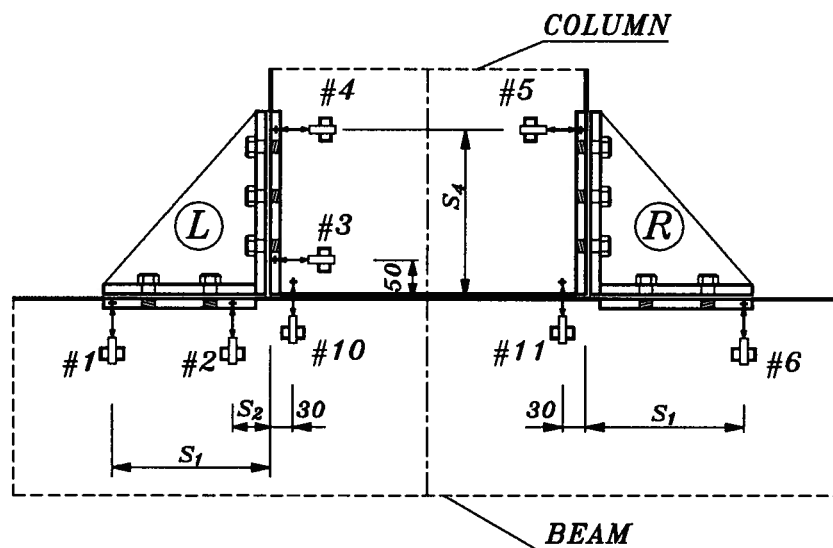


Fig.4.7 Locations of the gauges within the connection region.

The distances S_1 , S_2 , S_4 shown on Fig.4.7 varied according to the size of the plates used in different specimens. They will be quoted later when the specific tests are described.

4.4 MATERIALS.

GLULAM.

The glulam members were donated by Surrey Laminated Products Ltd, Surrey, B.C. They were beams and columns, grade 24-f made from Douglas Fir lumber. The elements were rectangular in shape and had the following dimensions:

columns: 130x418x1700mm

beams: 130x608x3250mm

REBARS.

Grade 400 (yield stress = 400MPa), deformed weldable reinforcing bars (rebars) were used. Two sizes of rebars were used: #15 and #20. Their nominal diameters were 16.0mm and 19.5mm respectively. Their nominal areas were 200mm² and 300mm² respectively. The nominal dimensions are equivalent to those of a plain round bar having the same mass per meter as the deformed bar. The results of the tension tests for #15 rebars have been already presented in chapter 2 (Table 2.2 and Fig.2.2). The results of the tension tests of #20 rebars are summarized in Table 4.3.

	yield		ultimate	
	load [kN]	stress [MPa]	load [kN]	stress [MPa]
Average (n=5)	144.2	481	202.2	674

Table 4.3 Results of tension tests performed on #20 rebars.

All rebars used in the tests were sandblasted prior to gluing.

PLATES.

The steel plates used for the testing were cut from flat bars of A-36 type steel (grade 300W). The specified minimum tensile strength of the steel was $F_u=450\text{MPa}$. The thickness of the plates was 12.7mm ($\frac{1}{2}$ "). There was only one location in the joint where the thicker plates ($\frac{3}{4}$ " or 1") were used in two last tests.

BOLTS.

The bolts used were imperial size 5/8, SAE-Grade 8, medium carbon alloy steel which were equivalent to grade ASTM-A490 specified in the steel design code (CAN3-S16.1-M89). Their characteristics were as follows:

nominal diameter [mm]:	15.88	
nominal area [mm ²]:	198	
specified minimum tensile strength, F_u [MPa]:	1035	(150,000psi)
factored shear resistance, [kN/bolt]:	57.6	(12,944lb)
factored tensile resistance, T_r [kN/bolt]:	103	(23,146lb)

The bolts' length were 24.5mm (1").

GLUE.

The epoxy glue IFC-SP was used for all connections. It is manufactured by Industrial Formulators of Canada Ltd., Burnaby, B.C. It consists of two parts: resin and hardener. The mixing ratio is 100 to 42 (by weight) respectively.

An average amount of glue use for gluing the rebars into the holes was as follows:

- #15 0.20 g/mm length of the rebar,
- #20 0.33 g/mm length of the rebar.

The pot life of the glue varied from 1 to 3 hours depending on the outside temperature and the volume of the glue used. The glued specimens were cured at least 7 days before testing in order to reach full strength of the glue.

4.5 JOINT DESIGN.

In this section, the design of the experimental connection is presented.

4.5.1 Joint Configuration.

The forces taking part in transferring the bending moment from the column to the beam are schematically shown on Fig.4.8.

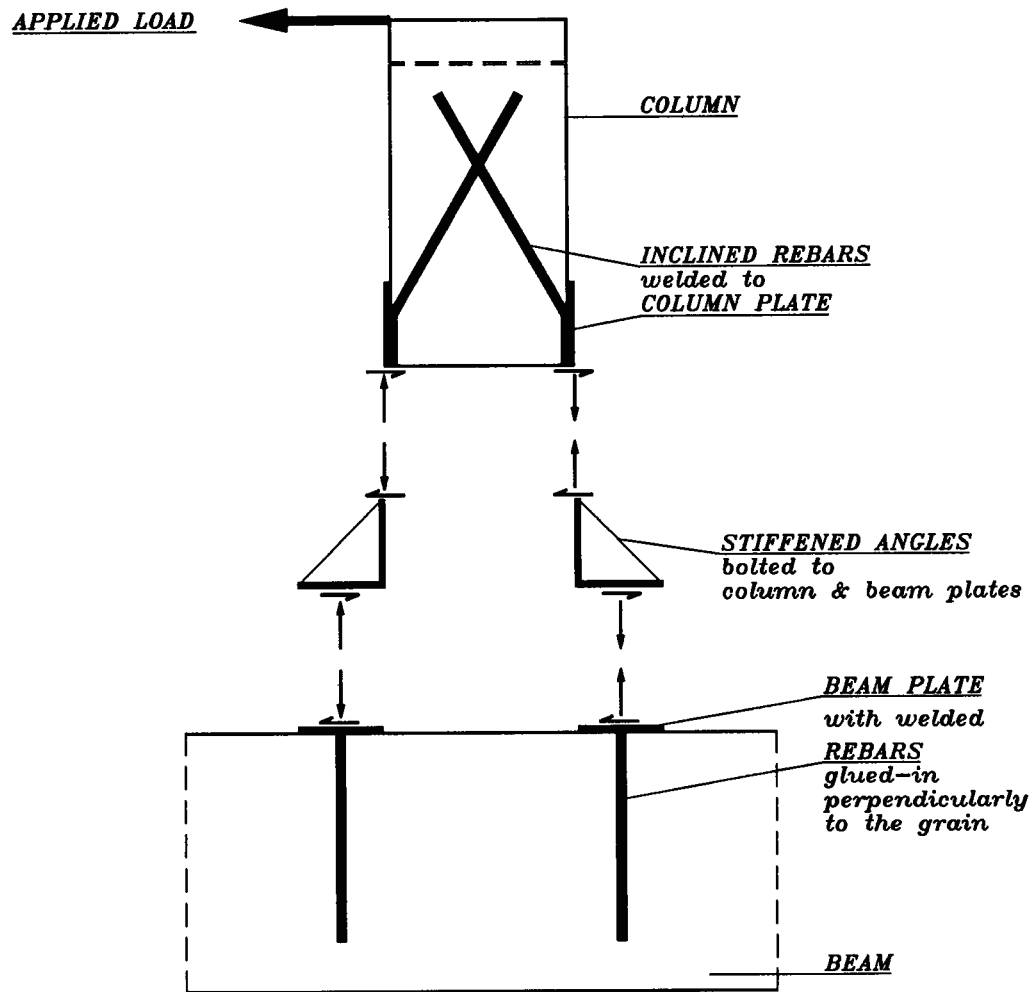


Fig.4.8 *Moment transfer from the column to the beam.*

It was assumed that the internal forces would be transferred from the column to the inclined, glued-in rebars and then to the column plates. The column plates and the beam plates were bolted to the stiffened angles. The beam plates were welded to the rebars glued perpendicularly to the grain into the beam. In effect, the moment from the column was transferred to the beam as a couple of forces.

4.5.2 Calculations.

It was assumed that the joint should be able to transfer the factored bending moment equal to 80kNm (see Table 4.1).

The first step was to determine the necessary number and size of the inclined rebars to carry that moment. As the top surface of the column plates was supposed to match the surface of the glulam it was calculated that the effective arm between the forces in the rebars (parallel to the column axis) was $a=377\text{mm}$ for #15 rebars or $a=373\text{mm}$ for #20 rebars (see Fig.4.9).

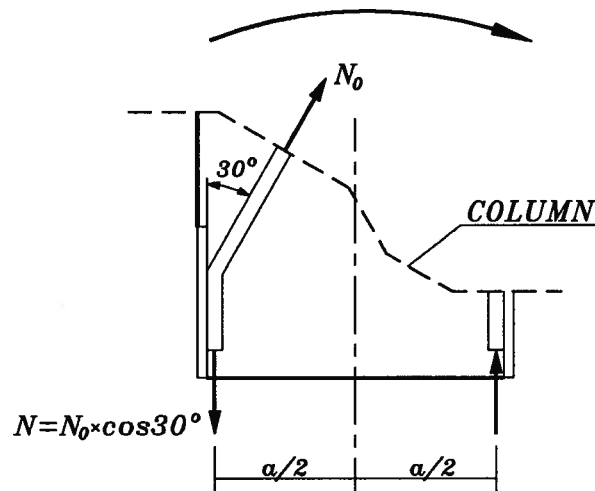


Fig.4.9 Forces created at the end of the column.

The tensile strength of the rebars N_O was established earlier during the material tests for both rebar sizes. The values used for the design are presented in Table 4.4.

rebar's size	yield load [kN]		ultimate load [kN]	
	0° N_{y0}	30° N_y	0° N_{u0}	30° N_u
#15	90	78	130	112
#20	140	121	200	173

Table 4.4 *Capability of glued-in rebars to transfer tension loads.*

It was desirable that the capacity of the rebars was close to the design moment (80kNm) at the yield level and close to the short term bending resistance of the column at the ultimate level. As the normal term loading resistance of the 130x418mm glulam section is 104kNm the short term resistance was estimated to be:

$$M_r = 104/0.8 = 130 \quad [\text{kNm}]$$

where 0.8 is the amplification factor due to the short term loading.

Two possible combinations of the rebars could be used to resist above moment: three #15 rebars (moment = $3 \times 112 \text{ kN} \times 0.377 \text{ m} = 127 \text{ kNm}$), or two #20 rebars (moment = $2 \times 173 \text{ kN} \times 0.373 \text{ m} = 129 \text{ kNm}$) per side of the connection. The second option was chosen. It was anticipated that the rebars would start to yield in tension at about 90kNm and would be able to transfer ultimate moment of 129kNm. Of course, to reach the ultimate level, the minimum embedment length for each rebar had to be ensured. For the rebars inclined at 30° to the grain this length was $L_e^{30} = 300 \text{ mm}$.

The second step was to establish the number of rebars glued into the beam. As #20 rebars were used in the column it was logical to use the same size rebars in the beam. The arm of the forces was larger than the arm in the column so the force in the beam rebars was smaller than in the column rebars. Therefore, it was decided to use two #20 rebars on each side of the connection. The minimum embedment length for those rebars was $L_e^{90} = 400 \text{ mm}$.

The next step was to design the bolted connection between the angle and the column as well as the beam plates. It was assumed that the column part would be loaded in shear only. The tension forces in those bolts weren't expected as any lateral force would be transfer in bearing between the column plate and the angle on the opposite side of the column. The shear force in all bolts was equal to the ultimate tension force in two inclined #20 rebars, i.e. $2 \times 173 = 346 \text{ kN}$. As the factored shear resistance of a single bolt was 57.6 kN , the required number of bolts for the column part was:

$$n_c = \frac{346}{57.6} = 6.0$$

The connection between the angle and the beam plate was loaded in tension (346 kN) as well as in shear. The total lateral force in the specimen at ultimate level was predicted to be:

$$P = \frac{125}{1.6} = 78.1 \text{ kN, assume } 80 \text{ kN.}$$

Therefore the shear force to be transferred by one side of the connection was 40 kN . According to the code CAN/CSA-S16.1-M89 the bolts should satisfy the relationship:

$$\frac{V_f^2}{m^2} + \beta T_f^2 \leq 0.56 \phi^2 \beta (A_b F_u)^2 n_b^2$$

where:

$$V_f = \text{total shear force} = 40 \text{ kN}$$

$$T_f = \text{total tension force} = 346 \text{ kN}$$

$$m = \text{number of shear planes} = 1$$

$$\beta = \text{an interaction factor} = 0.30$$

$$\phi = \text{resistance factor} = 0.67$$

$$A_b F_u = \text{specified minimum tensile force per bolt} = 205 \text{ kN}$$

$$n_b = \text{number of bolts}$$

therefore:

$$n_b \geq \left(\frac{\frac{V_f^2}{m^2} + \beta T_f^2}{0.56 \phi^2 \beta (A_b F_u)^2} \right)^{0.5}$$

$$n_b \geq \left(\frac{\frac{40^2}{1^2} + 0.30 \times 346^2}{0.56 \times 0.67^2 \times 0.30 \times 205^2} \right)^{0.5} = 3.4$$

As the bolted connections were not the parts of the joint which were intended to investigate, it was decided to overdesign them and use $n_c=8$ and $n_b=4$.

The last step was to check the strength of all welds between the rebars and the plates as well as in the angles. Because each of the specimens was different the sizes and location of welds varied accordingly. The general rule was to overdesign the welds and put them over the entire length provided by the elements.

4.5.3 Performance Expectations.

It was expected that the specimen would perform during the test as follows:

- at 78 kNm: nominal yielding point (400MPa) for the column rebars,
- 80 kNm: factored moment (design moment),
- 90 kNm: yielding point for the column rebars obtained from material tests,
- 124 kNm: short term shear resistance of the column (without considering the increase of the shear capacity due to the glued-in rebars),
- 129 kNm: ultimate strength of the column rebars (from tests),
- 130 kNm: short term bending resistance of the column,
- 148 kNm: nominal yielding point for the beam rebars,
- 173 kNm: yielding point for the beam rebars obtained from tests.

It was anticipated that the ultimate failure would take place in the column rebars on the tension side of the connection (both rebars at the same time).

The limits of the deformations for the building were as follows:

8 mm (4000mm/500) - total storey drift due to the specified wind load and gravity loads,

80 mm (4000mm/50) - interstorey deflection due to the earthquake loads.

The bending moments in the second storey column due to the specified wind and gravity loads were 37kNm and due to the earthquake loads were 77kNm.

As the specimen represented half of the storey height, the displacements measured during the tests by LVDT 7 (see Fig.4.6) reflected 50% of the storey drift. Therefore, it was desirable that the measured deflection would be less than 4mm at 37kNm and less than 40mm at 77kNm.

4.6 TEST T-1.

4.6.1 Joint Configuration.

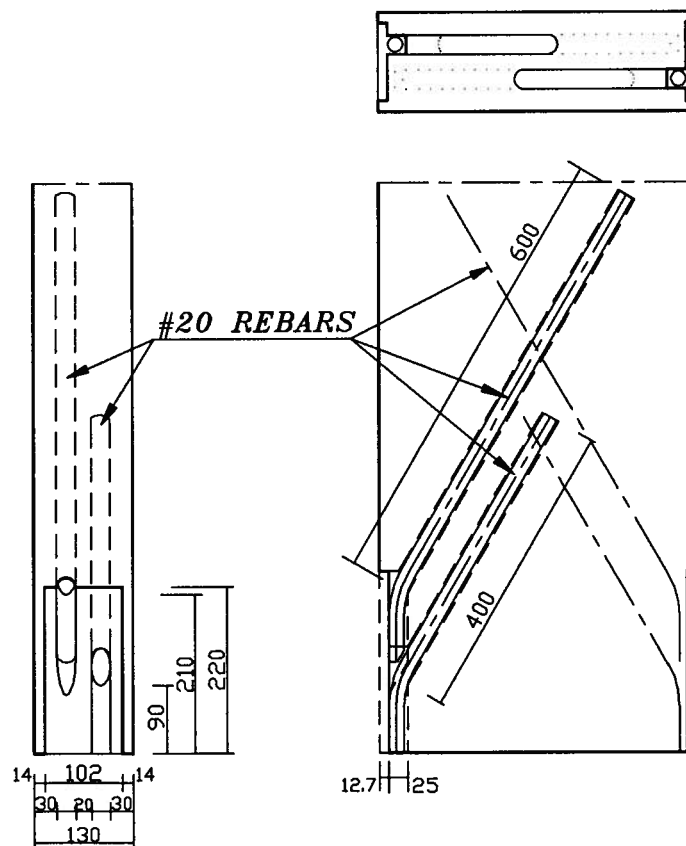


Fig.4.10 Locations of the column's plates and rebars in the specimen T-1.

Each side of the joint in the specimen T-1 consisted of:

- two inclined #20 rebars glued into the column (400mm and 600mm) located in two different planes,
- column plate 12.7x102x220mm with 8 tapped holes for 5/8 bolts,
- two #20 rebars glued into the beam perpendicularly to the grain (410mm each) located in one plane,
- beam plate 12.7x102x200mm with 4 tapped holes for 5/8 bolts,
- steel angle 12.7x200x220mm with a stiffener.

The joint in the specimen T-1 is shown on Fig.4.10 and Fig.4.11.

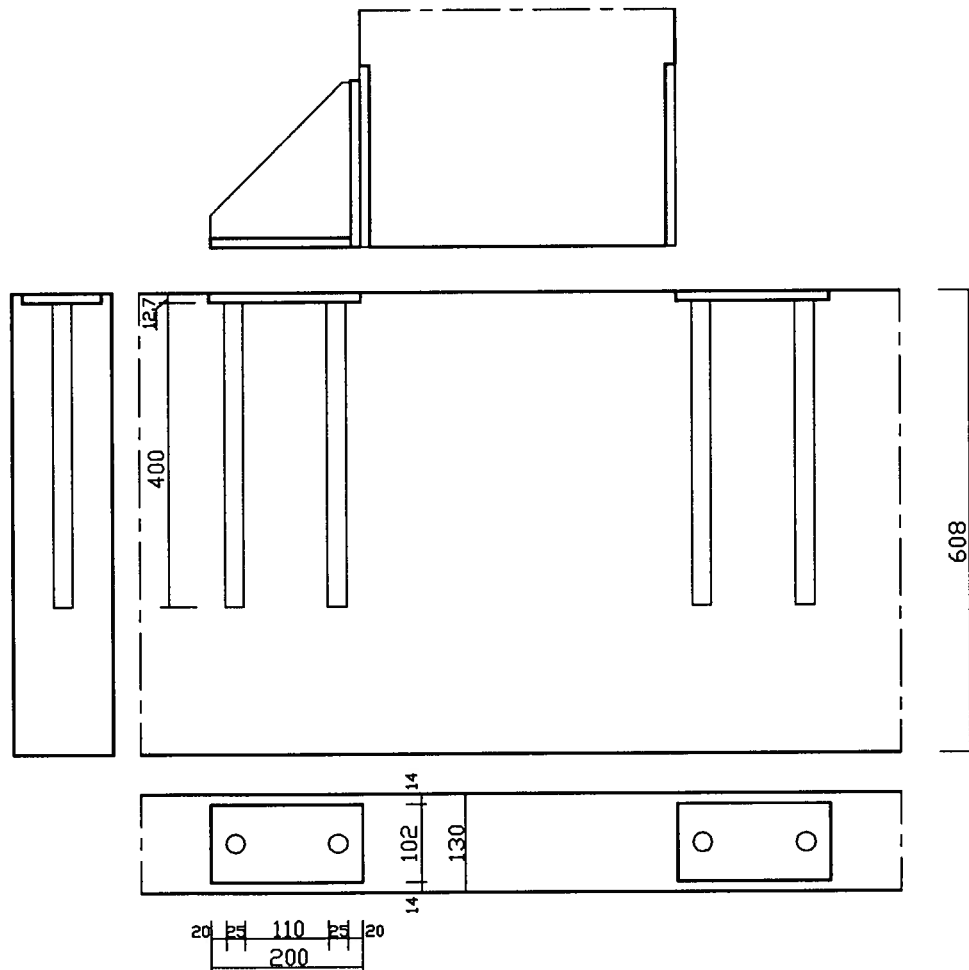


Fig.4.11 Locations of the beam's plates and rebars in the specimen T-1.

4.6.2 Manufacturing Steps.

The specimen T-1 was manufactured and assembled as follows:

1. woodworking on the column (routing grooves, drilling holes at 30° angle);
2. preparing the rebars and the plates for the column (cutting, bending and fitting the rebars, drilling and tapping the holes in the plates);
3. tackwelding the rebars to the plates, removing them from the holes and final welding away from the glulam;
4. sandblasting the steel assembly,
5. pouring the glue into the holes and inserting the rebars (one side of the column at a time);
6. repeating the procedures 1-5 with respect to the beam (the holes for the rebars were drilled at 90° angle);
7. preparing the angle plates (cutting and drilling) and welding the stiffeners,
8. bolting the stiffeners to the column plates and then to the beam plates,
9. curing the epoxy in the specimen at least 6 days.

The pictures of some of the above steps will be presented in section 4.7.2 as they were taken during manufacturing of the specimen T-2.

4.6.3 Testing Procedures.

After the glue set, the beam was positioned in the testing frame (refer to section 4.3), leveled, and bolted down to the frame. The column was then moved into the frame and bolted to the beam. The specimen T-1 in the testing frame is shown on Fig.4.12.

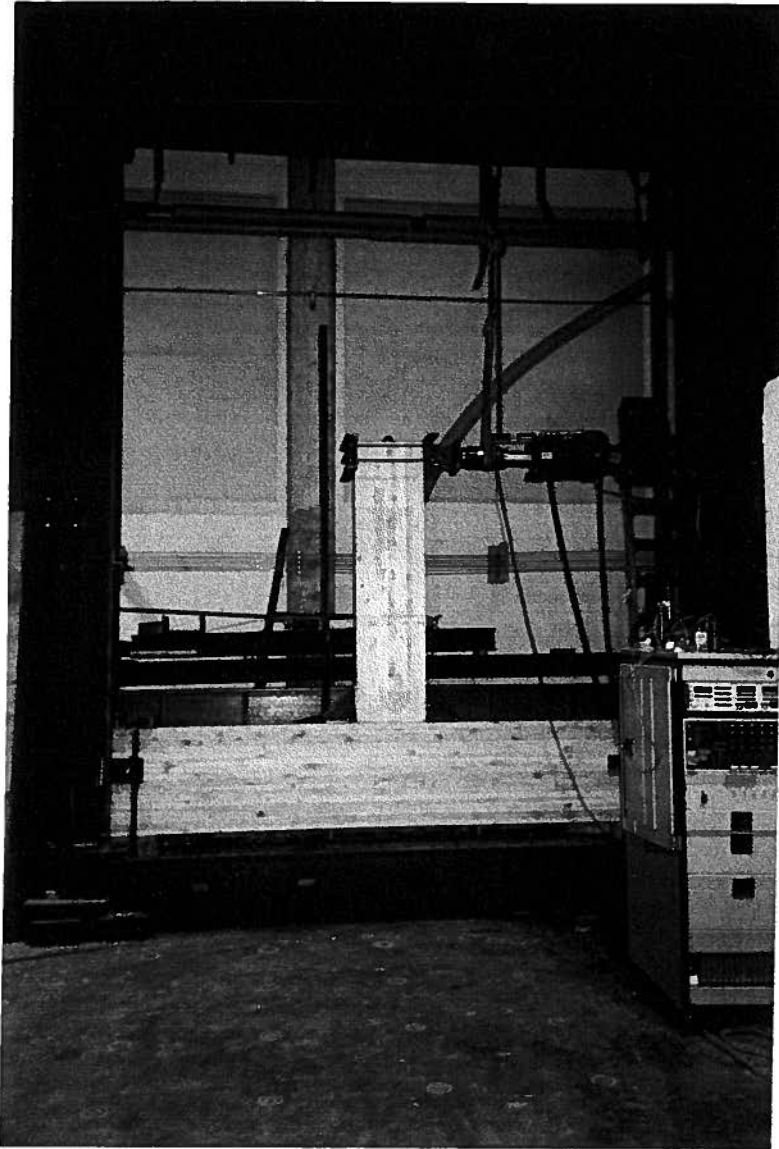


Fig.4.12 Specimen T-1 in the testing frame. Note: the lateral bracing has not been yet installed.

Next, the lateral bracing was installed and the hydraulic jack was connected to the column. Finally the displacement gauges were attached to the specimen and connected to the data acquisition system. The location of the gauges was described in section 4.3 and is shown on Fig.4.13. The distances shown on Fig.4.7 were: $S_1=180\text{mm}$, $S_2=50\text{mm}$, $S_4=200\text{mm}$.

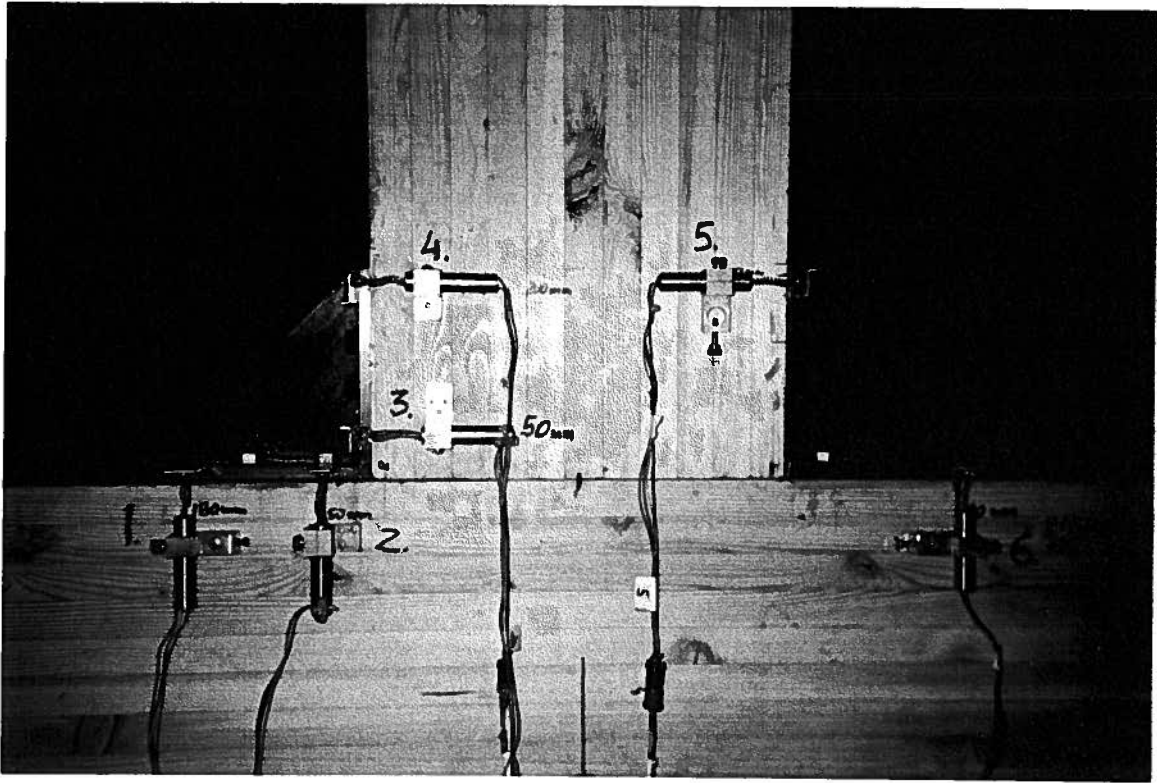


Fig.4.13 *Locations of the displacement gauges in the specimen T-1.*

The loading procedures for the test T-1 were as follows:

- | | |
|----------------------------------|-------------------------------|
| 1. load range from -10 to +10 kN | 2 cycles |
| 2. load range from -20 to +20 kN | 2 cycles |
| 3. load range from -40 to +40 kN | 4 cycles |
| 4. load range from -50 to +50 kN | 4 cycles |
| 5. final loading | from 0 to -54kN and to +60kN. |

Each cycle started from zero load point. The negative load was applied first (pushing the column from the right to the left) creating compression in the left hand side of the connection and tension in the right hand side of the connection. After reaching the desired load level the unloading started. After passing the zero load point the load was reversed (pulling the column) and increased to the similar level as the negative one. At that moment the compression was created in the right side of the connection and the tension in the left side.

The unloading to the zero load level ended the cycle.

As the displacement control was used during this test, the peak loads varied slightly from one cycle to the other.

The test was stopped after a characteristic loud sound (indicating rebar fracture) was heard.

4.6.4 Results.

OVERALL BEHAVIOUR.

The specimen T-1 failed by yielding and fracture of one of the inclined column rebars on the left side of the connection (see Fig.4.14 and Fig.4.15).



Fig.4.14 Joint in the specimen T-1 after failure.

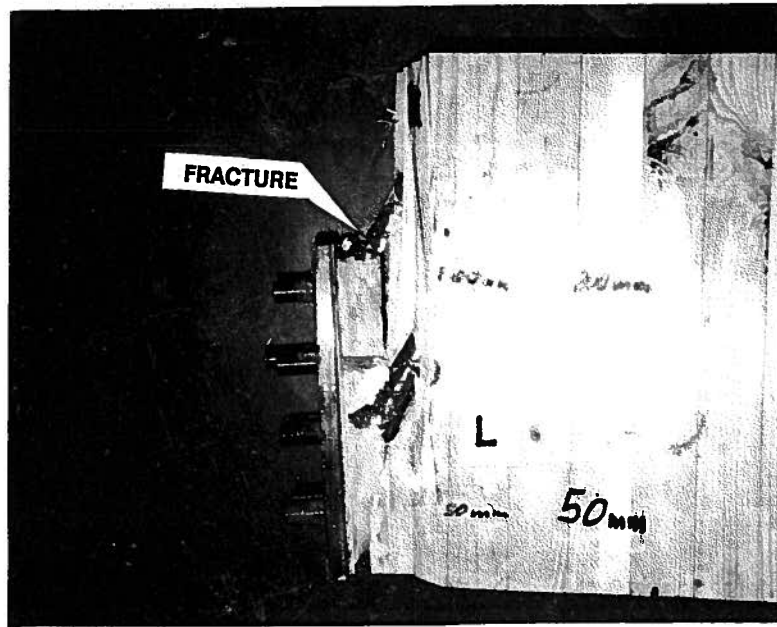


Fig.4.15 Left side of the column after exposing the rebars. Note the fracture of the upper rebar and the final inclination of the plate with respect to the laminations (originally parallel).

The ultimate load was 59.5kN which created the moment at the joint equal to 95kNm. Although, the moment was higher than the design requirement for the structure, this was only 74% of the expected ultimate moment (the bending stress in the glulam = 25.1MPa).

Surprisingly, only one rebar was broken - not both of them as was expected. That indicated uneven distribution of the load between the rebars.

Very large deformations of the glulam under the column plates were observed during the test (see Fig.4.14). An insufficient bearing resistance of the glulam was blamed for this effect. Probably, this was also the reason for uneven stress distribution between the column rebars.

MOMENT-DEFLECTION RELATIONSHIP.

The relationship between the moment at the joint and the deflection of the end of the column is presented on Fig.4.16.

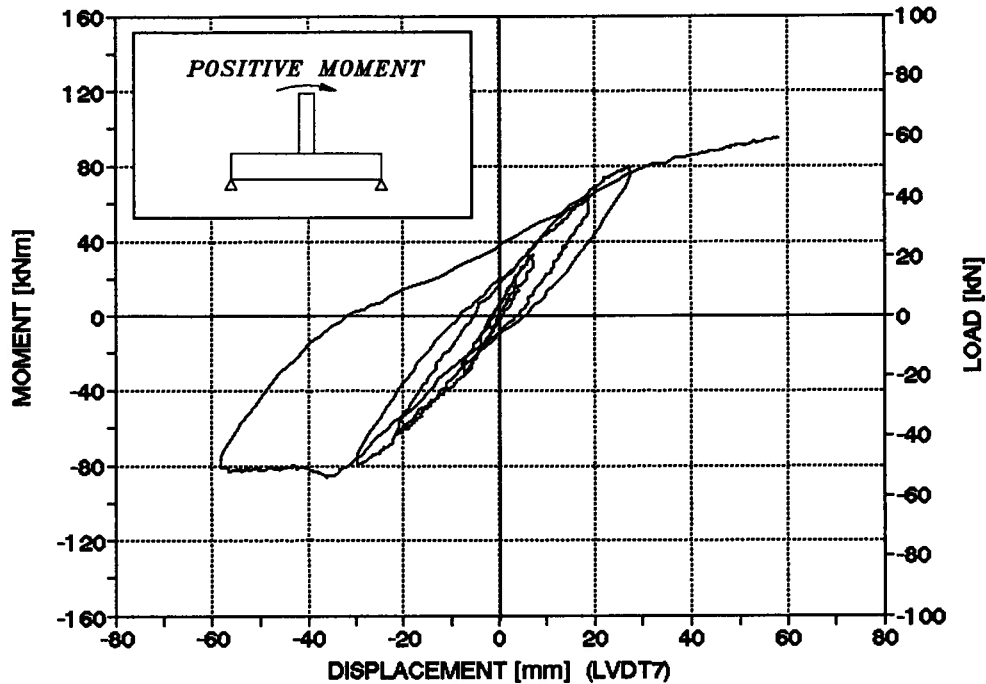


Fig.4.16 Deflections of the column's free end during the test T-1
(first cycles at each load level are presented).

The moment-deflection (M-D) relationship can be described as linear up to 32kNm (20kN load level). At that point the deflection of the top of the column reached 7.3mm. At higher loads, pinching of the M-D curve was observed. Approximately at the same time the crushing of the glulam under the column plates started. The average slope of the curve decreased as the load increased. At a load level 50kN it was only 55% of the slope observed in the first cycle (10kN level).

The specimen barely reached the design level of 80kNm. Immediately after that the column rebars on the right side of the connection started to yield (moment = -86kNm). Very large deformations of the joint region were observed. After the load was reversed, a similar effect was observed on the left side of the connection. Finally, the specimen failed by rebar fracture at a moment equal to 95kNm.

The serviceability limit for the wind loads (at 37kNm) was exceeded by more than

twice. The corresponding deflection was 9.4mm. However, the limit for the earthquake loads was satisfied with only 27.6mm deflection (equal to 69% of the limit). Also the final large deformations within the joint prior to the failure were desirable from the earthquake engineering point of view.

THE COMPONENTS OF THE TOTAL DEFLECTION.

The total deflection d_t (measured by LVDT 7) consisted of three main components:

- d_b - displacement due to the rotation of the beam,
- d_c - displacement due to the deformation of the glulam column,
- d_j - displacement due to the deformations between the glulam and the plates as well as rebars yielding.

There was also a component due to the transverse movement of the whole specimen (in the direction of applied force) but this was considered to be small with respect to the other components.

The percentage share of those three components in the total deflection of the column is presented in Table 4.5.

load kN	moment kNm	d_b %	d_c %	d_j %	d_t [100%] mm
10	16	19	48	33	2.7
20	32	12	35	53	7.5
40	64	12	27	61	19.3
50	80	10	22	68	29.4
60	96	6.5	13.5	80	58.2

Table 4.5 *Components of the total deflection in test T-1.*

In the table above, d_b was calculated from the test data (based on the readings from LVDT 8 and LVDT 9), d_c was calculated from the theoretical formula for displacement in a

cantilever glulam beam, d_j was calculated as $d_t - d_b - d_c$.

It is clear that the component associated with the plates and the rebars behaviour became dominant early in the test. At the ultimate load it counted for 75% of the total displacement. It is obvious that reducing d_j would improve the overall behaviour of the joint.

THE BEHAVIOUR OF THE COLUMN PART OF THE JOINT.

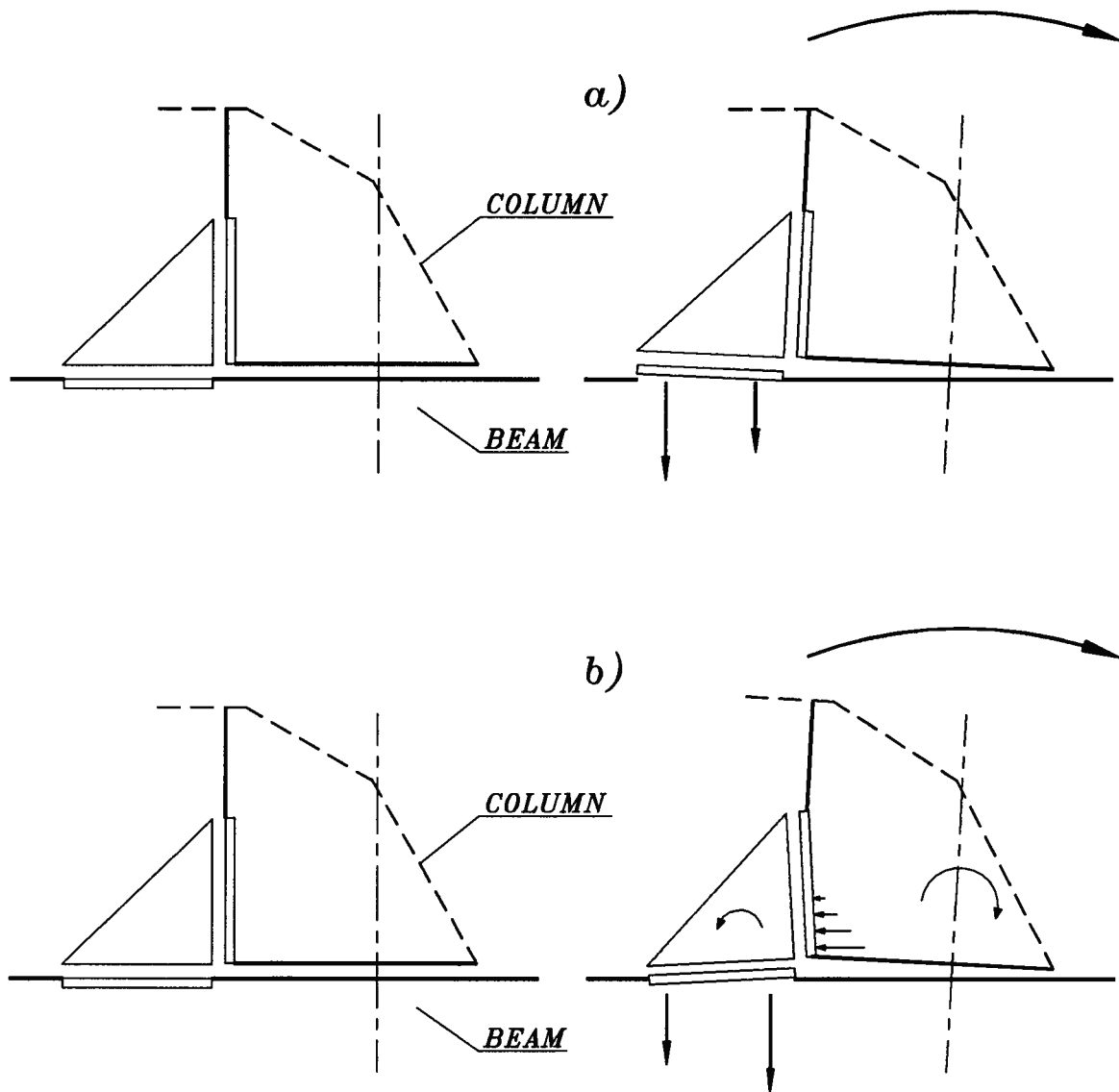


Fig.4.17 Behaviour of the tension side of the connection: a) desired, b) observed.

The main problem observed during the test was insufficient resistance of the glulam in bearing under the column plates. In fact, at a load level 40kN and higher, the connection between the column and the column plates could not be considered rigid. Therefore, the stress distribution in the rebars was different than assumed before the test. That could be the main reason why only the outer rebar was broken at the end of the test. The difference between the desired and observed behaviour of the connection is shown on Fig.4.17.

The bolted connection between the column plate and the angle did not cause any problems.

THE BEHAVIOUR OF THE BEAM PART OF THE JOINT.

The bearing problem under the column plates also affected the stress distribution in the beam rebars. As indicated on Fig.4.17, the tension forces, which were created in those rebars, were different from the assumed forces. Although the rebars behaved as expected (no yielding) there were problems with the bolted connection and the bending resistance of the plate. At the very end of the test the bolts closest to the inner beam rebar failed. In fact, it was the thread in the plate which failed in tension. It turned out that the stiffness of the beam plate was insufficient for those loads. Due to the overload of the inner bolts the moment created in the plate between the bolts and the inner rebar exceeded the bending resistance of the plate (see Fig.4.18)

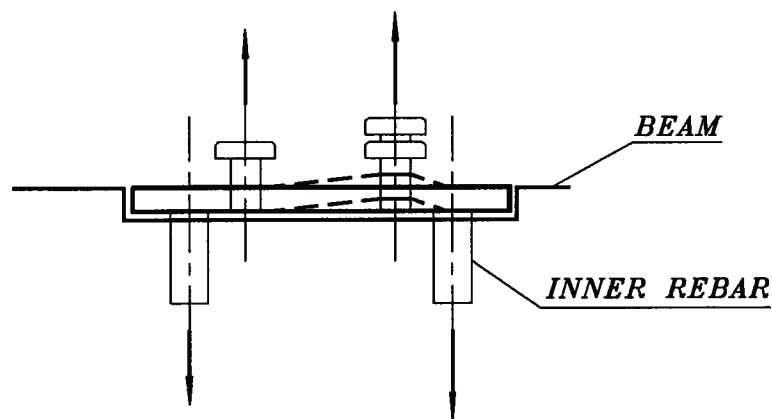


Fig.4.18 *Bending of the beam plate.*

4.6.5 Comments.

It was expected that some problems associated with bearing under the plates would arise during the test. It was decided, however, that specimen T-1 shouldn't be reinforced in compression perpendicular to the grain. The test showed how serious the bearing problem was and indicated that the reinforcement perpendicular to the grain was necessary under the column plates.

The magnitude of deformations did not come as a great surprise but the ultimate load was significantly less than expected. The analysis of the data indicated, however, that the compression perpendicular to the grain was the cause of the problems in both cases.

It was also decided that the thickness of the beam plates should be increased in the subsequent specimens. That would prevent bending of those plates. To avoid pull-out of the bolts from the beam plates, it was suggested to increase the number of the beam bolts from 4 to 6.

4.7 TEST T-2.

4.7.1 Joint Configuration.

The specimen T-2 was an improved version based upon the experience with the specimen T-1. The compression reinforcement added was two #15 rebars glued perpendicularly to the grain under the column plates (see Fig.4.19). They were going through the entire depth of the column. Those rebars were flush with the surface of the glulam under the plates. Some minor changes to the joint configuration are listed below:

- beam plates thickness was increased from 12.7 (½") to 25.4mm (1"),
- six instead of four bolts were used to connect the beam plates to the angles,
- the beam rebars and the beam bolts were located at the same cross section to reduce

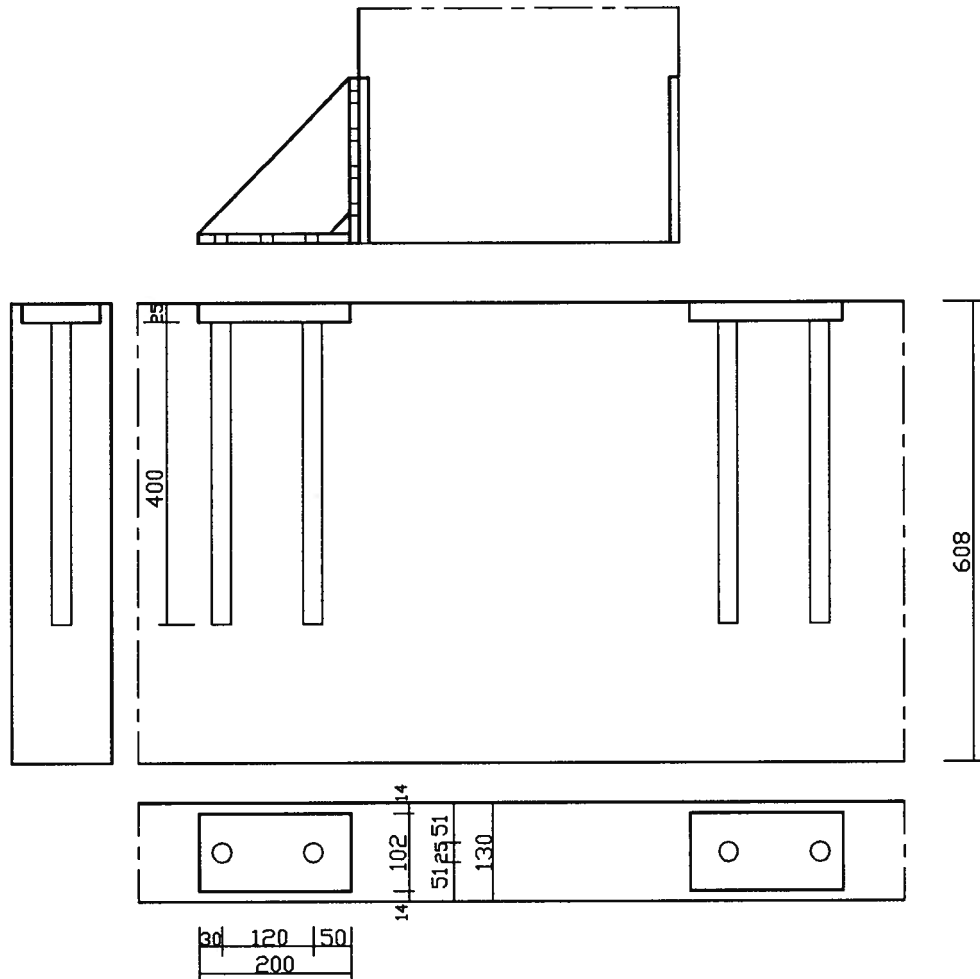


Fig.4.20 Locations of the beam's plates and rebar in the specimen T-2.

4.7.2 Manufacturing Steps.

The specimen T-2 was manufactured and assembled in a similar way as the specimen T-1 (refer to section 4.6.2). The only change was the gluing of the perpendicular rebar in the column. This activity was performed after routing the grooves for the column plates and before gluing the inclined rebar into the column.

Different phases of the manufacturing process of the column are presented on Fig.4.21 through 4.25.

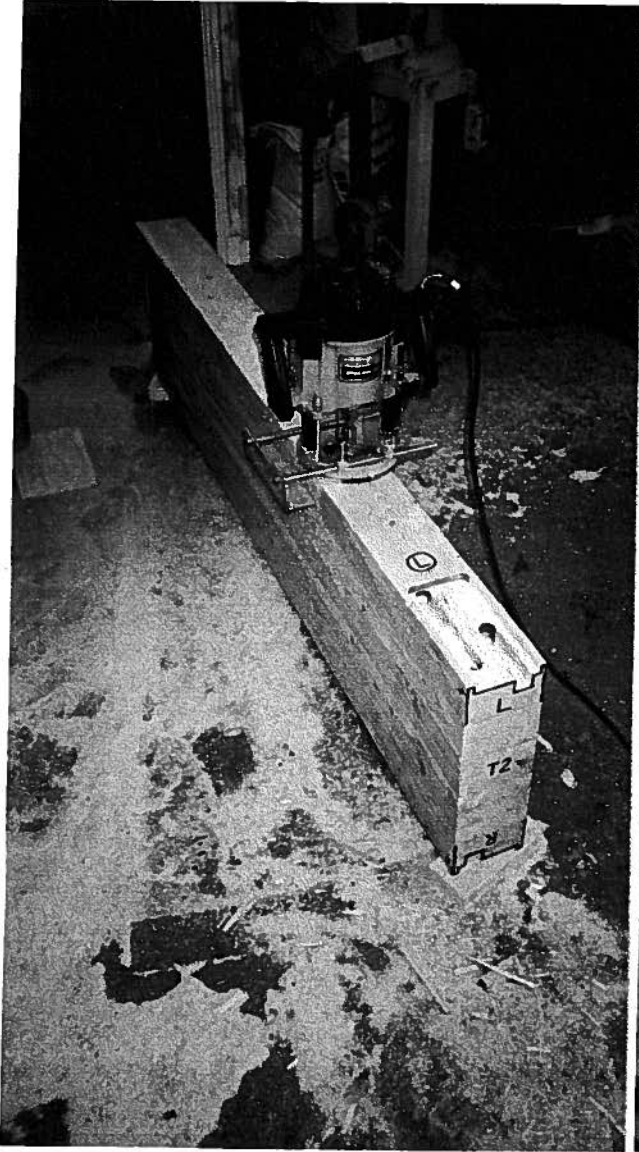


Fig.4.21 *Routing grooves.*

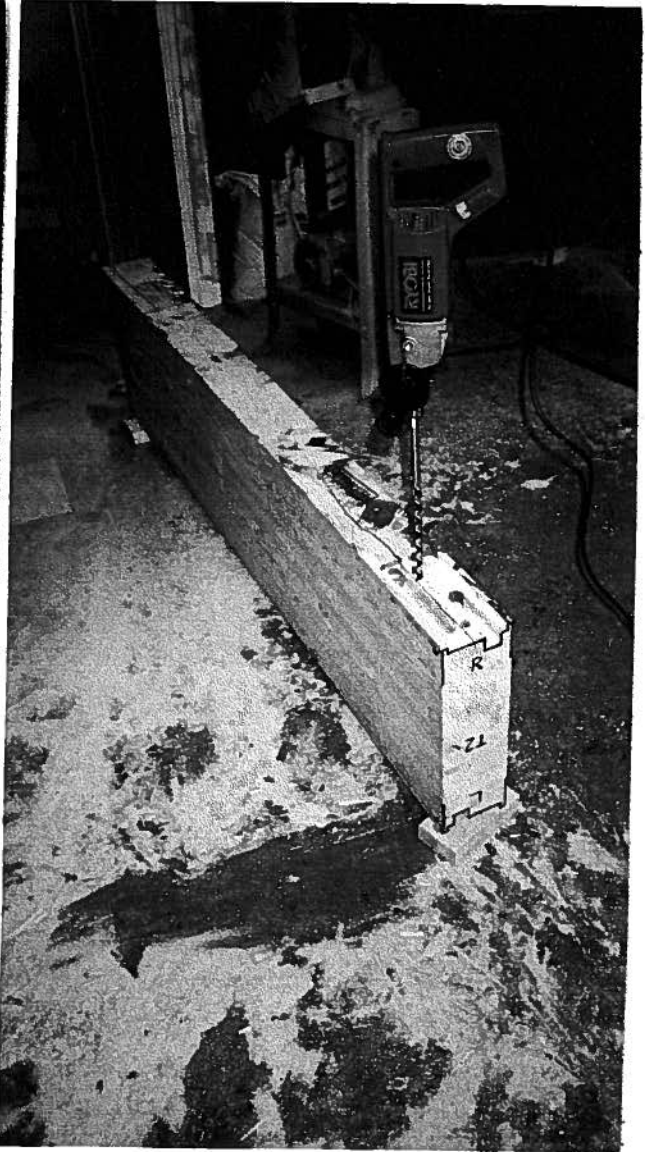


Fig.4.22 *Drilling perpendicular holes.*

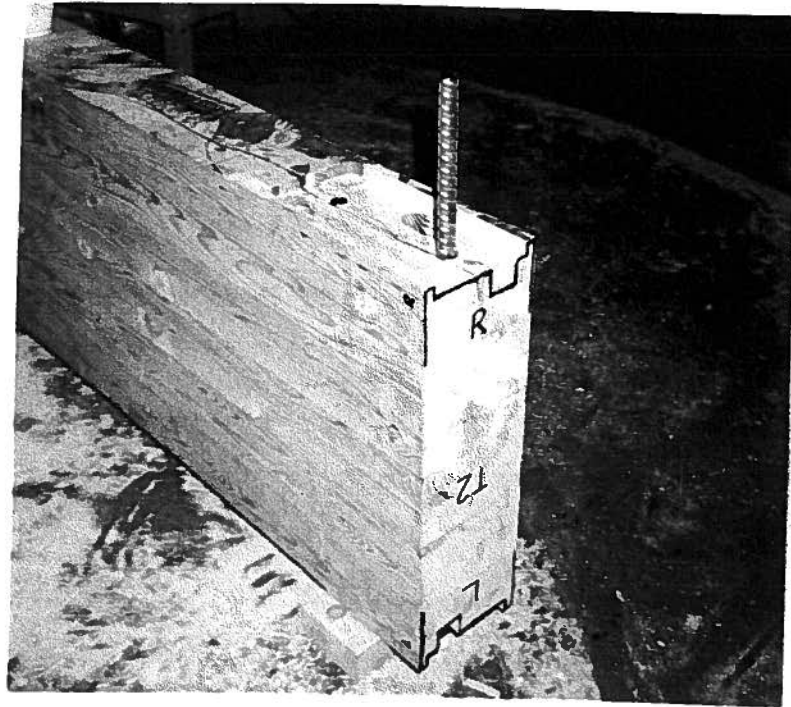


Fig.4.23 *Gluing perpendicular rebars.*



Fig.4.24 *Drilling inclined holes.*



Fig.4.25 Fitting inclined rebars and plates.

4.7.3 Testing Procedures.

The assembly of the specimen T-2 in the testing frame proceeded exactly the same as it was described for the specimen T-1 (see section 4.6.3).

The location of the gauges was slightly different than previously. The distances shown on Fig.4.7 were: $S_1=200\text{mm}$, $S_2=50\text{mm}$, $S_4=200\text{mm}$.

The loading procedures for the test T-2 were as follows:

1. load range from -10 to +10 kN 4 cycles
2. load range from -20 to +20 kN 4 cycles
3. load range from -30 to +30 kN 4 cycles
4. load range from -40 to +40 kN 4 cycles
5. load range from -50 to +50 kN 4 cycles
6. load range from -60 to +60 kN 4 cycles
7. final loading from 0 to -61kN and to +40kN.

Load control was used throughout the test (except the final loading) with sinusoidal wave form (see Fig.4.26).

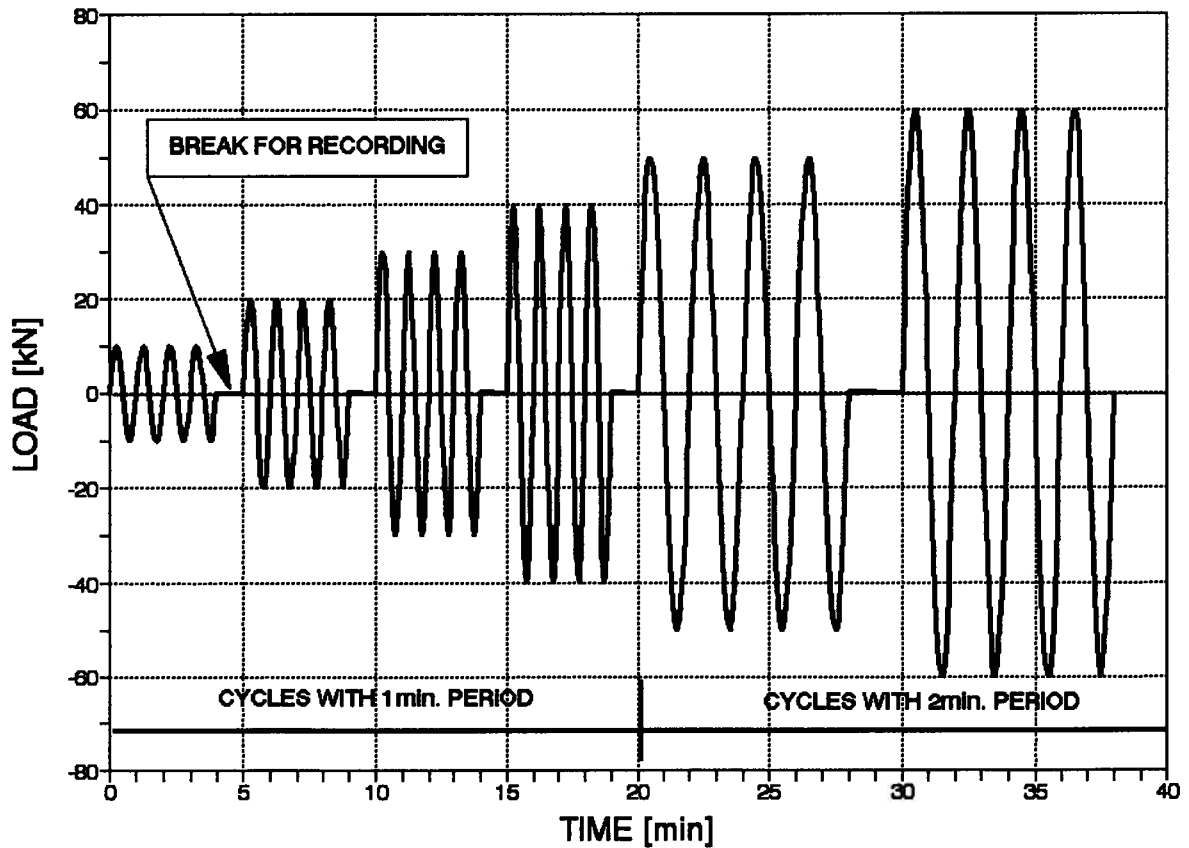


Fig.4.26 Loading procedures for the specimen T-2.

The period of the load cycles was 1 minute up to 40 kN load and 2 minutes over 40 kN load.

Each cycle started from zero load point. The positive load was applied first (pulling the column from the left to the right) creating compression in the right hand side of the connection and tension in the left hand side of the connection.

Displacement control was used during final loading (not shown on Fig.4.26) because of large displacements. In fact, the test was terminated without obvious failure of the glulam or steel elements due to the limitation of the stroke of the hydraulic jack.

4.7.4 Results.

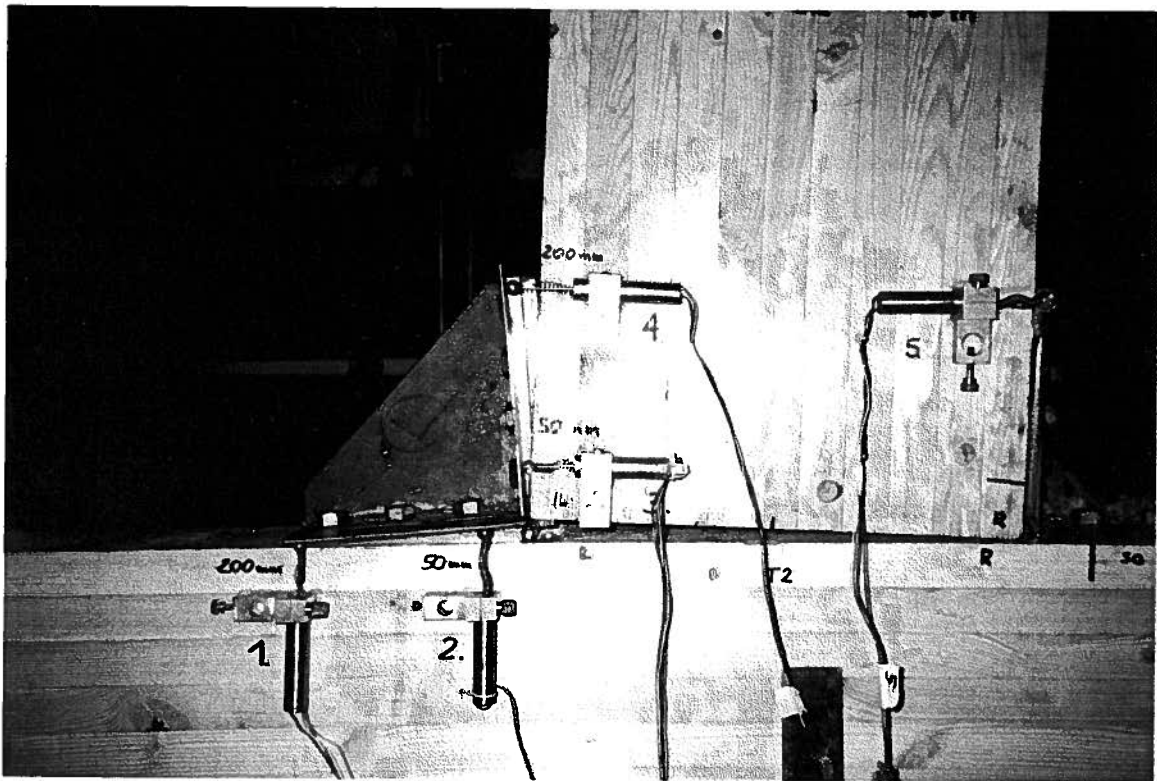


Fig.4.27 Joint in the specimen T-2 during final loading.

OVERALL BEHAVIOUR.

A rebar fracture in the specimen T-2 was not observed during the test. However the deformations of the joint (see Fig.4.27) indicated some kind of hidden failure.

After the test, the column rebars were exposed and it turned out that the weld between the outer rebar and the left column plate started to tear (see Fig.4.28). The fracture also involved some parts of that rebar so it was not a clear weld failure.

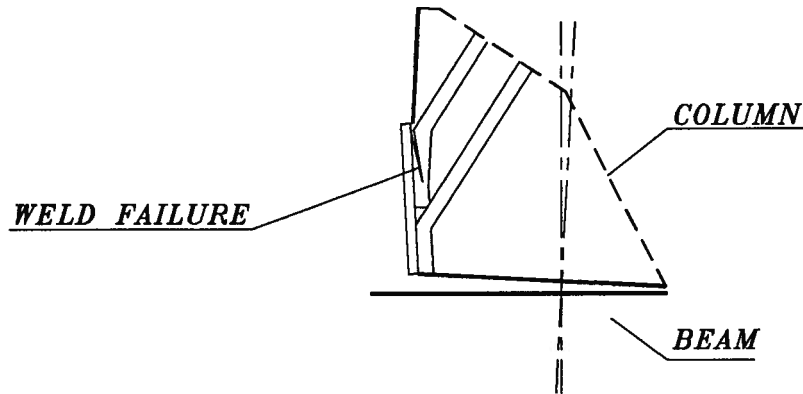


Fig.4.28 Failure of the specimen T-2.

The ultimate load during the test reached 60.5kN which created the moment at the joint equal to 97kNm (the bending stress in the glulam = 25.6MPa). This is almost identical result to the previous test T-1. Also the deformations of the joint were at the same level as before.

Apparently, the reinforcement which was used in the specimen T-2 was not effective as far as the overall behaviour of the specimen is concerned. It worked, however, locally.

MOMENT-DEFLECTION RELATIONSHIP.

The relationship between the moment at the joint and the deflection of the end of the column is presented on Fig.4.29.

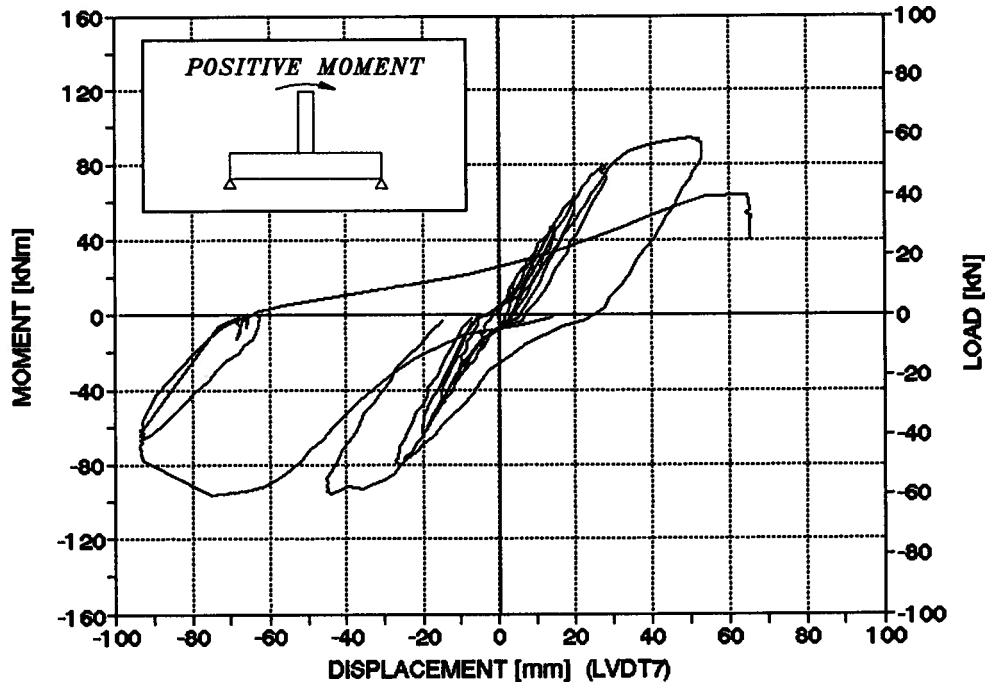


Fig.4.29 Deflections of the column's free end during the test T-2
(first cycles at each load level are presented).

The linear character of the M-D curve was observed only at the lowest load level (16kNm, 10kN). Immediately after that the pinching started. The average slope of the curve decreased by 26% with respect to the original. However the slope at 10kN load level was only 75% of the slope observed in the specimen T-1.

The specimen barely reached the design level of 80kNm. Immediately after that the column rebars started to yield. The specimen survived all 4 cycles at 60kN load level (moment =96kNm) but the deflections recorded by LVDT7 were 2.2 times larger than at the previous level (50kN).

The serviceability limit for the wind loads (at 37kNm) was exceeded almost three times. The corresponding deflection was 11.6mm. The limit for the earthquake loads was satisfied, similar to T-1 test, with only 27.0mm deflection (68%).

THE COMPONENTS OF THE TOTAL DEFLECTION.

The percentage share of three components in the total deflection of the column is presented in Table 4.6.

load kN	moment kNm	d_b %	d_c %	d_j %	d_t [100%] mm
10	16	19	29	52	4.5
20	32	15	29	56	9.1
30	48	12	27	61	14.6
40	64	11	25	64	20.9
50	80	10	22	68	30.0
60	96	6.5	12	81.5	65.0

Note: d_t - total deflection;
 d_b - displacement due to the rotation of the beam;
 d_c - displacement due to the elastic deformation of the column;
 d_j - displacement due to the deformation of the joint.

Table 4.6 *Components of the total deflection in test T-2.*

The specimen T-2 appears to be even more flexible than T-1 - specially within the lower range of the load. But the percentage share of three components is almost exactly the same as before.

THE BEHAVIOUR OF THE COLUMN PART OF THE JOINT.

The comparison of the LVDT 3 readings (refer to Fig.4.7 or 4.27 for the location) during the tests T-1 and T-2 is presented in Table 4.7 (positive moment).

load	moment	LVDT 3 [mm]		
		T-1	T-2	T2/T1
kN	kNm			
10	16	0.05	0.03	0.60
20	32	0.12	0.09	0.75
30	48	-	0.12	-
40	64	0.40	0.18	0.45
50	80	0.90	0.24	0.27
60	96	3.20	0.46	0.14

Table 4.7 *Local compression deformations of the glulam at the end of the column.*

The data collected by LVDT 3 shows that the bearing reinforcement did work. Unfortunately, its effect was only local and did not influence the overall behaviour of the specimen. The compression deformations in the column at the location of the reinforcement were much smaller than those recorded during T-1 test. The reinforcement became more and more effective as the load (and bearing stresses) increased. At the 60kN load level the deformations of the glulam were only 14% when compared to unreinforced specimen.

load	moment	LVDT 4 [mm]		
		T-1	T-2	T2/T1
kN	kNm			
10	16	0.06	0.09	1.50
20	32	0.45	0.51	1.13
30	48	-	0.99	-
40	64	1.39	1.68	1.21
50	80	2.43	2.96	1.22
60	96	4.70	11.3	2.40

Table 4.8 *Local "tension" deformations between the column and the column plate.*

At the same time, the gauge located on the top end of the column plate (LVDT 4) recorded the uplift displacements of the plate versus the glulam. Those readings are compared in Table 4.8.

The deformations were over 20% larger during the test T-2 than during the test T-1 (unlike the readings from LVDT 3). At the ultimate load they were 2.4 times larger but this was the effect of the weld failure.

The tension forces perpendicular to the plate were carried (in both specimens) by the inclined rebars only. Apparently, this was not enough. Some kind of "tension reinforcement" turned out to be necessary.

THE BEHAVIOUR OF THE BEAM PART OF THE JOINT.

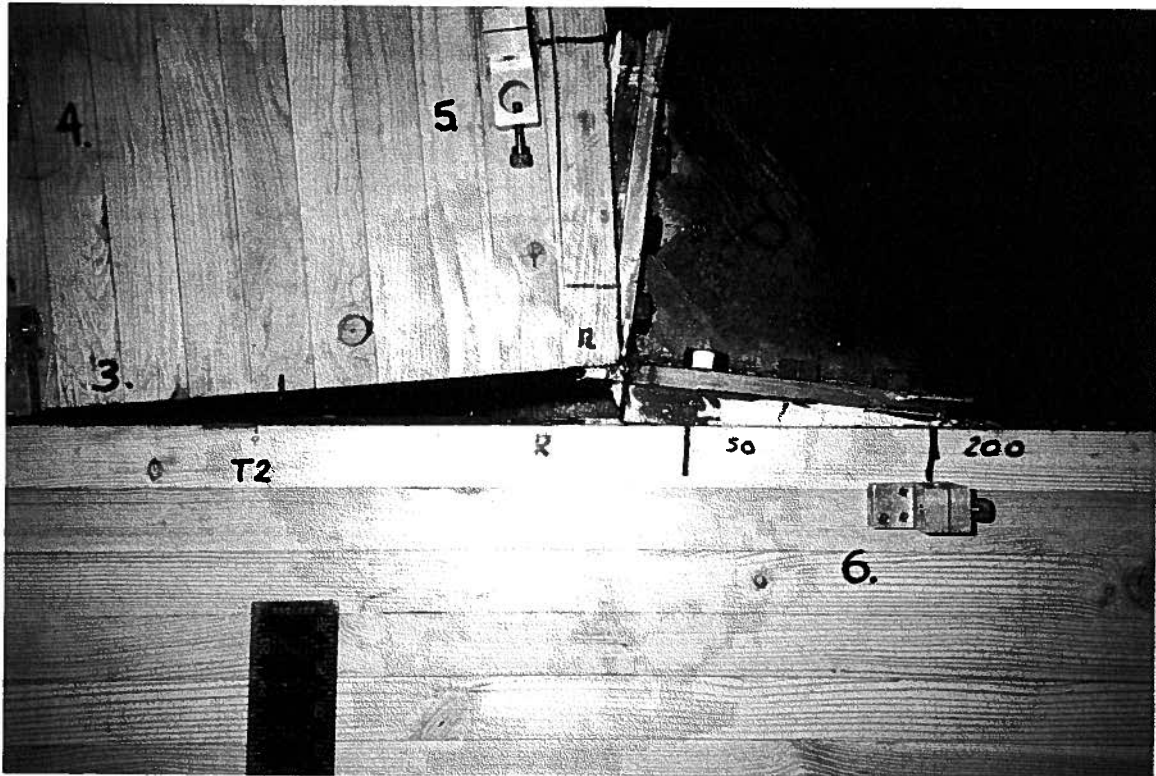


Fig.4.30 *Partial pullout of the beam rebar in the specimen T-2.*

The bending of the beam plates was successfully avoided in the specimen T-2. The resistance of the bolts was also sufficient. However, a new problem appeared at the very end of the test. The inner beam rebar on the right side of the joint was pulled out of the beam (see Fig.4.30).

It was very difficult to determine the reason for that kind of failure. It is possible that this particular rebar was not adequately cleaned before gluing. The corresponding rebar on the other side of the joint did not show any signs of pullout failure, although it experienced the same tension force. To avoid similar accidental situation, it was decided that the beam rebars in the next specimen should be extended from 400mm to 550mm.

4.7.5 Comments.

The lack of improvement in the behaviour of the specimen T-2 was obvious. In some aspects, T-2 was even worse than T-1. Although the compression deformations under the column plates were significantly reduced, the reinforcement caused even larger "tension" deformations.

After this test it became clear that the column plates and the glulam should be able to resist not only compression forces but also tension forces in the direction perpendicular to the axis of the column. Therefore, the plates should be permanently connected to the rebars glued perpendicularly to the grain.

The joint in the specimen T-3 was redesigned. The inclined column rebars (#20) were placed in one row and inclined out of the plane by 3° to allow crossing with the rebars from the other side. The length of the column plates was increased to 240mm and their width to 127mm (equal to the width of the column). Four #15 rebars were placed in the holes drilled perpendicularly to the grain. Those rebars went through the entire depth of the column and their ends were welded to the column plates, and were also glued to the glulam. In this way, the #15 rebars acted not only as bearing reinforcement (as it was in the specimen T-2), but were also able to resist tension forces. The column part of the joint is shown on Fig.4.31.

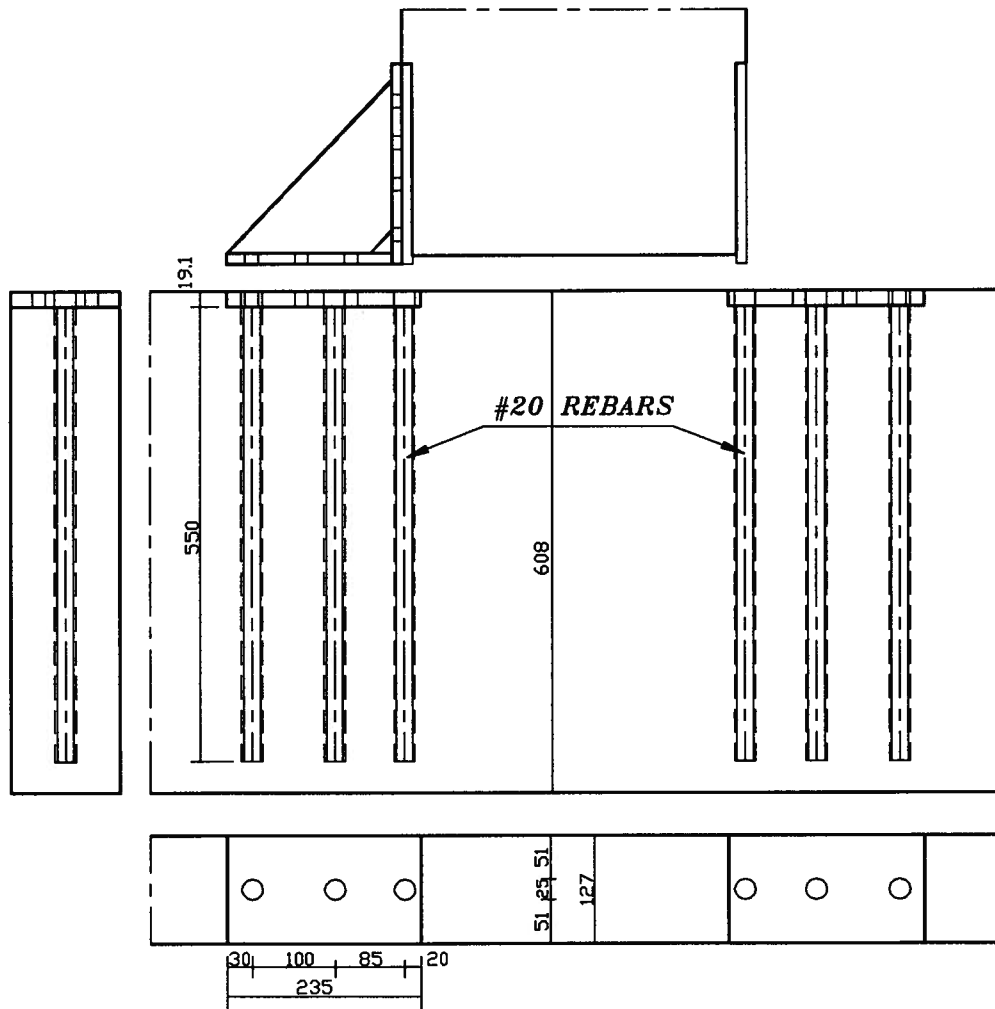


Fig.4.32 Locations of the beam's plates and rebars in the specimen T-3.

Some changes were also introduced to the beam part of the joint (see Fig.4.32.). The width of the beam plates was increased, as it was done in the column, to cover the full width of the beam. Three #20 rebars (instead of 2) were welded to the plate and glued into the beam. Their length was also increased to 550mm to eliminate any accidental pull-out (refer to section 4.7.4). In order to accommodate three rebars in one row it was necessary to increase the length of the beam plate to 235mm. As the bending of the plate was not observed in the specimen T-2 the thickness of the beam plates in the specimen T-3 was decreased to 19mm ($\frac{3}{4}$ ").

The dimensions of the angle with the stiffener were increased accordingly to the size of the plates.

4.8.2 Manufacturing Steps.

The specimen T-3 was manufactured in a way similar to the specimen T-1. However, some extra operations were necessary due to the perpendicular reinforcement in the columns. After the column plates with the inclined rebars (#20) were glued into both sides of the column, the holes perpendicular to the grain ($\frac{3}{4}$ " diameter) were drilled through the entire depth of the glulam (the plates were predrilled earlier). #15 rebars were placed in those holes and glued to the glulam. After the glue set, each end of the rebar was welded to the column plate.

4.8.3 Testing Procedures.

The assembly of the specimen T-3 in the testing frame proceeded in exactly the same manner as it was described for the specimen T-1 (see section 4.6.3).

The location of the gauges was slightly different than previously. The distances shown on Fig.4.7 were: $S_1=200\text{mm}$, $S_2=10\text{mm}$, $S_4=220\text{mm}$. The gauges LVDT10 and LVDT11 were used during this test.

The loading procedures for the test T-3 were as follows:

1. load range from +10 to -10 kN 4 cycles
2. load range from +20 to -20 kN 4 cycles
3. load range from +30 to -30 kN 4 cycles
4. load range from +40 to -40 kN 4 cycles
5. load range from +50 to -50 kN 4 cycles
6. load range from +60 to -60 kN 4 cycles
7. load range from +70 to -70 kN 4 cycles
8. load range from +80 to -80 kN 4 cycles
9. final loading from 0 to +90kN and to -86kN.

Load control was used throughout the test with sinusoidal wave form (see Fig.4.33).

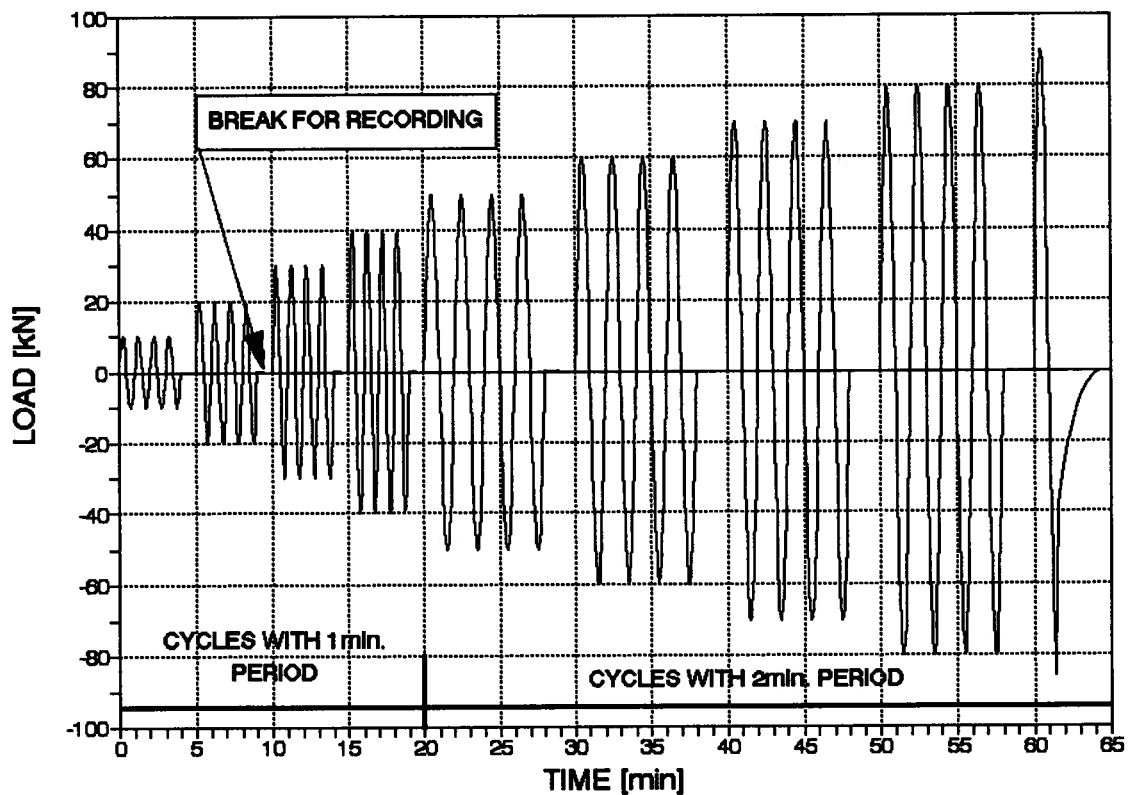


Fig.4.33 Loading procedures for the specimen T-3.

The period of the load cycles was 1 minute up to 40 kN load and 2 minutes over 40 kN load.

Each cycle started from zero load point. The positive load was applied first (pulling the column from the left to the right) creating compression in the right hand side of the

connection and tension in the left hand side of the connection.

The test was terminated after a shear failure occurred in the glulam column, without any sign of the failure in the rebars. The failure included delamination of the column (failure of the glue line) on the length equal to approximately 2/3 of the column height.

4.8.4 Results.

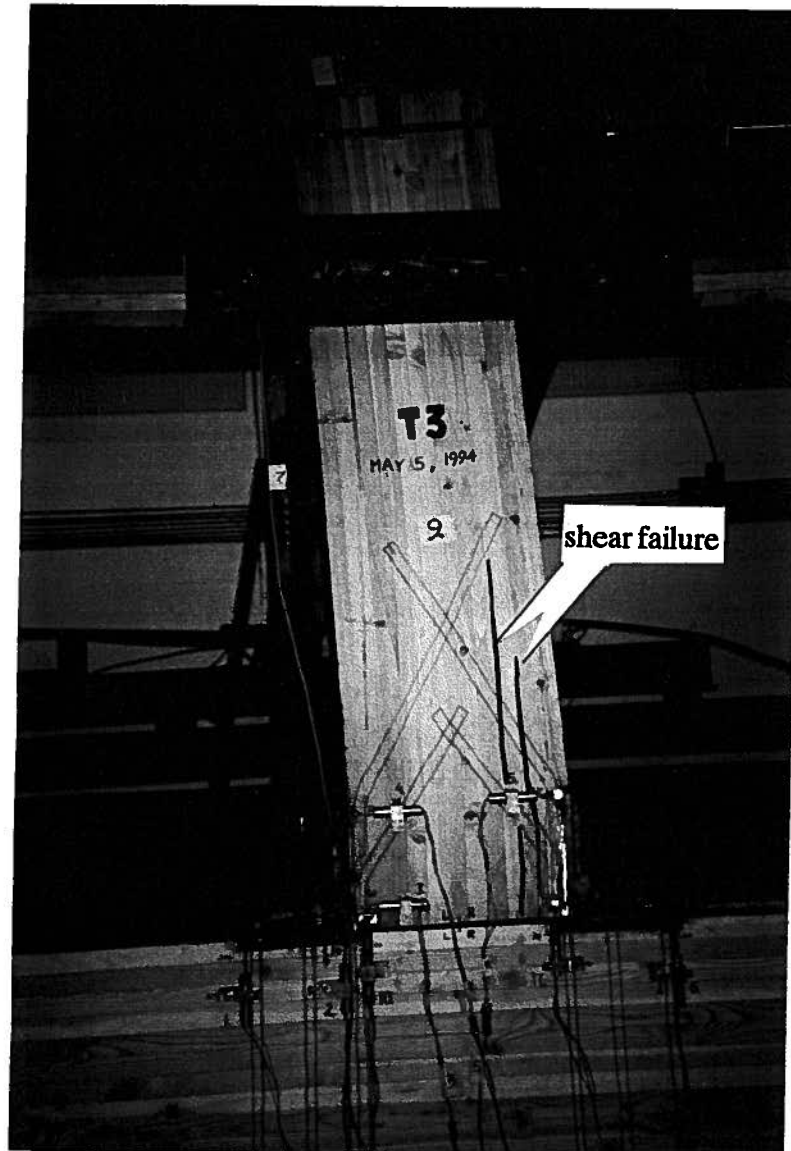


Fig.4.34 Specimen T-3 during final loading.

OVERALL BEHAVIOUR.

The behaviour of the specimen T-3 was much better than the behaviour of two previous specimens. Both, the stiffness and the strength of the connection were improved. The glulam column failed in shear at -86kN load (110% of the calculated resistance), however the specimen survived the load of +90kN (116%, shear stress = 2.48MPa). The shear took place on both sides of the column but away from the joint region, i.e. away from the location of inclined and perpendicular rebars. That proved the positive effect of gluing the rebars on the shear capacity of the glulam member. The shear failure of the specimen T-3 is shown on Fig.4.34 and Fig.4.35.

After the test, the column rebars were exposed to check where the fracture occurred. The inclined rebars as well as the perpendicular reinforcement did not show any sign of yielding. Also the welds performed very well.

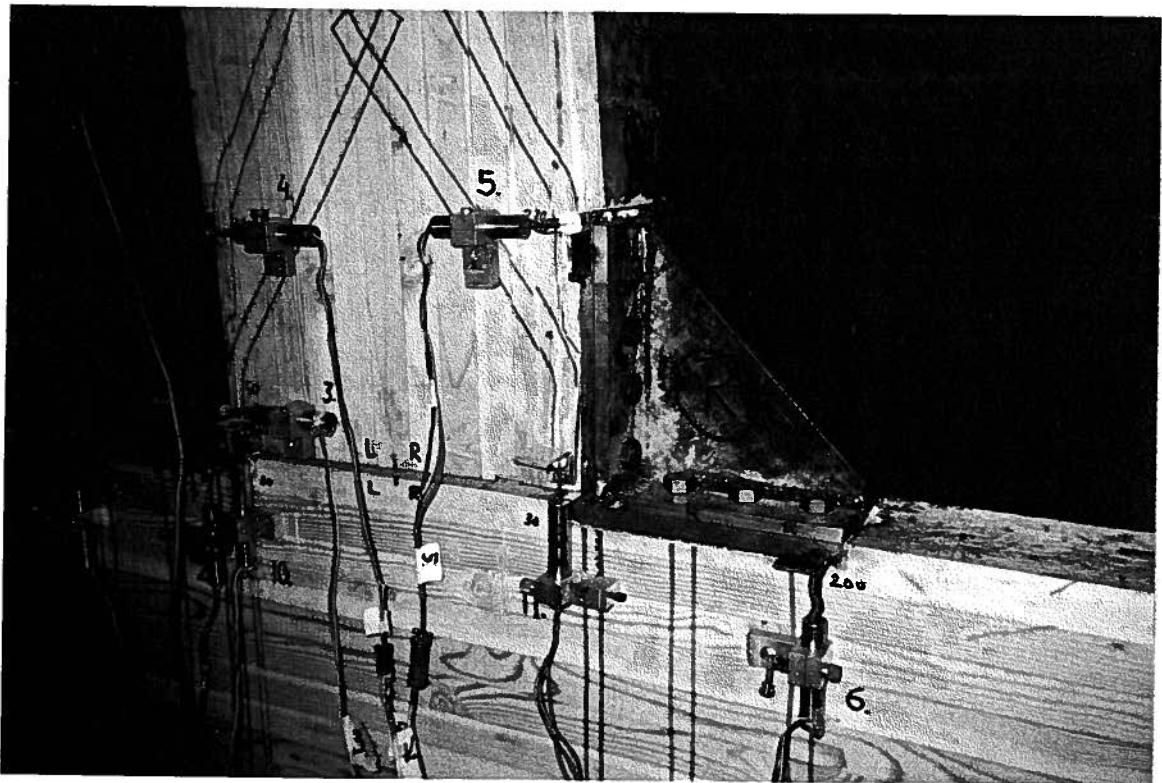


Fig.4.35 Joint in the specimen T-3 after failure.

The ultimate load during the test reached 90.0kN which created the moment at the joint equal to 144kNm. This is almost 50% more than in two previous tests and 80% more than the design requirement for the structure. The bending stress in the column reached:

$$\sigma_b = \frac{144000000}{\frac{1}{6} \times 130 \times 418^2} = 38.0 \text{ MPa}$$

The deformations of the joint were approx. half of those recorded previously at the ultimate level.

Apparently, the welding of the perpendicular rebars was the key for the improved behaviour of the joint.

MOMENT-DEFLECTION RELATIONSHIP.

The relationship between the moment at the joint and the deflection of the end of the column is presented on Fig.4.36.

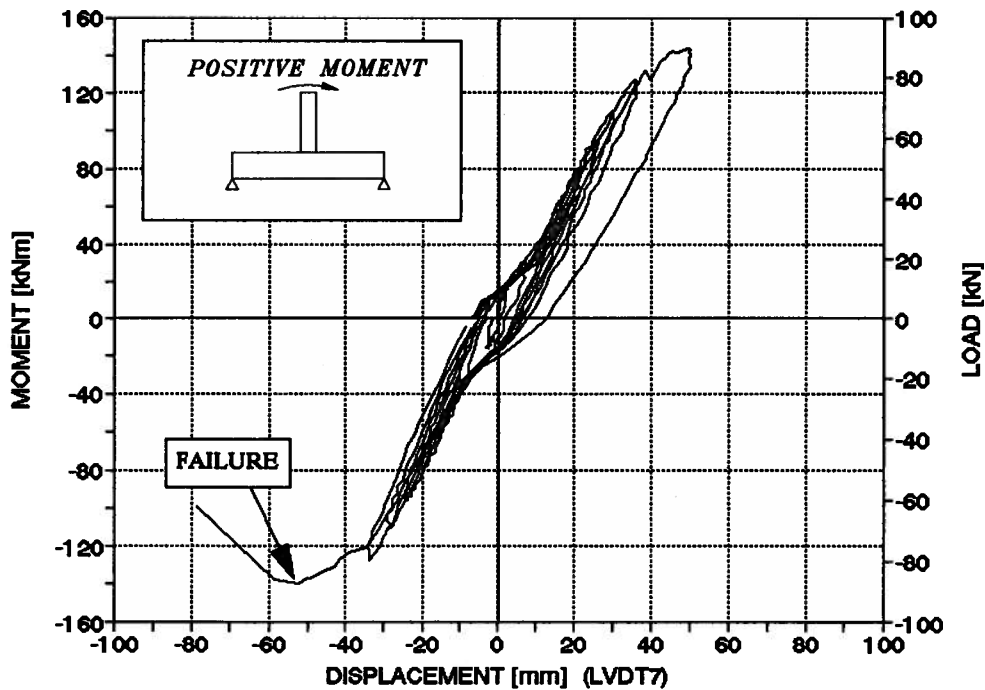


Fig.4.36 Deflections of the column's free end during the test T-3
(first cycles at each load level are presented).

The linear character of the M-D curve was observed only up to the moment of 32kNm (20kN load level). Immediately after that some pinching started. The average slope of the curve was over 30% greater than observed during the test T-1. The slope decreased during the test by 45%, but its final magnitude (at 80kN level) was equal to the slope of the specimen T-1 at 40kN (20kN for T-2).

The specimen quite easily reached the design level of 80kNm (50kN). The ultimate moment - 144kNm - was greater than anticipated moment resistance of the joint by 12.5% and greater than calculated short term moment resistance of the column by 11%.

The serviceability limit for the wind loads (4mm at 37kNm) was exceeded 2.5 times. The corresponding deflection was 9.9mm. The limit for the earthquake loads was satisfied - at 77kNm the deflection was only 19.7mm (50% of the limit).

THE COMPONENTS OF THE TOTAL DEFLECTION.

load kN	moment kNm	d_b %	d_c %	d_j %	d_t [100%] mm
10	16	20	50	30	2.6
20	32	15	37	48	7.1
30	48	13	31	56	12.8
40	64	12	31	57	16.9
50	80	13	30	57	21.7
60	96	12	30.5	57.5	25.9
70	112	12.5	30	57.5	30.9
80	128	12	28	60	37.4

Note: d_t - total deflection;
 d_b - displacement due to the rotation of the beam;
 d_c - displacement due to the elastic deformation of the column;
 d_j - displacement due to the deformation of the joint.

Table 4.9 Components of the total deflection in test T-3.

The percentage share of three components in the total deflection of the column is presented in Table 4.9.

The joint deformation component (d_j) is slightly smaller than in previous tests. The difference is more significant at lower load levels (by 40% at 10kN) than at higher (by 10% at 50kN when compared to T-2). That indicates greater stiffness of the specimen T-3.

THE BEHAVIOUR OF THE COLUMN PART OF THE JOINT.

The comparison of the LVDT 3 readings during the tests is presented in Table 4.10 (positive moment).

The data collected by LVDT 3 shows further improvement of the bearing reinforcement. The compression deformations in the specimen T-3 were 66% smaller than the corresponding deformations in the specimen T-2 and over 80% smaller than the deformations in the specimen T-1! The ultimate deformation of 0.14mm in the reinforced specimen (T-3) was reached in the unreinforced specimen (T-1) at about 22kN (at 4 times lower load!).

load kN	moment kNm	LVDT 3 [mm]			
		T-1	T-2	T-3	T3/T2
10	16	0.05	0.03	0.02	0.67
20	32	0.12	0.09	0.03	0.33
30	48	-	0.12	0.04	0.33
40	64	0.40	0.18	0.06	0.33
50	80	0.90	0.24	0.08	0.33
60	96	3.20	0.46	0.09	0.20
70	112	-	-	0.11	-
80	128	-	-	0.12	-
90	144	-	-	0.14	-

Table 4.10 *Local compression deformations of the glulam at the end of the column.*

load kN	moment kNm	LVDT 4 [mm]			
		T-1	T-2	T-3	T3/T2
10	16	0.06	0.09	0.02	0.22
20	32	0.45	0.51	0.02	0.04
30	48	-	0.99	0.03	0.03
40	64	1.39	1.68	0.04	0.02
50	80	2.43	2.96	0.05	0.02
60	96	4.70	11.3	0.06	0.01
70	112	-	-	0.07	-
80	128	-	-	0.12	-
90	144	-	-	0.49	-

Table 4.11 *Local tension deformations at the end of the column.*

Even more astonishing results were collected by the gauge LVDT 4 (see Table 4.11). The tension deformations were reduced to 2% of the values recorded during the test with the unreinforced specimens.

What is even more important, the compression and the tension deformations in the specimen T-3 had identical amplitudes. Additionally, their graphs were linear throughout entire test.

The welding of the perpendicular rebars to the plates turned to be a very effective way of decreasing compression and tension deformations between the glulam column and the column plates.

THE BEHAVIOUR OF THE BEAM PART OF THE JOINT.

The specimen T-3 did not experience any problems in the beam part of the connection. The beam's plates and rebars behaved perfectly well. The gauges measuring the deformations between the beam and the plates recorded linear relationship throughout the entire test. The deformations at the ultimate load level reached 0.5mm in tension and 0.1mm in compression. It was also observed that the required behaviour of the beam plates was

achieved, i.e. the outer end of the plate experienced larger deformations than the inner end (as shown on Fig.4.17a). In this situation the additional third rebar under the beam plate was not needed.

4.8.5 Comments.

The specimen T-3 showed great improvement in comparison to the other specimens. It survived the highest load and, at the same time, it displayed the smallest deflections of the column. The deformations measured by all gauges located within the joint region were smaller than any other recorded earlier. Compression and tension deformations had similar amplitudes and their behaviour was linear throughout the test. The overall stiffness of the joint, measured by the slope of the moment-deformation curve, was over 30% greater than previously recorded. Both, the shear resistance and the bending resistance of the column, calculated according to the code values, were exceeded during the test. The failure took place in the glulam which indicates that the joint can be made stronger than the member itself.

Most of the improvement described above should be credited to the perpendicular reinforcement used in this specimen. The welding of the perpendicular rebars to the plates seems to be the proper way of designing the column part of the connection. In the specimen T-3 the rebars were glued before they were welded to the plates. That caused some problems: the penetration of the weld was not complete and some toxic fumes were created during the process. Although the welds performed adequately during the test, in the future, welding should take place before gluing. This can be done by injecting the glue between the glulam and the rebar through an additional, small hole made in the side of the specimen.

This specimen met all design criteria except one: serviceability at low load levels. Further research should try to eliminate that problem.

4.9 CONCLUSIONS.

The tests described in this chapter showed that the glued-in rebar connections are able to transfer bending moments under reversed loading conditions in multi-storey frame structures. In fact, the connection may be stronger than the glulam member which is connected (glulam failure in the test T-3). However, to achieve an acceptable behaviour of the connection a very careful detailing is necessary. The reinforcement perpendicular to the grain under the plates is essential for obtaining satisfactory stiffness of the joint. This reinforcement should be able to transfer compression forces as well as tension forces.

CHAPTER 5

DESIGN GUIDELINES FOR GLUED-IN REBAR JOINTS.

5.1 OBJECTIVE.

The objective of this chapter is to provide basic information about a design method for moment resisting joints using glued-in rebars. Although the information is based on the beam-to-column tests described in chapter 4, it may be also used to design other moment resisting joints, such as column to foundation joint or beam splice.

The main aim for using the glued-in rebar connection method is to obtain timber connections with reliability equal to reliability of the steel joints. Whenever the embedment length of the rebar is larger than required minimum length, the failure takes place in the steel. Therefore, the connection may be designed as the steel joint. As a consequence of this approach, the designer should rely only on steel parts of the connection. Contact between the glulam members should be ignored because it may change the pattern of load transfer. For example, putting the column in contact with the beam would decrease the lever arm between the tension force and the resultant of the compression forces. It would also be very difficult to predict the location of that resultant. In effect, the connection would be less reliable than similar connection where the column and the beam are not in direct contact.

However, there are locations where relying only on steel would be too conservative. That is the case of bearing plates, which are widely used in the glued-in rebar joints. Usually the rebar is welded to the plate and, where subjected to compression load, the plate and the rebar act together. The compression load is transferred by the bearing under the plate and shear stress around the rebar. The tests described in Chapter 3 showed that the compression deformations

of the rebar glued perpendicularly to the grain and the deformations of the bearing plate are similar within elastic range. Therefore, with sufficient degree of accuracy, it may be assumed that the load carrying capacity of the plate with the rebar in compression perpendicular to the grain is the sum of the capacity of the rebar and the plate acting separately (refer to Chapter 3 for more details).

5.2 DESIGN PHILOSOPHY.

The design philosophy of the glued-in rebar connection is based on the following:

- the moment in the connection is transferred by the rebars glued into the glulam at an angle to the grain to involve the whole cross section of the element (or a significant portion of that section),
- the failure of the connection takes place in the steel,
- all forces are transferred through the steel parts of the connection (the contact between the glulam members is disregarded),
- wherever the bearing stress occur under the plate, the glulam should be reinforced by gluing additional rebars perpendicularly to the grain; furthermore, those rebars should be permanently attached to the plate so they can transfer tension and compression forces,
- the welding of the rebars to the plates should take place before gluing of the rebars, preferably away from the glulam,
- the connection should be designed in such way that all the gluing procedures take place in the plant, before delivery of the elements to the site,
- field welding should be avoided,
- bolted connection of the elements (their steel parts) on the site is preferred.

5.3 DESIGN ASSUMPTIONS.

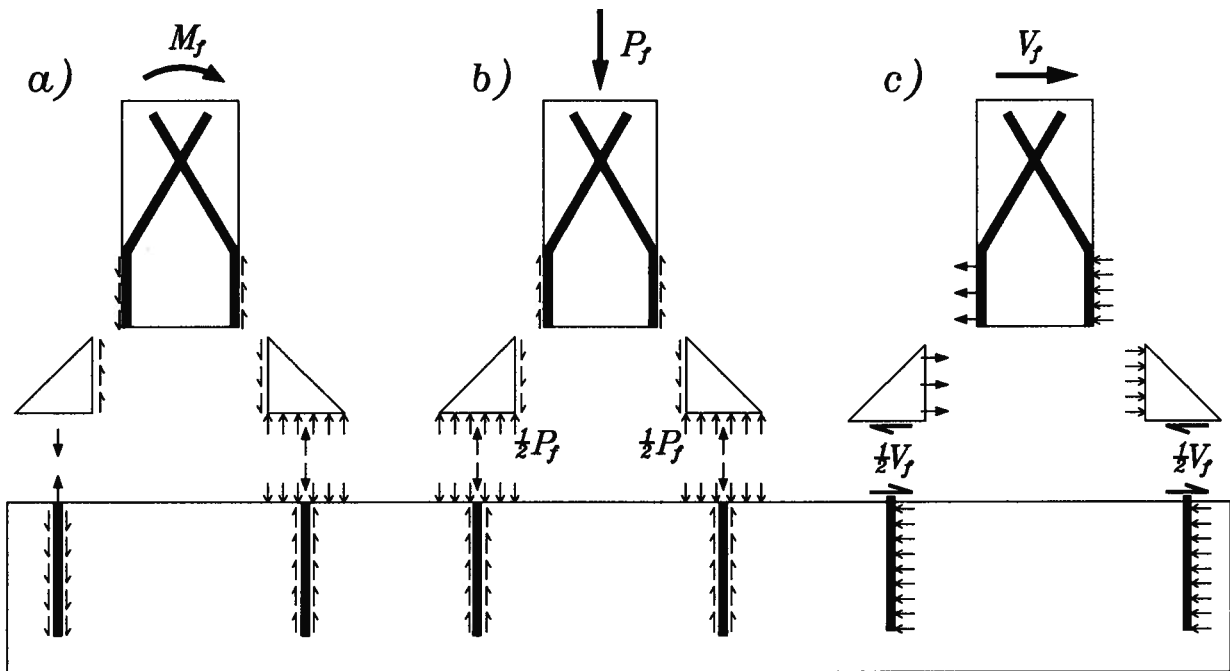


Fig.5.1 Forces in the connection:
a) bending, b) axial, c) shear.

The following assumptions have been made:

1. The failure of the glued-in rebar connection is a tension failure in the rebar.
2. The bending moment is transferred by the glued-in rebars acting in tension or compression and forming a moment couple (see Fig.5.1). The compression interaction of the glulam and the rebars takes place exclusively under the beam plates subjected to the compression forces (bearing).
3. An axial force in the column (not included during the tests described in chapter 4) is transferred by the glued-in rebars in the beam in conjunction with bearing under the plates.
4. The shear forces (usually insignificant in this configuration of the beam and the column) are carried by shear in the beam's rebars, bearing under the column plate, and tension in the column bolts.

5. The minimum embedment length is provided for all rebars in the connection, according to Table 5.1.

rebar size	embedment length at an angle to the grain [mm]	
	90°	30°
#10	200	150
#15	300	250
#20	400	300

Table 5.1 *Minimum embedment length for various size of the rebars.*

6. The diameter of the holes drilled in the glulam is 3-5mm larger than the nominal diameter of the rebars.
7. The glue provides enough resistance to yield the rebar in tension when the embedment length is greater than the length specified in Table 5.1.
8. Weldable rebars are used.
9. The buckling of the rebars subjected to compression loads is restrained by the glulam, therefore the compression resistance of the rebars may be calculated as being equal to the tension resistance of the rebars.
10. The design is in the elastic deformations range.
11. The stresses created in the rebars due to the factored loads should be smaller than the factored yield strength of reinforcing steel ($\phi \times F_{yr}$).

In the design guidelines presented below, it is assumed that the elements themselves (beams and columns) have already been designed according to section 6 of Canadian Wood Design Code CAN/CSA-O86.1-M89. Therefore the applicable formulas referring to the resistance of the glulam members are not quoted.

The formulas, which are introduced in the following sections, pertain to the resistance of the joint and its elements (i.e. resistance of the rebars, plates, and the glulam in direct contact with the plates) caused by the forces acting in the joint (i.e. bending moment, axial force, shear force).

5.4 MOMENT RESISTANCE OF THE JOINT.

The moment resistance of the joint should be greater than the factored bending moment acting in the joint:

$$M_f \leq (M_{rc}, M_{rb})$$

The moment resistance of the beam to column connection should be calculated as the lesser of the following:

$$M_{rc} = l_c \times F_c$$

or

$$M_{rb} = l_b \times F_b$$

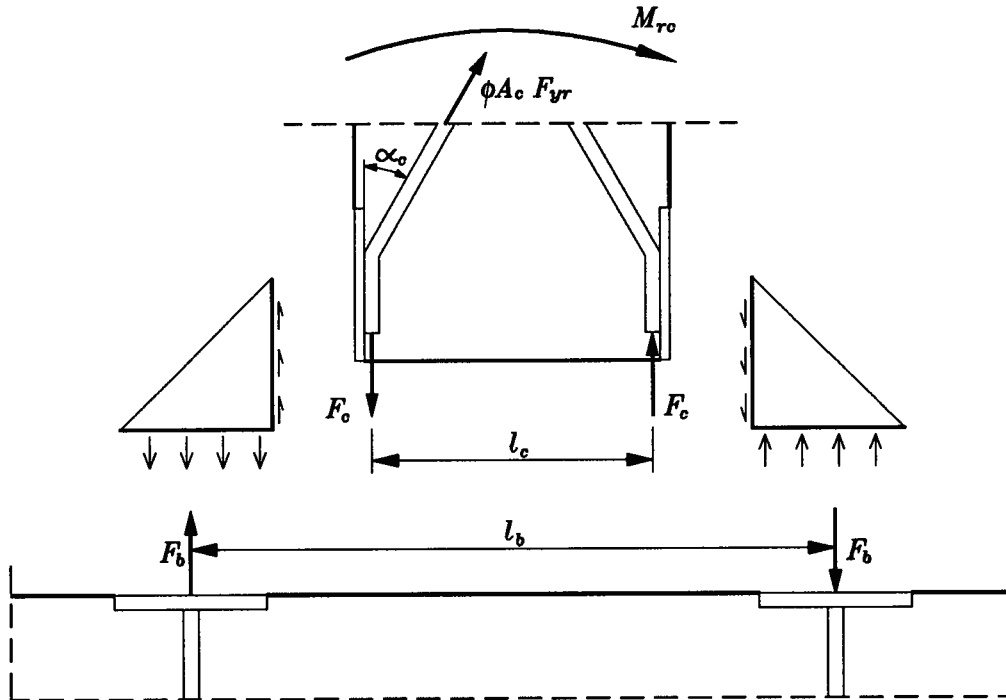


Fig.5.2 Geometry of the beam to column joint.

where

M_{rc} - moment resistance of the column part of the joint,

M_{rb} - moment resistance of the beam part of the joint,

- l_c - distance (centre to center) between the column rebars welded to the plates,
- l_b - distance between the beam rebars (or between groups of rebars),
- F_c - resistance of the column rebars on one side of the joint equal to:

$$F_c = \phi \times A_c \times F_{yr} \times \cos \alpha_c$$

- F_b - resistance of the beam rebars on one side of the joint equal to:

$$F_b = \phi \times A_b \times F_{yr}$$

- ϕ - resistance factor (suggested value 0.9),
- F_{yr} - specified yield strength of reinforcing steel,
- A_c - total area of the rebars glued in the column on one side of the joint,
- A_b - total area of the rebars glued in the beam on one side of the joint,
- α_c - angle of inclination of the column rebars.

The resistance of the glulam members has to be at least equal to the calculated resistance of the joint. The resistance of the column may be calculated as the moment resistance of the total cross section (based on gross area) of the member. The resistance of the beam should be calculated based on the net area of the member at the location of the beam rebars. This is a conservative approach but it should be adopted until the reduction of the moment capacity of the glulam member, caused by drilling the holes at 90° and gluing the rebars, is established.

5.5 BEARING REINFORCEMENT OF THE COLUMN PLATES.

The tests described in Chapter 4 showed that the bearing resistance of the glulam under the column plates was not sufficient. The bearing reinforcement, in the form of the rebars glued perpendicularly to the grain, was used to decrease local compression deformations of the glulam. The rebars were continuous over the entire depth of the column and connected by welding to the column plates on the opposite sides of the column.

This reinforcing method is recommended for the connection as means of providing sufficient stiffness. The rebars glued at 90° angle to the grain have to transfer the horizontal forces

$(A_c \times F_{yr} \times \sin \alpha_c)$ coming from the inclined rebar (see Fig. 5.3). Bearing in the glulam is not accounted for because the horizontal forces may create compression as well as tension in the perpendicular rebar, depending on the direction of the moment applied to the column.

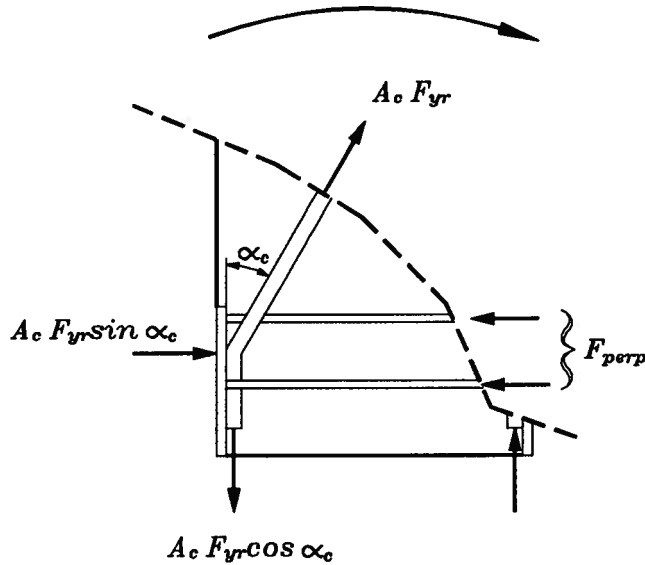


Fig.5.3 Forces perpendicular to the grain in the column

The tension and compression resistance of the perpendicular rebar in the column may be calculated as:

$$F_{perp} = \phi \times A_{perp} \times F_{yr}$$

where

F_{perp} - resistance of the perpendicular rebar,

ϕ - resistance factor (suggested value 0.67),

F_{yr} - specified yield strength of reinforcing steel,

A_{perp} - total area of the perpendicular rebar glued in the column and welded to the plates.

5.6 AXIAL RESISTANCE OF THE JOINT.

It is assumed that the axial force is carried by the steel parts only without direct contact between the column and the beam. The axial force resistance should be taken as the lesser of the following:

$$P_c = 2 \times F_c$$

or

$$P_b = 2 \times (F_b + Q_r)$$

and

$$P_f \leq (P_c, P_b)$$

where

P_c - axial resistance of the column part of the joint,

P_b - axial resistance of the beam part of the joint,

F_c - resistance of the column rebars on one side of the joint, calculated as in section 5.4,

F_b - resistance of the beam rebars on one side of the joint, calculated as in section 5.4,

Q_r - bearing resistance of the glulam under one beam plate, calculated according to CAN/CSA-O86.1-M89 section 6.5.9.

5.7 COMBINED AXIAL AND BENDING RESISTANCE OF THE JOINT.

In case of combined axial loads and bending the following interaction equations should be satisfied:

$$\frac{P_f}{F_c} + \frac{M_f}{l_c \times F_c} \leq 1.0$$

or

$$\frac{P_f}{F_b} + \frac{M_f}{l_b \times (F_b + Q_r)} \leq 1.0$$

where

P_f - applied axial load,

M_f - applied bending moment,

F_c, F_b, Q_r - as in section 5.6,

l_c, l_b - as in section 5.4.

5.8 SHEAR RESISTANCE OF THE JOINT.

It is assumed that shear force from the column is transferred to the stiffened angles (by bearing between the column plate on one side of the column, and tension in the bolts on the other side of the column) and then to the beam plates (creating shear in the bolts connecting the angles and the beam plates). Then the shear is transferred from the plates to the beam rebars. This is the critical section, where the resistance of the joint due to shear force should be checked.

The shear resistance of the joint should be calculated as follows:

$$V_{rb} = \phi \times 2 \times A_b \times 0.66 \times F_{yr}$$

and

$$V_f \leq V_{rb}$$

where

V_{rb} - shear resistance of the beam rebars,

ϕ - resistance factor (suggested value 0.9),

F_{yr} - specified yield strength of reinforcing steel,

A_b - total area of the rebars glued in the beam on one side of the joint.

The shear resistance of the glulam column has to be at least equal to the resistance of the joint calculated as above.

5.9 RESISTANCE OF THE BOLTS, PLATES, AND WELDS.

The resistance of the plates, bolts connecting the plates and the angles, and welds connecting the rebars to the plates has to be determined according to the appropriate sections of steel design code CAN/CSA-S16.1-M89.

5.9.1 Bolts.

The following resistances have to be determined:

1. the beam bolts on one side of the joint due to the combined tension (M_f / l_b) and shear forces ($\frac{1}{2}V_f$), according to CAN/CSA-S16.1-M89 clause 13.11.4;
2. the column bolts in shear due to the tension or compression force (whichever is greater) coming from combined bending moment and axial load ($P_f/2 + M_f/l_c$), according to CAN/CSA-S16.1-M89 clause 13.11.2.

It is possible to use welded connections instead of bolted connections. In that case, the appropriate resistances of the welds due to the loads described above, should be determined according to CAN/CSA-S16.1-M89 clause 13.13.

5.9.2 Welds.

The following resistances have to be determined, according to CAN/CSA-S16.1-M89 clause 13.13:

1. the weld between the inclined column rebars and the column plates due to the ultimate tension stress in those rebars ($1.5 \times F_{yr} \times \cos \alpha_c$);
2. the weld between the beam rebars and the beam plates due to the factored tension load (M_f / l_b);
3. the welds between the plates forming the angle and the triangular stiffener due to the combined tension and shear.

5.9.3 Plates.

The following plates have to be checked for bending, according to CAN/CSA-S16.1-M89 clause 13.5:

1. the beam plate due to tension forces in the beam bolts and the beam rebars (see Fig.5.4),
2. the stiffened angle due to the tension force in the beam bolts equal to their factored tensile resistance (the column side of the stiffener may be considered fixed to the column).

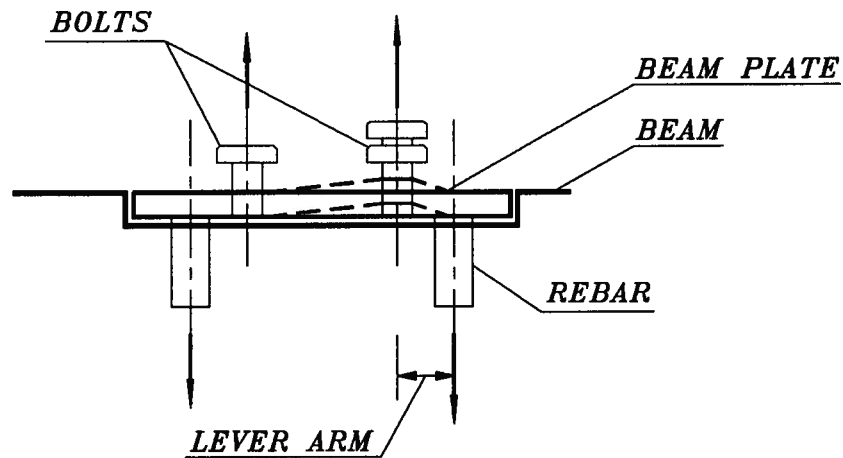


Fig.5.4 Bending of the beam plates.

5.10 SERVICEABILITY CHECK.

The deformations of the structure equipped with the glued-in rebar joints due to the specified loads can be calculated using any frame analysis computer program, which is able to simulate joints as rotational springs. The glued-in rebar joint should be modelled as a spring with known stiffness. The stiffness of the joints during the tests described in chapter 4 were:

T-1 8800 kNm/rad,

T-2 7500 kNm/rad,

T-3 12300 kNm/rad.

It is recommended to use the value obtained during the test T-3.

CHAPTER 6

COMPARISON WITH

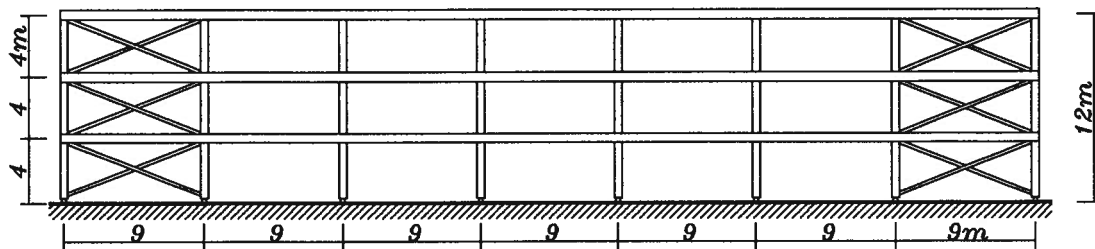
STATICALLY DETERMINATE FRAME

6.1 OBJECTIVE.

The objective of this chapter is to compare a traditional design of timber structures with the design based on the glued-in rebar technique. The same, 3-storey office building, which was described in chapter 4 (and in appendix B) was chosen for the comparison. The frame was designed again, this time, in a way which is commonly practiced in the industry, i.e. as a statically determinate structure. Then, the amounts of materials necessary to construct both frames were compared.

6.2 DESIGN OF THE PINNED FRAME.

The overall dimensions of the building remained the same as those described in chapter 4 (see Fig.4.1.). Because all joints between the columns and the beams were hinged, it was necessary to add the diagonal bracing elements which could resist the lateral forces acting on the frame. They were placed in the outside bays of the frame (see Fig.6.1).



CROSS SECTION

Fig.6.1 Braced frame of the building.

As this frame was designed only for the sake of the comparison, it was assumed that all design assumptions made for the rigid frame (presented in appendix B) were valid also for the hinged frame. This refers to the dimensions, loads and load combinations used in the analysis. The results of the statical analysis of the hinged frame are presented in Table 6.1.

element	internal	storey		
		1st	2nd	3rd
beams	bending moment [kNm]	244	244	223
	shear force [kN]	108.5	108.5	99.0
columns	compression force [kN]	631.8	414.9	198.0
diagonals	tension force [kN]	308.7	253.6	143.2

Table 6.1 *Maximum internal forces.*

6.3 DESIGN OF THE MEMBERS.

It is assumed that all applicable factors and material properties are identical to the factors and properties used in design of the elements of the rigid frame (see appendix B).

6.3.1 Beams.

6.3.1.1 floor beams (first and second storey)

Assume glulam section: 175 x 570 mm.

$$E_s I = 35400 \times 10^9 \text{ Nmm}^2$$

MOMENT RESISTANCE

The intermediate supports of the compression edge of the beam are assumed to be spaced at 600mm. Therefore:

$$L_e = 1.92 \times 600 = 1152 \text{ mm}$$

$$C_B = \left(\frac{1152 \times 570}{175^2} \right)^{0.5} = 4.6$$

$$K_L = 1.0$$

$$M_r = 0.9 \times 30.6 \times \frac{175 \times 570^2}{6} \times 1.0 \times 1.0 = 261 \times 10^6 \text{ Nmm} = 261 \text{ kNm}$$

O.K.

SHEAR RESISTANCE

$$V_r = \phi F_v \frac{2A}{3} K_N = 0.9 \times 2.0 \times \frac{2 \times 175 \times 570}{3} \times 1.0 = 119700 \text{ N} = 119.7 \text{ kN}$$

O.K.

DEFLECTION CHECK

The specified load acting on the beam was:

$$w = 17.55 \text{ N/mm}$$

The deflection limit is:

$$\Delta_{\max} \geq \frac{l}{180} = \frac{9000}{180} = 50 \text{ mm}$$

The deflection at the center of the beam is:

$$\Delta = \frac{5}{384} \frac{w l^4}{E_s I} = \frac{5}{384} \times \frac{17.55 \times 9000^4}{35400 \times 10^9} = 42.4 \text{ mm}$$

O.K.

6.3.1.2 roof beams

Assume glulam section: 175 x 532 mm.

$$E_s I = 28800 \times 10^9 \text{ Nmm}^2$$

MOMENT RESISTANCE

The intermediate supports of the compression edge of the beam are assumed to be spaced at 600mm. Therefore:

$$L_e = 1.92 \times 600 = 1152 \text{ mm}$$

$$C_B = \left(\frac{1152 \times 532}{175^2} \right)^{0.5} = 4.5$$

$$K_L = 1.0$$

$$M_r = 0.9 \times 30.6 \times \frac{175 \times 532^2}{6} \times 1.0 \times 1.0 = 227.3 \times 10^6 \text{ Nmm} = 227.3 \text{ kNm}$$

O.K.

SHEAR RESISTANCE

$$V_r = \phi F_v \frac{2A}{3} K_N = 0.9 \times 2.0 \times \frac{2 \times 175 \times 532}{3} \times 1.0 = 111700 \text{ N} = 111.7 \text{ kN}$$

O.K.

DEFLECTION CHECK

The specified load acting on the beam was:

$$w = 15.5 \text{ N/mm}$$

The deflection limit is:

$$\Delta_{\max} \geq \frac{l}{180} = \frac{9000}{180} = 50 \text{ mm}$$

The deflection at the center of the beam is:

$$\Delta = \frac{5}{384} \frac{wl^4}{E_s I} = \frac{5}{384} \times \frac{15.5 \times 9000^4}{28800 \times 10^9} = 46.0 \text{ mm}$$

O.K.

6.3.2 Columns.

Because the axial force is the only load acting on the columns, the buckling at weaker plane is considered below.

6.3.2.1 first storey

$$K_e = 1.0$$

$$L = 4000 - 570/2 = 3715 \text{ mm}$$

$$C_K = 20.6$$

Try glulam section: 175 x 342 mm

$$C_c = \frac{3715}{175} = 21.2$$

$$C_c > C_K$$

$$K_c = \frac{1}{2C_c^2} \frac{E_{05} K_{SE} K_T}{F_c} = \frac{1}{2 \times 21.2^2} \frac{11400 \times 1.0 \times 1.0}{20.4} = 0.62$$

$$P_r = 0.9 \times 20.4 \times 175 \times 342 \times 0.62 = 681300 \text{ N} = 681.3 \text{ kN}$$

O.K.

6.3.2.2 second storey

$$K_e = 1.0$$

$$L = 4000 - 570 = 3430 \text{ mm}$$

$$C_K = 20.6$$

Try glulam section: 175 x 190 mm

$$C_c = \frac{3430}{175} = 19.6$$

$$10 < C_c < C_K$$

$$K_c = 1 - \frac{1}{3} \left(\frac{C_c}{C_K} \right)^4 = 1 - \frac{1}{3} \left(\frac{19.6}{20.6} \right)^4 = 0.70$$

$$P_r = 0.9 \times 20.4 \times 175 \times 190 \times 0.70 = 427300 \text{ N} = 427.3 \text{ kN}$$

O.K.

6.3.2.3 third storey

$$K_e = 1.0$$

$$L = 4000 - 570/2 - 532/2 = 3449 \text{ mm}$$

$$C_K = 20.6$$

Try glulam section: 175 x 152 mm

$$C_c = \frac{3449}{152} = 22.7$$

$$C_c > C_K$$

$$K_c = \frac{1}{2C_c^2} \frac{E_{05} K_{SE} K_T}{F_c} = \frac{1}{2 \times 22.7^2} \frac{11400 \times 1.0 \times 1.0}{20.4} = 0.54$$

$$P_r = 0.9 \times 20.4 \times 175 \times 152 \times 0.54 = 263700 \text{ N} = 263.7 \text{ kN}$$

O.K.

6.3.3 Diagonals.

The gross section tensile resistance of the diagonals is calculated in this section.

$K_{St} = 1.0$ - service condition factor for tension

$f_{tg} = 15.3$ MPa - specified strength in tension parallel to the grain at gross section

$F_{tg} = f_{tg}(K_D K_H K_{St} K_T) = 15.3 \times (1.0) = 15.3$ MPa

6.3.3.1 first storey

Assume glulam section: 80 x 304 mm.

The factored tensile resistance parallel to the grain is:

$$T_r = \phi F_{tg} A_g = 0.9 \times 15.3 \times 80 \times 304 = 334900 N = 334.9 kN$$

O.K.

6.3.3.2 second storey

Assume glulam section: 80 x 266 mm.

The factored tensile resistance parallel to the grain is:

$$T_r = \phi F_{tg} A_g = 0.9 \times 15.3 \times 80 \times 266 = 293000 N = 293.0 kN$$

O.K.

6.3.3.3 third storey

Assume glulam section: 80 x 152 mm.

The factored tensile resistance parallel to the grain is:

$$T_r = \phi F_{tg} A_g = 0.9 \times 15.3 \times 80 \times 152 = 167400 N = 167.4 kN$$

O.K.

6.4 COST COMPARISON.

The comparison between the amount of the glulam used for both structures (hinged frame and rigid frame) is presented in Table 6.2. The numbers in the table represent the volume of the glulam, in m^3 , needed for one frame.

elements	hinged frame	rigid frame
beams	18.46	15.17
columns	3.52	5.60
diagonals	2.25	-
TOTAL	24.23	20.77

Table 6.2 *Volume of the glulam used for the frames [m^3].*

The volume of the glulam used for the rigid frame is 14.3% smaller than the volume needed for the hinged frame. Assuming the present price of the glulam in B.C. at approximately \$1,120 per cubic meter, the savings on the glulam can reach \$3,900 per one frame (\$35,000 on the whole building).

However, the glued-in rebar connections are more costly than the traditional non-rigid connections. The cost of materials used for the joint T-3, which was described in section 4.8, is as follows:

material	unit	unit price	quantity	cost
epoxy glue	l	\$11	1.5	\$17
rebars	kg	\$0.65	12	\$8
steel plates	kg	\$0.90	25	\$23
bolts (5/8")	pcs	\$0.42	28	\$12
total				\$60

Table 6.3 *Cost of the beam-to-column joint using glued-in rebar connection.*

The cost of the materials for a traditional joint between a beam and a column is estimated to be approximately \$40 (the joint consists of 4 shear plates and one steel beam hangers). This cost should be compared to the cost of joining a column to a beam in the rigid frame, which is \$60. Although the rigid connections are more expensive than the traditional ones, the total cost of the materials for the structure and the joints is smaller in case of the rigid frame with glued-in joints than in case of the traditional frame (see table 6.4).

	per frame		per building	
	glulam	joints	glulam	joints
hinged frame	\$27,140	\$1,680	\$244,000	\$15,000
rigid frame	\$23,260	\$2,640	\$209,000	\$24,000
cost difference (h-r)	\$3,880	-\$960	\$35,000	-\$9,000
total savings	\$2,920		\$26,000	

Table 6.4 *Cost comparison between hinged frame and rigid frame buildings.*

Above analysis does not take into consideration the cost of labor, which is very difficult to estimate at this stage. The glued-in rebar connections require more work in the plant, but the erection costs are much smaller than erection costs of the traditional frame. Therefore, it may be assumed that the combined cost of manufacturing and erection is similar in both cases.

CHAPTER 7

CONCLUSIONS

- 1. The effect of the moisture content changes and the temperature changes on the glued-in rebar connection has been investigated. The relative movement taking place at the interface between the glulam and the steel bar was examined. The tests showed that the behaviour of the specimens tested after cyclic temperature changes or cyclic moisture changes was similar to the behaviour of the specimens tested without any treatment. The only property which was affected by the treatment was a stiffness (decreased about 20%). The other properties, such as strength and ductility, remained unchanged.**

Therefore, the glued-in rebar connection may be considered reliable in the temperature and moisture conditions which can occur in the building. The connection was found to be influenced by those conditions to a lesser degree than the glulam structure itself.

- 2. A new method of increasing bearing capacity of the glulam has been developed. The gluing of the reinforcing bars under the bearing plate can increase the compressive resistance of the glulam in the direction perpendicular to the grain by 100%. This is possible because of the distribution of the local bearing stresses along the glued-in rebar through a significant portion of the glulam cross section.**
- 3. The rebars glued-in perpendicularly to the grain have an additional effect of increasing the shear capacity of the glulam members.**

4. A beam to column connection for glulam structures, based on the glued-in rebar idea, has been designed and tested, and its stiffness estimated. The connection is capable to transfer axial loads, shear loads and bending moments. Thus, it can be used in statically indeterminate structural systems, i.e. in the structures where the glulam was not successfully used before.

The connection proved to have a bending and shear resistance equal to or greater than the resistance of the glulam members which were joined. This allows more effective use of the glulam in the structure and "capacity design" approach in the design of the members.

A ductile behaviour of the connection prior to the failure was observed.

5. A suggested design method for the beam-to-column connection is outlined in the thesis.

The glued-in rebar connections can be designed as the steel connections whenever the minimum embedment length of the rebars glued into the glulam is ensured.

6. The rigid frame with the glued-in rebar joints is compared with a hinged frame utilizing the traditional connection methods. The savings on the glulam volume can reach 15%.

7. However, while the glued-in rebar connection methods seems to work very well in various configurations, there are still some questions to be amplified and thus the need for further investigation still exists.

Future research may include:

- the rebars' contribution to the shear capacity of the glulam,
- detailed studies of the embedment mechanism,
- development of the finite element model of the connection.

BIBLIOGRAPHY

1. Townsend, P.K., Buchanan, A.H., Moss, P.J.
"Steel Dowels Epoxy Bonded in Glue Laminated Timber", Report 90-11, Department of Civil Engineering, University of Canterbury, Christchurch, New Zealand, June 1990.
2. Fairweather, R.H., Buchanan, A.H., Dean, J.A.
"Beam Column Connections for Multi-Storey Timber Buildings", Report 92-5, Department of Civil Engineering, University of Canterbury, Christchurch, New Zealand, July 1992.
3. Barber, J., Buchanan, A.H.
"Fire Resistance of Epoxied Steel Rods in Glulam Timber", Report 94-1, Department of Civil Engineering, University of Canterbury, Christchurch, New Zealand, May 1994.
4. Buchanan, A.H., Fairweather, R.H.
"Epoxied Moment-Resisting Connections for Timber Buildings", Proceedings, International Workshop on Wood Connectors, Las Vegas, Nevada, USA, 1992.
5. Riberholt, H.
"Steel Bolts Glued into Glulam", Proceedings, Meeting of IUFRO Wood Engineering Group, Oxford, U.K., 1980.
6. Riberholt, H.
"Glued Bolts in Glulam", Department of Structural Engineering, Technical University of Denmark, Series R, Number 210, 1986.
7. Riberholt, H.
"Glued Bolts in Glulam, Part 2", Department of Structural Engineering, Technical University of Denmark, Series R, Number 228.

8. Riberholt, H.
"Glued Bolts in Glulam. Proposals for CIB Code", Proceedings, CIB Meeting 21, Parksville, British Columbia, Canada, 1988.
9. Foschi, R.O., Folz, B.R., Yao, F.Z.
"Reliability Based Design of Wood Structures", Report No.34, Department of Civil Engineering, University of British Columbia, Vancouver, Canada, 1990.
10. Madsen, B., Malczyk, R., Wiktor, R.
"Epoxyed Dowel Connections", Proceedings, International Workshop on Wood Connectors, Las Vegas, Nevada, USA, 1992.
11. Madsen, B.
"Structural Behaviour of Timber", Timber Engineering Ltd., Vancouver, Canada, 1992.
12. Malczyk, R.
"Glued-in Rebar Connections", M.A.Sc. Thesis, Department of Civil Engineering, University of British Columbia, Vancouver, Canada, October 1993.
13. McIntosh, K.A.
"From Theory to Reality - 30 Years in Glulam Manufacture", Proceedings of the Second Pacific Timber Engineering Conference, Auckland, New Zealand, 1989.
14. Turkovskij, S.
"Prefabricated Joints of Timber Structures with Inclined Glued-in Bars", Proceedings of the 1991 International Timber Engineering Conference, TRADA, London, U.K., 1991.
15. Turkovskij, S., Lukyanov, E.I., Pogoreltsev, A.A.
"Use of Glued-in Bars for Reinforcement of Wood Structures", Proceedings of the 1991 International Timber Engineering Conference, TRADA, London, U.K., 1991.
16. Turkovskij, S.B., Kurganskij, V.G., Pochernjaev, B.G.
"Opyt primienienija kliejnyh dierieviannyh konstrukcij v Moskovskoj oblasti" (in Russian), NTO strojindustrii, Moscow, USSR, 1987.

17. Bodig, J., Meyer, R.W., Kellogg, R.M.
"Structural Use of Wood in Adverse Environments. Moisture Effects on Structural Use of Wood", Society of Wood Science and Technology, New York, USA.
18. Schniewind, A.P.
"Concise Encyclopedia of Wood & Wood-Based Materials", Pergamon Press, New York, 1989.
19. Charleson, A.W., Patience, D.B.
"Review of Current Structural Timber Jointing Methods", New Zealand Timber Design Journal, Issue 3, Volume 2, 1993.
20. Forest Products Laboratory
"Wood Handbook: Wood as an Engineering Material", U.S. Department of Agriculture, Washington, D.C., 1974.
21. Wangaard, F.F.
"Wood: Its Structure and Properties", The Pennsylvania State University, 1979.
22. Canadian Institute of Steel Construction
"Handbook of Steel Construction", Canadian Institute of Steel Construction, Willowdale, Ontario, Canada, 1991.
23. Canadian Institute of Steel Construction
"Metric Design Notes for Limit States Design in Steel", Canadian Institute of Steel Construction, Willowdale, Ontario, Canada, 1979.
24. PZITB
"Poradnik inżyniera i technika budowlanego. Tom 5" (in Polish), Polish Association of Civil Engineers and Technicians, Warsaw, Poland, 1986.
25. Canadian Wood Council
"Wood Design Manual", Canadian Wood Council, Ottawa, Ontario, Canada, 1990.

APPENDIX A

THEORETICAL DEFORMATIONS AND STRESSES IN A GLUED-IN REBAR SPECIMEN DURING FREEZING/HEATING CYCLE

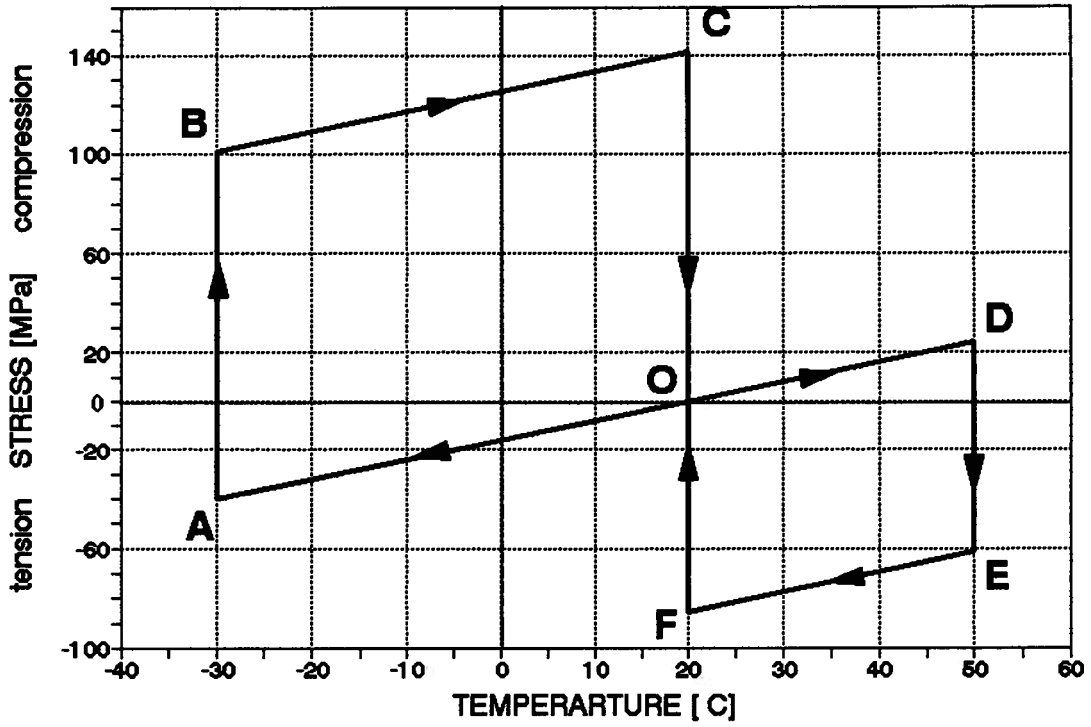
This Appendix presents detailed calculations of the stresses and deformations shown on Fig.2.20 in section 2.4.3. Please, refer to chapter 2 for information about the specimen and testing procedures.

1. ASSUMPTIONS.

The following assumptions have been made:

- there are no internal stresses in the specimen at the beginning of the cycle,
- the manufacturing temperature is +20°C and so is the temperature of the specimen (rebar and glulam) at the beginning of the cycle,
- a thin layer of glue is not taken into consideration in this calculations,
- the changes of the ambient temperature are instantaneous,
- linear elastic behaviour of both materials is considered,
- elastic modulus of steel (rebar) is $E_s=200\ 000\ \text{MPa}$,
- elastic modulus of glulam perpendicularly to the grain is $E_g=500\ \text{MPa}$ (test value),
- linear thermal expansion coefficient of steel is $c_s=11.3 \times 10^{-6}/^\circ\text{C}$,
- linear thermal expansion coefficient of wood in the direction perpendicular to the grain is $c_g=40 \times 10^{-6}/^\circ\text{C}$,
- thermal conductivity of steel is 58 W/m/K,
- thermal conductivity of wood perpendicularly to the grain is 0.16 W/m/K,
- the dimensional changes of the rebar due to the change of the outside temperature are completed before the glulam starts to contract or expand - this is not exactly accurate but, due to a very big difference between the conductivities of both materials, is acceptable.

STRESS IN REBAR



STRESS IN GLULAM

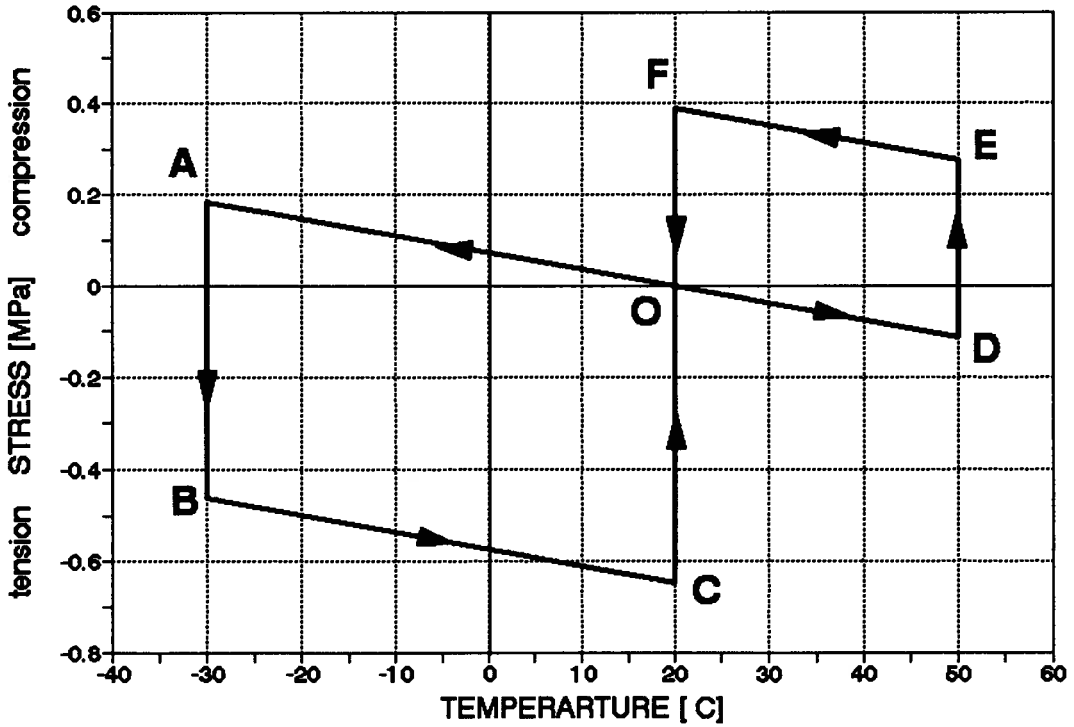


Fig. A.1 Internal stresses in the specimen due to temperature changes.

2. FREEZING CYCLE: from +20°C to -30°C.

There are no stresses in the rebar nor in the glulam. Outside temperature is +20°C. The starting point of the graph (Fig.A.1) is O.

phase 1 - line OA

The outside temperature changes from +20°C to -30°C ($\Delta T = -50^\circ\text{C}$). Only the rebar is affected by the changed temperature in this phase.

The rebar contracts and puts the glulam into compression. The tension stress develops in the rebar. An equilibrium is reached when the tension force in the rebar is equal to the compression force in the glulam.

The final contraction of the whole specimen in phase 1, X_1 , is calculated by solving the equation below [A4].

$$F_s = F_g \quad [A1]$$

$$\sigma_s A_s = \sigma_g A_g \quad [A2]$$

$$\epsilon_s E_s A_s = \epsilon_g E_g A_g \quad [A3]$$

$$\frac{\Delta_s}{L} E_s A_s = \frac{\Delta_g}{L} E_g A_g \quad [A4]$$

where subscripts s g refer to steel and glulam respectively, and

F - force at equilibrium,

σ - stress at equilibrium,

A - area,

ϵ - strain in the material,

L - length of the specimen,

Δ - change of the length.

The glulam is subjected to compression deformation $\Delta_g = X_1$.

The rebar's tension deformation is equal to the difference between free contraction of the rebar due to the temperature change Δ_r^{-50} and the shortening of the specimen at equilibrium X_1 (equation [A5]).

$$\Delta_s = \Delta_r^{-50} - X_1 \quad [A5]$$

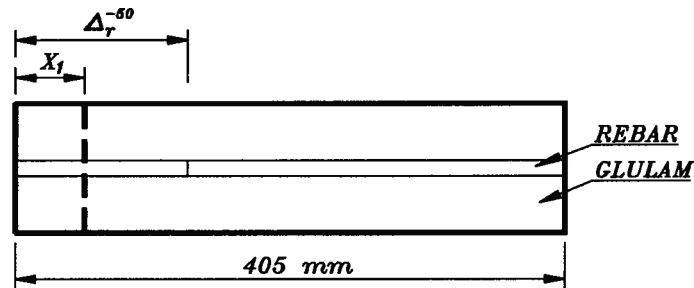


Fig.A.2 Deformation of the specimen in phase 1 ($\Delta T = -50^\circ\text{C}$).

Free contraction of the rebar is

$$\Delta_r = c_r L \Delta T \quad [A6]$$

$$\Delta_r^{-50} = 11.3 \times 10^{-6} \times 405 \times 50 = 0.23 \text{ mm}$$

Substituting the following values:

$$E_s = 200\,000 \text{ MPa}, \quad E_g = 500 \text{ MPa}, \quad L = 405 \text{ mm}$$

$$A_s = 200 \text{ mm}^2, \quad A_g = 175 \times 250 = 43\,750 \text{ mm}^2,$$

the equation [A4] becomes

$$\frac{(0.23 - X_1)}{405} \times 200\,000 \times 200 = \frac{X_1}{405} \times 500 \times 43\,750 \quad [A7]$$

Solving equation [A7] for X_1 gives

$$X_1 = 0.149 \text{ mm} \quad (\text{contraction})$$

Now, the compression stress in the glulam can be found:

$$\sigma_g = \frac{X_1}{L} E_g = \frac{0.149}{405} \times 500 = 0.184 \text{ MPa}$$

Therefore the equilibrium force is:

$$F_g = \sigma_g A_g = 0.184 \times 43750 = 8050 \text{ N} = F_s$$

Finally, the tension stress in the rebar can be calculated:

$$\sigma_s = \frac{F_s}{A_s} = \frac{8050}{200} = 40.25 \text{ MPa}$$

phase 2 - line AB

The glulam cools and shrinks, releasing the tension stress in the rebar and then, shrinking even more, puts the rebar into compression. The equilibrium is reached when the temperature of the glulam matches the surrounding temperature, i.e. -30°C (it is assumed that the rebar reached -30°C in phase 1).

The final contraction of the specimen after phase 2, X_2 , can be found by solving the same relationship as before (equation [A4]). Now, however, the change of the length of the rebar and the glulam are as follows (see Fig.A.3):

$$\Delta_s = X_2 - \Delta_r^{-50} \quad [\text{A8}]$$

$$\Delta_g = \Delta_g^{-50} - X_2 \quad [\text{A9}]$$

where

Δ_r^{-50} - free contraction of the rebar ($\Delta T = -50^\circ\text{C}$),

Δ_g^{-50} - free contraction of the glulam ($\Delta T = -50^\circ\text{C}$).

$$\Delta_r^{-50} = 0.23 \text{ mm}$$

$$\Delta_g^{-50} = 40 \times 10^{-6} \times 405 \times 50 = 0.81 \text{ mm}$$

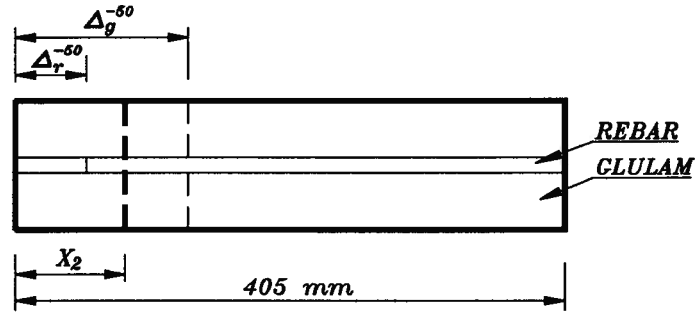


Fig.A.3 Deformation of the specimen in phase 2 ($\Delta T = -50^\circ\text{C}$).

After substituting relations [A8] and [A9] the equation [A4] may be written as:

$$\frac{(X_2 - 0.23)}{405} \times 200000 \times 200 = \frac{(0.81 - X_2)}{405} \times 500 \times 43750 \quad [\text{A10}]$$

After solving above, the contraction of the specimen in phase 2 is:

$$X_2 = 0.435 \text{ mm} \quad (\text{contraction})$$

Now, the tension stress in the glulam can be found:

$$\sigma_g = \frac{\Delta_g}{L} E_g = \frac{(0.81 - 0.435)}{405} \times 500 = 0.463 \text{ MPa}$$

Therefore, the equilibrium force is:

$$F_g = \sigma_g A_g = 0.463 \times 43750 = 20256 \text{ N} = F_s$$

Finally, the compression stress in the rebar can be calculated:

$$\sigma_s = \frac{F_s}{A_s} = \frac{20256}{200} = 101.28 \text{ MPa}$$

phase 3 - line BC

The outside temperature changes from -30°C to $+20^{\circ}\text{C}$ ($\Delta T = +50^{\circ}\text{C}$). Similarly as it was in phase 1, only the rebar is affected by the changed temperature at first.

At the end of phase 2 the rebar was in compression. Now, it wants to expand due to the rising temperature but is restrained by the glulam. The compression stress in the rebar increases and so does the tension stress in the glulam. The total shortening of the specimen ($X_3 < X_2$) decreases, when compared to the previous phase.

To calculate X_3 , the equation [A4] may be used again. Because the rebar returned to its starting temperature, the change of its length is equal to X_3 ($\Delta_s = X_3$). The change of the length of the glulam is:

$$\Delta_g = \Delta_g^{-50} - X_3 \quad [\text{A11}]$$

where $\Delta_g^{-50} = 0.81 \text{ mm}$, as before.

The equation [A4] can be written as:

$$\frac{X_3}{405} \times 200000 \times 200 = \frac{(0.81 - X_3)}{405} \times 500 \times 43750 \quad [\text{A12}]$$

In result, the contraction of the specimen after phase 3 is:

$$X_3 = 0.286 \text{ mm} \quad (\text{contraction})$$

Now, the tension stress in the glulam can be found:

$$\sigma_g = \frac{\Delta_g}{L} E_g = \frac{(0.81 - 0.286)}{405} \times 500 = 0.647 \text{ MPa}$$

Therefore, the equilibrium force is:

$$F_g = \sigma_g A_g = 0.647 \times 43750 = 28306 \text{ N} = F_s$$

Finally, the compression stress in the rebar can be calculated:

$$\sigma_s = \frac{F_s}{A_s} = \frac{28306}{200} = 141.53 \text{ MPa}$$

phase 4 - line CO

The glulam expands until it reaches the original dimension. All stresses, in the rebar and in the glulam, are released.

$$X_4 = 0 \text{ mm}$$

$$\sigma_g = 0 \text{ MPa}$$

$$\sigma_s = 0 \text{ MPa}$$

3. HEATING CYCLE: from +20°C to +50°C.

There are no stresses in the rebar nor in the glulam. Outside temperature is +20°C. The starting point of the graph (Fig.A.1) is O. The calculations of the stresses are analogues to those presented in section 2.

phase 5 - line OD

The outside temperature changes from +20°C to +50°C ($\Delta T = +30^\circ\text{C}$). Similarly as it was in phase 1, only the rebar is affected by the changed temperature at first.

The rebar wants to expand due to the rising temperature but is restrained by the glulam. This causes the compression stress in the rebar and the tension stress in the glulam. The specimen expands by the length X_5 .

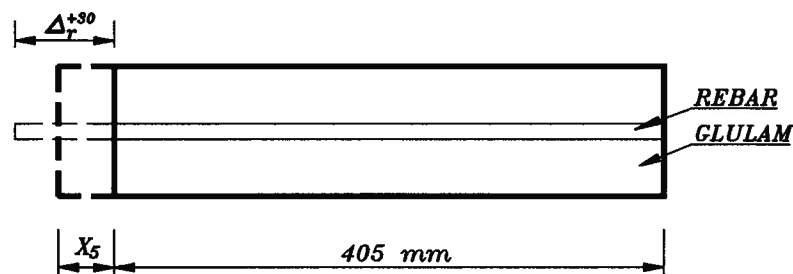


Fig.A.4 Deformation of the specimen in phase 5 ($\Delta T = +30^\circ\text{C}$).

Repeating the process used previously, the following results are obtained:

$$\Delta_g = X_5$$

$$\Delta_s = \Delta_r^{+30} - X_5$$

$$\Delta_r^{+30} = 11.3 \times 10^{-6} \times 405 \times 30 = 0.14 \text{ mm}$$

the equation [A4] becomes

$$\frac{(0.14 - X_5)}{405} \times 200000 \times 200 = \frac{X_5}{405} \times 500 \times 43750 \quad [\text{A13}]$$

therefore

$$X_5 = 0.091 \text{ mm} \quad (\text{expansion})$$

and

$$\sigma_g = \frac{X_5}{L} E_g = \frac{0.091}{405} \times 500 = 0.112 \text{ MPa} \quad (\text{tension})$$

$$F_g = \sigma_g A_g = 0.112 \times 43750 = 4900 \text{ N} = F_s$$

$$\sigma_s = \frac{F_s}{A_s} = \frac{4900}{200} = 24.50 \text{ MPa} \quad (\text{compression}).$$

phase 6 - line DE

The glulam warms and expands, releasing the compression stress in the rebar and then, expanding even more, creates the tension stress in the rebar. The equilibrium is reached when the temperature of the glulam matches the surrounding temperature, i.e. +50°C (it is assumed that the rebar reached +50°C in phase 5).

The final expansion of the specimen after phase 6, X_6 , is shown on Fig.A.5.

Repeating the process used previously, the following results are obtained:

$$\Delta_g = \Delta_g^{+30} - X_6$$

$$\Delta_s = X_6 - \Delta_r^{+30}$$

$$\Delta_g^{+30} = 40 \times 10^{-6} \times 405 \times 30 = 0.49 \text{ mm}$$

$$\Delta_r^{+30} = 0.14 \text{ mm}$$

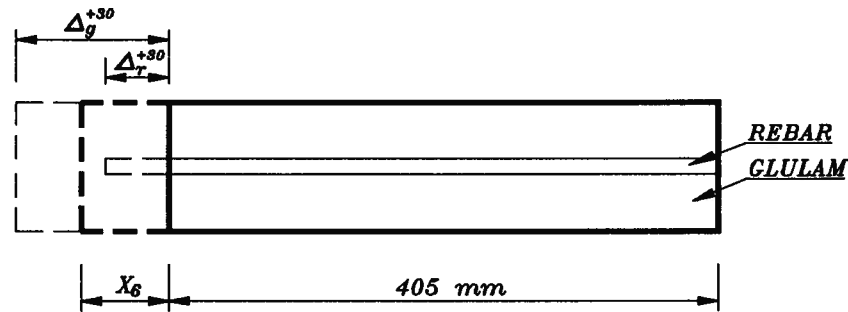


Fig.A.5 Deformation of the specimen in phase 6 ($\Delta T = +30^\circ C$).

the equation [A4] becomes

$$\frac{(X_6 - 0.14)}{405} \times 200000 \times 200 = \frac{(0.49 - X_6)}{405} \times 500 \times 43750 \quad [A13]$$

therefore

$$X_6 = 0.264 \text{ mm} \quad (\text{expansion})$$

and

$$\sigma_g = \frac{(\Delta_g^{+30} - X_6)}{L} E_g = \frac{(0.49 - 0.264)}{405} \times 500 = 0.279 \text{ MPa} \quad (\text{compression})$$

$$F_g = \sigma_g A_g = 0.279 \times 43750 = 12206 \text{ N} = F_s$$

$$\sigma_s = \frac{F_s}{A_s} = \frac{12206}{200} = 61.03 \text{ MPa} \quad (\text{tension}).$$

phase 7 - line EF

The outside temperature changes from +50°C to +20°C ($\Delta T = -30^\circ\text{C}$). Similarly as it was in phase 5, only the rebar is affected by the changed temperature at first.

At the end of phase 6 the rebar was in tension. Now, it wants to shrink due to the dropping temperature but is restrained by the glulam. The tension stress in the rebar increases and so does the compression stress in the glulam. The total expansion of the specimen decreases ($X_7 < X_6$), when compared to the previous phase.

Repeating the process used previously, the following results are obtained:

$$\Delta_g = \Delta_g^{+30} - X_7$$

$$\Delta_s = X_7$$

the equation [A4] becomes

$$\frac{X_6}{405} \times 200000 \times 200 = \frac{(0.49 - X_7)}{405} \times 500 \times 43750 \quad [\text{A14}]$$

therefore

$$X_7 = 0.173 \text{ mm} \quad (\text{expansion})$$

and

$$\sigma_g = \frac{(\Delta_g^{+30} - X_7)}{L} E_g = \frac{(0.49 - 0.173)}{405} \times 500 = 0.391 \text{ MPa} \quad (\text{compression})$$

$$F_g = \sigma_g A_g = 0.391 \times 43750 = 17106 \text{ N} = F_s$$

$$\sigma_s = \frac{F_s}{A_s} = \frac{17106}{200} = 85.53 \text{ MPa} \quad (\text{tension}).$$

phase 8 - line FO

The whole specimen returns to its original temperature (+20°C). All stresses are released completely.

$$X_g = 0 \text{ mm}$$

$$\sigma_g = 0 \text{ MPa}$$

$$\sigma_s = 0 \text{ MPa}$$

4. SUMMARY.

The maximum stresses and deformations occur during the freezing cycle because of the largest change of the temperature ($\Delta T = 50^\circ\text{C}$). The largest dimensional change of the specimen's length can be observed at the end of phase 2 when the contraction reaches 0.44mm (0.11% of the initial length). The peak stresses occur at the end of phase 3 and are as follows:

141.5MPa compression in the rebar (35% of the specified yield strength),

0.647MPa tension in the glulam (78% of the specified strength of the glulam perpendicularly to the grain).

APPENDIX B

THE ANALYSIS OF THE RIGID FRAME FOR A MULTI-STOREY OFFICE BUILDING

This Appendix presents the analysis of the frame for a 3-storey office building. Testing of a portion of this frame (a second storey beam-to-column joint) was described in chapter 4 of this thesis.

1. GENERAL DESIGN ASSUMPTIONS.

I. Location.

The building is located in Vancouver, British Columbia.

II. Dimensions.

The building is rectangular in shape, 63.0m long and 36.0m wide. It consists of 3 stories.

The requirements for the clear heights are:

ground floor	3 000 mm
2 nd and 3 rd floors	2 700 mm.

Ceiling space must accommodate the mechanical ducts.

III. Structural System.

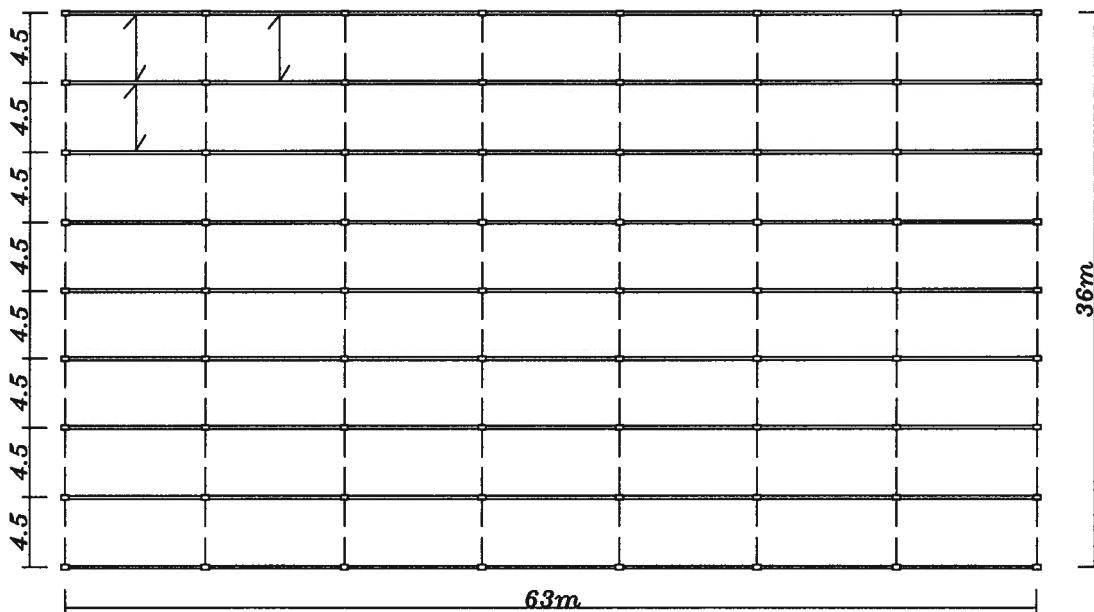
The main frame is placed in the longitudinal direction of the building. It consists of the glulam members connected using the glued-in rebar method. The joints between the beams

and the columns, and beam splices are moment resisting. The first storey columns are pin connected to the foundation.

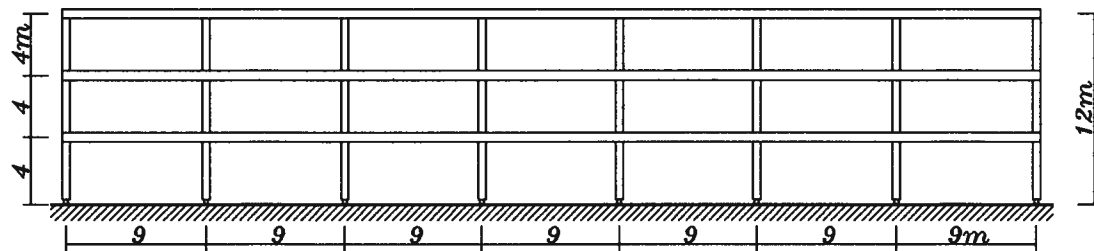
The dimensions of the main frame are as follows (see Fig.B.1):

span	9.0 m
spacing	4.5 m
storey height	4.0 m.

The lateral forces in the direction perpendicular to the plane of the rigid frame are resisted by a bracing system between the frames.



PLAN



CROSS SECTION

Fig.B.1 Overall dimensions of the building.

IV. Specified Design Loads.

The following specified loads have to be considered:

office floor live load	2.40 kPa	
partition allowance	1.20 kPa	
ground snow load	2.50 kPa	
reference wind pressure $q(1/10)$	0.45 kPa	(serviceability limit states)
reference wind pressure $q(1/30)$	0.55 kPa	(strength limit states)
earthquake loads.		

2. LOADS.

I. Dead Loads.

a) floor dead load

floor finish	0.10 kN/m ²
plywood decking on I-joists	0.20 kN/m ²
mechanical ducts and ceiling	0.40 kN/m ²
self weight of supporting structure	0.10 kN/m ²
partition allowance	1.20 kN/m ²

TOTAL: 2.00 kN/m²

b) roof dead load

felt and gravel	0.35 kN/m ²
insulation	0.10 kN/m ²

plywood decking on I-joists	0.20 kN/m ²
mechanical ducts and ceiling	0.40 kN/m ²
self weight of supporting structure	0.10 kN/m ²

TOTAL: 1.15 kN/m²

II. Live Loads.

a) floor live load

occupancy load	2.40 kN/m ²
tributary area of the beam $A=9.0 \times 4.5$	40.5 m ²

because $A > 20\text{m}^2$, the floor live load can be reduced multiplying the specified occupancy load by factor (t_r) calculated below:

$$t_r = 0.3 + \left(\frac{9.8}{A}\right)^{0.5} = 0.3 + \left(\frac{9.8}{40.5}\right)^{0.5} = 0.79$$

therefore the floor live load is:

$$lf = 0.79 \times 2.40 = 1.90 \text{ kN/m}^2.$$

b) roof live load

S_s	specified ground snow load	2.50 kN/m ²	
S_r	associated rain load	0.30 kN/m ²	
C_b	basic roof snow load factor	0.80	
C_w	wind exposure factor	1.00	
C_f	roof slope factor	1.00	(flat roof)
C_a	accumulation factor	1.00	

The specified snow load, S, can be calculated follows:

$$S = S_s (C_b C_w C_f C_a) + S_r$$
$$S = 2.5 \times (0.8 \times 1.0 \times 1.0 \times 1.0) + 0.3 = 2.3 \text{ kN/m}^2.$$

III. Wind Loads.

$q_{(1/30)}$	reference velocity pressure (1/30)	0.55 kN/m ²
$q_{(1/10)}$	reference velocity pressure (1/10)	0.45 kN/m ²
h	reference height of the building	13.0 m

It is assumed that exposure factor C_e is constant over the entire height of the building and is equal to:

$$C_e = \left(\frac{h}{10} \right)^{0.2} = \left(\frac{13.0}{10} \right)^{0.2} = 1.05$$

a) wind pressure on the windward wall

$C_p C_g$	peak pressure coefficient	0.75
-----------	---------------------------	------

The specified external pressure is equal to:

$$p = q C_e C_p C_g$$

therefore

$$p_{(1/30)} = 0.55 \times 1.05 \times 0.75 = 0.43 \text{ kN/m}^2$$

$$p_{(1/10)} = 0.45 \times 1.05 \times 0.75 = 0.35 \text{ kN/m}^2$$

b) wind suction on the leeward wall

$C_p C_g$	peak pressure coefficient	0.55
-----------	---------------------------	------

The specified external suction is equal to:

$$p = q C_e C_p C_g$$

therefore

$$P_{(1/30)} = 0.55 \times 1.05 \times 0.55 = 0.32 \text{ kN/m}^2$$

$$P_{(1/10)} = 0.45 \times 1.05 \times 0.55 = 0.26 \text{ kN/m}^2$$

c) wind suction on the roof

$C_p C_g$ peak pressure coefficient 1.30

The specified external suction is equal to:

$$p = q C_e C_p C_g$$

therefore

$$P_{(1/30)} = 0.55 \times 1.05 \times 1.30 = 0.75 \text{ kN/m}^2$$

$$P_{(1/10)} = 0.45 \times 1.05 \times 1.30 = 0.61 \text{ kN/m}^2$$

IV. Earthquake Loads.

U calibration factor 0.6

R force modification factor 2.0 (moment-resisting wood frame with ductile connectors)

Note: The values of the factor R, permitted by the code, do not include the case of glued-in rebar connections. Assuming rigidity of the joints and failure in the steel, this structure could be treated as a steel structure.

v zonal velocity ratio 0.2 (Vancouver)

Z_a acceleration seismic zone 4 (Vancouver)

Z_v velocity seismic zone 4 (Vancouver)

F	foundation factor	1.0	(dense soil)
I	seismic importance factor	1.0	(nominal)
N	number of storeys	3	

The fundamental period of the building, T, is:

$$T = 0.1 N = 0.1 \times 3 = 0.3 \text{ s}$$

therefore, the seismic response factor, S, is equal to:

$$S = 3.0 - 3.6 \times (T - 0.25) = 3.0 - 3.6 \times (0.3 - 0.25) = 2.82$$

The weight, W, of the structure is estimated to be as follows:

25% of the snow load	$0.25 \times 2.30 \times 4.5 \times 63.0$	164 kN
100% of roof dead load	$1.15 \times 4.5 \times 63.0$	326 kN
100% of floors dead load	$2 \times 1.90 \times 4.5 \times 63.0$	1077 kN
100% of self weight of frame	$20 \text{ m}^3 \times 5.3 \text{ kN/m}^3$	101 kN
<hr style="border-top: 3px double #000;"/>		
TOTAL:		1668 kN

The equivalent lateral seismic force, V_e , can be calculated in accordance with the following formula:

$$V_e = v S I F W$$

therefore

$$V_e = 0.2 \times 2.82 \times 1.0 \times 1.0 \times 1668 = 941 \text{ kN.}$$

The minimum lateral seismic force (base shear), V, is equal to:

$$V = (V_e/R)U$$

therefore

$$V = (941/2.0) \times 0.8 = 282 \text{ kN.}$$

The above seismic force at the base of the structure, V, is calculated for one frame, i.e. it is 1/8 of the total base shear of the whole building.

The distribution of the minimum lateral seismic force along the height of the building is calculated according to the formula given below:

$$F_x = \frac{(V - F_t)W_x h_x}{\sum_{i=1}^N W_i h_i}$$

a) roof seismic force

The concentrated force at the top $F_t = 0$, because period $T < 0.7s$.

The weight of the roof (including snow) is equal to:

$$W_r = 164 + 326 + 101/3 = 524 \text{ kN}$$

The seismic force at the roof level is:

$$F_r = \frac{(V - F_t)W_r h_r}{\sum_{i=1}^N W_i h_i}$$

$$F_r = \frac{(282 - 0) \times 524 \times 12.0}{524 \times 12.0 + 572 \times 8.0 + 572 \times 4.0} = 131 \text{ kN}$$

b) second storey seismic force

The weight of the floor is equal to:

$$W_s = 1077/2 + 101/3 = 572 \text{ kN}$$

The seismic force at the second floor level is:

$$F_s = \frac{(V - F_t)W_s h_s}{\sum_{i=1}^N W_i h_i}$$

$$F_s = \frac{(282 - 0) \times 572 \times 8.0}{524 \times 12.0 + 572 \times 8.0 + 572 \times 4.0} = 101 \text{ kN}$$

c) first storey seismic force

The weight of the roof (including snow) is equal to:

$$W_f = W_s = 572 \text{ kN}$$

The seismic force at the first floor level is:

$$F_f = \frac{(V - F_t)W_f h_f}{\sum_{i=1}^N W_i h_i}$$

$$F_f = \frac{(282-0) \times 572 \times 4.0}{524 \times 12.0 + 572 \times 8.0 + 572 \times 4.0} = 50 \text{ kN}$$

3. LOAD COMBINATIONS.

The following factored load combinations are included in the analysis:

- a. 1.25x(Dead Loads) + 1.5x(Live Loads)
- b. 1.25x(Dead Loads) + 1.5x(Wind Loads)
- c. 0.85x(Dead Loads) + 1.5x(Wind Loads)
- d. 1.25x(Dead Loads) + 1.0x(Seismic Forces)
- e. 0.85x(Dead Loads) + 1.0x(Seismic Forces)
- f. 1.25x(Dead Loads) + 0.7x{1.5x(Live Loads) + 1.5x(Wind Loads)}
- g. 1.25x(Dead Loads) + 0.7x{1.5x(Live Loads) + 1.0x(Seismic Forces)}

A load combination giving the largest internal forces in the element is chosen to design that element.

The load combinations involving partial loading of the structure were found to give less critical internal forces than full loading.

4. FRAME ANALYSIS.

The static analysis of the frame was performed using a finite element method program called PLANE 3. The model of the structure used for the computations is presented on Fig.B.2.

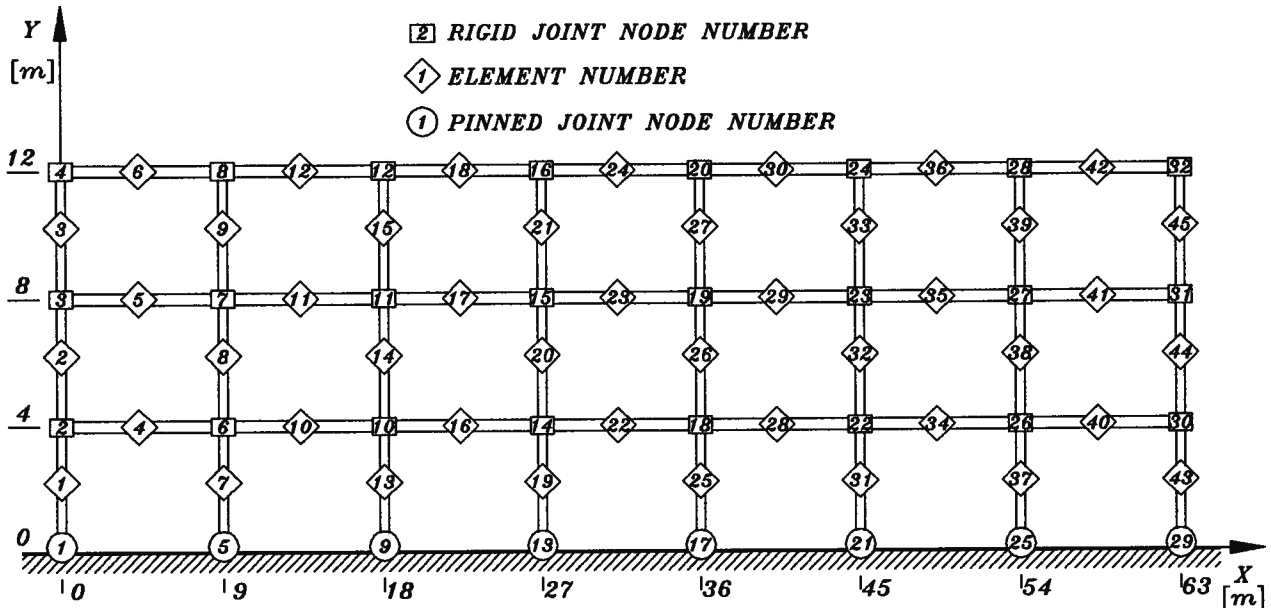


Fig.B.2 Model of the frame used in the numerical analysis.

The factored loads applied to the frame in each load case are shown in Table B.1.

uniformly distr. loads [kN/m]	element No.	direc.	load combinations						
			a	b	c	d	e	f	g
roof beams	6,12,18,24,30,36,42	-Y	22.0	1.4	-0.7	6.5	4.4	13.8	17.3
floor beams	4,5,10,11,16,17,22,23, 28,29,34,35,40,41	-Y	24.1	11.3	7.7	11.3	7.6	20.2	20.2
windward columns	1,2,3	X	-	2.9	2.9	-	-	2.0	-
leeward columns	43,44,45	X	-	2.1	2.1	-	-	1.5	-

Table B.1 ...continues on the next page...

concentrated loads [kN]	node No.	direc.	load combinations						
			a	b	c	d	e	f	g
1 st st. seismic force	2,6,10,14,18,22,26	X	-	-	-	7.2	7.2	-	5.0
2 nd st. seismic force	3,7,11,15,19,23,27	X	-	-	-	14.4	14.4	-	10.1
roof seismic force	4,8,12,16,20,24,28	X	-	-	-	18.7	18.7	-	13.1

Table B.1 *Load cases used in the numerical analysis of the frame.*

5. RESULTS OF THE ANALYSIS.

The internal forces in the frame, due to the load combinations described in section 4, are presented below.

Load combination "A" 1.25*D+1.5*L						
Beam Forces						
member	axial1 [kN]	shear1 [kN]	bm1 [kNm]	axial2 [kN]	shear2 [kN]	bm2 [kNm]
1	-290.9	-15.9	0.0	-290.9	-15.9	-63.7
2	-189.8	-26.3	49.9	-189.8	-26.3	-55.2
3	-88.6	-34.6	60.2	-88.6	-34.6	-78.3
4	10.3	101.0	-113.6	10.3	-115.9	-180.3
5	8.3	101.2	-115.3	8.3	-115.7	-180.3
6	-34.6	88.6	-78.3	-34.6	-109.4	-172.0
7	-659.7	1.6	0.0	-659.7	1.6	6.4

Table B.2 *...continues on the next page...*

8	-434.4	2.5	-5.3	-434.4	2.5	4.9
9	-209.9	5.7	-9.5	-209.9	5.7	13.3
10	9.4	109.4	-168.6	9.4	-107.5	-160.4
11	5.2	108.9	-165.8	5.2	-108.0	-161.8
12	-28.9	100.5	-158.7	-28.9	-97.5	-145.5
13	-628.4	-0.3	0.0	-628.4	-0.3	-1.3
14	-412.5	-0.2	0.4	-412.5	-0.2	-0.4
15	-196.2	-0.2	-0.1	-196.2	-0.2	-0.7
16	9.3	108.4	-162.1	9.3	-108.5	-162.8
17	5.1	108.3	-162.1	5.1	-108.6	-163.1
18	-29.1	98.7	-146.2	-29.1	-99.3	-149.4
19	-632.3	0.0	0.0	-632.3	0.0	0.0
20	-415.4	0.0	-0.1	-415.4	0.0	0.0
21	-198.3	0.3	-0.5	-198.3	0.3	0.7
22	9.2	108.5	-162.8	9.2	-108.5	-162.8
23	4.8	108.5	-162.6	4.8	-108.5	-162.6
24	-28.8	99.0	-148.7	-28.8	-99.0	-148.7
25	-632.3	0.0	0.0	-632.3	0.0	0.0
26	-415.4	0.0	0.1	-415.4	0.0	0.0
27	-198.3	-0.3	0.5	-198.3	-0.3	-0.7
28	9.3	108.5	-162.8	9.3	-108.4	-162.1
29	5.1	108.6	-163.1	5.1	-108.3	-162.1
30	-29.1	99.3	-149.4	-29.1	-98.7	-146.2
31	-628.4	0.3	0.0	-628.4	0.3	1.3
32	-412.5	0.2	-0.4	-412.5	0.2	0.4
33	-196.2	0.2	0.1	-196.2	0.2	0.7
34	9.4	107.5	-160.4	9.4	-109.4	-168.6

Table B.2 ...continues on the next page...

35	5.2	108.0	-161.8	5.2	-108.9	-165.8
36	-28.9	97.5	-145.5	-28.9	-100.5	-158.7
37	-659.7	-1.6	0.0	-659.7	-1.6	-6.4
38	-434.4	-2.5	5.3	-434.4	-2.5	-4.9
39	-209.9	-5.7	9.5	-209.9	-5.7	-13.3
40	10.3	115.9	-180.3	10.3	-101.0	-113.6
41	8.3	115.7	-180.3	8.3	-101.2	-115.3
42	-34.6	109.4	-172.0	-34.6	-88.6	-78.3
43	-290.9	15.9	0.0	-290.9	15.9	63.7
44	-189.8	26.3	-49.9	-189.8	26.3	55.2
45	-88.6	34.6	-60.2	-88.6	34.6	78.3
Support Reactions						
node	Rx [kN]	Ry [kN]	M [kNm]			
1	15.9	290.9	0.0			
5	-1.6	659.7	0.0			
9	0.3	628.4	0.0			
13	0.0	632.3	0.0			
17	0.0	632.3	0.0			
21	-0.3	628.4	0.0			
25	1.6	659.7	0.0			
29	-15.9	290.9	0.0			

Table B.2 *Internal forces due to the load combination "a".*

Load combination "B" 1.25*D+1.5*Wo						
Beam Forces						
member	axial1 [kN]	shear1 [kN]	bm1 [kNm]	axial2 [kN]	shear2 [kN]	bm2 [kNm]
1	-93.8	2.5	0.0	-93.8	-9.1	-13.2
2	-51.2	-5.3	17.0	-51.2	-16.9	-27.3
3	-6.3	0.2	12.7	-6.3	-11.4	-9.8
4	-3.8	42.6	-30.2	-3.8	-59.1	-104.8
5	-17.1	45.0	-40.0	-17.1	-56.7	-92.9
6	-11.4	6.3	-9.8	-11.4	-6.3	-10.2
7	-225.6	7.8	0.0	-225.6	7.8	31.3
8	-119.1	6.5	-11.7	-119.1	6.5	14.1
9	-12.2	1.9	-4.3	-12.2	1.9	3.2
10	-2.5	47.4	-61.8	-2.5	-54.3	-92.6
11	-12.5	50.2	-74.5	-12.5	-51.5	-80.7
12	-9.6	5.8	-7.0	-9.6	-6.8	-11.2
13	-215.0	6.7	0.0	-215.0	6.7	26.9
14	-113.8	4.1	-7.4	-113.8	4.1	8.9
15	-12.8	1.2	-2.0	-12.8	1.2	3.0
16	0.2	46.9	-58.4	0.2	-54.8	-93.9
17	-9.6	49.5	-69.8	-9.6	-52.2	-82.3
18	-8.3	6.0	-8.3	-8.3	-6.6	-10.8
19	-216.2	6.9	0.0	-216.2	6.9	27.5
20	-114.4	4.2	-7.6	-114.4	4.2	9.3

Table B.3 ...continues on the next page...

21	-12.6	1.3	-2.3	-12.6	1.3	2.9
22	2.8	47.0	-58.8	2.8	-54.7	-93.7
23	-6.7	49.6	-70.6	-6.7	-52.1	-82.0
24	-7.0	6.0	-7.9	-7.0	-6.6	-10.9
25	-216.1	6.9	0.0	-216.1	6.9	27.6
26	-114.4	4.0	-7.2	-114.4	4.0	8.9
27	-12.6	1.3	-2.2	-12.6	1.3	2.9
28	5.7	47.0	-58.9	5.7	-54.7	-93.5
29	-3.9	49.7	-70.9	-3.9	-52.0	-81.3
30	-5.8	6.0	-8.0	-5.8	-6.6	-11.1
31	-215.2	7.0	0.0	-215.2	7.0	28.0
32	-113.8	4.2	-7.3	-113.8	4.2	9.3
33	-12.7	1.3	-2.5	-12.7	1.3	2.9
34	8.5	46.7	-58.1	8.5	-55.0	-95.5
35	-1.1	49.1	-69.5	-1.1	-52.6	-85.4
36	-4.4	6.1	-8.2	-4.4	-6.5	-10.4
37	-223.5	6.5	0.0	-223.5	6.5	26.0
38	-118.9	2.3	-4.2	-118.9	2.3	5.0
39	-12.7	0.6	-0.1	-12.7	0.6	2.1
40	12.7	49.6	-65.3	12.7	-52.1	-76.6
41	0.6	53.6	-80.2	0.6	-48.1	-55.1
42	-3.9	6.1	-8.3	-3.9	-6.5	-9.8
43	-106.6	15.7	0.0	-106.6	7.3	46.0
44	-54.5	20.0	-30.6	-54.5	11.6	32.7
45	-6.5	12.3	-22.4	-6.5	3.9	9.8

Table B.3 ...continues on the next page...

Support Reactions			
node	Rx [kN]	Ry [kN]	M [kNm]
1	-2.5	93.8	0.0
5	-7.8	225.6	0.0
9	-6.7	215.0	0.0
13	-6.9	216.2	0.0
17	-6.9	216.1	0.0
21	-7.0	215.2	0.0
25	-6.5	223.5	0.0
29	-15.7	106.6	0.0

Table B.3 *Internal forces due to the load combination "b".*

Load combination "C" $0.85 \cdot D + 1.5 \cdot W_o$						
Beam Forces						
member	axial1 [kN]	shear1 [kN]	bm1 [kNm]	axial2 [kN]	shear2 [kN]	bm2 [kNm]
1	-54.3	4.9	0.0	-54.3	-6.7	-3.5
2	-27.3	-1.1	9.2	-27.3	-12.7	-18.3
3	2.3	4.2	4.9	2.3	-7.4	-1.7
4	-5.6	27.1	-12.7	-5.6	-41.3	-77.1
5	-16.8	29.6	-23.2	-16.8	-38.8	-65.0
6	-7.4	-2.3	-1.7	-7.4	4.0	6.0

Table B.4 *...continues on the next page...*

7	-136.5	7.6	0.0	-136.5	7.6	30.4
8	-64.5	5.9	-10.7	-64.5	5.9	13.1
9	7.7	1.3	-3.1	7.7	1.3	2.0
10	-4.0	30.6	-36.0	-4.0	-37.8	-68.0
11	-12.2	33.4	-48.8	-12.2	-35.0	-55.9
12	-6.2	-3.7	8.0	-6.2	2.6	2.7
13	-129.9	6.8	0.0	-129.9	6.8	27.1
14	-61.9	4.1	-7.4	-61.9	4.1	9.0
15	6.0	1.2	-2.0	6.0	1.2	3.0
16	-1.3	30.3	-33.5	-1.3	-38.1	-68.9
17	-9.3	32.8	-45.0	-9.3	-35.6	-57.2
18	-4.9	-3.4	5.7	-4.9	2.9	3.4
19	-130.6	6.9	0.0	-130.6	6.9	27.5
20	-62.1	4.2	-7.6	-62.1	4.2	9.3
21	6.4	1.3	-2.2	6.4	1.3	2.8
22	1.4	30.3	-33.9	1.4	-38.1	-68.7
23	-6.4	32.9	-45.7	-6.4	-35.5	-57.0
24	-3.7	-3.5	6.2	-3.7	2.8	3.3
25	-130.6	6.9	0.0	-130.6	6.9	27.6
26	-62.1	4.1	-7.3	-62.1	4.1	8.9
27	6.3	1.3	-2.3	6.3	1.3	3.0
28	4.2	30.3	-33.9	4.2	-38.1	-68.6
29	-3.6	33.0	-45.8	-3.6	-35.4	-56.5
30	-2.3	-3.5	6.3	-2.3	2.8	3.0
31	-130.1	7.0	0.0	-130.1	7.0	27.8
32	-61.9	4.1	-7.3	-61.9	4.1	9.2

Table B.4 ...continues on the next page...

33	6.1	1.3	-2.5	6.1	1.3	2.8
34	7.1	30.2	-33.5	7.1	-38.2	-69.7
35	-0.8	32.6	-44.8	-0.8	-35.8	-59.6
36	-1.0	-3.3	5.8	-1.0	3.0	4.6
37	-134.4	6.7	0.0	-134.4	6.7	26.9
38	-64.4	2.8	-5.2	-64.4	2.8	6.1
39	7.2	1.1	-1.3	7.2	1.1	3.3
40	11.0	31.8	-37.6	11.0	-36.6	-59.1
41	0.8	35.7	-52.2	0.8	-32.7	-38.3
42	0.1	-4.2	7.9	0.1	2.1	-1.7
43	-67.2	13.3	0.0	-67.2	4.9	36.3
44	-30.6	15.8	-22.8	-30.6	7.4	23.7
45	2.1	8.3	-14.6	2.1	-0.1	1.7
Support Reactions						
node	Rx [kN]	Ry [kN]	M [kNm]			
1	-4.9	54.3	0.0			
5	-7.6	136.5	0.0			
9	-6.8	129.9	0.0			
13	-6.9	130.6	0.0			
17	-6.9	130.6	0.0			
21	-7.0	130.1	0.0			
25	-6.7	134.4	0.0			
29	-13.3	67.2	0.0			

Table B.4 *Internal forces due to the load combination "c".*

Load combination "D" 1.25*D+1.0*Eq						
Beam Forces						
member	axial1 [kN]	shear1 [kN]	bm1 [kNm]	axial2 [kN]	shear2 [kN]	bm2 [kNm]
1	-73.2	19.5	0.0	-73.2	19.5	78.1
2	-54.8	6.7	-9.9	-54.8	6.7	17.0
3	-21.2	-0.5	3.0	-21.2	-0.5	1.0
4	5.6	18.4	88.0	5.6	-83.3	-204.0
5	-7.2	33.6	14.0	-7.2	-68.1	-141.4
6	-19.2	21.2	1.0	-19.2	-37.3	-71.4
7	-283.1	39.8	0.0	-283.1	39.8	159.2
8	-171.3	34.9	-66.8	-171.3	34.9	72.8
9	-62.9	20.3	-38.4	-62.9	20.3	42.9
10	3.3	28.5	21.9	3.3	-73.2	-179.0
11	-7.0	40.3	-30.1	-7.0	-61.4	-125.1
12	-17.6	25.6	-28.5	-17.6	-32.9	-61.6
13	-259.4	37.3	0.0	-259.4	37.3	149.4
14	-158.9	31.5	-59.7	-158.9	31.5	66.2
15	-57.9	17.6	-33.2	-57.9	17.6	37.2
16	1.9	27.3	30.1	1.9	-74.4	-182.0
17	-7.5	39.6	-25.6	-7.5	-62.1	-126.6
18	-18.7	25.0	-24.5	-18.7	-33.5	-62.9
19	-262.3	37.7	0.0	-262.3	37.7	150.7
20	-160.4	31.8	-60.3	-160.4	31.8	66.7

Table B.5 ...continues on the next page...

21	-58.6	17.8	-33.6	-58.6	17.8	37.7
22	0.7	27.5	29.0	0.7	-74.2	-181.5
23	-8.0	39.7	-26.3	-8.0	-62.0	-126.2
24	-19.6	25.1	-25.2	-19.6	-33.4	-62.6
25	-262.0	37.7	0.0	-262.0	37.7	150.7
26	-160.3	31.6	-60.0	-160.3	31.6	66.5
27	-58.6	17.6	-33.3	-58.6	17.6	37.3
28	-0.5	27.4	29.2	-0.5	-74.3	-181.9
29	-8.4	39.8	-26.5	-8.4	-61.9	-125.9
30	-20.6	25.2	-25.3	-20.6	-33.3	-62.2
31	-261.9	37.6	0.0	-261.9	37.6	150.4
32	-159.8	31.5	-59.7	-159.8	31.5	66.4
33	-58.2	17.6	-33.2	-58.2	17.6	37.3
34	-1.6	27.8	28.2	-1.6	-73.9	-179.4
35	-8.9	39.7	-26.3	-8.9	-62.0	-127.0
36	-21.7	24.9	-24.8	-21.7	-33.6	-64.0
37	-263.2	38.3	0.0	-263.2	38.3	153.1
38	-163.7	31.5	-60.3	-163.7	31.5	65.8
39	-60.4	16.5	-31.3	-60.4	16.5	34.9
40	-2.0	25.5	34.0	-2.0	-76.2	-193.9
41	-8.3	41.3	-29.9	-8.3	-60.4	-116.0
42	-23.8	26.8	-29.1	-23.8	-31.7	-50.9
43	-168.3	34.2	0.0	-168.3	34.2	136.8
44	-92.1	32.2	-57.1	-92.1	32.2	71.5
45	-31.7	23.8	-44.5	-31.7	23.8	50.9

Table B.5 ...continues on the next page...

Support Reactions			
node	Rx [kN]	Ry [kN]	M [kNm]
1	-19.5	73.2	0.0
5	-39.8	283.1	0.0
9	-37.3	259.4	0.0
13	-37.7	262.3	0.0
17	-37.7	262.0	0.0
21	-37.6	261.9	0.0
25	-38.3	263.2	0.0
29	-34.2	168.3	0.0

Table B.5 *Internal forces due to the load combination "d".*

Load combination "E" 0.85*D+1.0*Eq						
Beam Forces						
member	axial1 [kN]	shear1 [kN]	bm1 [kNm]	axial2 [kN]	shear2 [kN]	bm2 [kNm]
1	-33.7	21.9	0.0	-33.7	21.9	87.7
2	-30.8	10.9	-17.7	-30.8	10.9	26.0
3	-12.7	3.5	-4.8	-12.7	3.5	9.1
4	3.8	2.9	105.5	3.8	-65.5	-176.3
5	-6.9	18.2	30.8	-6.9	-50.2	-113.4
6	-15.2	12.7	9.1	-15.2	-26.9	-55.2

Table B.6 *...continues on the next page...*

7	-194.0	39.6	0.0	-194.0	39.6	158.3
8	-116.7	34.4	-65.8	-116.7	34.4	71.7
9	-43.0	19.7	-37.3	-43.0	19.7	41.6
10	1.8	11.7	47.8	1.8	-56.7	-154.4
11	-6.7	23.5	-4.4	-6.7	-44.9	-100.3
12	-14.2	16.0	-13.6	-14.2	-23.6	-47.7
13	-174.3	37.4	0.0	-174.3	37.4	149.6
14	-107.0	31.5	-59.7	-107.0	31.5	66.3
15	-39.1	17.6	-33.3	-39.1	17.6	37.2
16	0.5	10.6	55.0	0.5	-57.8	-157.0
17	-7.2	23.0	-0.8	-7.2	-45.4	-101.6
18	-15.3	15.6	-10.5	-15.3	-24.0	-48.6
19	-176.7	37.7	0.0	-176.7	37.7	150.8
20	-108.2	31.7	-60.2	-108.2	31.7	66.7
21	-39.7	17.8	-33.6	-39.7	17.8	37.6
22	-0.8	10.8	54.0	-0.8	-57.6	-156.6
23	-7.7	23.1	-1.3	-7.7	-45.3	-101.3
24	-16.2	15.6	-11.0	-16.2	-24.0	-48.4
25	-176.4	37.7	0.0	-176.4	37.7	150.7
26	-108.1	31.6	-60.0	-108.1	31.6	66.5
27	-39.6	17.7	-33.3	-39.6	17.7	37.3
28	-1.9	10.7	54.2	-1.9	-57.7	-157.0
29	-8.1	23.1	-1.5	-8.1	-45.3	-101.1
30	-17.2	15.7	-11.1	-17.2	-23.9	-48.2
31	-176.8	37.5	0.0	-176.8	37.5	150.2
32	-107.9	31.5	-59.6	-107.9	31.5	66.3

Table B.6 ...continues on the next page...

33	-39.5	17.6	-33.2	-39.5	17.6	37.3
34	-3.1	11.3	52.8	-3.1	-57.1	-153.6
35	-8.6	23.1	-1.5	-8.6	-45.3	-101.2
36	-18.3	15.6	-10.9	-18.3	-24.0	-49.0
37	-174.1	38.5	0.0	-174.1	38.5	154.1
38	-109.2	32.1	-61.3	-109.2	32.1	66.9
39	-40.5	17.1	-32.4	-40.5	17.1	36.1
40	-3.8	7.7	61.7	-3.8	-60.7	-176.4
41	-8.1	23.4	-1.9	-8.1	-45.0	-99.2
42	-19.9	16.5	-12.9	-19.9	-23.1	-42.7
43	-128.8	31.8	0.0	-128.8	31.8	127.1
44	-68.1	28.0	-49.3	-68.1	28.0	62.5
45	-23.1	19.9	-36.7	-23.1	19.9	42.7
Support Reactions						
node	Rx [kN]	Ry [kN]	M [kNm]			
1	-21.9	33.7	0.0			
5	-39.6	194.0	0.0			
9	-37.4	174.3	0.0			
13	-37.7	176.7	0.0			
17	-37.7	176.4	0.0			
21	-37.5	176.8	0.0			
25	-38.5	174.1	0.0			
29	-31.8	128.8	0.0			

Table B.6 *Internal forces due to the load combination "e".*

Load combination "F" $1.25*D+0.7*(1.5*I+1.5*W_o)$						
Beam Forces						
member	axial1 [kN]	shear1 [kN]	bm1 [kNm]	axial2 [kN]	shear2 [kN]	bm2 [kNm]
1	-220.5	-6.5	0.0	-220.5	-14.5	-41.9
2	-139.2	-16.9	37.2	-139.2	-24.9	-46.6
3	-55.9	-19.3	41.4	-55.9	-27.3	-51.7
4	2.5	81.3	-79.1	2.5	-100.5	-165.2
5	-5.7	83.3	-88.0	-5.7	-98.5	-156.6
6	-27.3	55.9	-51.7	-27.3	-68.3	-107.6
7	-509.6	6.3	0.0	-509.6	6.3	25.2
8	-320.1	5.7	-10.6	-320.1	5.7	12.0
9	-131.0	4.6	-8.2	-131.0	4.6	10.0
10	3.1	89.0	-129.4	3.1	-92.8	-146.6
11	-4.6	90.6	-136.4	-4.6	-91.2	-139.1
12	-22.7	62.7	-97.6	-22.7	-61.5	-92.6
13	-485.2	4.5	0.0	-485.2	4.5	18.2
14	-304.3	2.7	-4.9	-304.3	2.7	6.0
15	-123.2	0.8	-1.5	-123.2	0.8	1.6
16	4.9	88.1	-123.5	4.9	-93.7	-148.8
17	-2.6	89.9	-131.6	-2.6	-91.9	-140.7
18	-21.9	61.7	-91.0	-21.9	-62.5	-94.6
19	-488.2	4.8	0.0	-488.2	4.8	19.2
20	-306.3	3.0	-5.3	-306.3	3.0	6.5

Table B.7 ...continues on the next page...

21	-124.4	1.1	-1.9	-124.4	1.1	2.4
22	6.8	88.2	-124.2	6.8	-93.6	-148.6
23	-0.8	90.0	-132.3	-0.8	-91.8	-140.3
24	-20.8	61.9	-92.2	-20.8	-62.3	-94.3
25	-488.2	4.8	0.0	-488.2	4.8	19.3
26	-306.3	2.8	-5.1	-306.3	2.8	6.3
27	-124.4	0.7	-1.3	-124.4	0.7	1.6
28	8.8	88.2	-124.3	8.8	-93.6	-148.1
29	1.4	90.1	-132.7	1.4	-91.7	-139.6
30	-20.1	62.1	-92.6	-20.1	-62.1	-92.9
31	-485.4	5.1	0.0	-485.4	5.1	20.3
32	-304.3	3.0	-5.4	-304.3	3.0	6.7
33	-123.2	1.0	-1.6	-123.2	1.0	2.5
34	10.8	87.5	-122.5	10.8	-94.3	-152.9
35	3.4	89.5	-131.3	3.4	-92.3	-143.9
36	-19.1	61.0	-90.4	-19.1	-63.2	-100.0
37	-508.1	3.7	0.0	-508.1	3.7	14.9
38	-320.0	0.5	-0.5	-320.0	0.5	1.4
39	-131.3	-2.9	5.2	-131.3	-2.9	-6.3
40	14.1	93.8	-137.6	14.1	-88.0	-111.5
41	6.7	96.4	-147.7	6.7	-85.4	-98.6
42	-22.0	68.2	-106.3	-22.0	-56.0	-51.7
43	-229.5	19.2	0.0	-229.5	13.2	64.8
44	-141.5	27.3	-46.7	-141.5	21.3	50.4
45	-56.0	28.0	-48.2	-56.0	22.0	51.7

Table B.7 ...continues on the next page...

Support Reactions			
node	Rx [kN]	Ry [kN]	M [kNm]
1	6.5	220.5	0.0
5	-6.3	509.6	0.0
9	-4.5	485.2	0.0
13	-4.8	488.2	0.0
17	-4.8	488.2	0.0
21	-5.1	485.4	0.0
25	-3.7	508.1	0.0
29	-19.2	229.5	0.0

Table B.7 *Internal forces due to the load combination "f".*

Load combination "G" $1.25 \cdot D + 0.7 \cdot (1.5 \cdot L + 1.0 \cdot Eq)$						
Beam Forces						
member	axial1 [kN]	shear1 [kN]	bm1 [kNm]	axial2 [kN]	shear2 [kN]	bm2 [kNm]
1	-205.8	5.5	0.0	-205.8	5.5	22.0
2	-141.4	-8.5	18.3	-141.4	-8.5	-15.6
3	-66.1	-19.6	34.5	-66.1	-19.6	-43.9
4	9.0	64.4	3.7	9.0	-117.4	-234.7
5	1.0	75.3	-50.1	1.0	-106.5	-190.6
6	-32.7	66.1	-43.9	-32.7	-89.6	-149.9

Table B.8 *...continues on the next page...*

7	-549.1	28.7	0.0	-549.1	28.7	114.7
8	-356.0	25.6	-49.3	-356.0	25.6	53.2
9	-165.8	17.5	-32.2	-165.8	17.5	37.8
10	7.0	75.7	-70.7	7.0	-106.1	-207.1
11	-0.9	83.7	-105.3	-0.9	-98.1	-170.2
12	-28.3	76.2	-112.2	-28.3	-79.5	-127.4
13	-515.7	26.0	0.0	-515.7	26.0	103.8
14	-335.3	22.0	-41.6	-335.3	22.0	46.2
15	-154.2	12.2	-23.4	-154.2	12.2	25.6
16	6.0	74.4	-61.6	6.0	-107.4	-210.5
17	-1.3	83.0	-100.6	-1.3	-98.8	-171.8
18	-29.2	74.7	-101.8	-29.2	-81.0	-130.6
19	-519.9	26.4	0.0	-519.9	26.4	105.5
20	-337.9	22.2	-42.3	-337.9	22.2	46.7
21	-156.0	12.7	-23.8	-156.0	12.7	26.8
22	5.2	74.5	-62.7	5.2	-107.3	-210.1
23	-1.9	83.1	-101.3	-1.9	-98.7	-171.3
24	-29.6	74.9	-103.8	-29.6	-80.8	-130.0
25	-519.6	26.4	0.0	-519.6	26.4	105.5
26	-337.8	22.2	-42.0	-337.8	22.2	46.6
27	-156.0	12.2	-23.0	-156.0	12.2	25.7
28	4.4	74.5	-62.6	4.4	-107.3	-210.0
29	-2.0	83.2	-101.7	-2.0	-98.6	-170.9
30	-30.5	75.2	-104.3	-30.5	-80.5	-128.2
31	-517.5	26.5	0.0	-517.5	26.5	105.9
32	-335.9	22.2	-42.1	-335.9	22.2	46.7

Table B.8 ...continues on the next page...

33	-154.4	12.4	-23.2	-154.4	12.4	26.6
34	3.6	74.3	-62.0	3.6	-107.5	-211.7
35	-2.3	82.9	-101.0	-2.3	-98.9	-173.1
36	-31.2	73.9	-101.6	-31.2	-81.8	-137.0
37	-535.2	26.0	0.0	-535.2	26.0	103.8
38	-350.7	21.0	-39.8	-350.7	21.0	44.0
39	-164.1	8.3	-16.7	-164.1	8.3	16.7
40	3.6	76.9	-68.0	3.6	-104.9	-193.7
41	0.2	87.7	-112.5	0.2	-94.1	-141.2
42	-36.0	82.3	-120.3	-36.0	-73.4	-80.2
43	-272.3	32.1	0.0	-272.3	32.1	128.3
44	-167.5	35.7	-65.3	-167.5	35.7	77.6
45	-73.4	36.0	-63.6	-73.4	36.0	80.2
Support Reactions						
node	Rx [kN]	Ry [kN]	M [kNm]			
1	-5.5	205.8	0.0			
5	-28.7	549.1	0.0			
9	-26.0	515.7	0.0			
13	-26.4	519.9	0.0			
17	-26.4	519.6	0.0			
21	-26.5	517.5	0.0			
25	-26.0	535.2	0.0			
29	-32.1	272.3	0.0			

Table B.8 *Internal forces due to the load combination "g".*

The internal maximum forces governing the design of the elements of the frame are summarized in Table B.9.

element	internal force governing design		load combination
first storey beam	bending moment	235 kNm	G
second storey beam	bending moment	191 kNm	G
roof beam	bending moment	172 kNm	A
first storey column	bending moment	159 kNm	D
	axial force	283 kN	
second storey column	bending moment	78 kNm	G
	axial force	168 kN	
third storey column	bending moment	80 kNm	G
	axial force	73 kN	

Table B.9 *Internal forces governing the design of the elements.*

6. DESIGN OF THE MEMBERS.

The design calculations are performed according to section 6 of CAN/CSA-O86.1-M89.

The glulam 24f-E, D.Fir-L. shall be used as material for the frame's members.

I. Design of the Beams.

The following factors and material properties are used in calculations of the factored bending moment resistance and the factored shear resistance:

ϕ	resistance factor	0.9	
K_D	load duration factor	1.0	(standard term)
K_H	system factor	1.0	(nominal)
K_{Sb}	service condition factor for bending	1.0	(dry service conditions)

K_{Sv}	service condition factor for shear	1.0	(dry service conditions)
K_{SE}	service condition factor for M.O.E.	1.0	(dry service conditions)
K_T	treatment factor	1.0	(non-treated glulam)
K_X	curvature factor for glulam	1.0	(straight members)
K_N	notch factor	1.0	(free of notches)
f_b	specified strength in bending	30.6 MPa	
f_v	specified strength in shear	2.0 MPa	
E	Modulus of elasticity	13100 MPa	

The factored moment resistance of the beam is given by the formula:

$$M_r = \phi F_b S K_L K_x$$

where

$$F_b = f_b (K_D K_H K_{Sb} K_T) = 30.6 \text{ MPa}$$

S section modulus

K_L lateral stability factor

$$K_x = (0.97 E K_{SE} K_T / F_b)^{0.5} = 20.38$$

The factored shear resistance of the beam is calculated according to the formula:

$$V_r = \phi F_v 0.6 A K_N C_V Z^{-0.18} \geq W_f$$

where

$$F_v = f_v (K_D K_H K_{Sv} K_T) = 2.0 \text{ MPa}$$

A cross-sectional area of beam, mm^2

C_V shear load coefficient

Z Beam volume, m^3

a) first storey beam

$$M_f = 235 \text{ kNm}$$

Assume glulam section 130x684mm.

$$A = 130 \times 684 = 88\,920 \text{ mm}^2$$

$$S = 130 \times 684^2 / 6 = 10.14 \times 10^6 \text{ mm}^3$$

$$Z = 0.13 \times 0.684 \times 9.0 = 0.8 \text{ m}^3$$

$$\text{theoretical length } l = 9000 \text{ mm}$$

MOMENT RESISTANCE

The unsupported length of the beam, l_u , is assumed to be $l/3$ because this is the approximate length of the bottom edge of the beam subjected to compression stresses.

The effective length of the beam, L_e , is:

$$L_e = 1.92 l_u = 1.92 \times 9000 / 3 = 5760 \text{ mm}$$

The slenderness ratio of the beam, C_B , is:

$$C_B = \left(\frac{L_e d}{b^2} \right)^{0.5} = \left(\frac{5760 \times 684}{130^2} \right)^{0.5} = 15.27$$

$$10 \leq C_B \leq C_K$$

The lateral stability factor is, therefore, equal to:

$$K_L = 1 - \frac{1}{3} \left(\frac{C_B}{C_K} \right)^4 = 1 - \frac{1}{3} \left(\frac{15.27}{20.38} \right)^4 = 0.89$$

Now, the moment resistance may be calculated:

$$M_r = 0.9 \times 30.6 \times 10.14 \times 10^6 \times 0.89 \times 1.0 = 249.8 \times 10^6 \text{ Nmm} = 249.8 \text{ kNm}$$

$$M_r > M_f = 235 \text{ kNm}$$

O.K.

SHEAR RESISTANCE

The sum of all factored loads, W_f , acting on the beam is:

$$W_f = 9.0 \times 24.1 = 216.900 \text{ kN}$$

The shear load coefficient is:

$$C_V = 3.74$$

Now, the shear resistance of the beam may be calculated:

$$V_r = 0.9 \times 2.0 \times 0.6 \times 88920 \times 1.0 \times 3.74 \times 0.8^{-0.18} = 378300 \text{ N}$$

$$V_r > W_f$$

O.K.

b) second storey beam

$$M_f = 191 \text{ kNm}$$

Assume glulam section 130x608mm.

$$A = 130 \times 608 = 79\,040 \text{ mm}^2$$

$$S = 130 \times 608^2 / 6 = 8.01 \times 10^6 \text{ mm}^3$$

$$Z = 0.13 \times 0.608 \times 9.0 = 0.71 \text{ m}^3$$

$$\text{theoretical length } l = 9000 \text{ mm}$$

MOMENT RESISTANCE

The effective length of the beam, L_e , is:

$$L_e = 1.92 l_u = 1.92 \times 9000 / 3 = 5760 \text{ mm}$$

The slenderness ratio of the beam, C_B , is:

$$C_B = \left(\frac{L_e d}{b^2} \right)^{0.5} = \left(\frac{5760 \times 608}{130^2} \right)^{0.5} = 14.40$$

$$10 \leq C_B \leq C_K$$

The lateral stability factor is, therefore, equal to:

$$K_L = 1 - \frac{1}{3} \left(\frac{C_B}{C_K} \right)^4 = 1 - \frac{1}{3} \left(\frac{14.40}{20.38} \right)^4 = 0.92$$

Now, the moment resistance may be calculated:

$$M_r = 0.9 \times 30.6 \times 8.01 \times 10^6 \times 0.92 \times 1.0 = 202.3 \times 10^6 \text{ Nmm} = 202.3 \text{ kNm}$$

$$M_r > M_f = 191 \text{ kNm} \quad \text{O.K.}$$

SHEAR RESISTANCE

The sum of all factored loads, W_f , acting on the beam is:

$$W_f = 9.0 \times 24.1 = 216.900 \text{ kN}$$

The shear load coefficient is:

$$C_V = 3.70$$

Now, the shear resistance of the beam may be calculated:

$$V_r = 0.9 \times 2.0 \times 0.6 \times 79040 \times 1.0 \times 3.70 \times 0.71^{-0.18} = 339000 \text{ N}$$

$$V_r > W_f \quad \text{O.K.}$$

c) roof beam

$$M_f = 172 \text{ kNm}$$

Assume glulam section 130x570mm.

$$A = 130 \times 570 = 74\,100 \text{ mm}^2$$

$$S = 130 \times 570^2 / 6 = 7.04 \times 10^6 \text{ mm}^3$$

$$Z = 0.13 \times 0.570 \times 9.0 = 0.67 \text{ m}^3$$

$$\text{theoretical length } l = 9000 \text{ mm}$$

MOMENT RESISTANCE

The effective length of the beam, L_e , is:

$$L_e = 1.92 l_u = 1.92 \times 9000/3 = 5760 \text{ mm}$$

The slenderness ratio of the beam, C_B , is:

$$C_B = \left(\frac{L_e d}{b^2} \right)^{0.5} = \left(\frac{5760 \times 570}{130^2} \right)^{0.5} = 13.94$$

$$10 \leq C_B \leq C_K$$

The lateral stability factor is, therefore, equal to:

$$K_L = 1 - \frac{1}{3} \left(\frac{C_B}{C_K} \right)^4 = 1 - \frac{1}{3} \left(\frac{13.94}{20.38} \right)^4 = 0.93$$

Now, the moment resistance may be calculated:

$$M_r = 0.9 \times 30.6 \times 7.04 \times 10^6 \times 0.93 \times 1.0 = 179.7 \times 10^6 \text{ Nmm} = 179.7 \text{ kNm}$$

$$M_r > M_f = 172 \text{ kNm} \quad \text{O.K.}$$

SHEAR RESISTANCE

The sum of all factored loads, W_f , acting on the beam is:

$$W_f = 9.0 \times 22.0 = 198.900 \text{ kN}$$

The shear load coefficient is:

$$C_V = 3.69$$

Now, the shear resistance of the beam may be calculated:

$$V_r = 0.9 \times 2.0 \times 0.6 \times 74100 \times 1.0 \times 3.69 \times 0.67^{-0.18} = 320000 \text{ N}$$

$$V_r > W_f \quad \text{O.K.}$$

II. Design of the Columns.

The following factors and material properties are used in calculations of the factored resistance to combined bending and axial load:

ϕ	resistance factor	0.9	
K_D	load duration factor	1.0	(standard term)
K_H	system factor	1.0	(nominal)
K_{Sb}	service condition factor for bending	1.0	(dry service conditions)
K_{Sc}	service cond. factor for compr. parallel	1.0	(dry service conditions)
K_{SE}	service condition factor for M.O.E.	1.0	(dry service conditions)
K_T	treatment factor	1.0	(non-treated glulam)
K_X	curvature factor for glulam	1.0	(straight members)
f_b	specified strength in bending	30.6 MPa	
f_c	specified strength in compr. parallel	20.4 MPa	
E	modulus of elasticity	13100 MPa	
E_{05}	modulus of elasticity - 5th percentile	11400 MPa	

The factored compressive load resistance parallel to the grain, P_r , of the column is given by the formula:

$$P_r = \phi F_c A K_c$$

where

$$F_c = f_c (K_D K_H K_{Sb} K_T) = 20.4 \text{ MPa}$$

A cross-sectional area of member, mm^2

K_c slenderness factor

The factored bending moment resistance of the column is calculated as in section 6.I.

The columns should satisfy the following interaction equation:

$$\frac{P_f}{P_r} + \frac{M_f}{M_r} \leq 1.0$$

where

P_f factored compressive axial load

M_f factored bending moment amplified due to axial loads

a) first storey column

$$P_f = 283 \text{ kN}$$

$$M_f' = 159 \text{ kNm}$$

Assume glulam section 175x532mm.

$$A = 175 \times 532 = 93\,100 \text{ mm}^2$$

$$S = 175 \times 532^2 / 6 = 8.26 \times 10^6 \text{ mm}^3$$

$$I = 175 \times 532^3 / 12 = 2.20 \times 10^9 \text{ mm}^4$$

$$\text{theoretical length } l = 4000 \text{ mm}$$

$$\text{clear length } l_c = 4000 - 684/2 = 3658 \text{ mm}$$

The effective length factor is assumed to be $K_e = 0.85$, because the column can rotate freely at the bottom end and the top end rotation is restrained by the moment resisting connection to the beam.

IN-PLANE RESISTANCE (MOMENT AND AXIAL FORCE COMBINED)

The effective length of the column, L_e , is:

$$L_e = K_e l_c = 3658 \times 0.85 = 3109 \text{ mm}$$

The slenderness ratio of the column, C_c , is:

$$C_c = \frac{L_e}{d} = \frac{3109}{532} = 5.8 \quad < 50 \quad \underline{\text{O.K.}}$$

therefore

$$K_C = 1.0$$

Now, the compression resistance parallel to the grain may be calculated:

$$P_r = 0.9 \times 20.4 \times 93100 \times 1.0 = 1709300 \text{ N}$$

The bending resistance of the column is determined as follows:

$$C_B = \left(1.92 l_c \frac{d}{b^2} \right)^{0.5} = \left(1.92 \times 3658 \times \frac{532}{175^2} \right)^{0.5} = 11.0$$

$$C_K = 20.4, \text{ as before}$$

$$K_L = 1 - \frac{1}{3} \left(\frac{C_B}{C_K} \right)^4 = 1 - \frac{1}{3} \left(\frac{11.0}{20.4} \right)^4 = 0.97$$

$$M_r = 0.9 \times 30.6 \times 8.26 \times 10^6 \times 0.97 \times 1.0 = 220.7 \times 10^6 \text{ Nmm}$$

The amplification factor due to the axial load is equal to:

$$\frac{1}{1 - \frac{P_f}{\pi^2 E_{05} \frac{I}{(L_e)^2}}} = \frac{1}{1 - \frac{283000}{\pi^2 11400 \frac{2.20 \times 10^9}{3109^2}}} = 1.01$$

$$M_f = 159 \times 1.01 = 161 \text{ kNm}$$

Now, the interaction equation may be checked:

$$\frac{P_f}{P_r} + \frac{M_f}{M_r} = \frac{283}{1709.3} + \frac{161}{220.7} = 0.90$$

O.K.

OUT OF PLANE RESISTANCE (AXIAL FORCE ONLY)

The effective length factor is $K_e = 1.0$ and:

$$L_e = K_e l_c = 3658 \times 1.0 = 3658 \text{ mm}$$

The slenderness ratio of the column, C_c , is:

$$C_c = \frac{L_e}{b} = \frac{3658}{175} = 20.90 \quad < 50 \quad \text{O.K.}$$

and

$$C_k = \left(\frac{0.76 E_{os} K_{SE} K_T}{F_c} \right)^{0.5} = \left(\frac{0.76 \times 11400 \times 1.0 \times 1.0}{20.4} \right)^{0.5} = 20.60$$

$$C_c > C_k$$

therefore

$$K_c = \frac{1}{2C_c^2} \frac{E_{os} K_{SE} K_T}{F_c} = \frac{1}{2 \times 20.90^2} \frac{11400 \times 1.0 \times 1.0}{20.4} = 0.64$$

Now, the compression resistance parallel to the grain may be calculated:

$$P_r = 0.9 \times 20.4 \times 93100 \times 0.64 = 1093000 \text{ N}$$

$$P_r > P_f = 283000 \text{ N} \quad \text{O.K.}$$

b) second storey column

$$P_f = 168 \text{ kN}$$

$$M_f' = 78 \text{ kNm}$$

Assume glulam section 130x418mm.

$$A = 130 \times 418 = 54340 \text{ mm}^2$$

$$S = 130 \times 418^2 / 6 = 3.79 \times 10^6 \text{ mm}^3$$

$$I = 130 \times 418^3 / 12 = 791 \times 10^6 \text{ mm}^4$$

$$\text{theoretical length } l = 4000 \text{ mm}$$

$$\text{clear length } l_c = 4000 - 684/2 - 608/2 = 3354 \text{ mm}$$

The effective length factor is assumed to be $K_e=0.80$, because the column can not rotate freely at any end. The amount of rotation of the top and bottom joints depends on the relative stiffness between all members adjacent to those joints.

IN-PLANE RESISTANCE (MOMENT AND AXIAL FORCE COMBINED)

The effective length of the column, L_e , is:

$$L_e = K_e l_c = 3354 \times 0.80 = 2683 \text{ mm}$$

The slenderness ratio of the column, C_c , is:

$$C_c = \frac{L_e}{d} = \frac{2683}{418} = 6.4 \quad < 50 \quad \text{O.K.}$$

therefore

$$K_C = 1.0$$

Now, the compression resistance parallel to the grain may be calculated:

$$P_r = 0.9 \times 20.4 \times 54340 \times 1.0 = 997700 \text{ N}$$

The bending resistance of the column is determined as follows:

$$C_B = \left(1.92 l_c \frac{d}{b^2} \right)^{0.5} = \left(1.92 \times 3354 \times \frac{418}{130^2} \right)^{0.5} = 12.6$$

$$C_K = 20.4, \text{ as before}$$

$$K_L = 1 - \frac{1}{3} \left(\frac{C_B}{C_K} \right)^4 = 1 - \frac{1}{3} \left(\frac{12.60}{20.4} \right)^4 = 0.95$$

$$M_r = 0.9 \times 30.6 \times 3.77 \times 10^6 \times 0.95 \times 1.0 = 98.6 \times 10^6 \text{ Nmm}$$

The amplification factor due to the axial load is equal to:

$$\frac{1}{1 - \frac{P_f}{\pi^2 E_{05} \frac{I}{(L_e)^2}}} = \frac{1}{1 - \frac{168000}{\pi^2 11400 \frac{791 \times 10^6}{2683^2}}} = 1.01$$

$$M_f = 78 \times 1.01 = 79 \text{ kNm}$$

Now, the interaction equation may be checked:

$$\frac{P_f}{P_r} + \frac{M_f}{M_r} = \frac{168}{997.7} + \frac{79}{98.6} = 0.97 \quad \text{O.K.}$$

OUT OF PLANE RESISTANCE (AXIAL FORCE ONLY)

The effective length factor is $K_e = 1.0$ and:

$$L_e = K_e l_c = 3354 \times 1.0 = 3354 \text{ mm}$$

The slenderness ratio of the column, C_c , is:

$$C_c = \frac{L_e}{b} = \frac{3354}{130} = 25.80 \quad < 50 \quad \text{O.K.}$$

and

$$C_c > C_k = 20.40$$

therefore

$$K_c = \frac{1}{2C_c^2} \frac{E_{0.5} K_{SE} K_T}{F_c} = \frac{1}{2 \times 25.8^2} \frac{11400 \times 1.0 \times 1.0}{20.4} = 0.42$$

Now, the compression resistance parallel to the grain may be calculated:

$$P_r = 0.9 \times 20.4 \times 54340 \times 0.42 = 419000 \text{ N}$$

$$P_r > P_f = 168000 \text{ N} \quad \text{O.K.}$$

c) third storey column

$$P_f = 73 \text{ kN}$$

$$M_f' = 80 \text{ kNm}$$

Assume glulam section 130x418mm, the same as in b).

$$A = 54\,340 \text{ mm}^2$$

$$S = 3.79 \times 10^6 \text{ mm}^3$$

$$I = 791 \times 10^6 \text{ mm}^4$$

$$\text{theoretical length } l = 4000 \text{ mm}$$

$$\text{clear length } l_c = 4000 - 608/2 - 570/2 = 3411 \text{ mm}$$

The effective length factor is assumed to be $K_e=0.75$, because the column can not rotate freely at any end. The amount of rotation of the top and bottom joints depends on the relative stiffness between all members adjacent to those joints, which is greater than in b).

IN-PLANE RESISTANCE (MOMENT AND AXIAL FORCE COMBINED)

The effective length of the column, L_e , is:

$$L_e = K_e l_c = 3411 \times 0.75 = 2558 \text{ mm}$$

The slenderness ratio of the column, C_c , is:

$$C_c = \frac{L_e}{d} = \frac{2558}{418} = 6.1 \quad < 50 \quad \text{O.K.}$$

therefore

$$K_C = 1.0$$

Now, the compression resistance parallel to the grain may be calculated:

$$P_r = 0.9 \times 20.4 \times 54340 \times 1.0 = 997700 \text{ N}$$

The bending resistance of the column is determined as follows:

$$C_B = \left(1.92 l_c \frac{d}{b^2} \right)^{0.5} = \left(1.92 \times 3411 \times \frac{418}{130^2} \right)^{0.5} = 12.7$$

$C_K = 20.4$, as before

$$K_L = 1 - \frac{1}{3} \left(\frac{C_B}{C_K} \right)^4 = 1 - \frac{1}{3} \left(\frac{12.7}{20.4} \right)^4 = 0.95$$

$$M_r = 0.9 \times 30.6 \times 3.77 \times 10^6 \times 0.95 \times 1.0 = 98.6 \times 10^6 \text{ Nmm}$$

The amplification factor due to the axial load is equal to:

$$\frac{1}{1 - \frac{P_f}{\pi^2 E_{05} \frac{I}{(L_e)^2}}} = \frac{1}{1 - \frac{73000}{\pi^2 11400 \frac{791 \times 10^6}{2558^2}}} = 1.01$$

$$M_f = 80 \times 1.01 = 81 \text{ kNm}$$

Now, the interaction equation may be checked:

$$\frac{P_f}{P_r} + \frac{M_f}{M_r} = \frac{73}{997.7} + \frac{81}{98.6} = 0.89 \quad \text{O.K.}$$

OUT OF PLANE RESISTANCE (AXIAL FORCE ONLY)

The effective length factor is $K_e = 1.0$ and:

$$L_e = K_e l_c = 3411 \times 1.0 = 3411 \text{ mm}$$

The slenderness ratio of the column, C_c , is:

$$C_c = \frac{L_e}{b} = \frac{3411}{130} = 26.24 \quad < 50 \quad \text{O.K.}$$

and

$$C_c > C_k = 20.40$$

therefore

$$K_c = \frac{1}{2C_c^2} \frac{E_{05} K_{SE} K_T}{F_c} = \frac{1}{2 \times 26.24^2} \frac{11400 \times 1.0 \times 1.0}{20.4} = 0.41$$

Now, the compression resistance parallel to the grain may be calculated:

$$P_r = 0.9 \times 20.4 \times 54340 \times 0.41 = 409000 \text{ N}$$

$$P_r > P_f = 73000 \text{ N}$$

O.K.